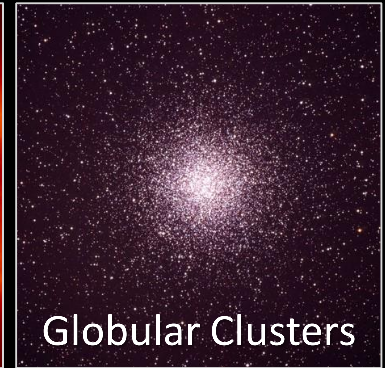

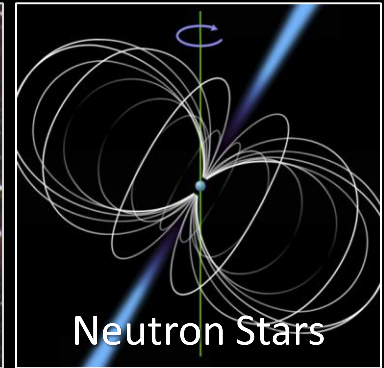

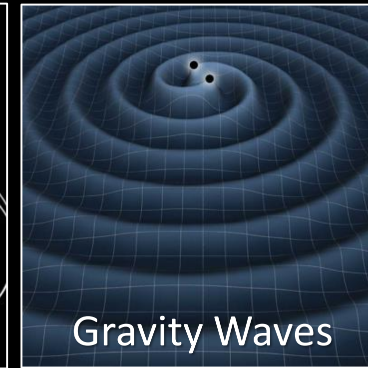

Particle-Physics Constraints from Stars

MAX-PLANCK-GESELLSCHAFT

Max-Planck-Institut für Physik
(Werner-Heisenberg-Institut)

SFB 1258 | Neutrinos Dark Matter Messengers

Georg G. Raffelt, Max-Planck-Institut für Physik, München

Particle-Physics Constraints from Stars

Low-mass particles (neutrinos, axions and friends, hidden photons, low-mass carriers of new forces, ...) can be probed by stars.

- **Particles from the Sun and their detection**
- **Impact of new energy-loss channels on low-mass stars**
- **Supernova 1987A**
- **Neutron-star cooling**
- **Axion conversion in pulsar magnetospheres**
- **Superradiance of ultra-light bosons from black holes**

In this lecture focus on the astrophysics of these arguments (often not so clear to particle physicists) and not so much on the latest results for all types of particles

EVOLUTION OF STARS

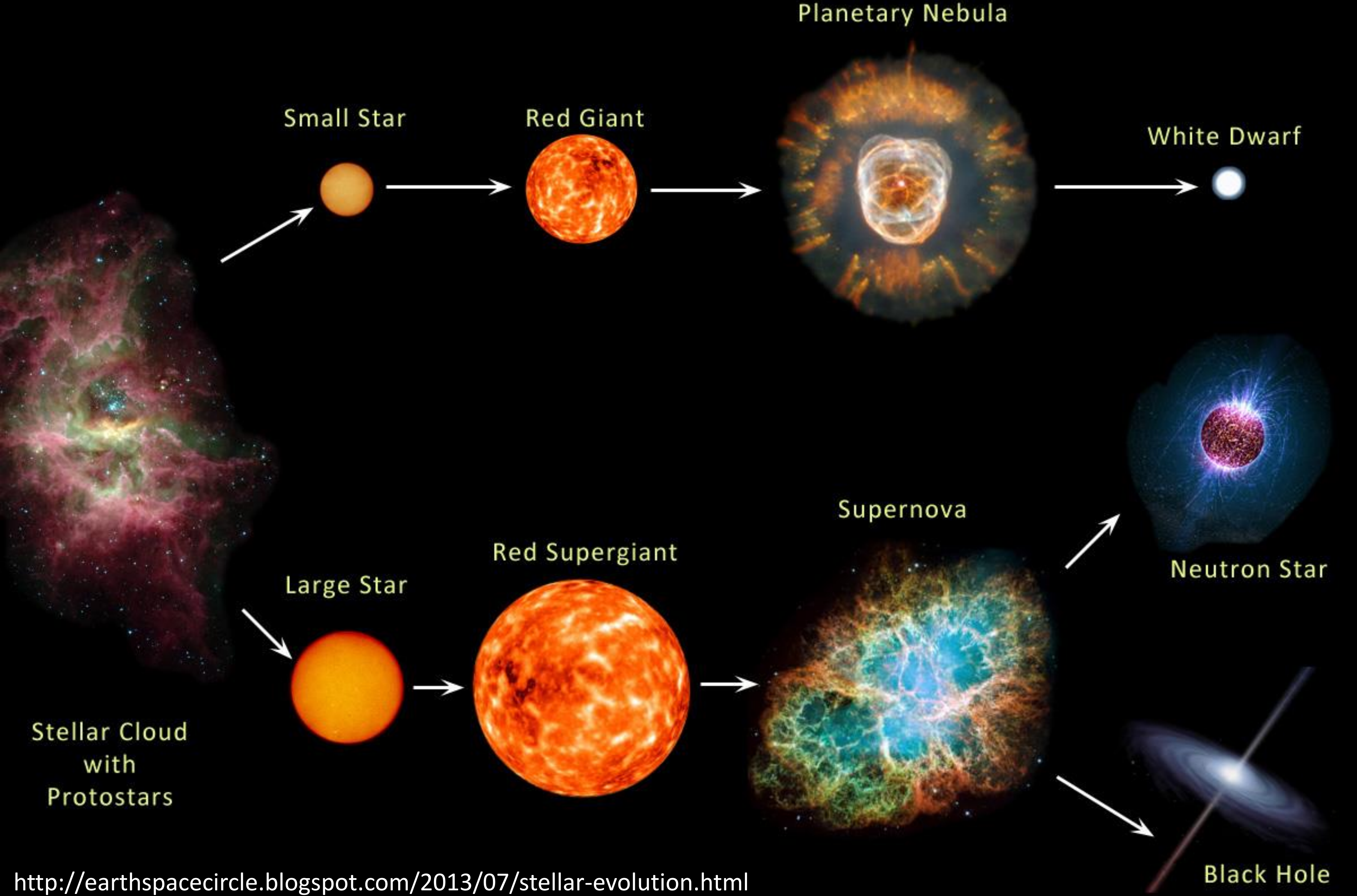

http://earthspacecircle.blogspot.com/2013/07/stellar-evolution.html

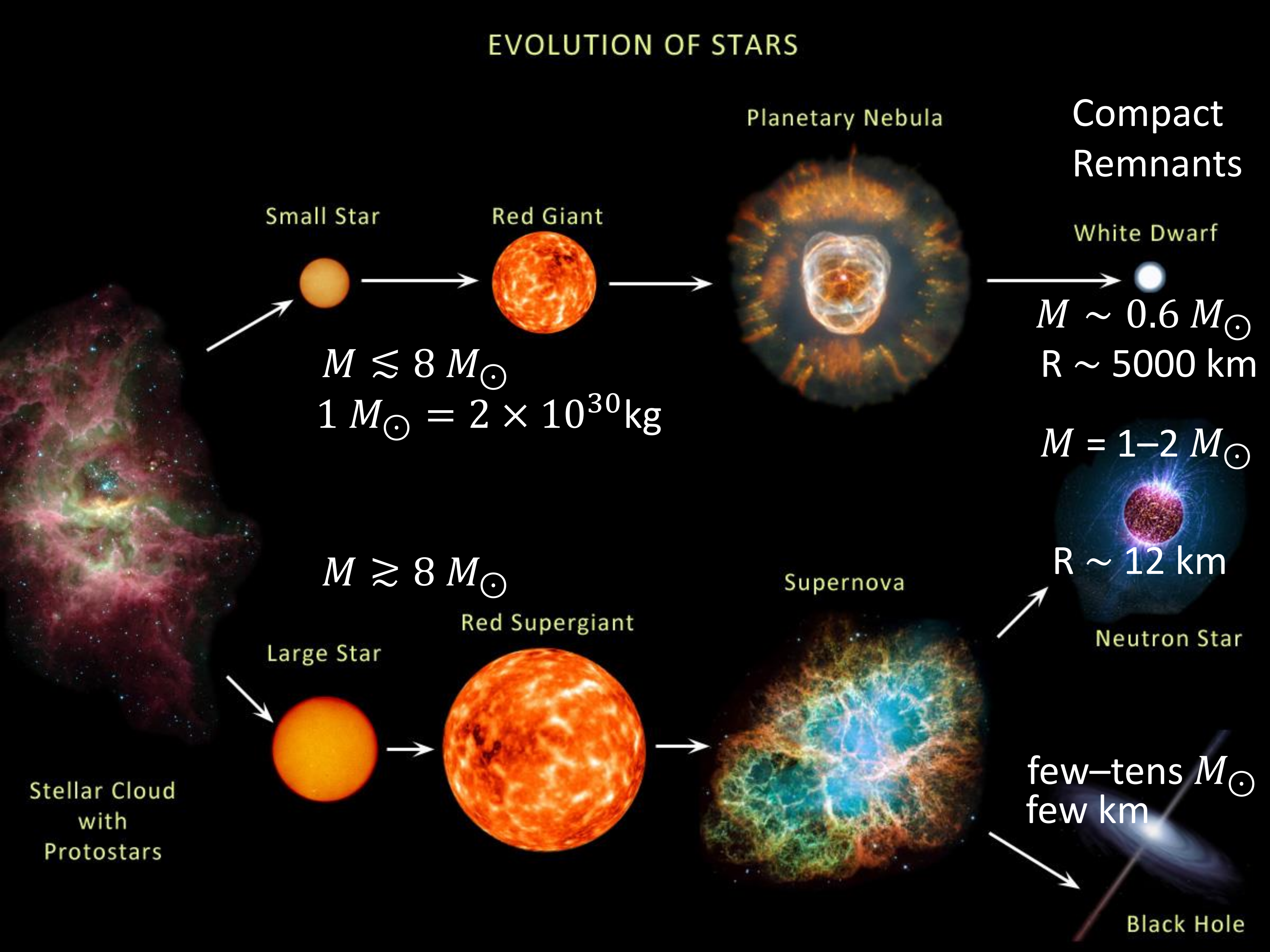
EVOLUTION OF STARS
Compact Remnants
Planetary Nebula
Small Star
Red Giant
White Dwarf
$M \sim 0.6\ M_\odot$
R ~ 5000 km
$M \lesssim 8\ M_\odot$
$1\ M_\odot = 2 \times 10^{30}$kg
M = 1–2 $M_\odot$
R ~ 12 km
$M \gtrsim 8\ M_\odot$
Supernova
Red Supergiant
Large Star
Neutron Star
few–tens $M_\odot$
few km
Stellar Cloud with Protostars
Black Hole

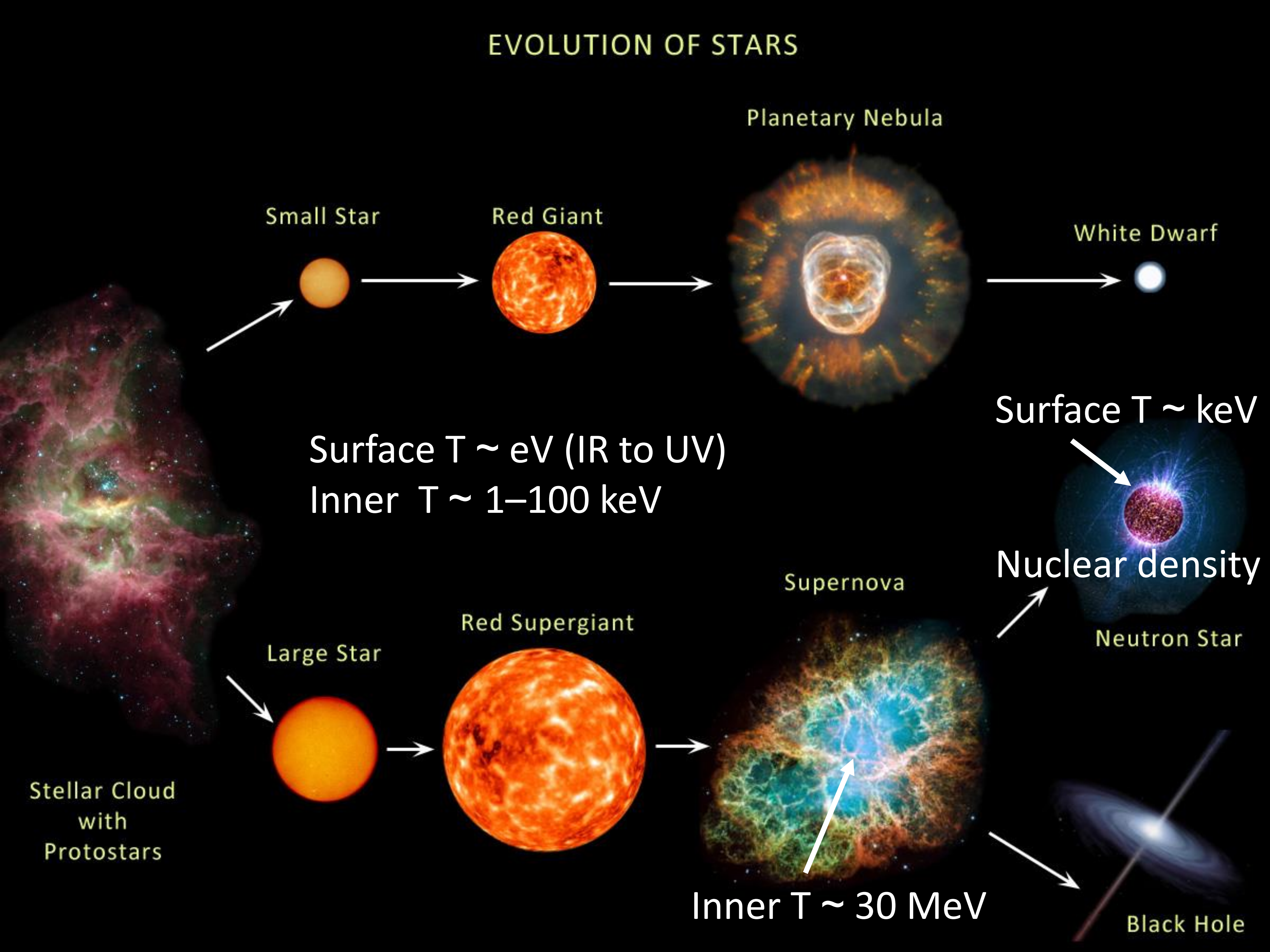

EVOLUTION OF STARS
Planetary Nebula
Small Star
Red Giant
White Dwarf
Surface T ~ keV
Surface T ~ eV (IR to UV)
Inner T ~ 1–100 keV
Nuclear density
Supernova
Red Supergiant
Neutron Star
Large Star
Stellar Cloud with Protostars
Inner T ~ 30 MeV
Black Hole

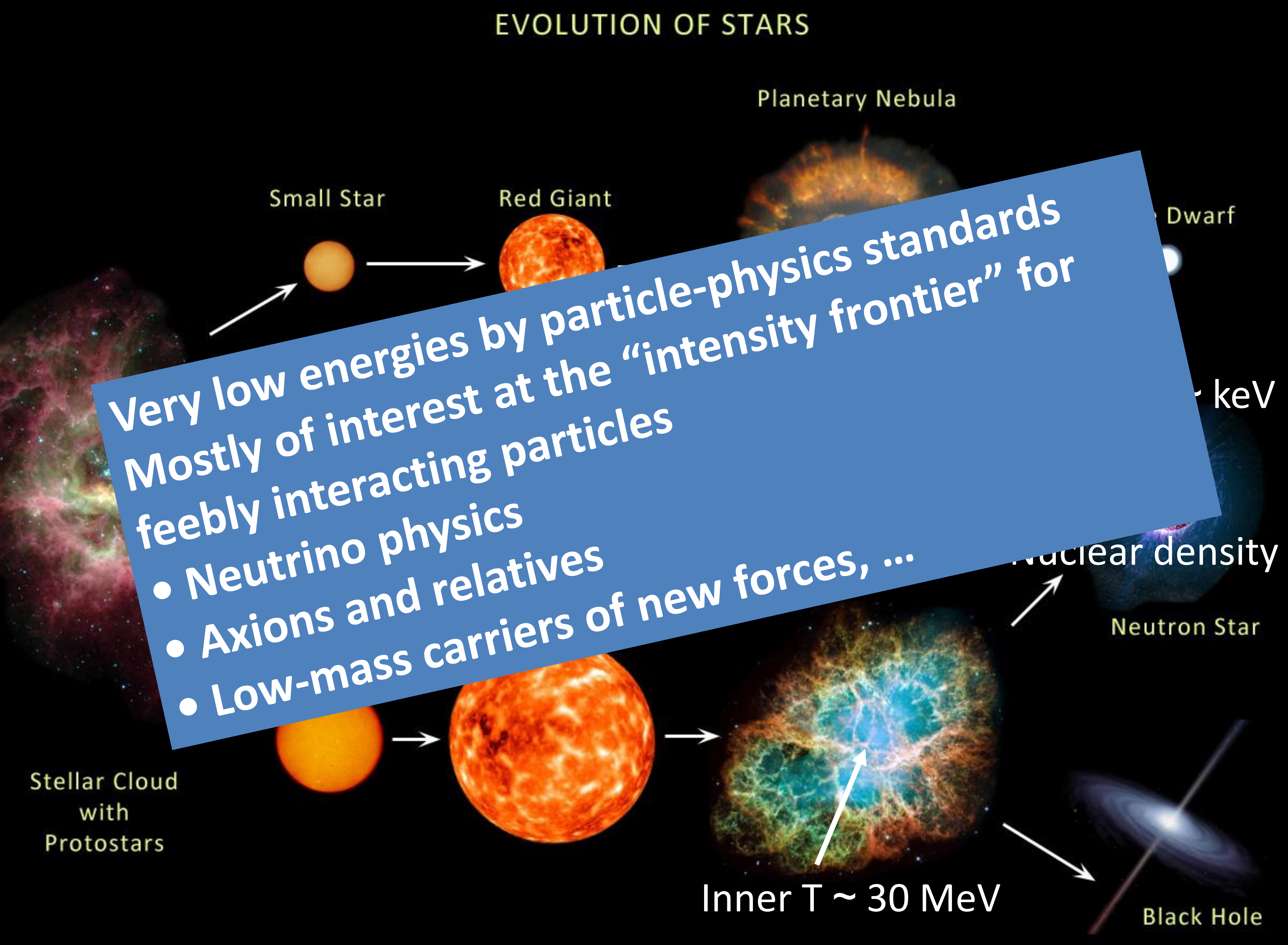

Very low energies by particle-physics standards

Mostly of interest at the "intensity frontier" for feebly interacting particles

- **Neutrino physics**
- **Axions and relatives**
- **Low-mass carriers of new forces, …**

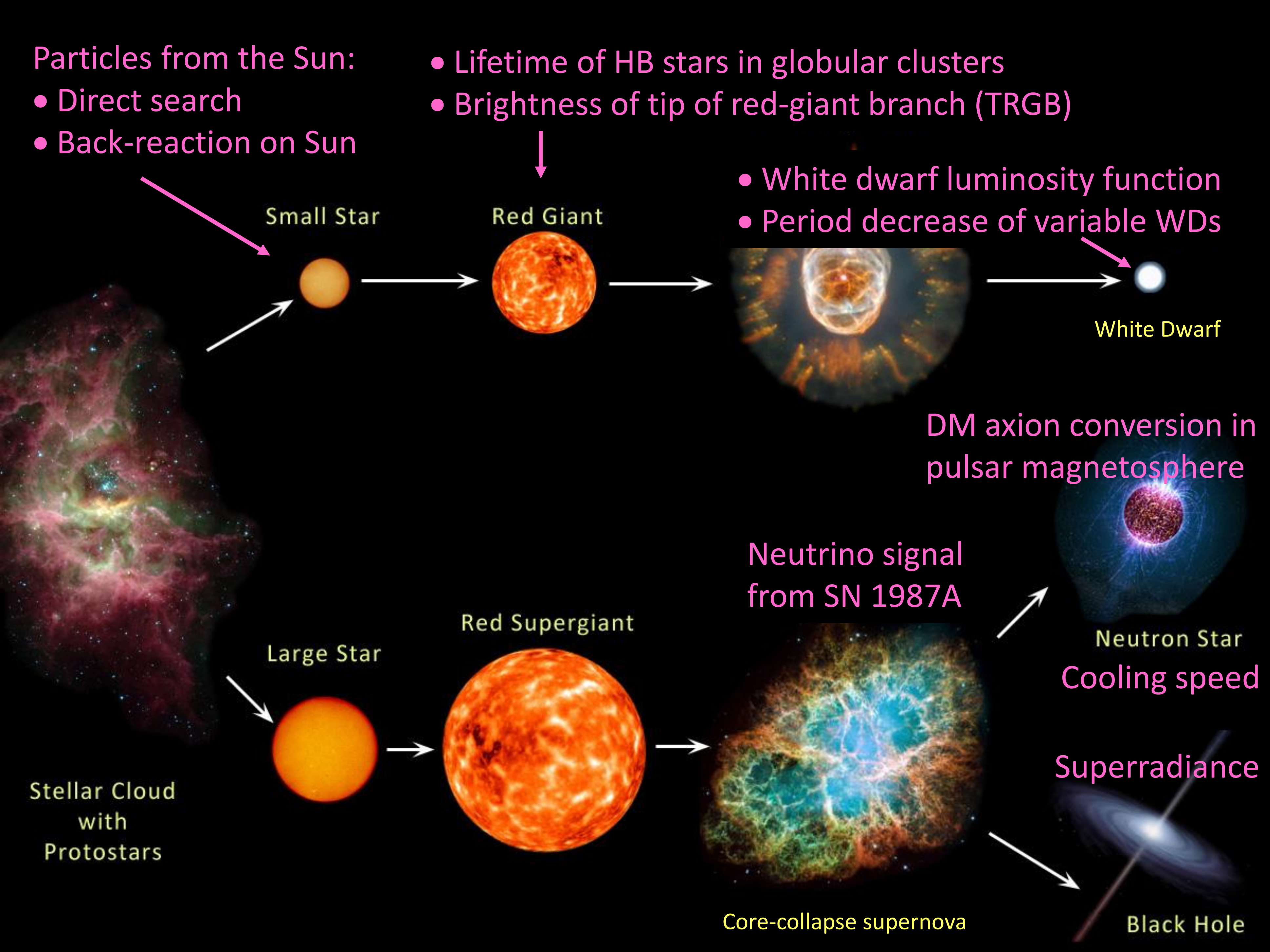

Particles from the Sun:
• Direct search
• Back-reaction on Sun
• Lifetime of HB stars in globular clusters
• Brightness of tip of red-giant branch (TRGB)
• White dwarf luminosity function
• Period decrease of variable WDs
Small Star
Red Giant
White Dwarf
DM axion conversion in pulsar magnetosphere
Neutrino signal from SN 1987A
Neutron Star
Cooling speed
Large Star
Red Supergiant
Superradiance
Stellar Cloud with Protostars
Core-collapse supernova
Black Hole

Particles from the Sun

2002 Solar Neutrinos (R.Davis, M.Koshiba)

2015 Solar Nu Oscillations (A.McDonald)

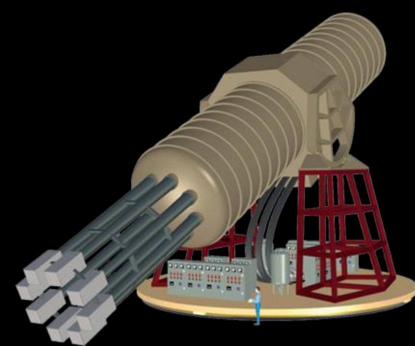

Search for solar axions with CAST and future IAXO

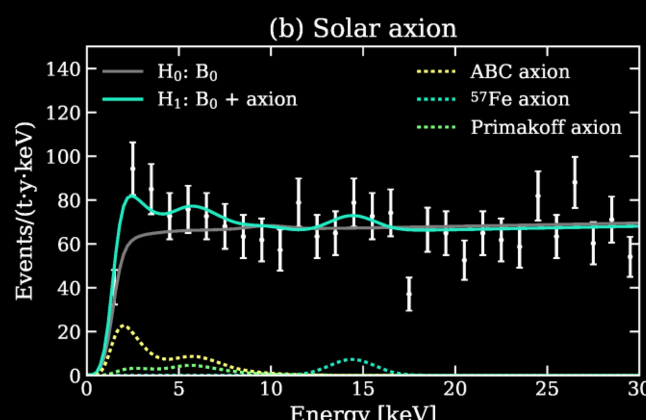

Excess events in XENON1T DM search. Solar axions? arXiv:2006.09721

Bethe's Classic Paper on Nuclear Reactions in Stars

MARCH 1, 1939 PHYSICAL REVIEW VOLUME 55

Energy Production in Stars*

H. A. Bethe
Cornell University, Ithaca, New York
(Received September 7, 1938)

It is shown that the *most important source of energy in ordinary stars is the reactions of carbon and nitrogen with protons*. These reactions form a cycle in which the original nucleus is reproduced, *viz.* $C^{12}+H=N^{13}$, $N^{13}=C^{13}+\epsilon^+$, $C^{13}+H=N^{14}$, $N^{14}+H=O^{15}$, $O^{15}=N^{15}+\epsilon^+$, $N^{15}+H=C^{12}+He^4$. Thus carbon and nitrogen merely serve as catalysts for the combination of four protons (and two electrons) into an α-particle (§7).

The carbon-nitrogen reactions are unique in their cyclical character (§8). For all nuclei lighter than carbon, reaction with protons will lead to the emission of an α-particle so that the original nucleus is permanently destroyed. For all nuclei heavier than fluorine, only radiative capture of the protons occurs, also destroying the original nucleus. Oxygen and fluorine reactions mostly lead back to nitrogen. Besides, these heavier nuclei react much more slowly than C and N and are therefore unimportant for the energy production.

The agreement of the carbon-nitrogen reactions with observational data (§7, 9) is excellent. In order to give the correct energy evolution in the sun, the central temperature of the sun would have to be 18.5 million degrees while integration of the Eddington equations gives 19. For the brilliant star Y Cygni the corresponding figures are 30 and 32. This good agreement holds for all bright stars of the main sequence, but, of course, not for giants.

For fainter stars, with lower central temperatures, the reaction $H+H=D+\epsilon^+$ and the reactions following it, are believed to be mainly responsible for the energy production. (§10)

It is shown further (§5–6) that *no elements heavier than* He^4 *can be built up in ordinary stars*. This is due to the fact, mentioned above, that all elements up to boron are disintegrated by proton bombardment (α-emission!) rather than built up (by radiative capture). The instability of Be^8 reduces the formation of heavier elements still further. The production of neutrons in stars is likewise negligible. The heavier elements found in stars must therefore have existed already when the star was formed.

Finally, the suggested mechanism of energy production is used to draw conclusions about astrophysical problems, such as the mass-luminosity relation (§10), the stability against temperature changes (§11), and stellar evolution (§12).

§1. Introduction

THE progress of nuclear physics in the last few years makes it possible to decide rather definitely which processes can and which cannot occur in the interior of stars. Such decisions will be attempted in the present paper, the discussion being restricted primarily to main sequence stars. The results will be at variance with some current hypotheses.

The first main result is that, under present conditions, no elements heavier than helium can be built up to any appreciable extent. Therefore we must assume that the heavier elements were built up *before* the stars reached their present state of temperature and density. No attempt will be made at speculations about this previous state of stellar matter.

The energy production of stars is then due entirely to the combination of four protons and two electrons into an α-particle. This simplifies the discussion of stellar evolution inasmuch as the amount of heavy matter, and therefore the opacity, does not change with time.

The combination of four protons and two electrons can occur essentially only in two ways. The first mechanism starts with the combination of two protons to form a deuteron with positron emission, *viz.*

$$H+H=D+\epsilon^+. \quad (1)$$

The deuteron is then transformed into He^4 by further capture of protons; these captures occur very rapidly compared with process (1). The second mechanism uses carbon and nitrogen as catalysts, according to the chain reaction

$$\begin{aligned} &C^{12}+H=N^{13}+\gamma, \qquad N^{13}=C^{13}+\epsilon^+\\ &C^{13}+H=N^{14}+\gamma,\\ &N^{14}+H=O^{15}+\gamma, \qquad O^{15}=N^{15}+\epsilon^+\\ &N^{15}+H=C^{12}+He^4. \end{aligned} \quad (2)$$

The catalyst C^{12} is reproduced in all cases except about one in 10,000, therefore the abundance of carbon and nitrogen remains practically unchanged (in comparison with the change of the number of protons). The two reactions (1) and

* Awarded an A. Cressy Morrison Prize in 1938, by the New York Academy of Sciences.

434

No neutrinos from nuclear reactions in 1938 …

The combination of four protons and two electrons can occur essentially only in two ways. The first mechanism starts with the combination of two protons to form a deuteron with positron emission, *viz.*

$$H+H=D+\epsilon^+. \quad (1)$$

The deuteron is then transformed into He^4 by further capture of protons; these captures occur very rapidly compared with process (1). The second mechanism uses carbon and nitrogen as catalysts, according to the chain reaction

$$\begin{aligned} &C^{12}+H=N^{13}+\gamma, \qquad N^{13}=C^{13}+\epsilon^+\\ &C^{13}+H=N^{14}+\gamma,\\ &N^{14}+H=O^{15}+\gamma, \qquad O^{15}=N^{15}+\epsilon^+\\ &N^{15}+H=C^{12}+He^4. \end{aligned} \quad (2)$$

Predicting Neutrinos from Stars

The Possible Role of Neutrinos in Stellar Evolution

It can be considered at present as definitely established that the energy production in stars is caused by various types of thermonuclear reactions taking place in their interior. Since these reaction chains usually contain the processes of β-disintegration accompanied by the emission of high speed neutrinos, and since the neutrinos can pass almost without difficulty through the body of the star, we must assume that a certain part of the total energy produced escapes into interstellar space without being noticed as the actual thermal radiation of the star. Thus, for example, in the case of the carbon-nitrogen cycle in the sun, about 7 percent of the energy produced is lost in the form of neutrino radiation. However, since, in such reaction chains, the energy taken away by neutrinos represents a definite fraction of the total energy liberation, these losses are of but secondary importance for the problem of stellar equilibrium and evolution.

More detailed calculations on this collapse process are now in progress.

G. Gamow

The George Washington University,
Washington, D. C.,

M. Schoenberg*

University of São Paulo,
São Paulo, Brazil,
November 23, 1940.

* Fellow of the Guggenheim Memorial Foundation. Now in Washington, D. C.

Phys. Rev. 58:1117 (1940)

Neutrinos from the Sun

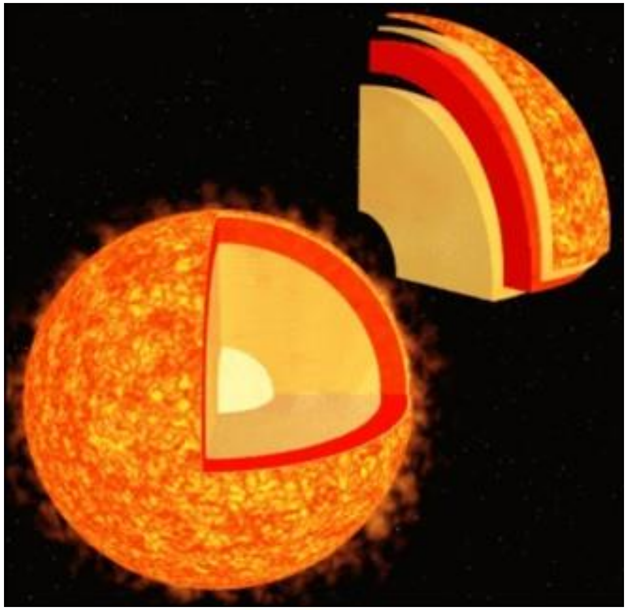

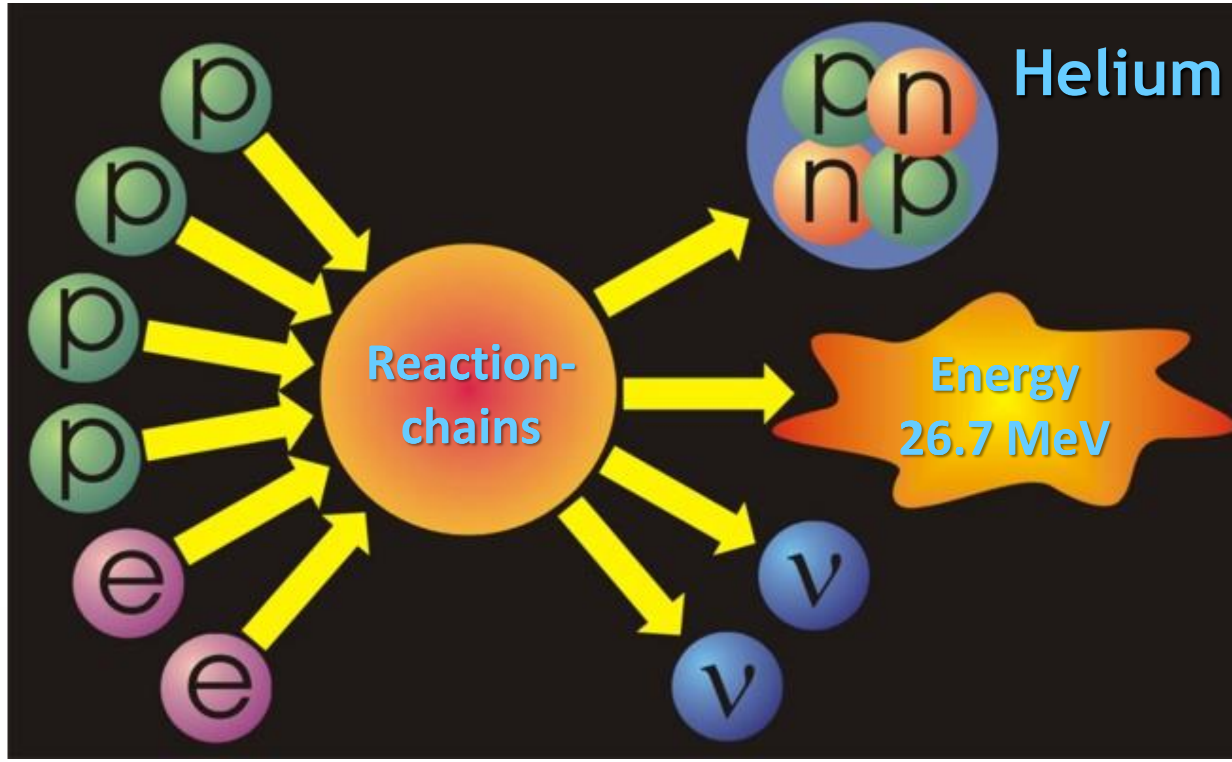

Solar radiation: 98 % light (photons)

2 % neutrinos

At Earth 66 billion neutrinos/cm^2 sec

Hans Bethe (1906–2005, Nobel prize 1967)
Thermonuclear reaction chains (1938)

Hydrogen Burning

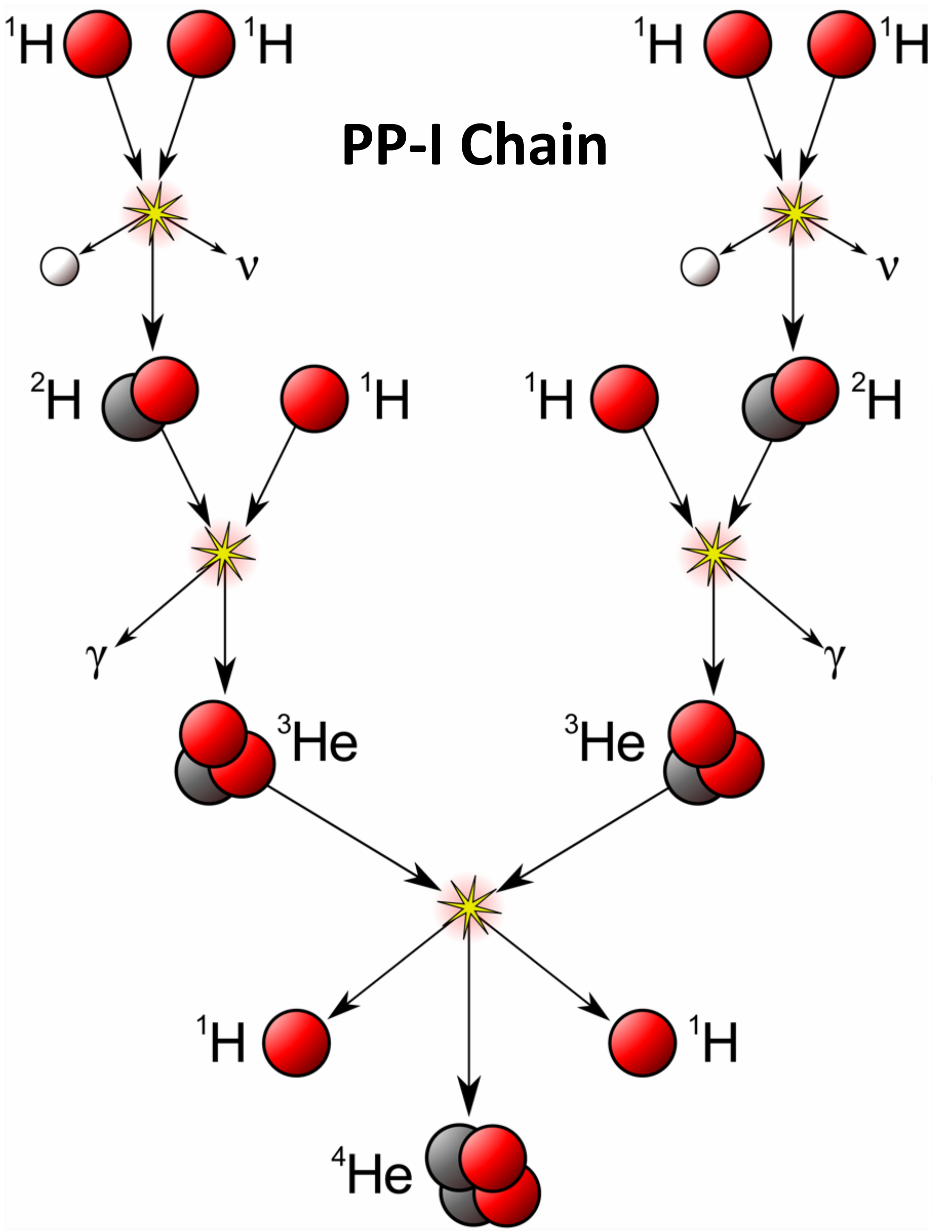

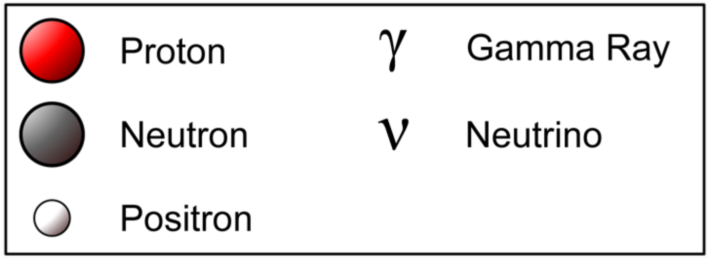

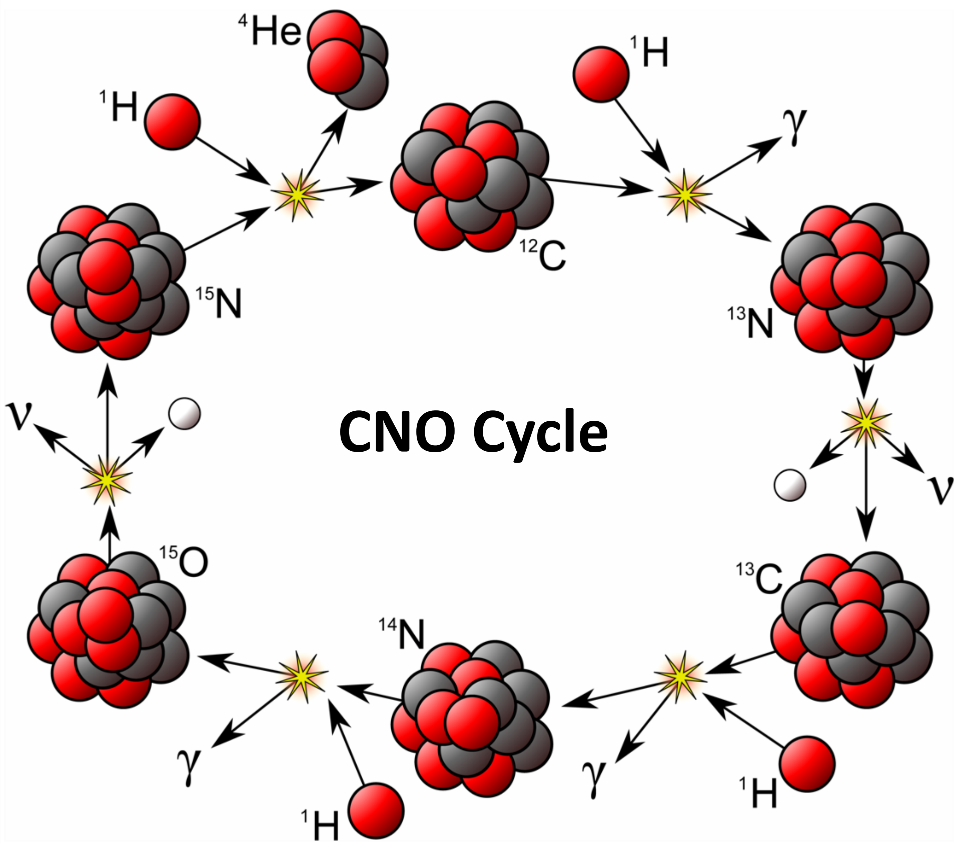

Solar Neutrinos from Nuclear Reactions

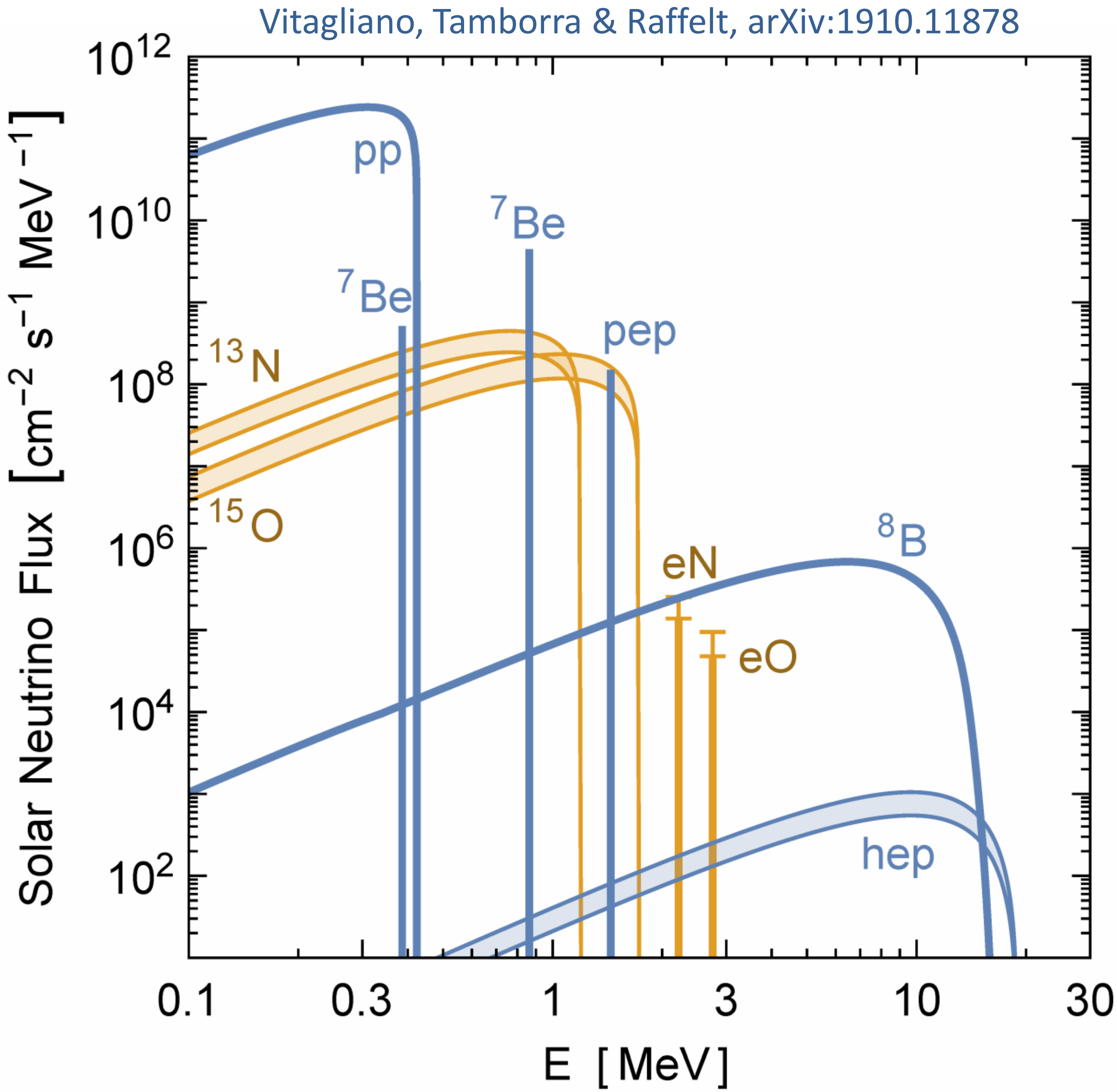

All components of pp chains (blue) have been measured

Very recently direct experimental evidence for CNO fluxes (orange) in Borexino
arXiv:2006.15115 (06/2020)

Solar Neutrino Spectroscopy with Borexino

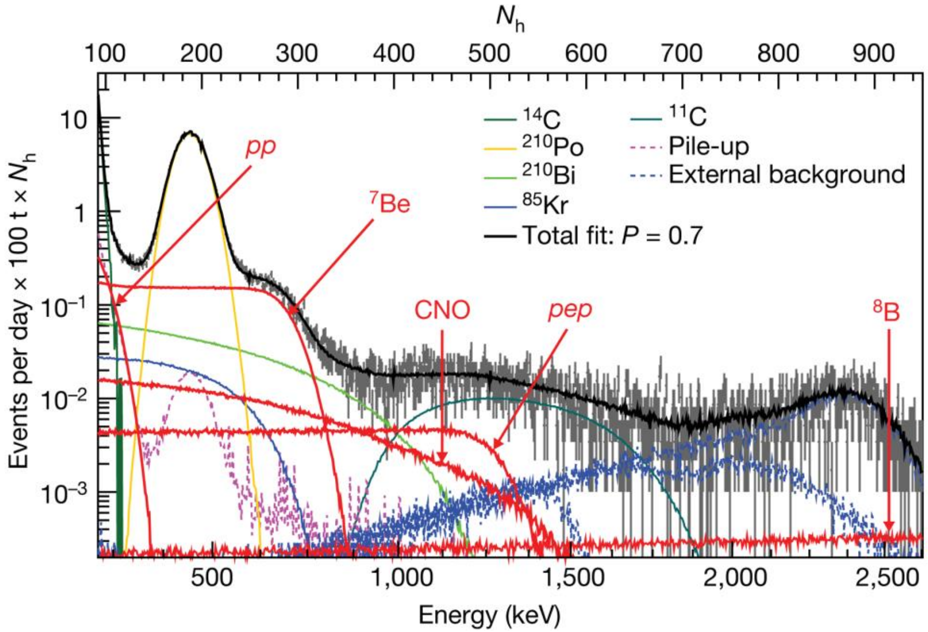

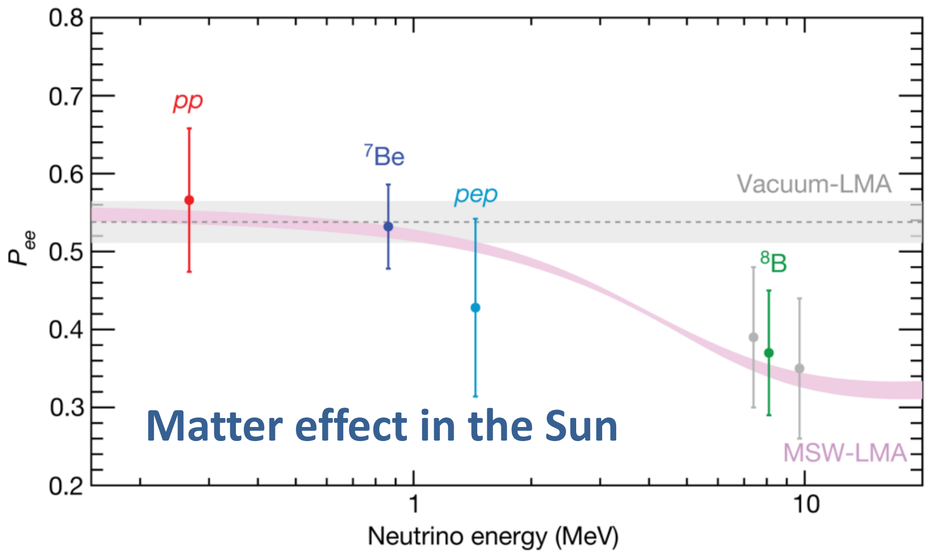

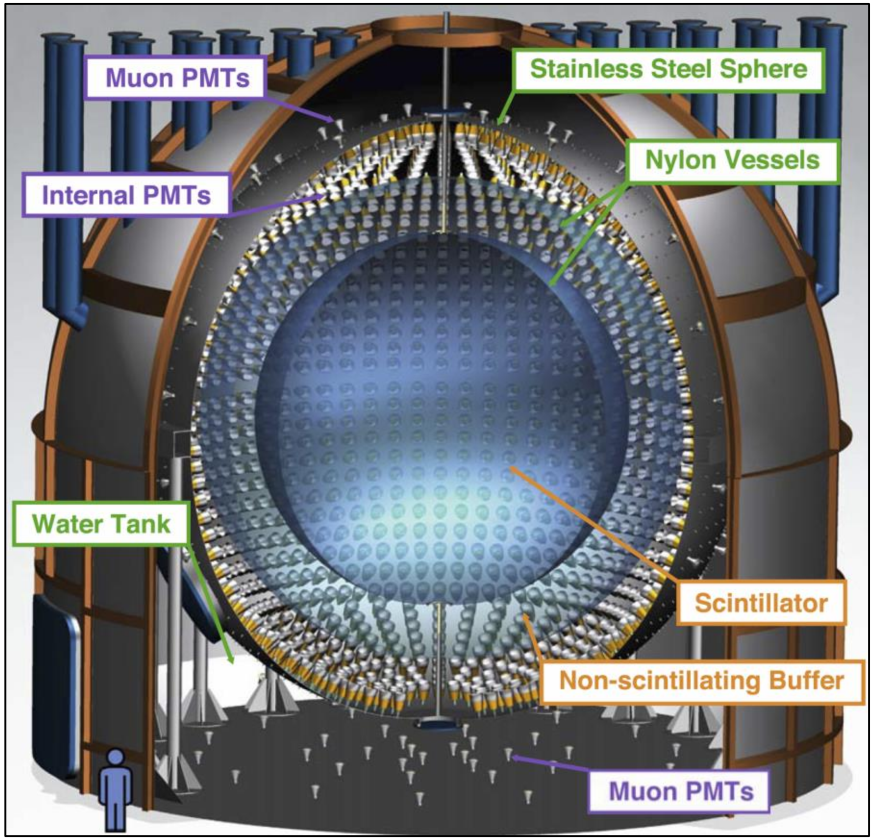

Borexino Collaboration:
Comprehensive measurement of pp-chain solar neutrinos
Nature 562 (2018) 505

Thermal Neutrinos: Production Processes

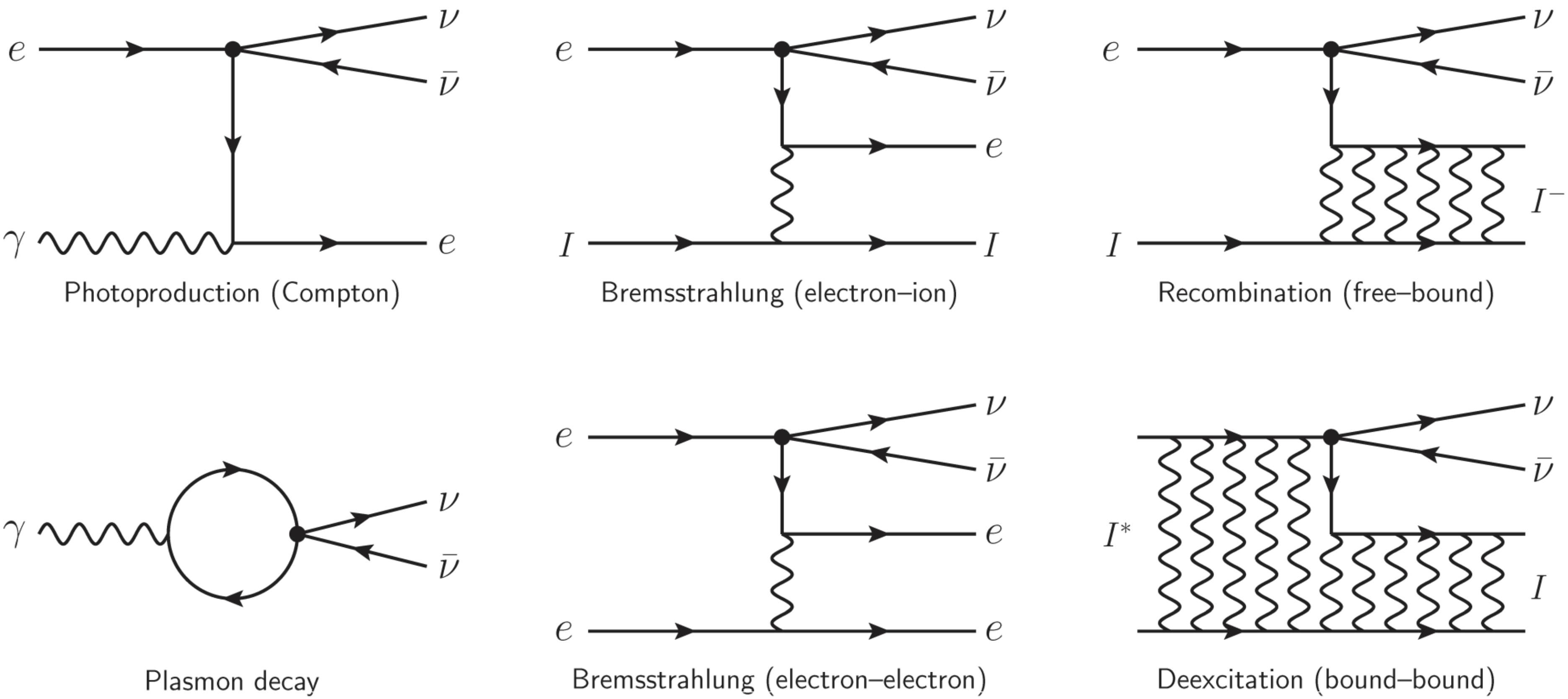

Figure 1. Processes for thermal neutrino pair production in the Sun.

Vitagliano, Redondo & Raffelt, arXiv:1708.02248

Solar neutrino flux at keV energies

- Thermally produced neutrinos and antineutrinos dominate at keV energies
- Future detection opportunities?

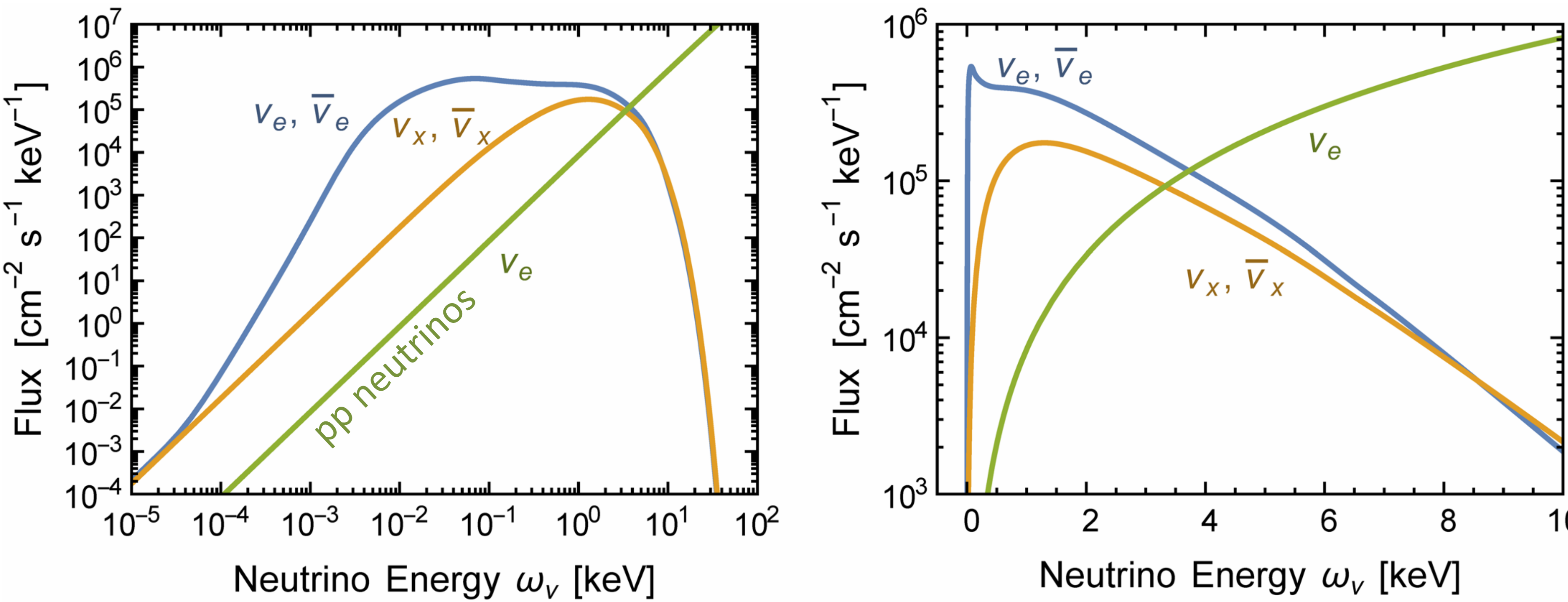

Vitagliano, Raffelt & Redondo, *JCAP 1712 (2017) 010* [arXiv:1708.02248]

Grand Unified Neutrino Spectrum (GUNS) at Earth

Vitagliano, Tamborra & Raffelt, arXiv:1910.11878

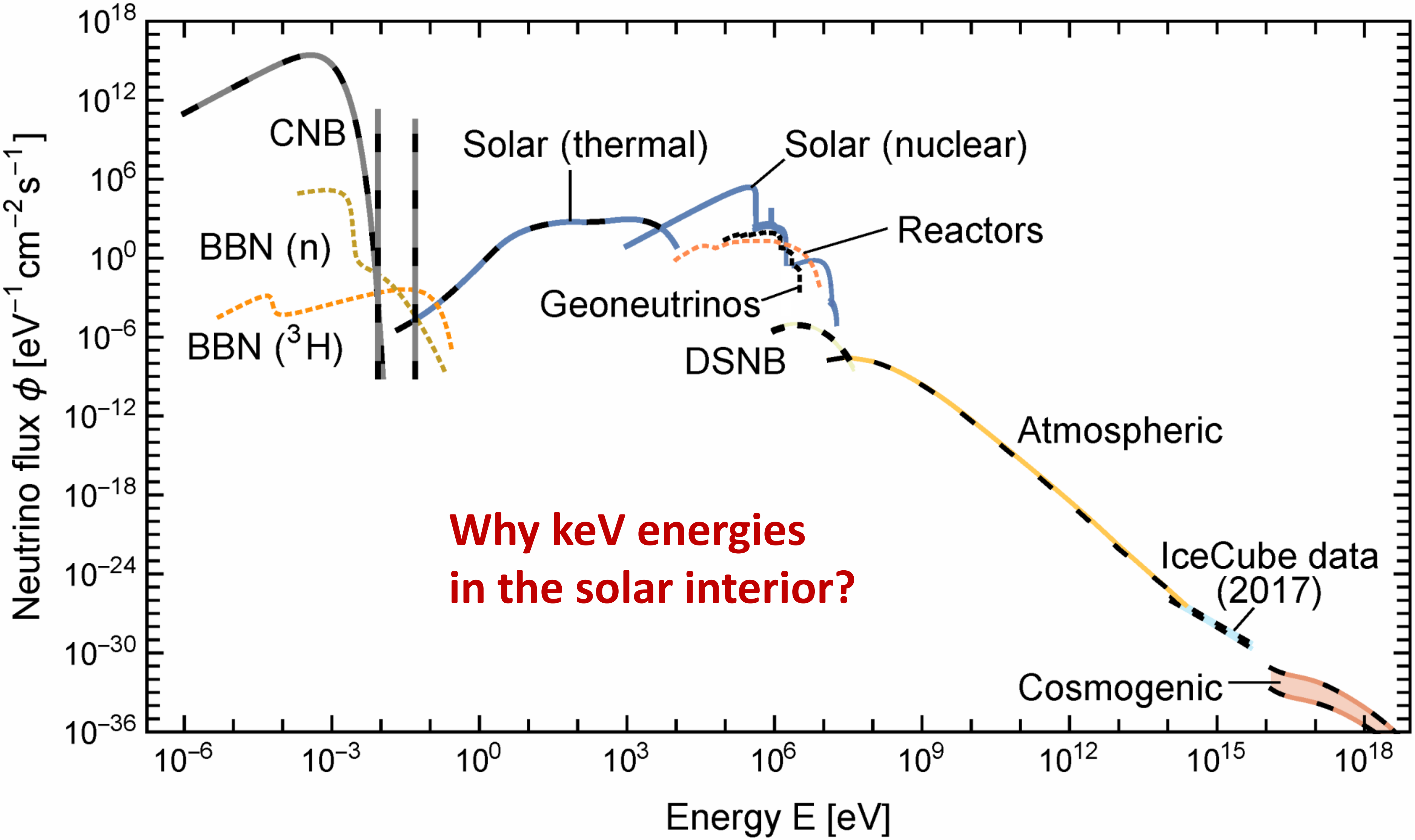

Why keV energies in the solar interior?

Virial Theorem – Dark Matter in Galaxy Clusters

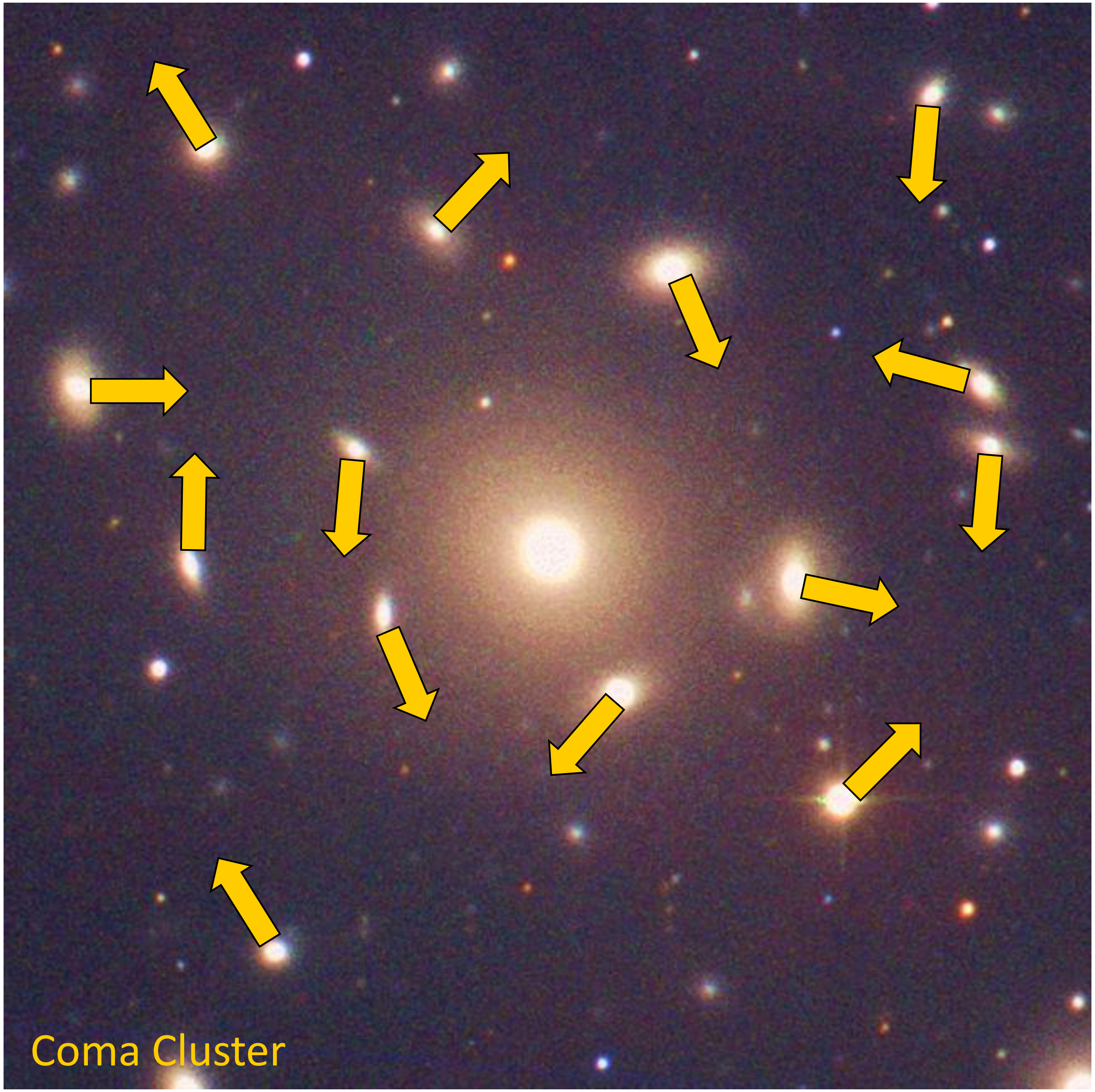

A gravitationally bound system of many particles obeys the virial theorem

$$2\langle E_{\rm kin}\rangle = -\langle E_{\rm grav}\rangle$$

$$2\left\langle\frac{mv^2}{2}\right\rangle = \left\langle\frac{G_N M_r m}{r}\right\rangle$$

$$\langle v^2\rangle \approx G_N M_r \langle r^{-1}\rangle$$

Velocity dispersion from Doppler shifts and geometric size

↓

Total Mass

Virial Theorem Applied to the Sun

Virial Theorem $\langle E_{\rm kin}\rangle = -\frac{1}{2}\langle E_{\rm grav}\rangle$

Approximate Sun as a homogeneous sphere with

Mass $M_{\rm sun} = 1.99\times 10^{33}\,{\rm g}$

Radius $R_{\rm sun} = 6.96\times 10^{10}\,{\rm cm}$

Gravitational potential energy of a proton near center of the sphere

$$\langle E_{\rm grav}\rangle = -\frac{3}{2}\frac{G_N M_{\rm sun} m_p}{R_{\rm sun}} = -3.2\ {\rm keV}$$

Thermal velocity distribution

$$\langle E_{\rm kin}\rangle = \frac{3}{2}k_{\rm B}T = -\frac{1}{2}\langle E_{\rm grav}\rangle$$

Estimated temperature

$$T = 1.1\ {\rm keV}$$

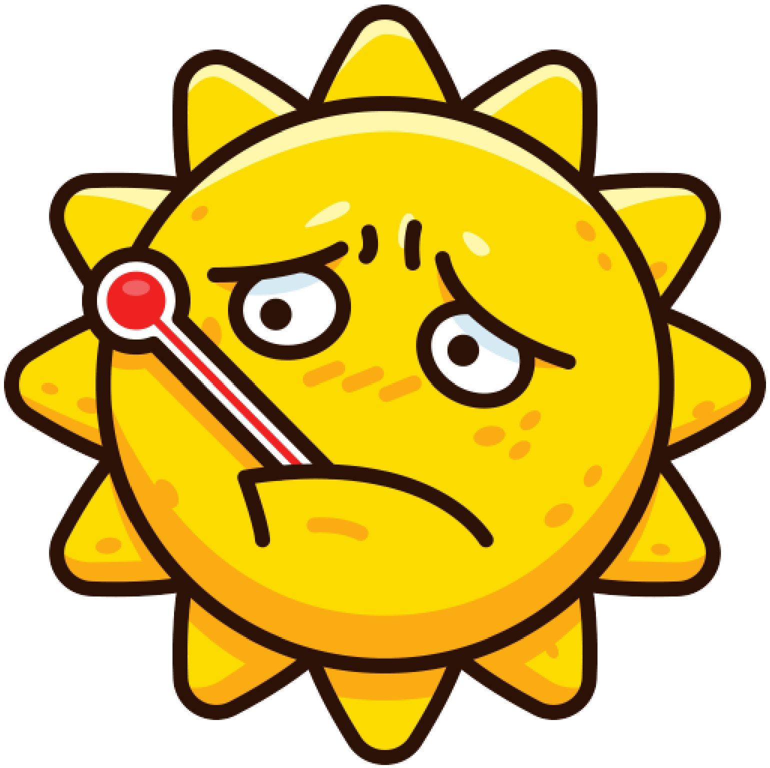

Central temperature from standard solar models

$$T_{\rm c} = 1.56\times 10^{7}\,{\rm K} = 1.34\ {\rm keV}$$

Standard Solar Model: Internal Structure

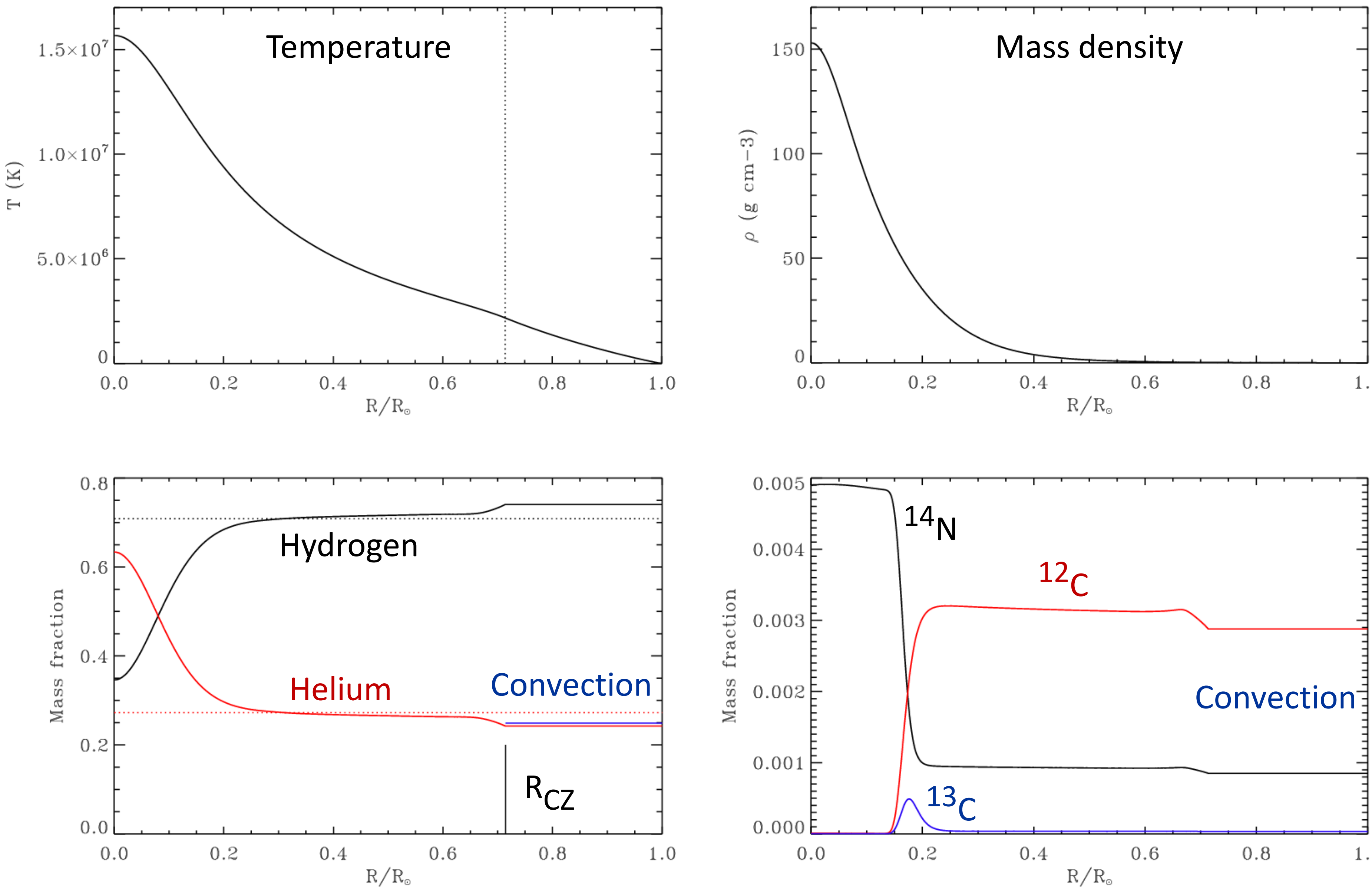

VOLUME 51, NUMBER 16 PHYSICAL REVIEW LETTERS 17 OCTOBER 1983

Experimental Tests of the "Invisible" Axion

P. Sikivie
Physics Department, University of Florida, Gainesville, Florida 32611
(Received 13 July 1983)

Experiments are proposed which address the question of the existence of the "invisible" axion for the whole allowed range of the axion decay constant. These experiments exploit the coupling of the axion to the electromagnetic field, axion emission by the sun, and/or the cosmological abundance and presumed clustering of axions in the halo of our galaxy.

Primakoff effect:

Axion-photon transition in external static E or B field
(Originally discussed for π^0 by Henri Primakoff 1951)

Pierre Sikivie:

Macroscopic B-field can provide a large coherent transition rate over a big volume (low-mass axions)

- Axion helioscope:
  Look at the Sun through a dipole magnet
- Axion haloscope:
  Look for dark-matter axions with
  A microwave resonant cavity

Let's point a magnet at the sun…

…and look for X-Rays!

By CAST student Sebastian Baum

LHC Magnet Mounted as a Telescope to Follow the Sun

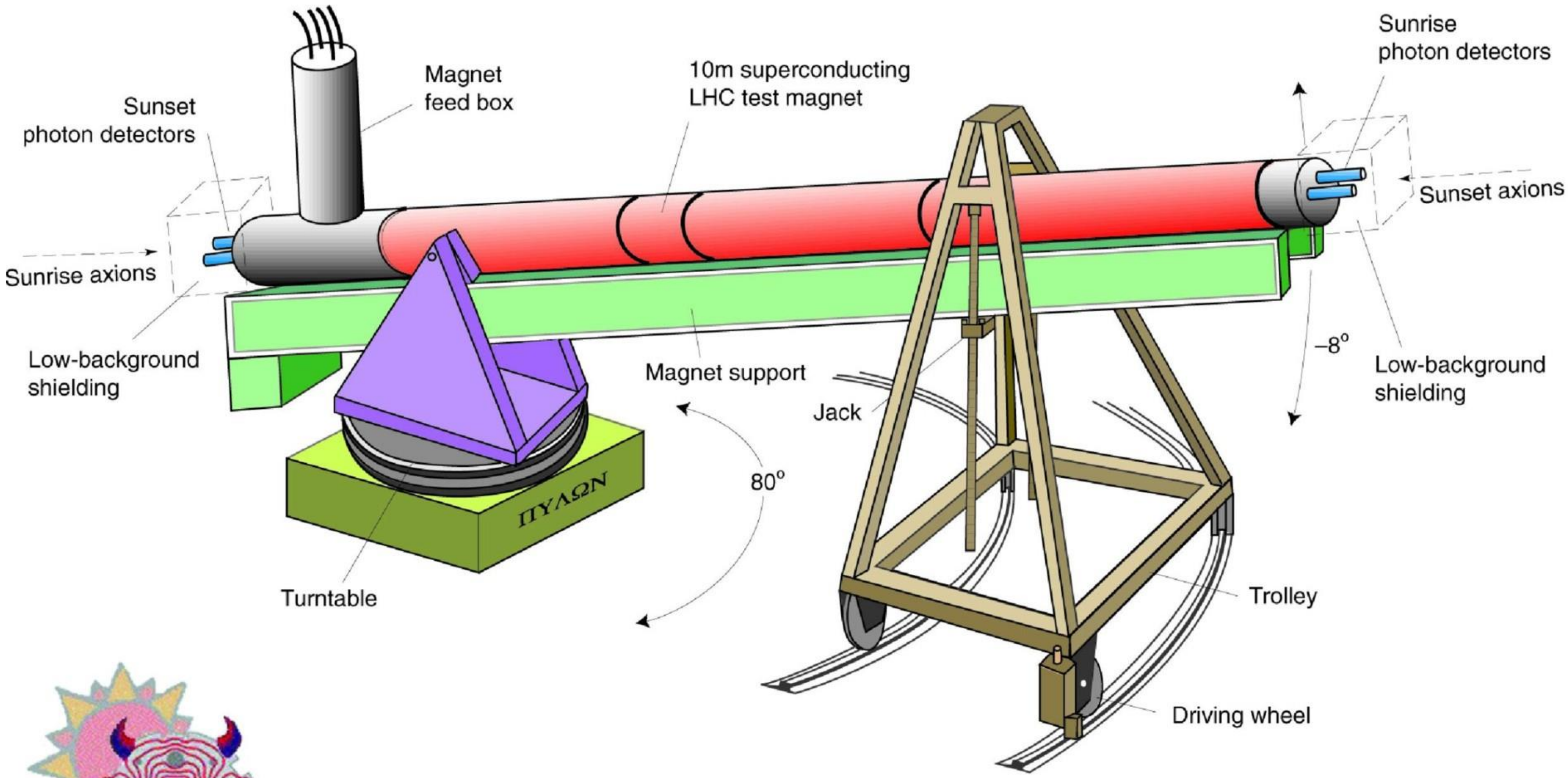

Cern **A**xion **S**olar **T**elescope

→ CAST Movie

Searching for Solar Axions with CAST

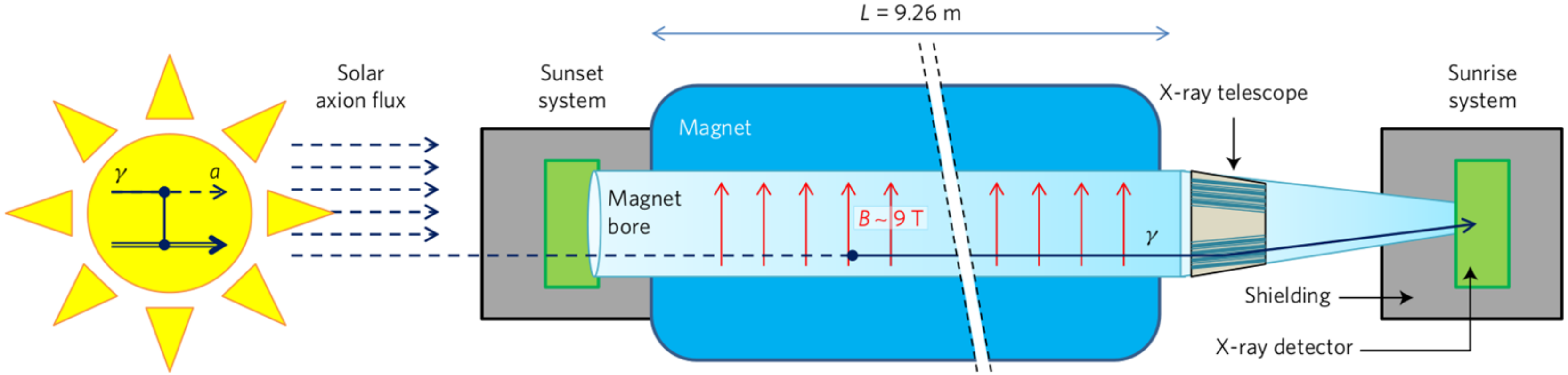

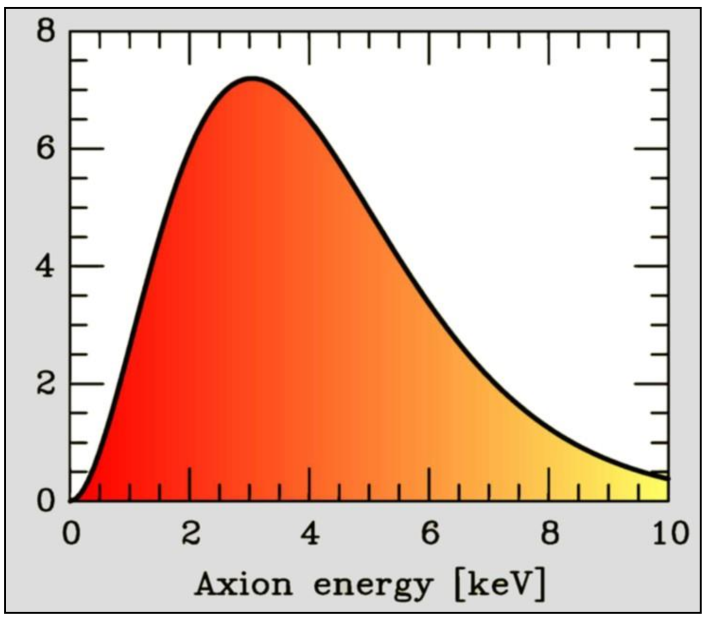

Flux: $g_{10}^2\ 3.7 \times 10^{11}\ \mathrm{cm}^{-2}\mathrm{s}^{-1}$

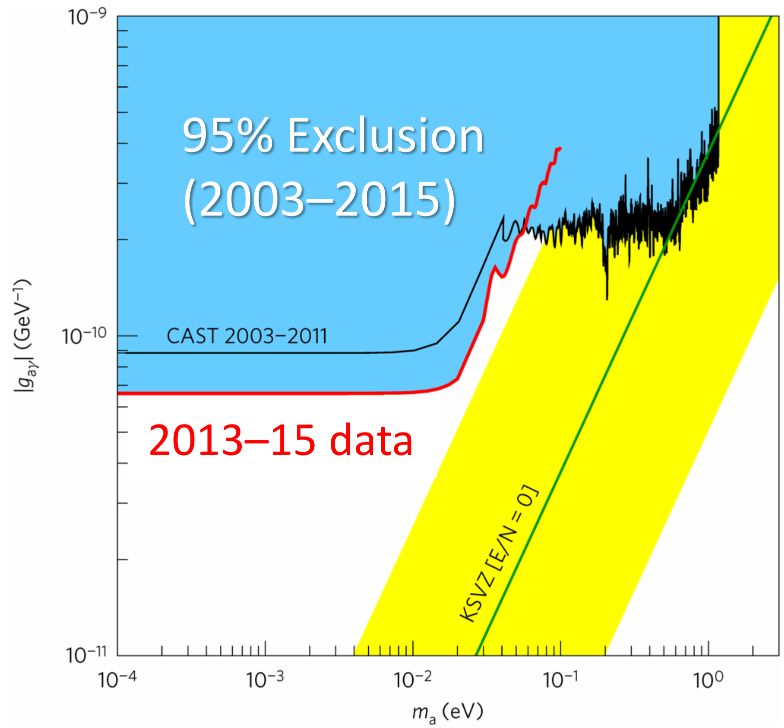

New CAST limit on the axion-photon interaction, Nature Physics 13 (2017) 584 [1705.02290]

Next Generation Axion Helioscope (IAXO)

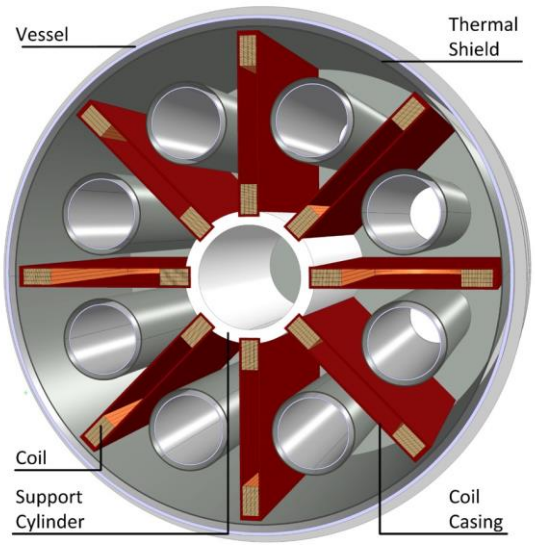

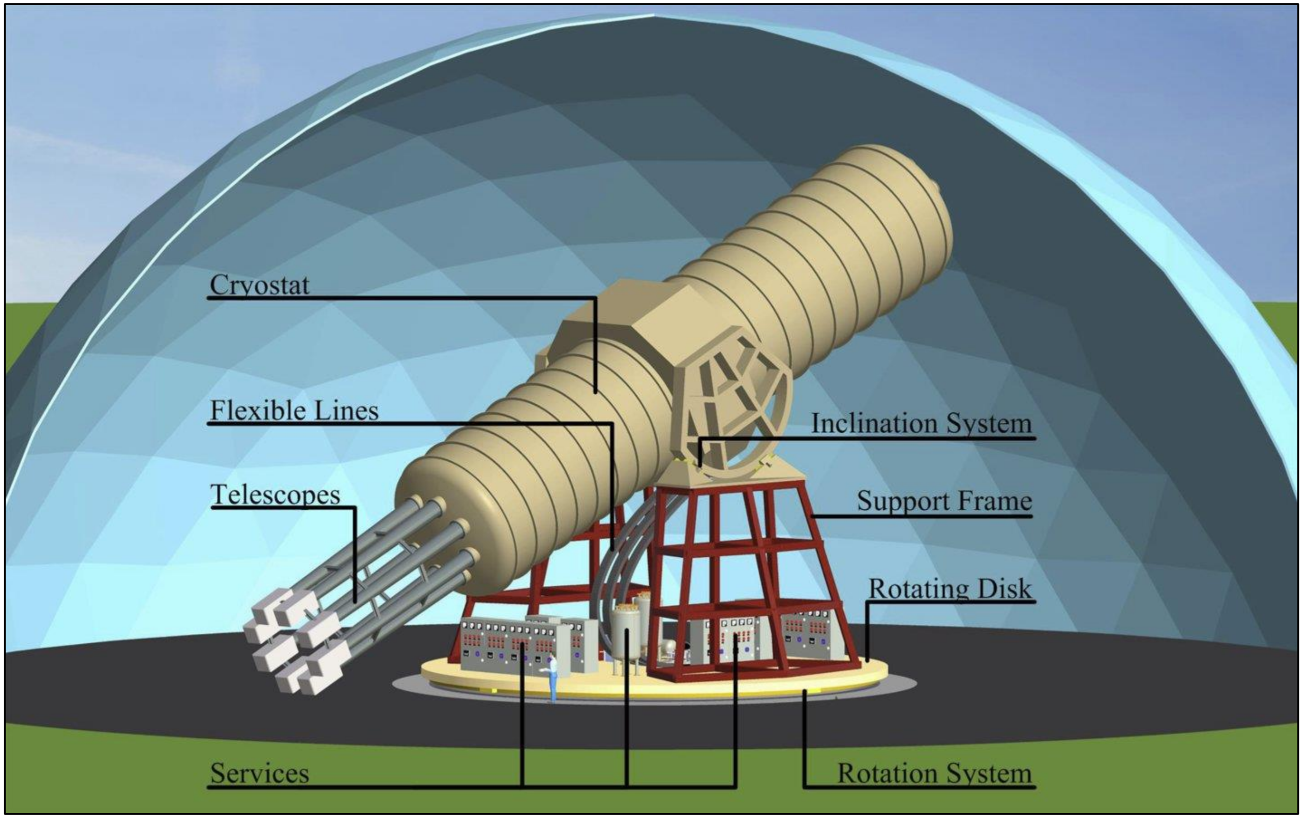

Need new magnet w/
– Much bigger aperture: $\sim$1 m^2 per bore
– Lighter (no iron yoke)
– Bores at T_{room}

- Irastorza et al.: Towards a new generation axion helioscope, arXiv:1103.5334
- Armengaud et al.: Conceptual Design of the International Axion Observatory (IAXO), arXiv:1401.3233

IAXO Sensitivty Forecast

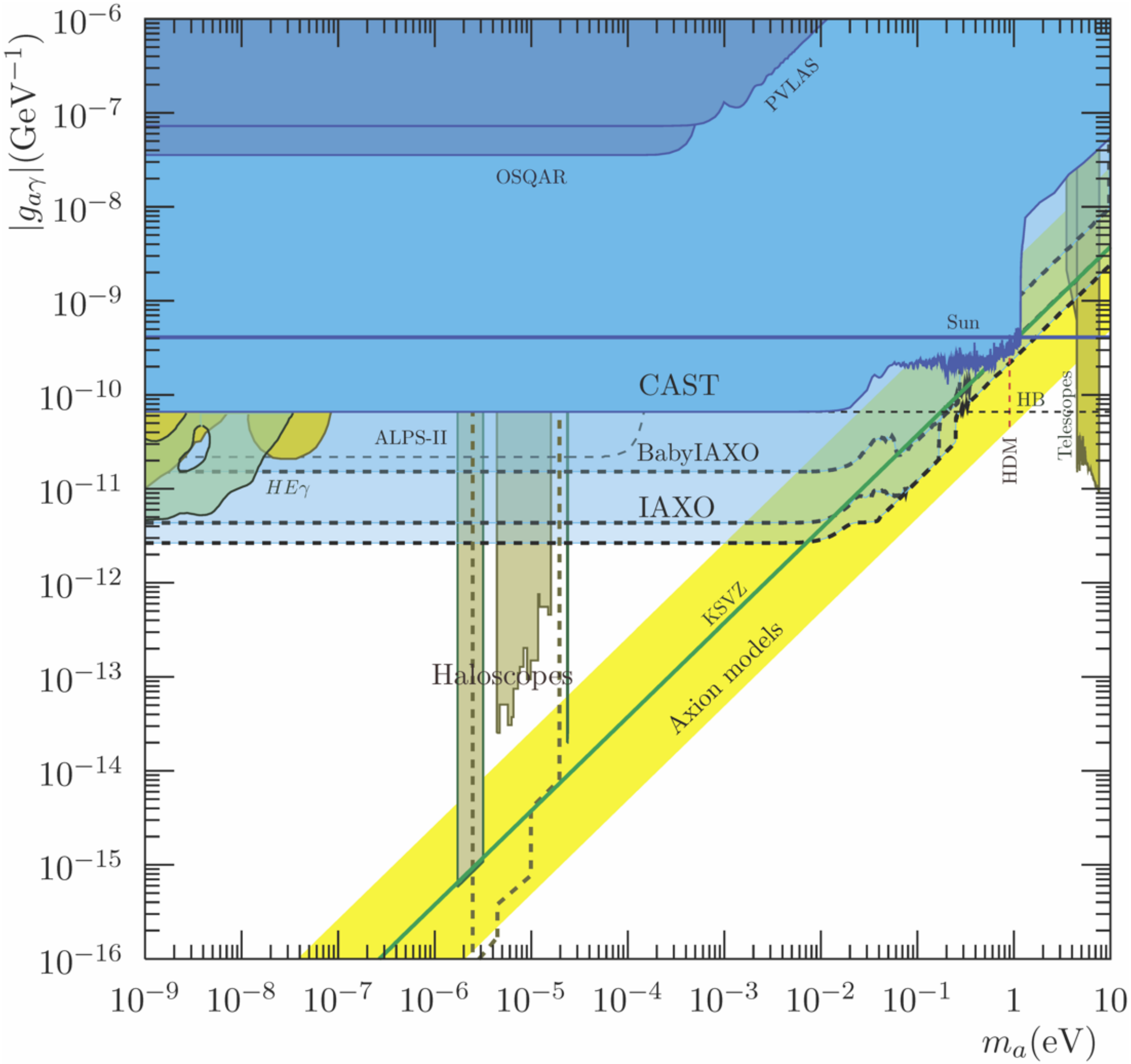

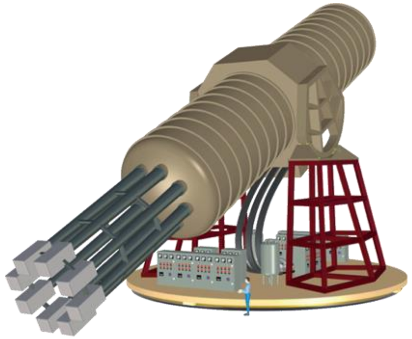

Physics potential of the International Axion Observatory (IAXO)
JCAP 1906 (2019) 047, arXiv:1904.09155

Observation of Excess Electronic Recoil Events in XENON1T

arXiv:2006.09721 (17 June 2020)
~ 150 citations

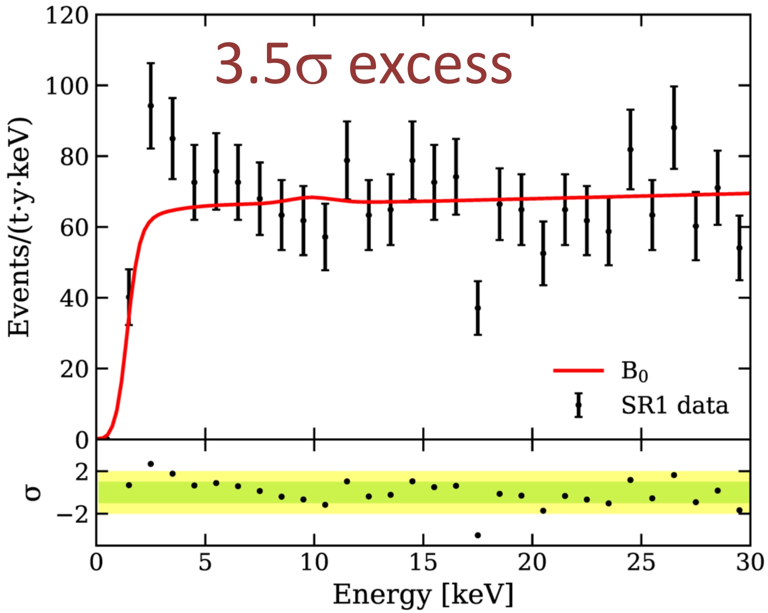

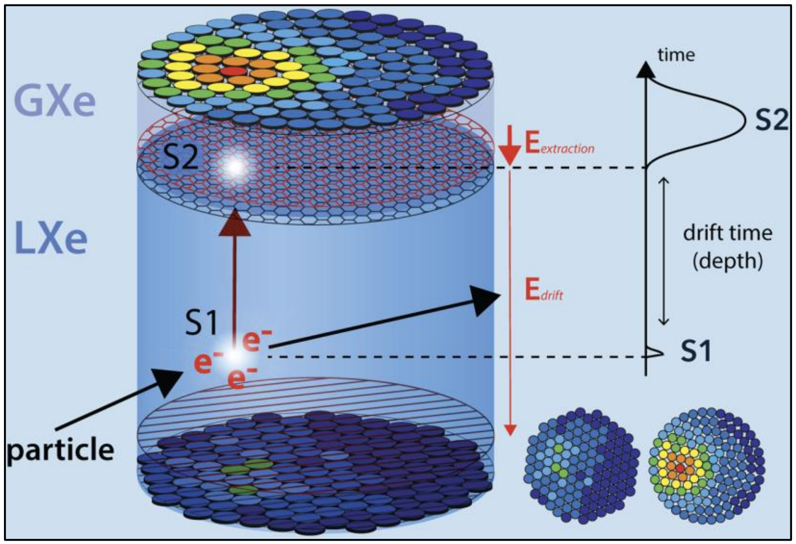

Caused by solar axions or other particles from the Sun?

Some Quick Blog Links

17 June Resonannes, Particle Physics Blog: **Hail the XENON excess**
http://resonaances.blogspot.com/

The Reference Frame https://motls.blogspot.com/2020/06/xenon1t-our-excess-is-due-to-tritium.html
XENON1T: our excess is due to tritium junk, axions, or magnetic neutrinos

18 June CosmoQuest: **Observation of Excess Events in the XENON1T Dark Matter Experiment**
https://cosmoquest.org/x/2020/06/observation-of-excess-events-in-the-xenon1t-dark-matter-experiment/

19 June physicsworld, Particle and nuclear
XENON1T may have detected something very interesting, or maybe not
https://physicsworld.com/a/xenon1t-may-have-detected-something-very-interesting-or-maybe-not/

22 June Centrales Forschungsnetz Aussergewöhnlicher Himmels-Phänomene
Astronomie: Observation of Excess Events in the XENON1T Dark Matter Experiment
https://www.hjkc.de/_blog/2020/06/22/15595-astronomie-observation-of-excess-events-in-the-xenon1t-dark-matter-experiment/

30 June ParticleBites: The high energy physics reader's digest
The XENON1T Excess : The Newest Craze in Particle Physics
https://www.particlebites.com/?p=7260

AlphaGalileo
Observation of Excess Events in the XENON1T Dark Matter Experiment
https://www.alphagalileo.org/en-gb/Item-Display/ItemId/194613

keV-Range Energy Depositions

Nuclear recoil

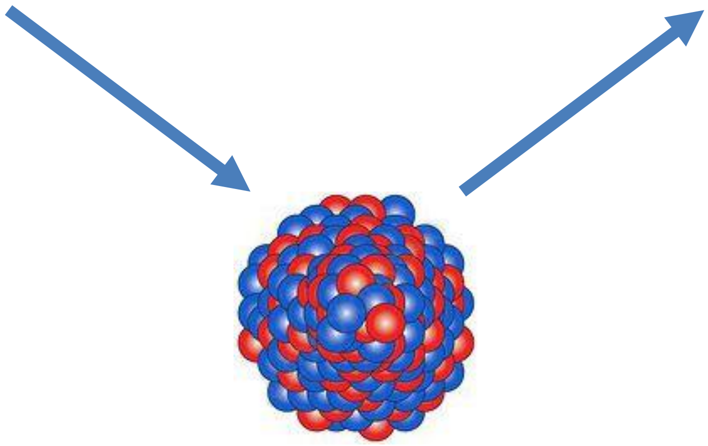

Dark-matter WIMPs

Coherent scattering of
10 MeV solar neutrinos

Electronic recoil (ER)

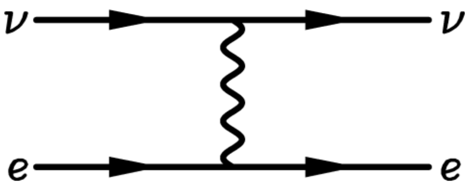

Solar neutrinos with large
dipole moments

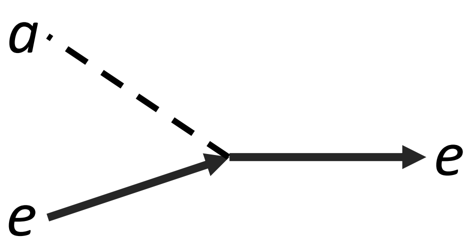

Solar axions (keV energies)

keV-mass bosonic DM particles
(ALP-like, hidden photons, …)

Observation of Excess Electronic Recoil Events in XENON1T

arXiv:2006.09721 (17 June 2020), accepted in PRD

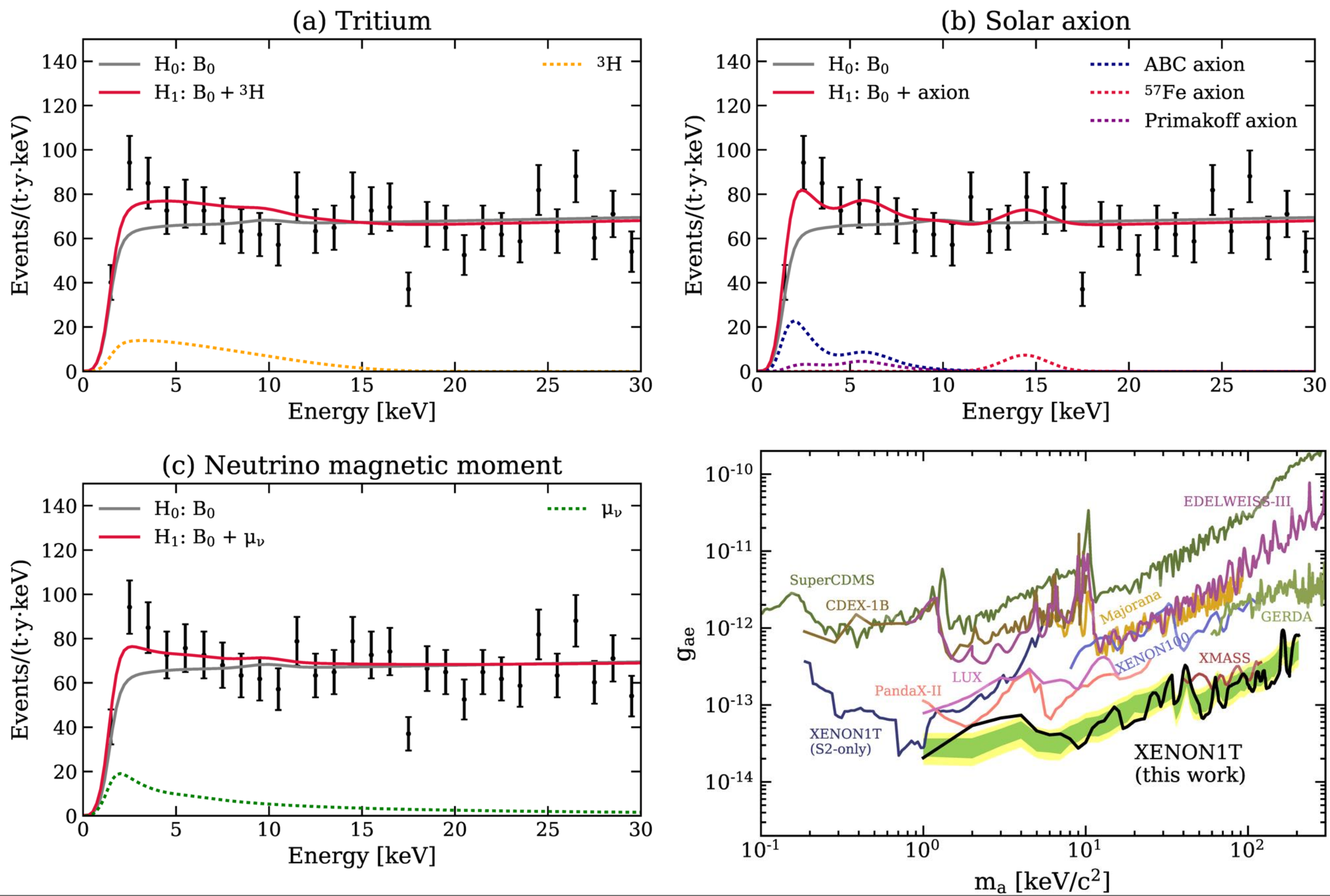

Solar Axions/ALPs

Redondo, arXiv:1310.0823

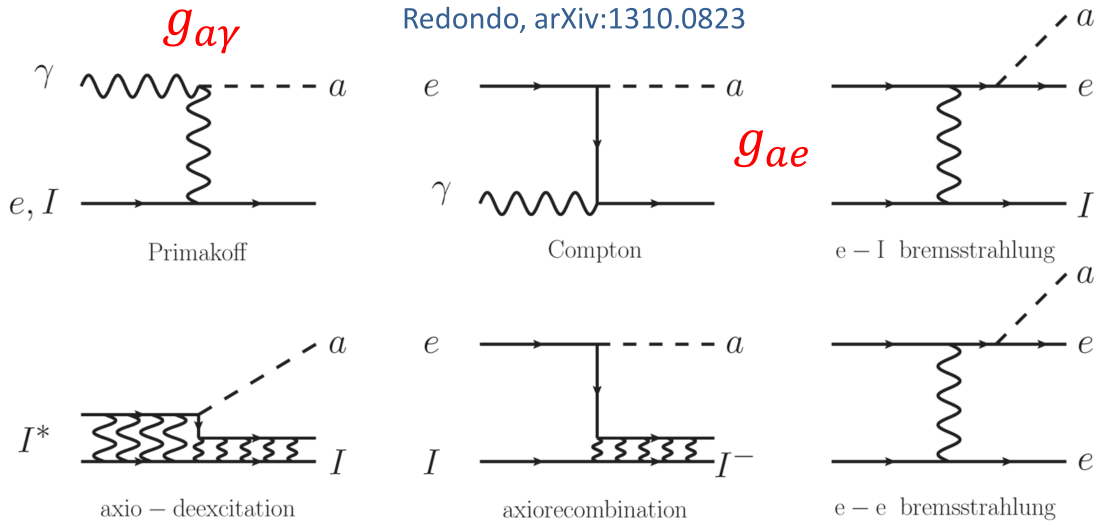

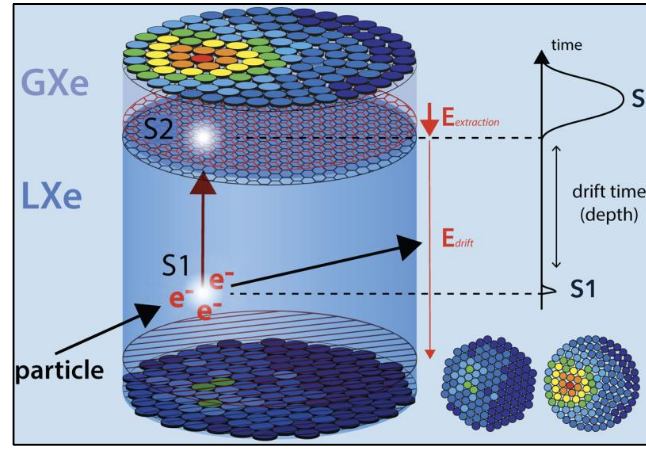

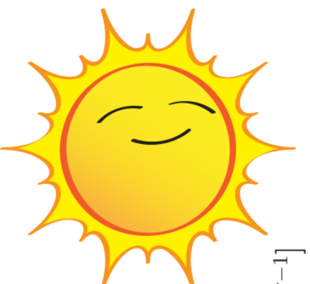

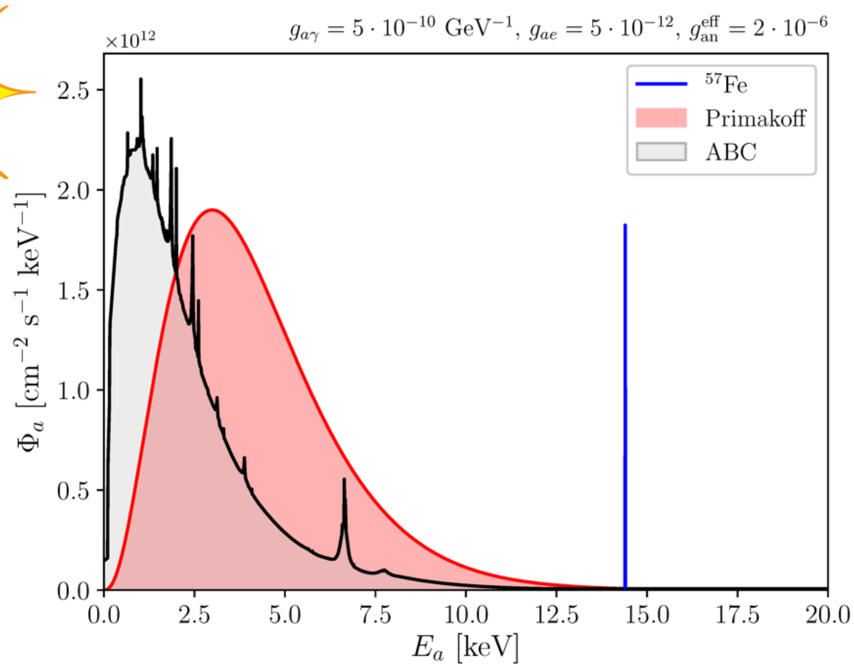

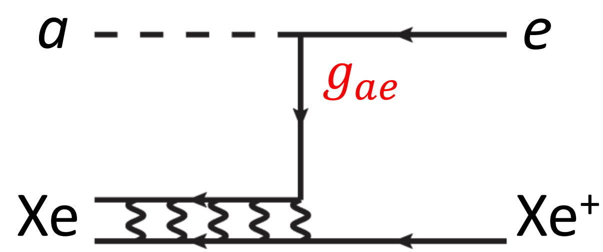

XENON Collab. 2006.09721

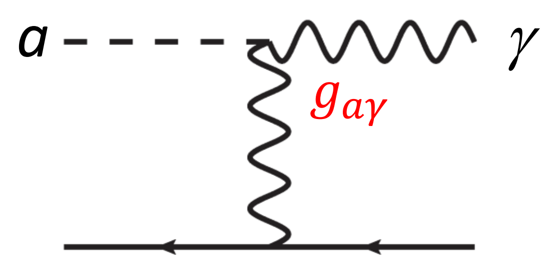

Dent+ 2006.15118, Gao+ 2006.14598

XENON1T Results for Solar Axions/ALPs

Gao+ 2006.14598

Including Primakoff detection

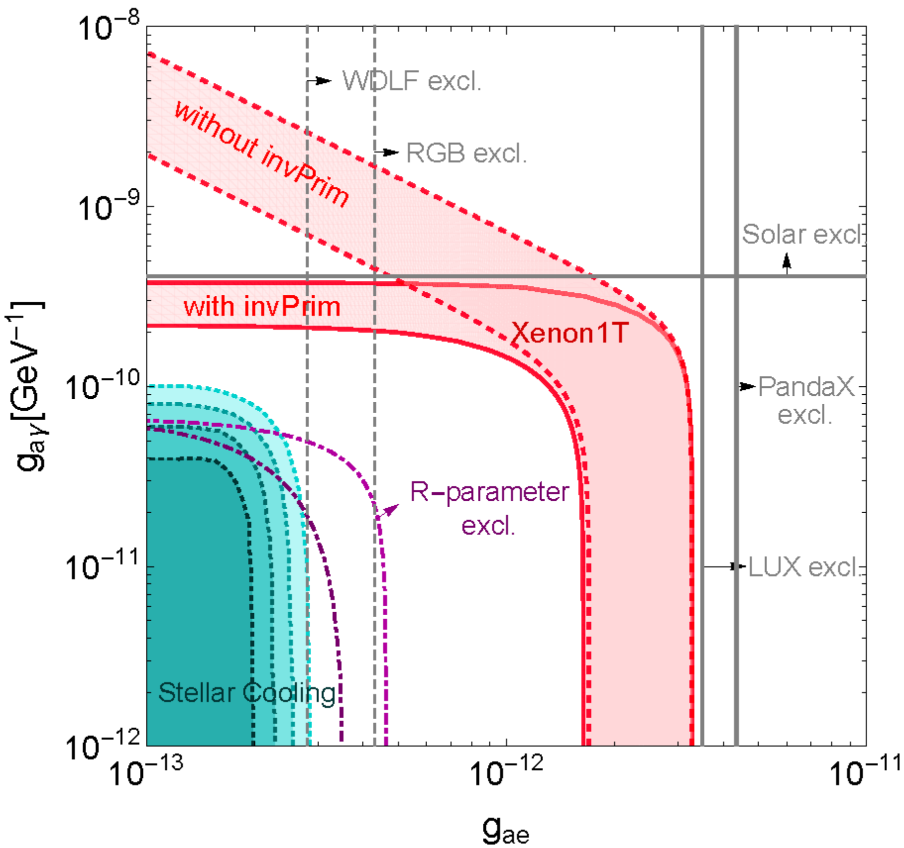

XENON Collab. 2006.09721

Only axio-electric detection

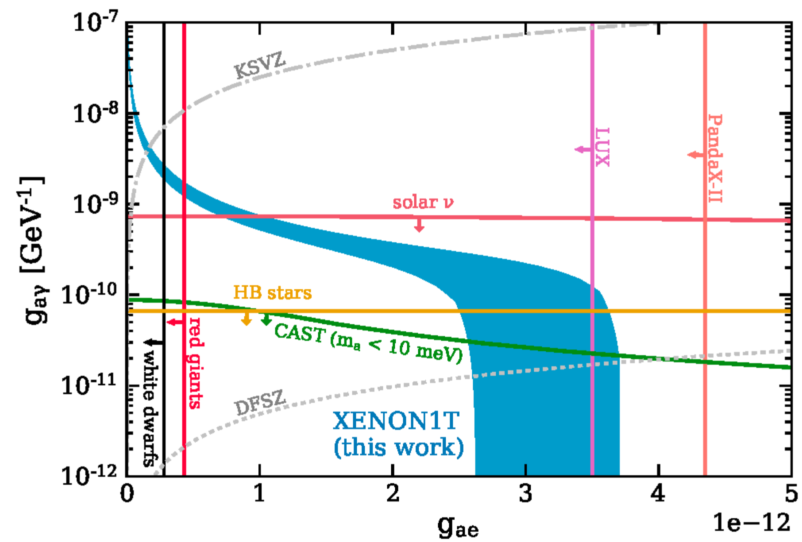

XENON1T excess cannot be due to solar axions/ALPs by a large margin

IAXO Sensitivity Forecast

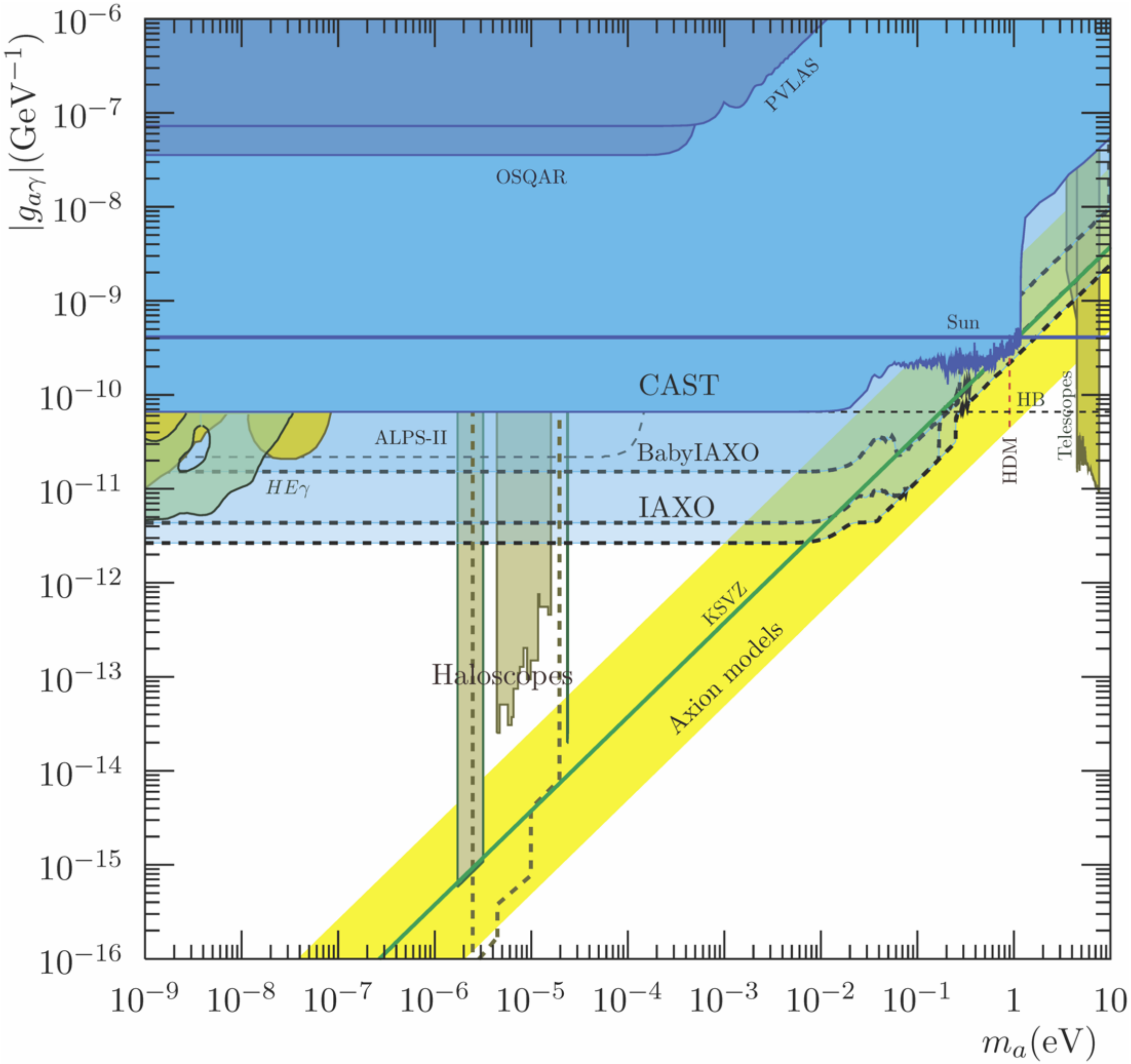

XENON1T Excess

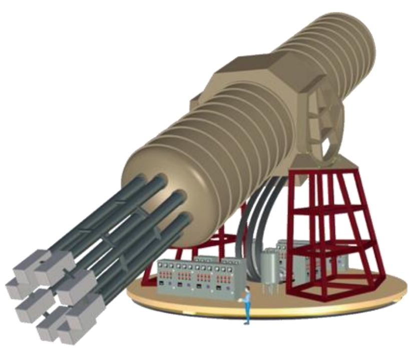

Physics potential of the International Axion Observatory (IAXO)
JCAP 1906 (2019) 047, arXiv:1904.09155

Summary on XENON1T Excess

Electron-recoil excess events in XENON1T (3.5 σ) can be attributed to

- **Statistical fluctuation**
  (“extraordinary claims require extraordinary evidence”)
- **Tritium contamination (~3 atoms per kg xenon)**
  – strong conflict with estimated purification
  – but not proven or disproven
- **Dark matter signal (MANY scenarios, e.g. keV-range hidden photons)**
- **Solar neutrinos with non-standard interactions**

Solar axion or neutrino MDM interpretation in strong conflict with CAST and/or stellar energy-loss limits

Solar hidden photons provide poor spectral fit

Editors' Suggestion

Solar Axions Cannot Explain the XENON1T Excess

Luca Di Luzio,[1,*] Marco Fedele,[2,†] Maurizio Giannotti,[3,‡] Federico Mescia,[2,§] and Enrico Nardi[4,∥]
[1]*Deutsches Elektronen-Synchrotron DESY, Notkestraße 85, D-22607 Hamburg, Germany*
[2]*Department de Física Quàntica i Astrofísica, Institut de Ciències del Cosmos (ICCUB), Universitat de Barcelona, Martí i Franquès 1, E-08028 Barcelona, Spain*
[3]*Physical Sciences, Barry University, 11300 NE 2nd Avenue, Miami Shores, Florida 33161, USA*
[4]*INFN, Laboratori Nazionali di Frascati, C.P. 13, 100044 Frascati, Italy*

(Received 3 July 2020; revised 23 July 2020; accepted 30 July 2020; published 24 September 2020)

We argue that the interpretation in terms of solar axions of the recent XENON1T excess is not tenable when confronted with astrophysical observations of stellar evolution. We discuss the reasons why the emission of a flux of solar axions sufficiently intense to explain the anomalous data would radically alter the distribution of certain type of stars in the color-magnitude diagram in the first place and would also clash with a certain number of other astrophysical observables. Quantitatively, the significance of the discrepancy ranges from 3.3σ for the rate of period change of pulsating white dwarfs and exceeds 19σ for the R parameter and for $M_{I,\mathrm{TRGB}}$.

DOI: 10.1103/PhysRevLett.125.131804

Introduction.—The XENON1T collaboration [1] has reported an excess in low-energy electronic recoil data below 7 keV and peaking around 2–3 keV. The collaboration cautions that the excess could be due to an unaccounted background from β decays due to a trace amount of tritium, but they also explore the possibility that the and because the location of the peak around 2–3 keV corresponds roughly to the maximum of the axion energy spectrum for the ABC processes, the Primakoff and ^{57}Fe components are both allowed to be absent as long as there is a nonzero ABC component. This selects g_{ae} as the crucial coupling to attempt to explain the data in terms of the QCD

Editors' Suggestion

Solar Axions Cannot Explain the XENON1T Excess

Luca Di Luzio,[1,*] Marco Fedele,[2,†] Maurizio Giannotti,[3,‡] Federico Mescia ...

[1]*Deutsches Elektronen-Synchrotron DESY, Notkestraße 85, D-2...*

[2]*Department de Física Quàntica i Astrofísica, Institut de Cièn...*

Martí i Franquè...

[3]*Physical Sciences, Barry Uni...*

What are these astrophysical limits?

Where do they come from?

...ould also ... the significance of the ... white dwarfs and exceeds 19σ for

Introduction.—The XENON1T collaboration [1] has reported an excess in low-energy electronic recoil data below 7 keV and peaking around 2–3 keV. The collaboration cautions that the excess could be due to an unaccounted background from β decays due to a trace amount of tritium, but they also explore the possibility that the and because the location of the peak around 2–3 keV corresponds roughly to the maximum of the axion energy spectrum for the ABC processes, the Primakoff and ^{57}Fe components are both allowed to be absent as long as there is a nonzero ABC component. This selects g_{ae} as the crucial coupling to attempt to explain the data in terms of the QCD

Equations of Stellar Structure

Assume spherical symmetry and static structure (neglect kinetic energy)
Excludes: Rotation, convection, magnetic fields, supernova-dynamics, …

Hydrostatic equilibrium

$$\frac{dP}{dr} = -\frac{G_N M_r \rho}{r^2}$$

Energy conservation

$$\frac{dL_r}{dr} = 4\pi r^2 \epsilon\rho$$

Energy transfer

$$L_r = \frac{4\pi r^2}{3\kappa\rho}\frac{d(aT^4)}{dr}$$

Literature

- Clayton: Principles of stellar evolution and nucleosynthesis (Univ. Chicago Press 1968)
- Kippenhahn & Weigert: Stellar structure and evolution (Springer 1990)

r	Radius from center
P	Pressure
G_N	Newton's constant
ρ	Mass density
M_r	Integrated mass up to r
L_r	Luminosity (energy flux)
ϵ	Local rate of energy generation $[\mathrm{erg\,g^{-1}s^{-1}}]$ $\epsilon = \epsilon_{\rm nuc} + \epsilon_{\rm grav} - \epsilon_\nu$
κ	Opacity $\kappa^{-1} = \kappa_\gamma^{-1} + \kappa_{\rm c}^{-1}$
κ_γ	Radiative opacity $\kappa_\gamma\rho = \langle\lambda_\gamma\rangle_{\rm Rosseland}^{-1}$
$\kappa_{\rm c}$	Electron conduction

Convection in Main-Sequence Stars

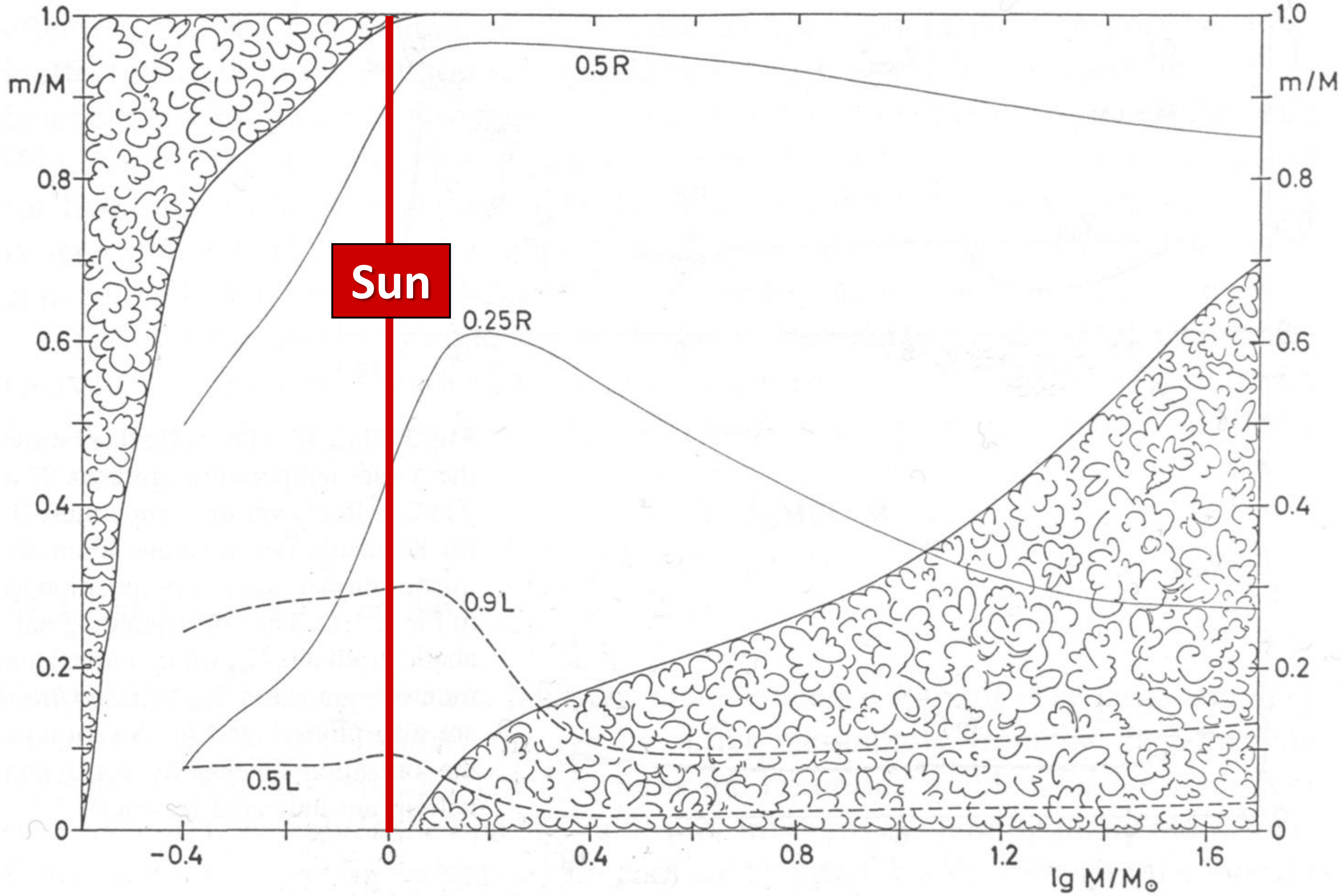

Fig. 22.7. The mass values m from centre to surface are plotted against the stellar mass M for the same zero-age main-sequence models as in Fig. 22.1. "Cloudy" areas indicate the extension of convective zones inside the models. Two solid lines give the m values at which r is 1/4 and 1/2 of the total radius R. The dashed lines show the mass elements inside which 50% and 90% of the total luminosity L are produced

Kippenhahn & Weigert, Stellar Structure and Evolution

Self-Regulated Nuclear Burning

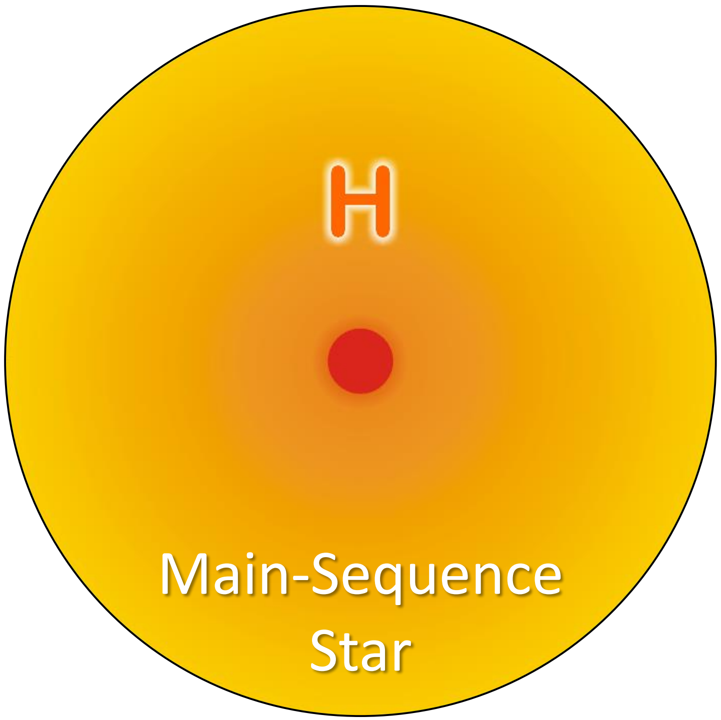

Virial Theorem: $\langle E_{\mathrm{kin}} \rangle = -\frac{1}{2} \langle E_{\mathrm{grav}} \rangle$

Small Contraction
$\to$ Heating
$\to$ Increased nuclear burning
$\to$ Increased pressure
$\to$ Expansion

Additional energy loss (“cooling”)
$\to$ Loss of pressure
$\to$ Contraction
$\to$ Heating
$\to$ Increased nuclear burning

Hydrogen burning at nearly fixed T
$\to$ Gravitational potential nearly fixed:
$G_{\mathrm{N}} M / R \sim \mathrm{constant}$
$\to$ $R \propto M$ (More massive stars bigger)

Nuclear Binding Energy

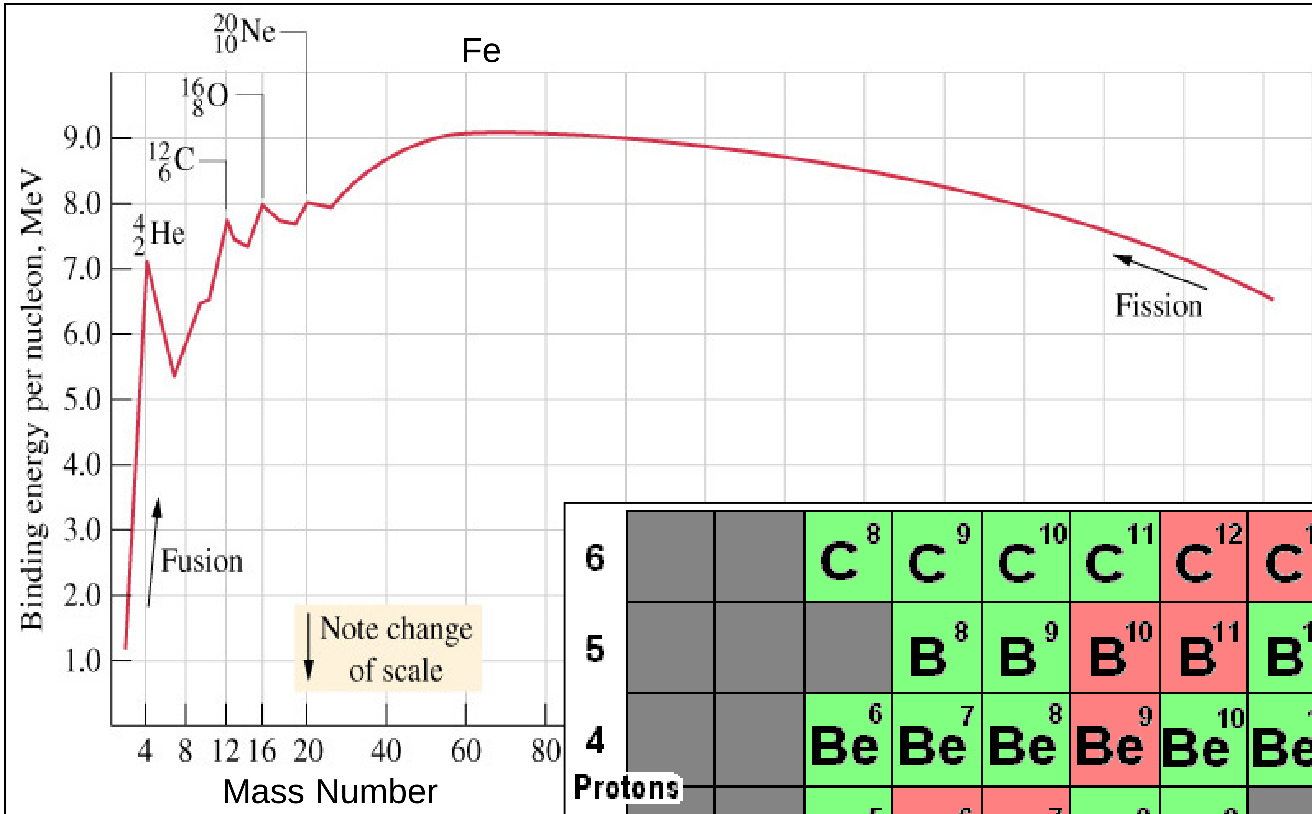

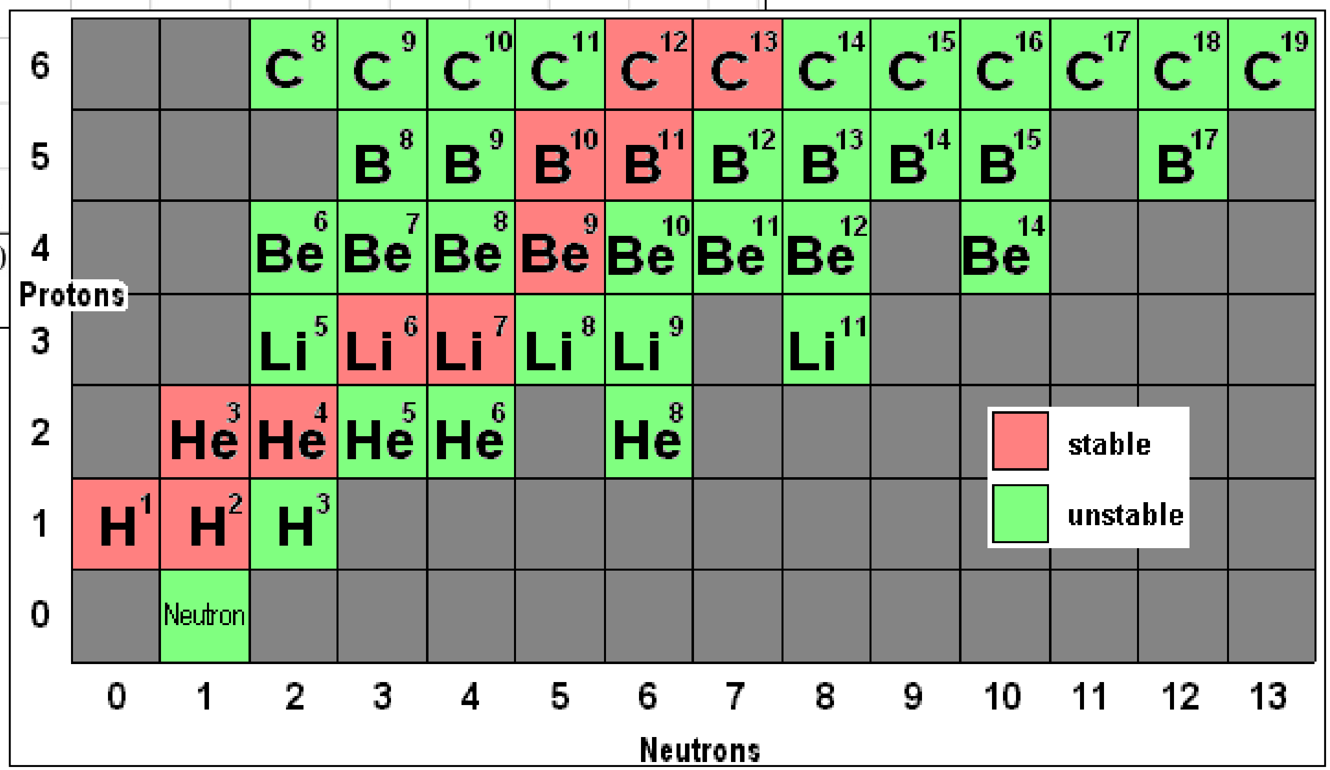

Thermonuclear Reactions and Gamow Peak

Coulomb repulsion prevents nuclear reactions, except for Gamow tunneling

Tunneling probability

$$p \propto E^{-1/2} e^{-2\pi\eta}$$

where the Sommerfeld parameter is

$$\eta = \left(\frac{m}{2E}\right)^{1/2} Z_1 Z_2 e^2$$

Parameterize cross section with astrophysical S-factor

$$S(E) = \sigma(E)\, E\, e^{2\pi\eta(E)}$$

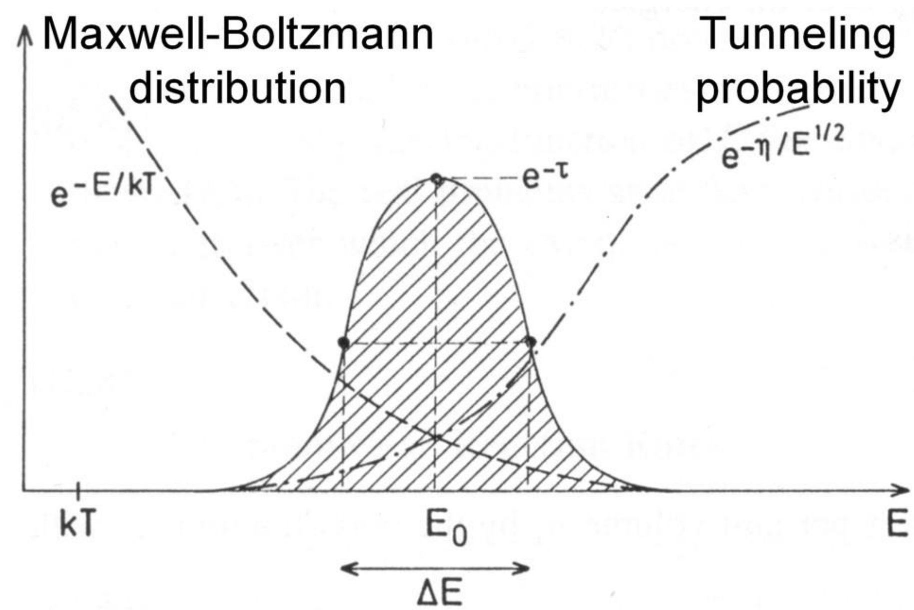

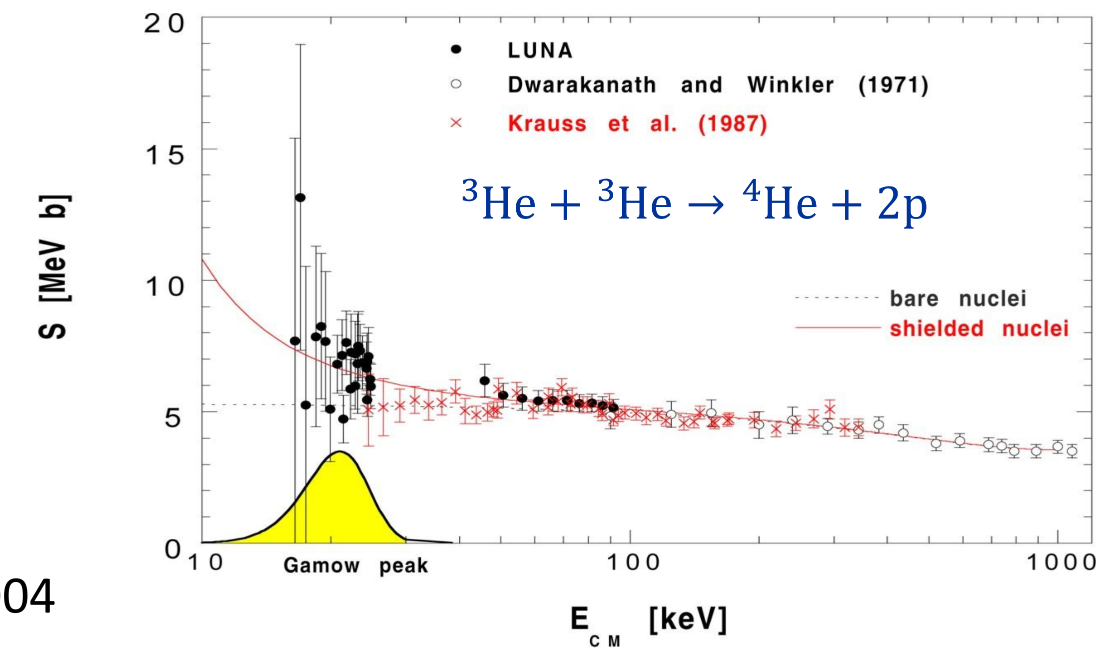

LUNA Collaboration, nucl-ex/9902004

Main Nuclear Burning Stages

Hydrogen burning $4\mathrm{p} + 2\mathrm{e}^- \rightarrow {}^4\mathrm{He} + 2\nu_e$

- Proceeds by pp chains and CNO cycle
- No higher elements are formed because no stable isotope with mass number 8
- Neutrinos from $\mathrm{p} \rightarrow \mathrm{n}$ conversion
- Typical temperatures: 10^7 K (~1 keV)

Helium burning

$${}^4\mathrm{He} + {}^4\mathrm{He} + {}^4\mathrm{He} \leftrightarrow {}^8\mathrm{Be} + {}^4\mathrm{He} \rightarrow {}^{12}\mathrm{C}$$

"Triple alpha reaction" because ${}^8\mathrm{Be}$ unstable, builds up with concentration $\sim 10^{-9}$

$${}^{12}\mathrm{C} + {}^4\mathrm{He} \rightarrow {}^{16}\mathrm{O}$$

$${}^{16}\mathrm{O} + {}^4\mathrm{He} \rightarrow {}^{20}\mathrm{Ne}$$

Typical temperatures: 10^8 K (~10 keV)

Carbon burning

Many reactions, for example

$${}^{12}\mathrm{C} + {}^{12}\mathrm{C} \rightarrow {}^{23}\mathrm{Na} + \mathrm{p} \text{ or } {}^{20}\mathrm{Ne} + {}^4\mathrm{He} \text{ etc}$$

Typical temperatures: 10^9 K (~100 keV)

- Each type of burning occurs at a very different T but a broad range of densities
- Never co-exist in the same location

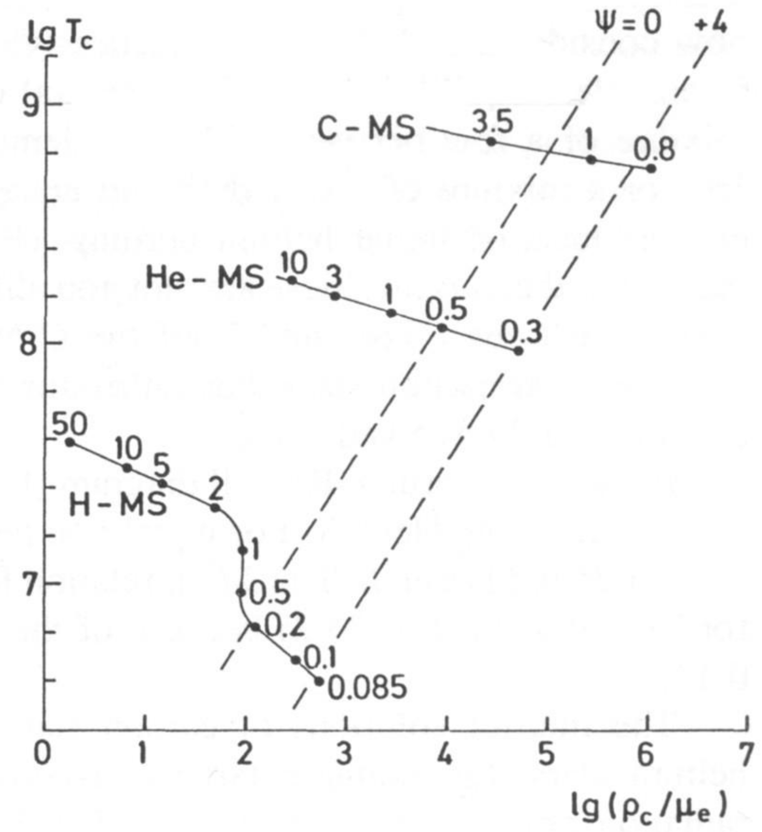

Hydrogen Exhaustion

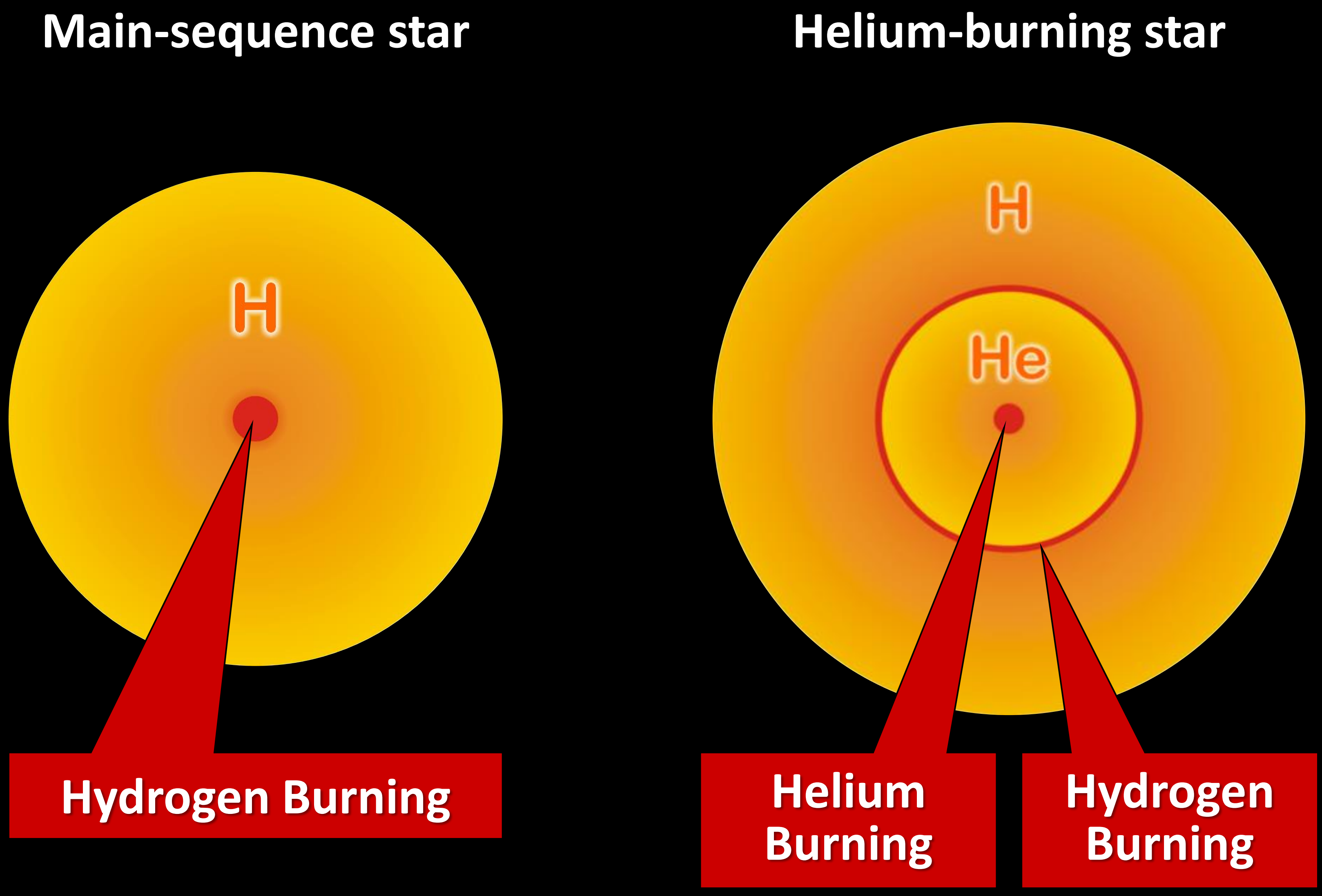

Burning Phases of a 15 Solar-Mass Star

Burning Phase		Dominant Process	T_c [keV]	ρ_c [g/cm^3]	L_γ [10^4 L_{sun}]	L_ν/L_γ	Duration [years]
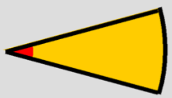	Hydrogen	H $\rightarrow$ He	3	5.9	2.1	–	1.2×10^7
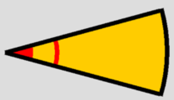	Helium	He $\rightarrow$ C, O	14	1.3×10^3	6.0	1.7×10^{-5}	1.3×10^6
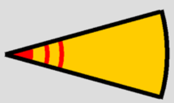	Carbon	C $\rightarrow$ Ne, Mg	53	1.7×10^5	8.6	1.0	6.3×10^3
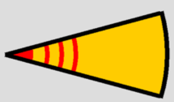	Neon	Ne $\rightarrow$ O, Mg	110	1.6×10^7	9.6	1.8×10^3	7.0
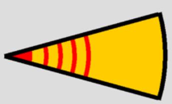	Oxygen	O $\rightarrow$ Si	160	9.7×10^7	9.6	2.1×10^4	1.7
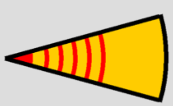	Silicon	Si $\rightarrow$ Fe, Ni	270	2.3×10^8	9.6	9.2×10^5	6 days

Degenerate Stars ("White Dwarfs")

Assume temperature very small
$\rightarrow$ No thermal pressure
$\rightarrow$ Electron degeneracy is pressure source

Pressure ~ Momentum density × Velocity

- Electron density $n_e = p_\mathrm{F}^3/(3\pi^3)$
- Momentum p_F (Fermi momentum)
- Velocity $v \propto p_\mathrm{F}/m_e$
- Pressure $P \propto p_\mathrm{F}^5 \propto \rho^{5/3} \propto M^{5/3}R^{-5}$
- Density $\rho \propto MR^{-3}$

Hydrostatic equilibrium

$$\frac{dP}{dr} = -\frac{G_\mathrm{N} M_r \rho}{r^2}$$

With $dP/dr \sim -P/R$ we have

$$P \propto G_\mathrm{N} M \rho R^{-1} \propto G_\mathrm{N} M^2 R^{-4}$$

Inverse mass radius relationship

$$R \propto M^{-1/3}$$

$$R = 10{,}500~\mathrm{km}\left(\frac{0.6\,M_\odot}{M}\right)^{1/3}(2Y_e)^{5/3}$$

(Y_e electrons per nucleon)

For sufficiently large stellar mass M, electrons become relativistic

- Velocity = speed of light
- Pressure

$$P \propto p_\mathrm{F}^4 \propto \rho^{4/3} \propto M^{4/3}R^{-4}$$

No stable configuration

Chandrasekhar mass limit

$$M_\mathrm{Ch} = 1.457\,M_\odot\,(2Y_e)^2$$

Galactic Globular Cluster M55

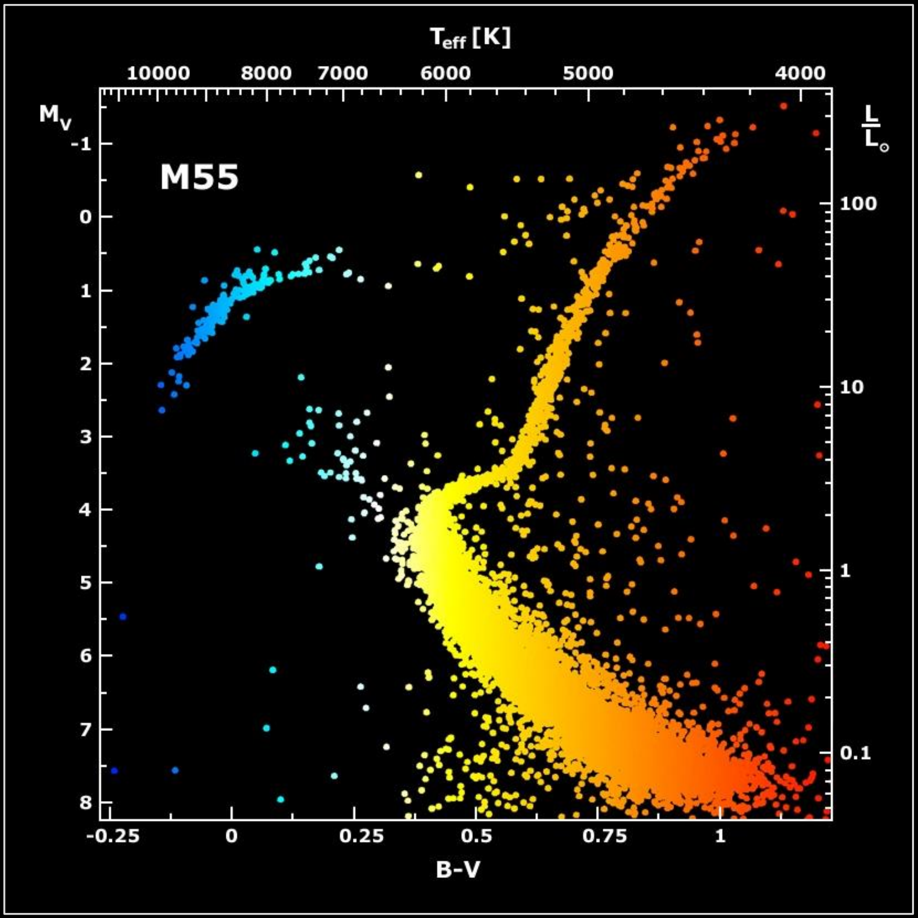

Color-Magnitude Diagram for Globular Clusters

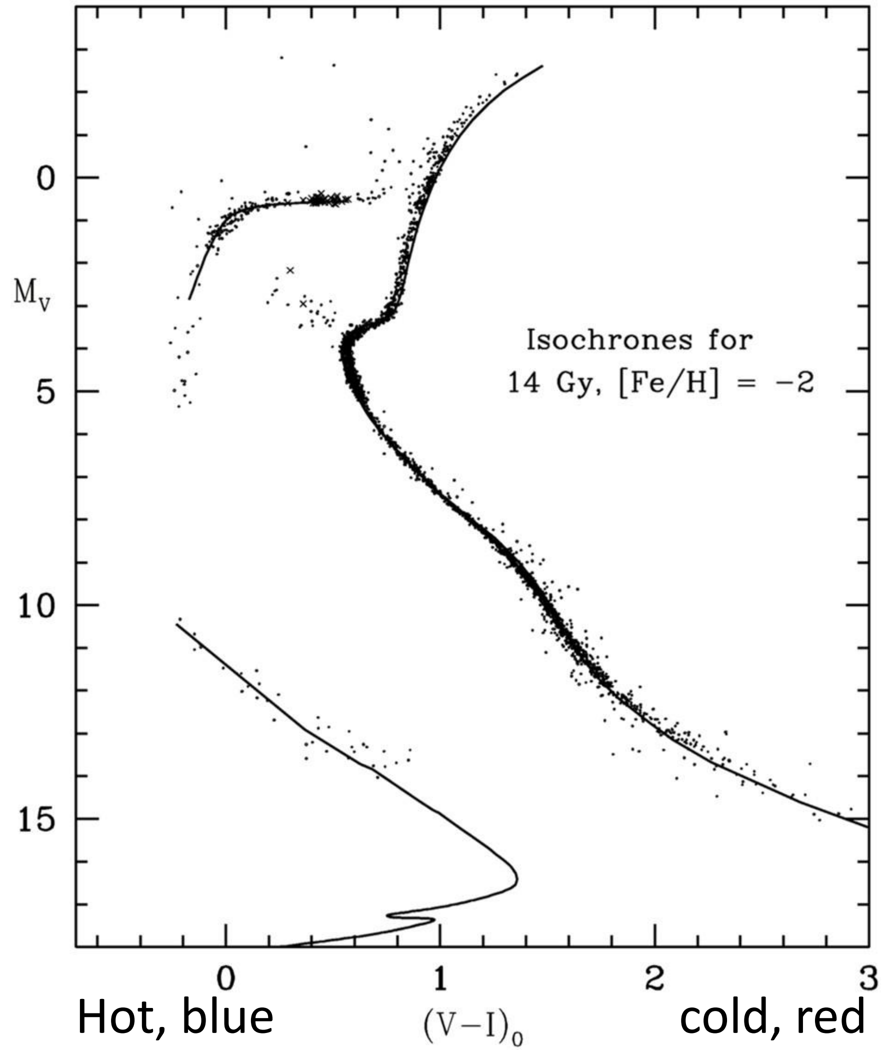

Color-magnitude diagram synthesized from several low-metallicity globular clusters and compared with theoretical isochrones (W.Harris, 2000)

Color-Magnitude Diagram for Globular Clusters

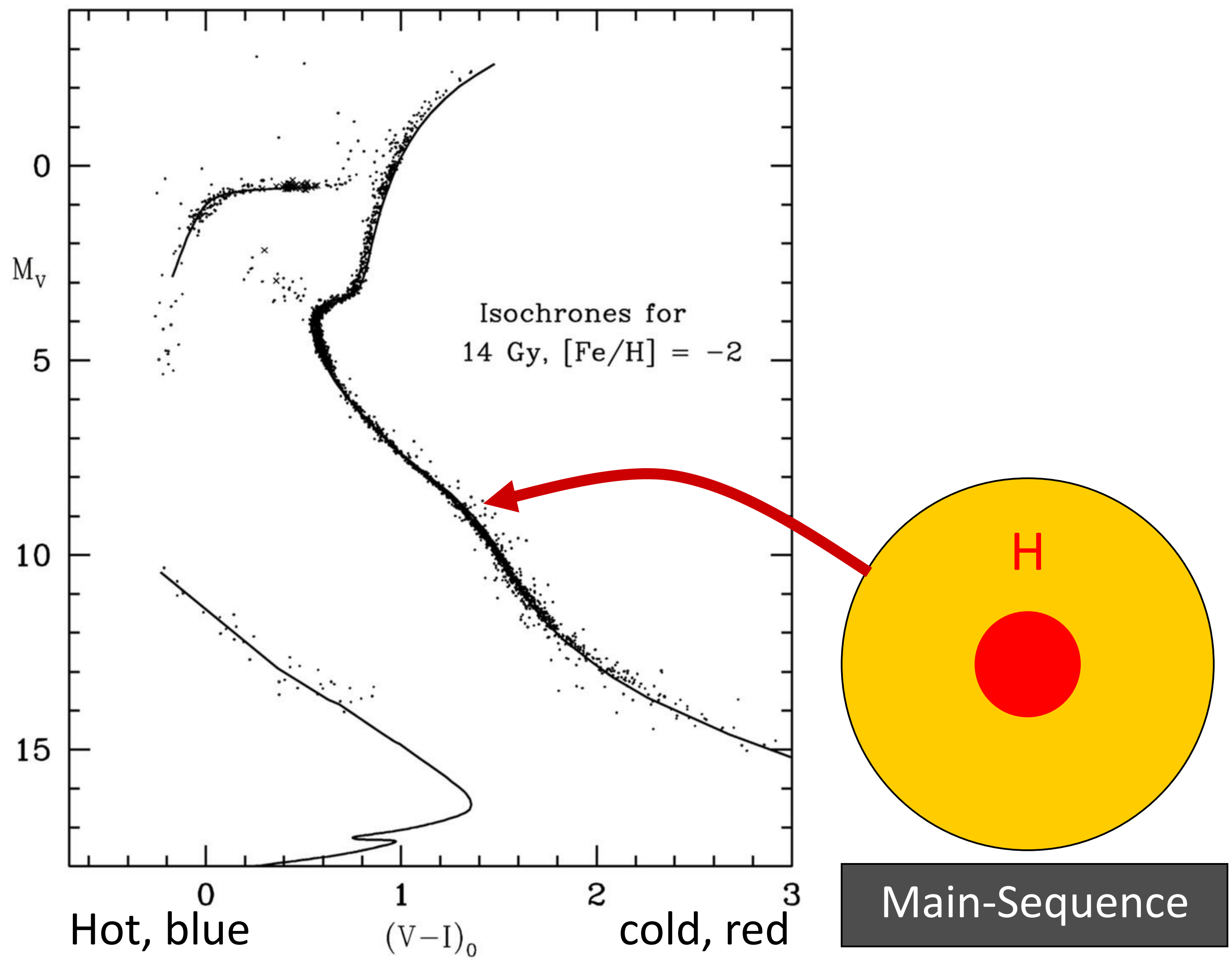

Color-magnitude diagram synthesized from several low-metallicity globular clusters and compared with theoretical isochrones (W.Harris, 2000)

Color-Magnitude Diagram for Globular Clusters

- Stars with M so large that they have burnt out in a Hubble time
- No new star formation in globular clusters

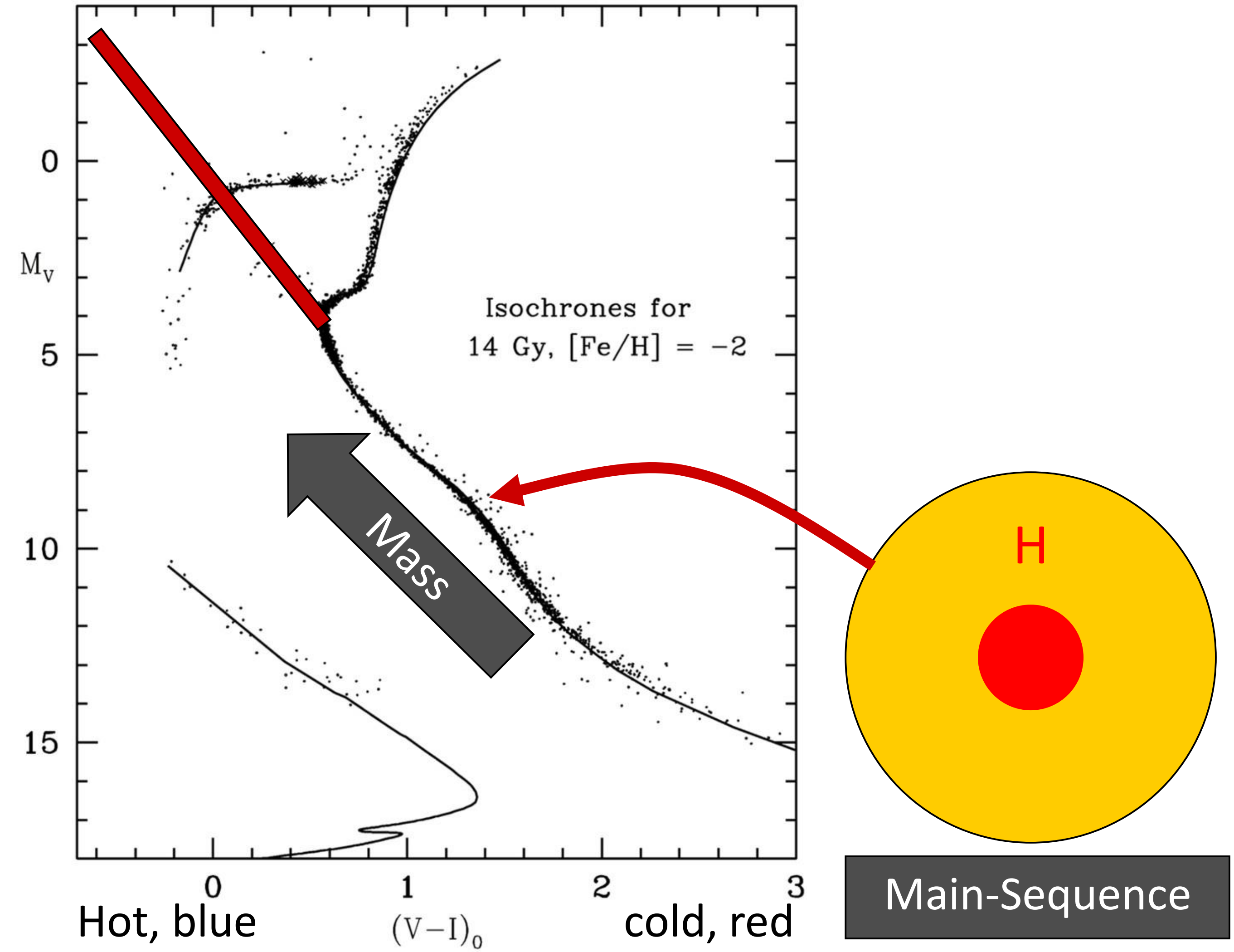

Color-magnitude diagram synthesized from several low-metallicity globular clusters and compared with theoretical isochrones (W.Harris, 2000)

Color-Magnitude Diagram for Globular Clusters

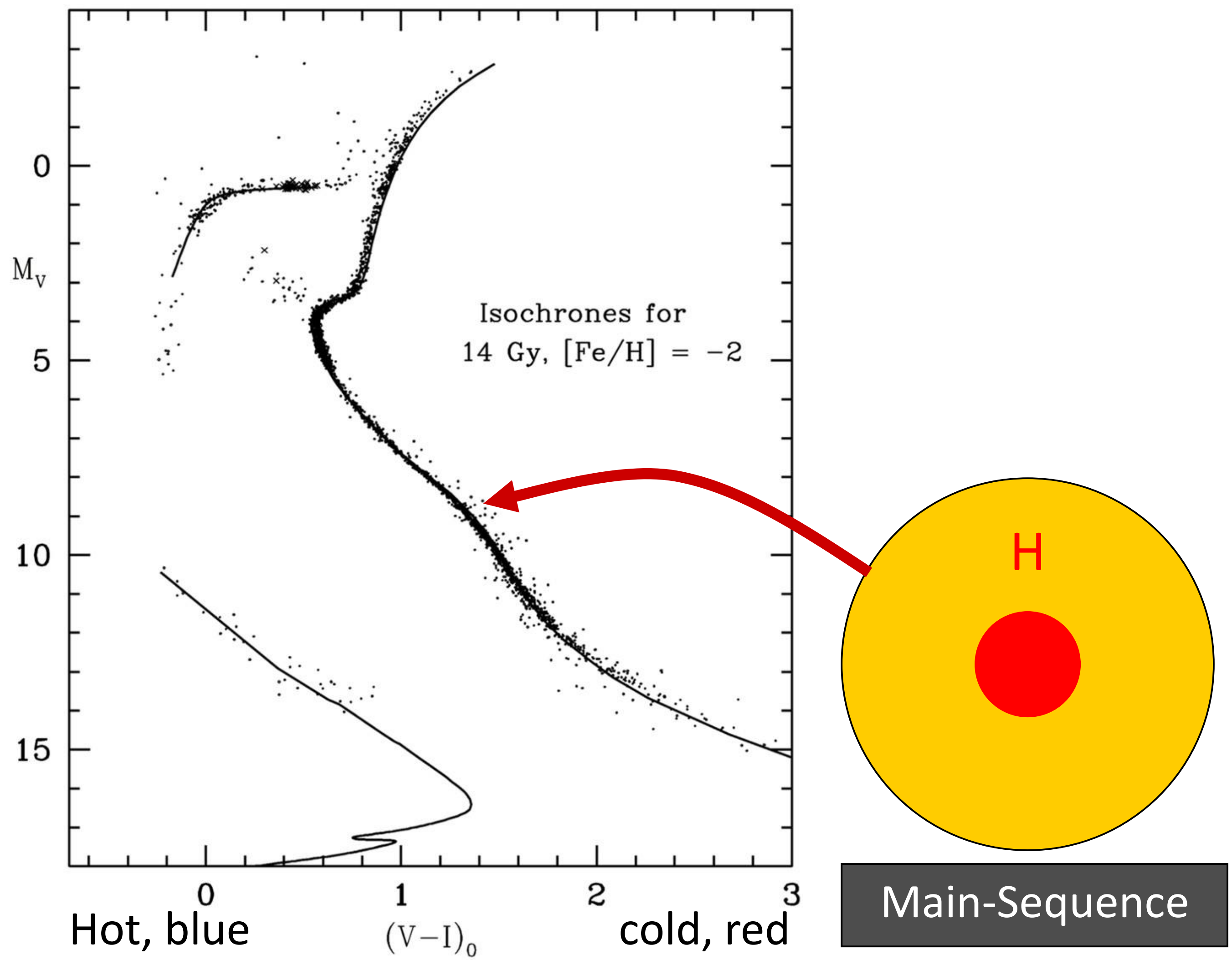

Color-magnitude diagram synthesized from several low-metallicity globular clusters and compared with theoretical isochrones (W.Harris, 2000)

Color-Magnitude Diagram for Globular Clusters

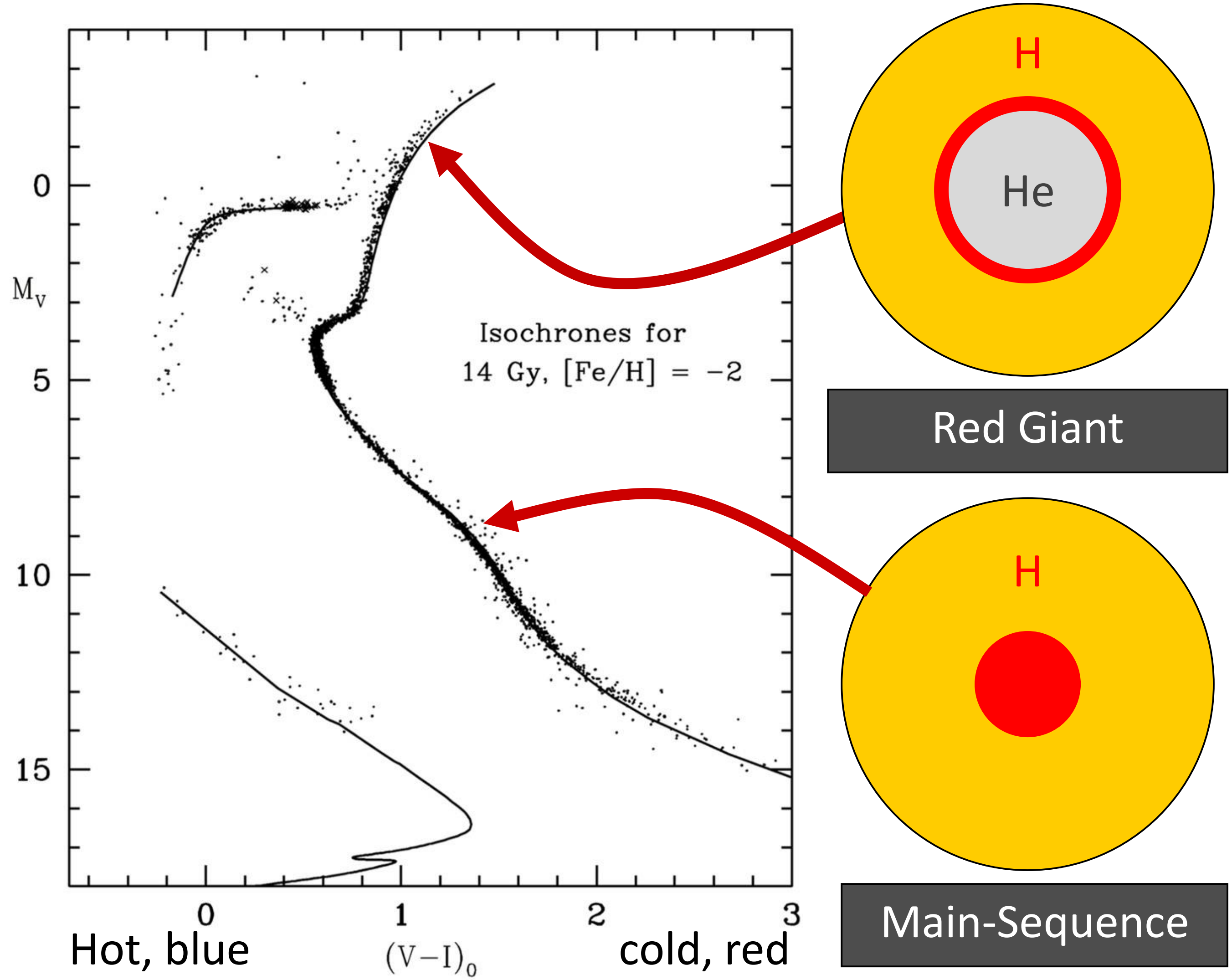

Color-magnitude diagram synthesized from several low-metallicity globular clusters and compared with theoretical isochrones (W.Harris, 2000)

Color-Magnitude Diagram for Globular Clusters

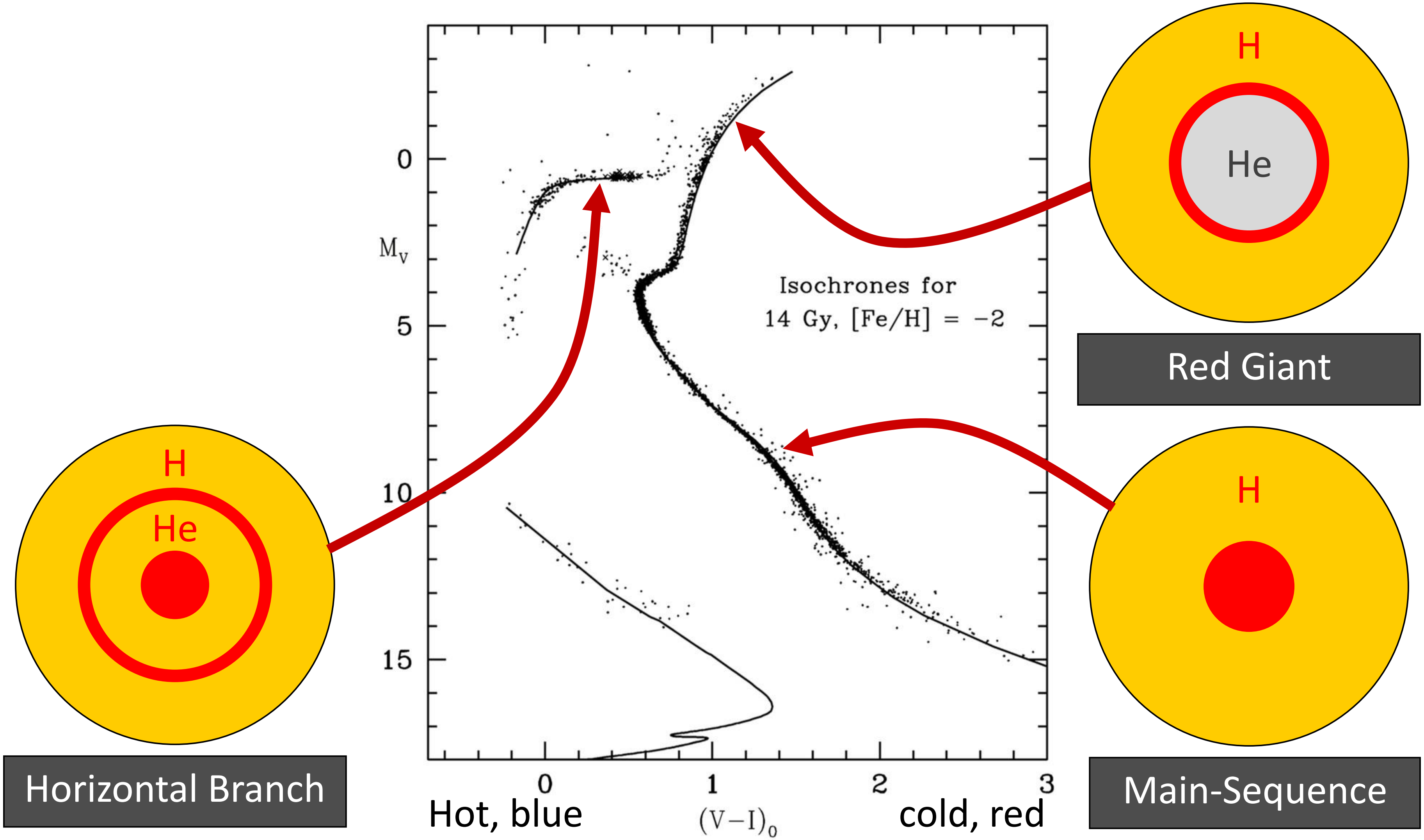

Color-magnitude diagram synthesized from several low-metallicity globular clusters and compared with theoretical isochrones (W.Harris, 2000)

Color-Magnitude Diagram for Globular Clusters

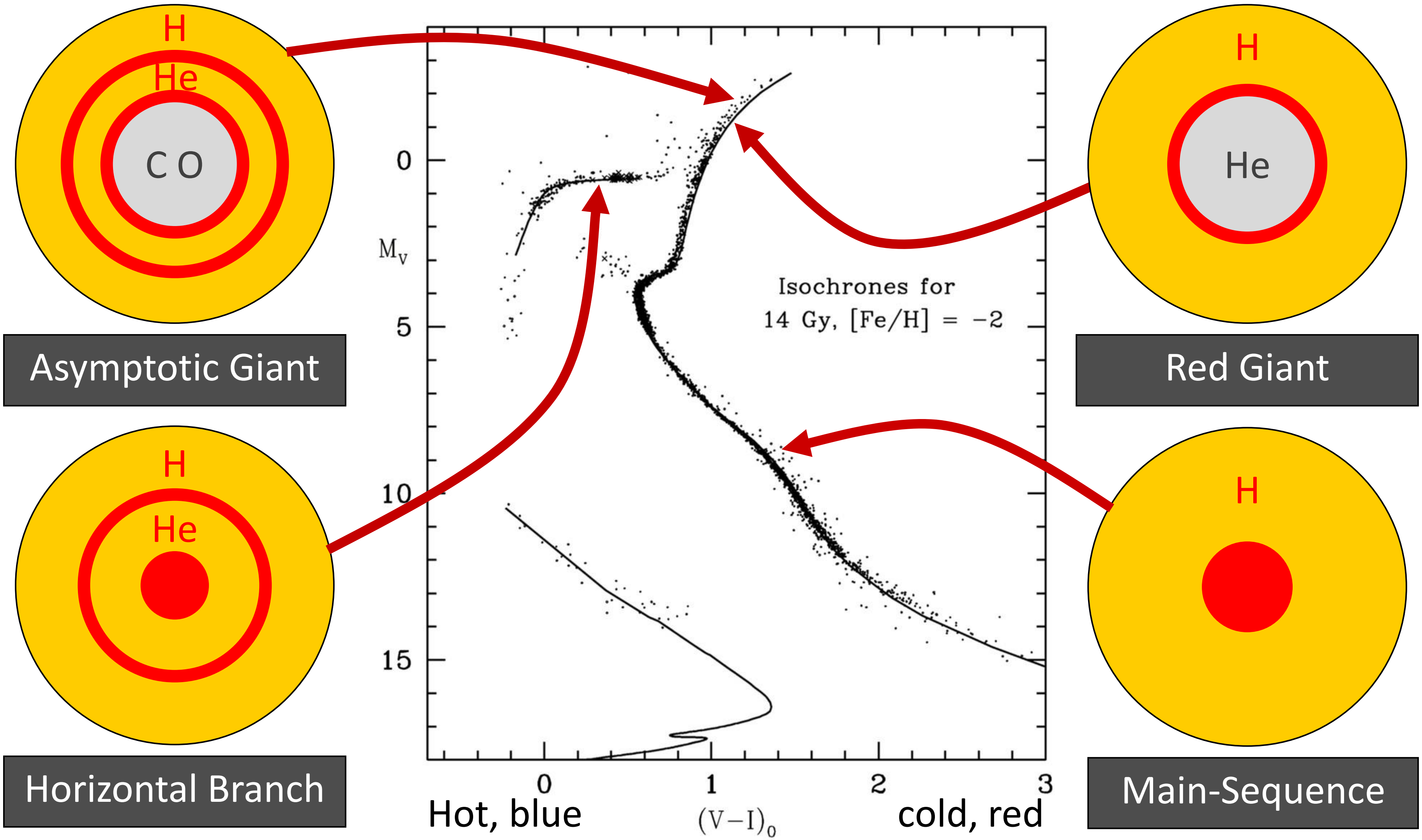

Color-magnitude diagram synthesized from several low-metallicity globular clusters and compared with theoretical isochrones (W.Harris, 2000)

Color-Magnitude Diagram for Globular Clusters

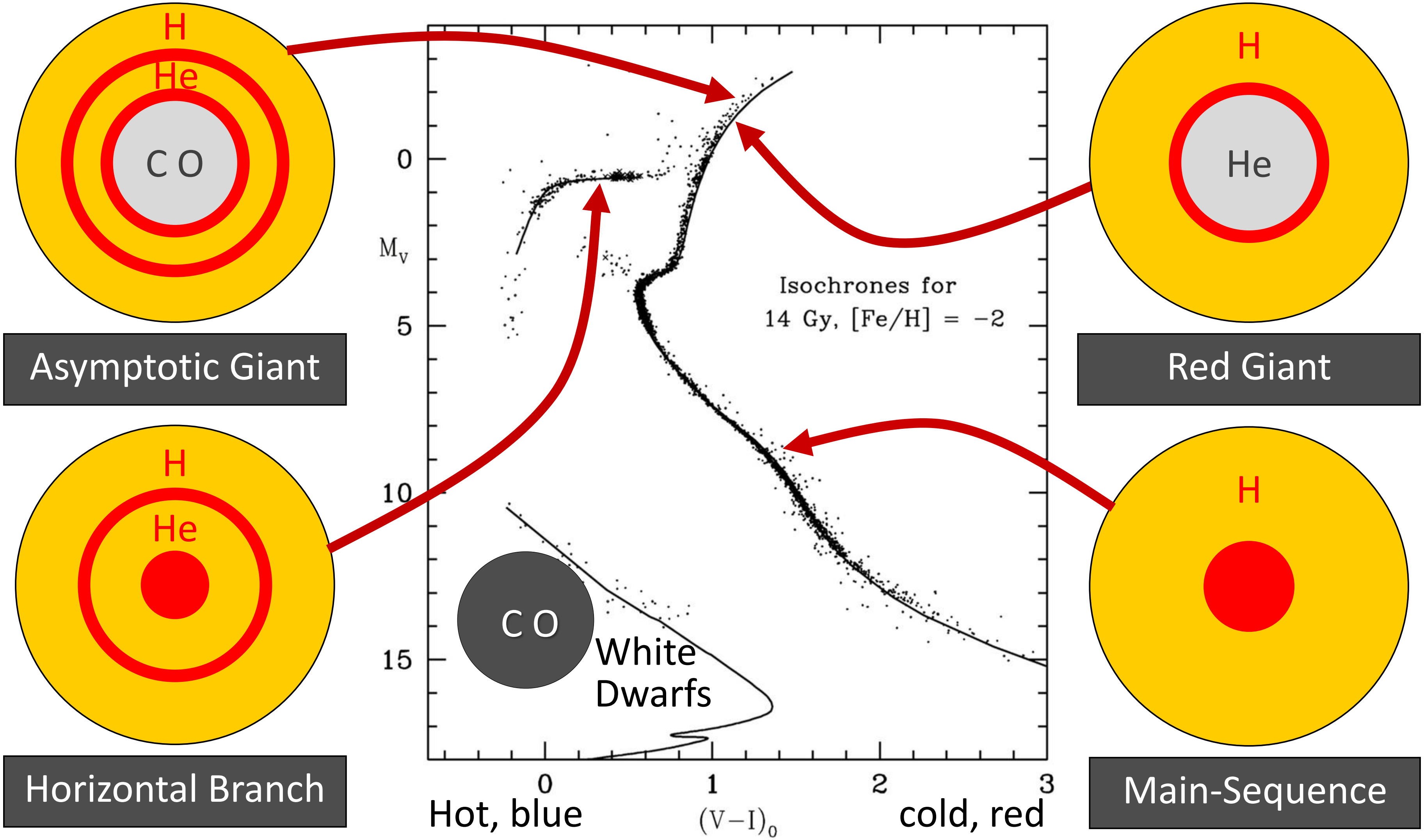

Color-magnitude diagram synthesized from several low-metallicity globular clusters and compared with theoretical isochrones (W.Harris, 2000)

Planetary Nebulae

Hour Glass Nebula

Helix Nebula

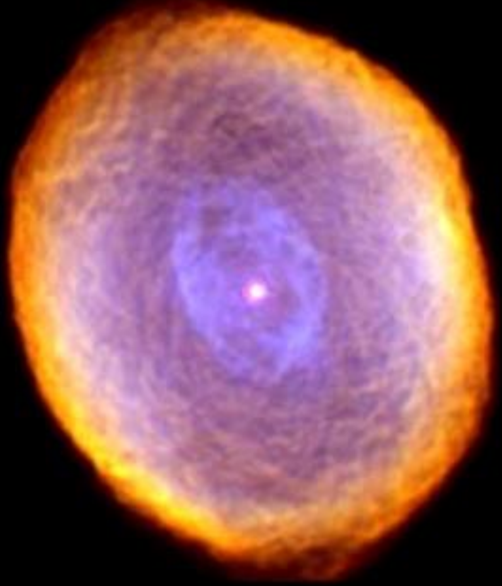

Planetary Nebula IC 418

Planetary Nebula NGC 3132

Eskimo Nebula

Evolution of Stars

$M < 0.08\ M_{sun}$	Never ignites hydrogen → cools ("hydrogen white dwarf")		Brown dwarf
$0.08 < M \lesssim 0.8\ M_{sun}$	Hydrogen burning not completed in Hubble time		Low-mass main-squence star
$0.8 \lesssim M \lesssim 2\ M_{sun}$	Degenerate helium core after hydrogen exhaustion		• Carbon-oxygen white dwarf • Planetary nebula
$2 \lesssim M \lesssim 8\ M_{sun}$	Helium ignition non-degenerate		
$8\ M_{sun} \lesssim M < ???$	All burning cycles → Onion skin structure with degenerate iron core	Core collapse supernova	• Neutron star (often pulsar) • Sometimes black hole • Supernova remnant (SNR), e.g. crab nebula

Color-Magnitude Diagram for Globular Clusters

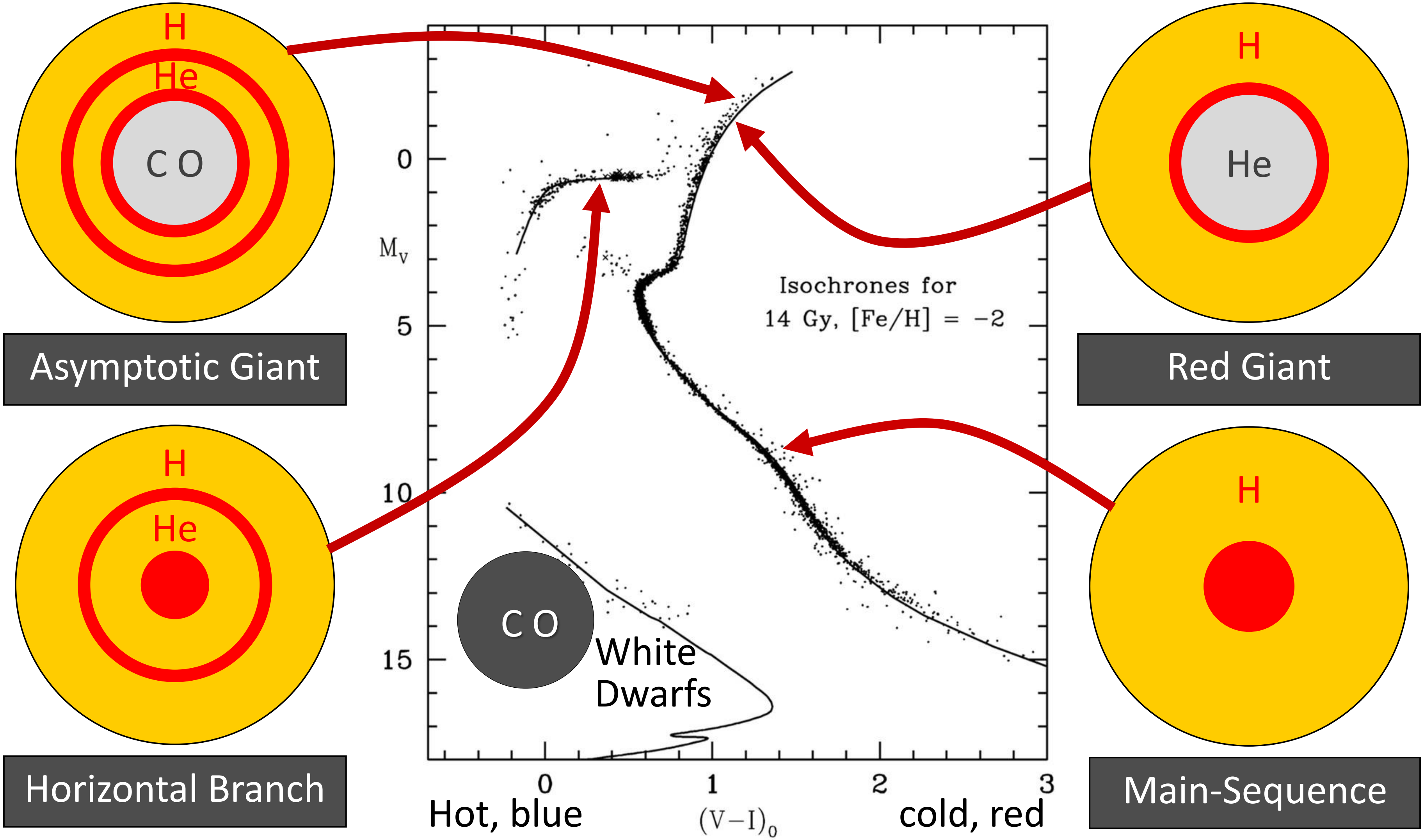

Color-magnitude diagram synthesized from several low-metallicity globular clusters and compared with theoretical isochrones (W.Harris, 2000)

Color-Magnitude Diagram for Globular Clusters

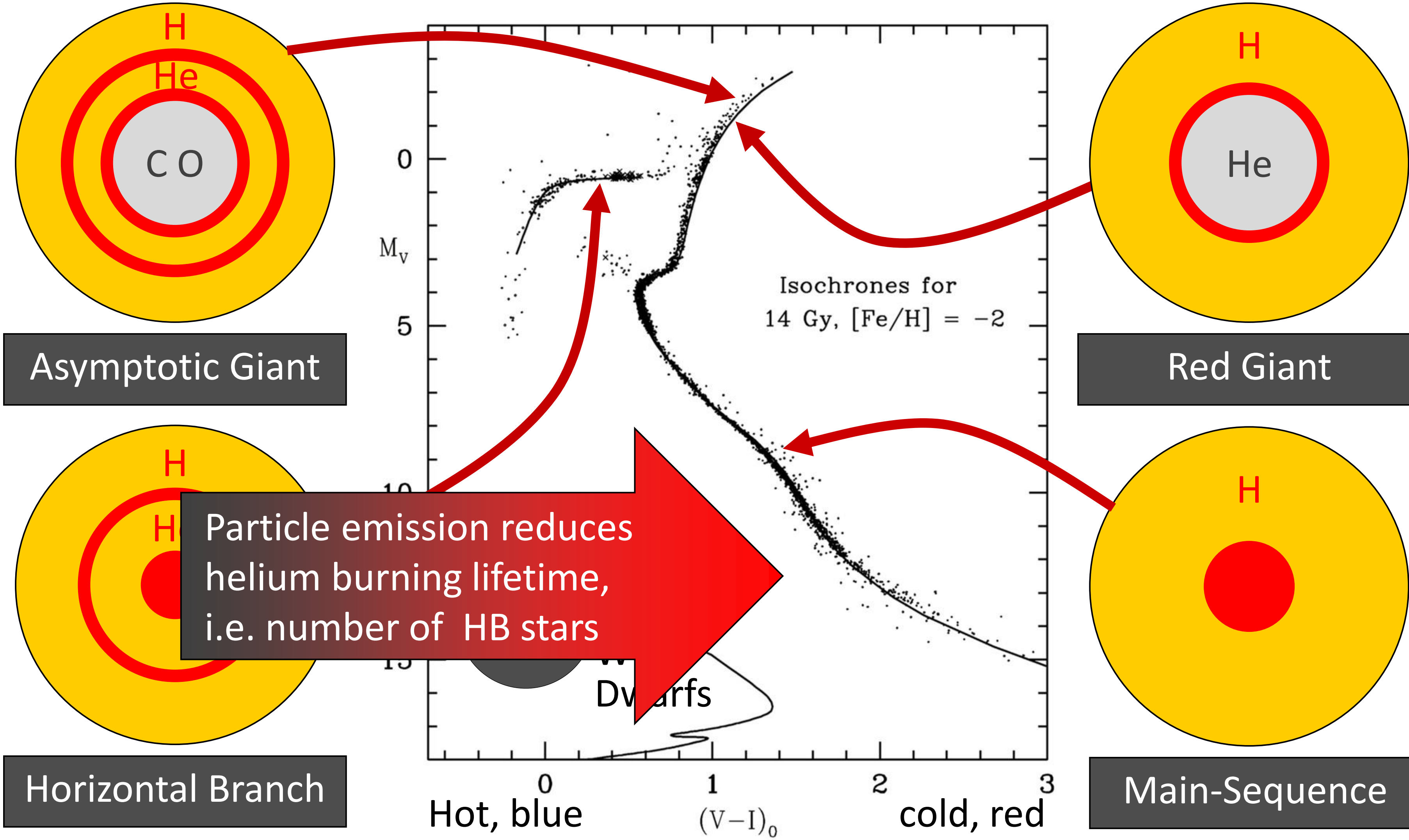

Color-magnitude diagram synthesized from several low-metallicity globular clusters and compared with theoretical isochrones (W.Harris, 2000)

Color-Magnitude Diagram for Globular Clusters

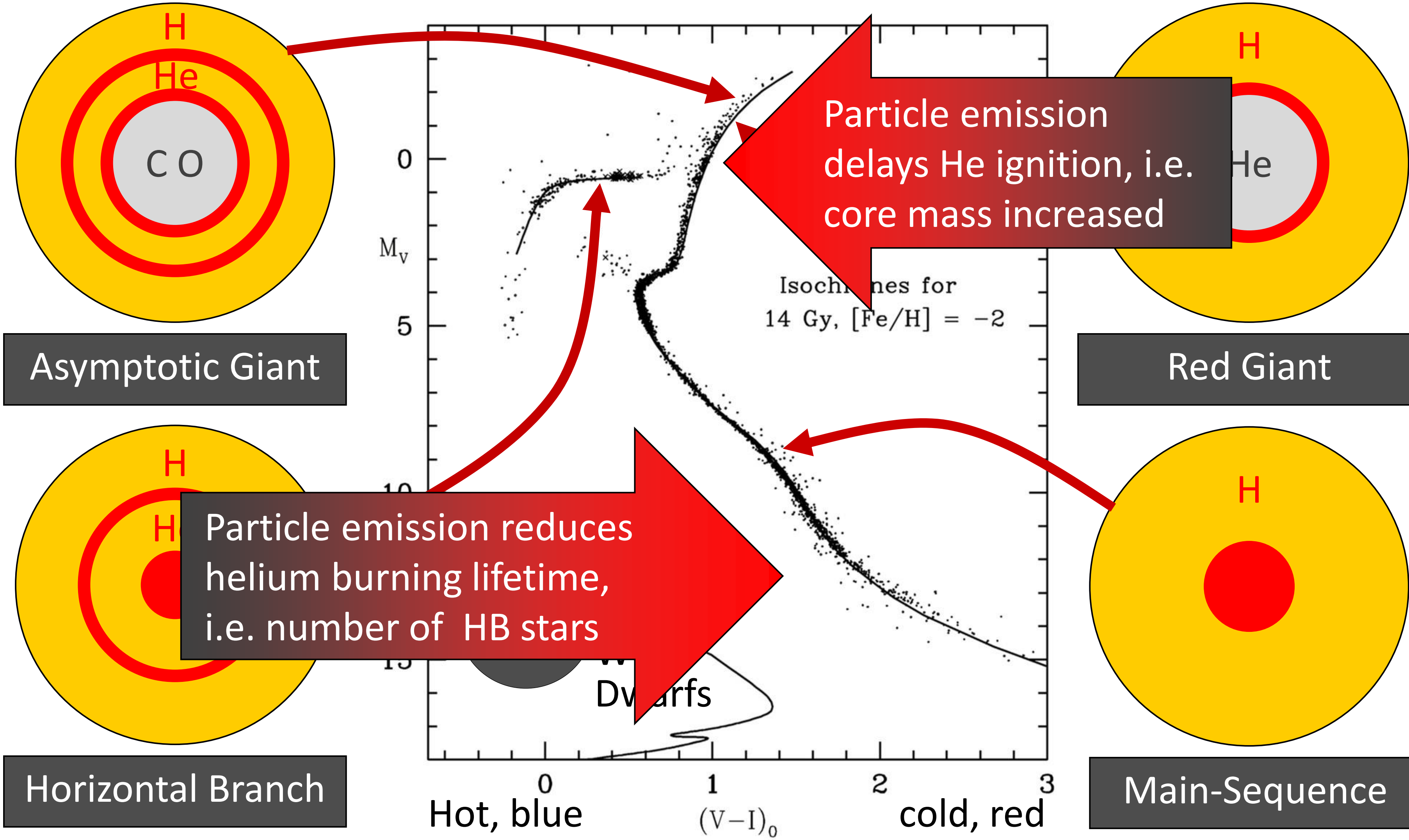

Color-magnitude diagram synthesized from several low-metallicity globular clusters and compared with theoretical isochrones (W.Harris, 2000)

Neutrinos from Thermal Processes

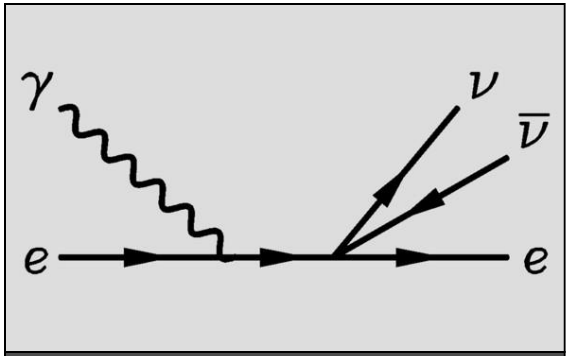

Photo (Compton)

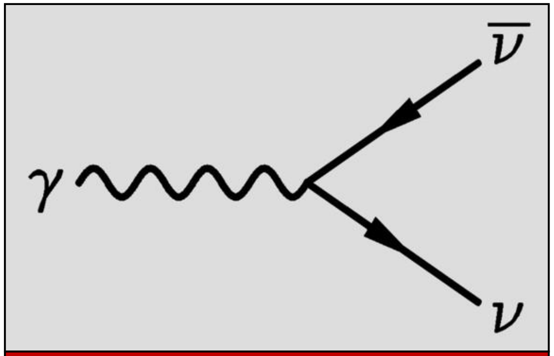

Plasmon decay

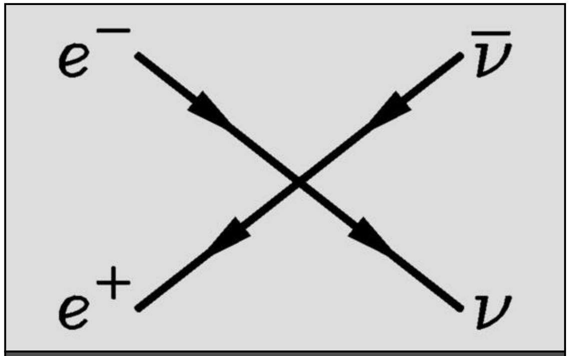

Pair annihilation

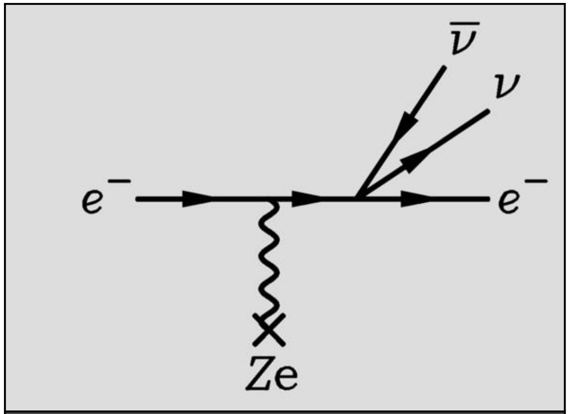

Bremsstrahlung

These processes were first discussed in 1961–63 after V–A theory

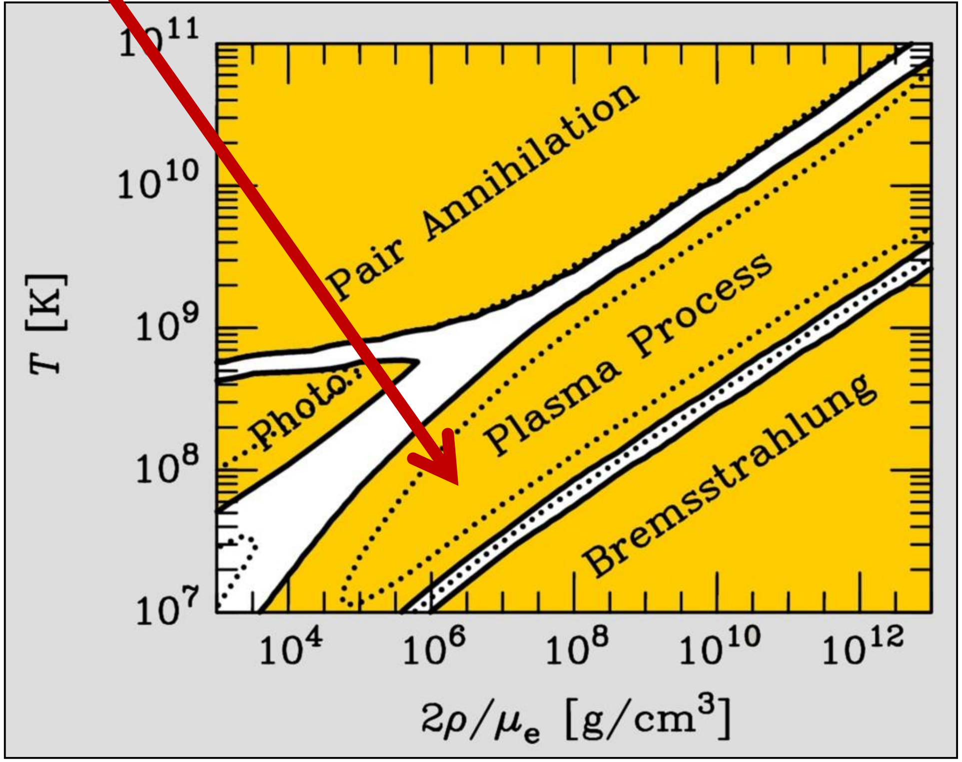

Brightness and Core Mass at TRGB

Raffelt & Weiss, Astron. Astrophys. 264 (1992) 536

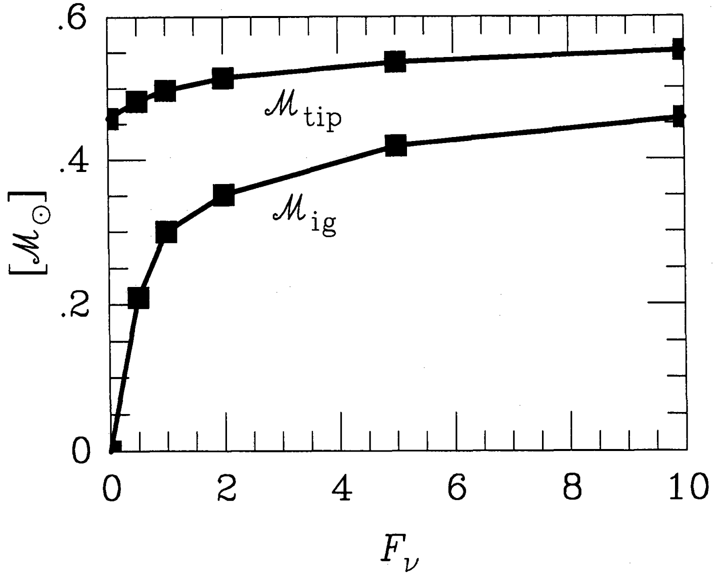

Fig. 2. Core mass at helium flash, $\mathcal{M}_{tip}$, and mass-coordinate of the ignition point, $\mathcal{M}_{ig}$, as a function of F_ν for $\mathcal{M} = 0.80$, $Z = 10^{-4}$, and $Y_0 = 0.22$ (see Table 2).

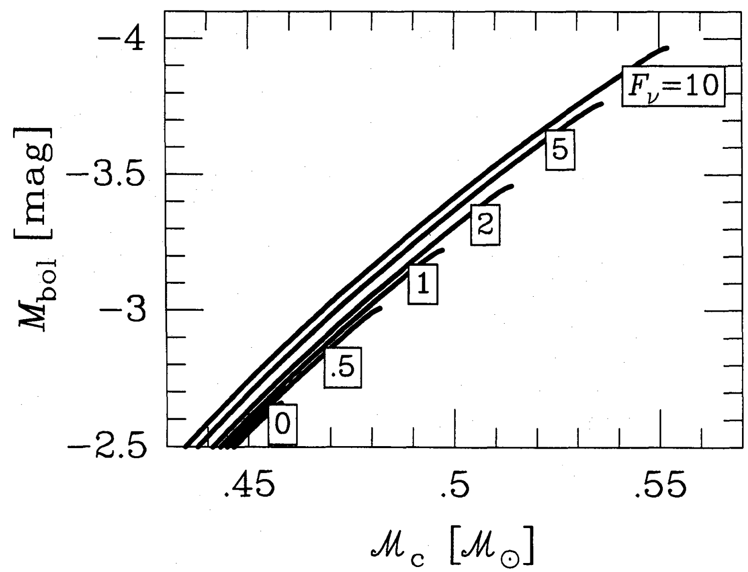

Fig. 3. Absolute surface brightness as a function of core mass for the $Z = 10^{-4}$ runs of Table 2. The curves are marked with the relevant F_ν values.

Parametric study: Vary standard neutrino losses with a fudge factor F_ν
($F_\nu = 1$ standard, $F_\nu = 0$ no losses at all, etc.)

- Helium ignition point (mass coordinate $\mathcal{M}_{ig}$)
- Core mass at ignition $\mathcal{M}_{tip}$
- Bolometric brightness at ignition M_{tip}

Particle Emission from Red-Giant Core or White Dwarf

Large Neutrino Dipole Moment
- Requires BSM physics
- Direct coupling to EM field
- Enhances plasmon decay

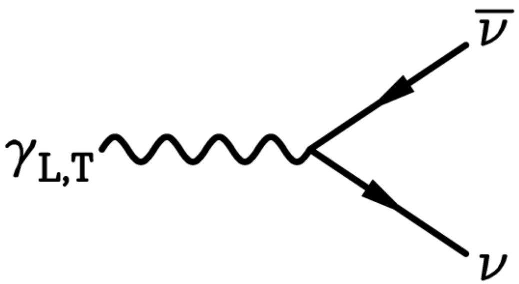

$\mu_\nu < 1.5 \times 10^{-12} \mu_B$ (95% CL)

Axions (or friends) with direct coupling to electrons
- Bremsstrahlung emission by degenerate electrons

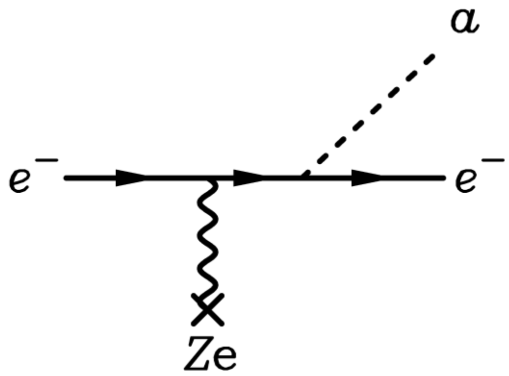

$g_{ae} < 1.6 \times 10^{-13}$ (95% CL)

Helium Ignition for Low-Mass Red Giants

Brightness increase at He ignition by nonstandard neutrino losses (increased plasmon decay by neutrino dipole moment)

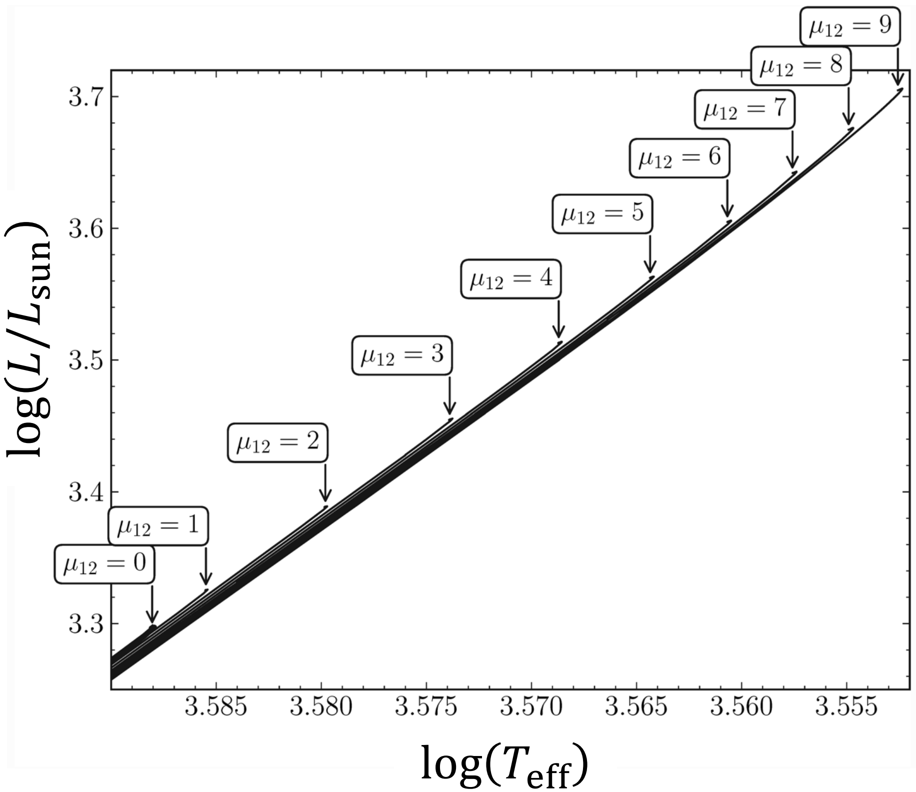

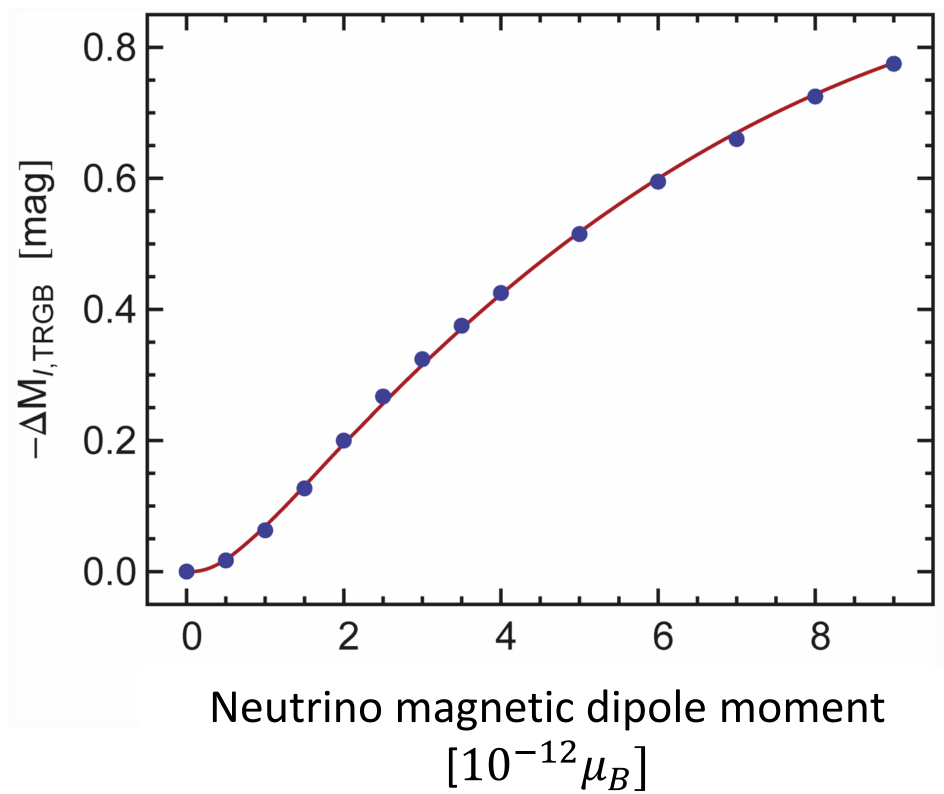

Viaux, Catelan, Stetson, Raffelt, Redondo, Valcarce & Weiss, arXiv:1308.4627

Upper Red Giant Branch of Globular Clusters

Brightest red giant
measures nonstandard energy loss

Beccari et al., arXiv:astro-ph/0610289

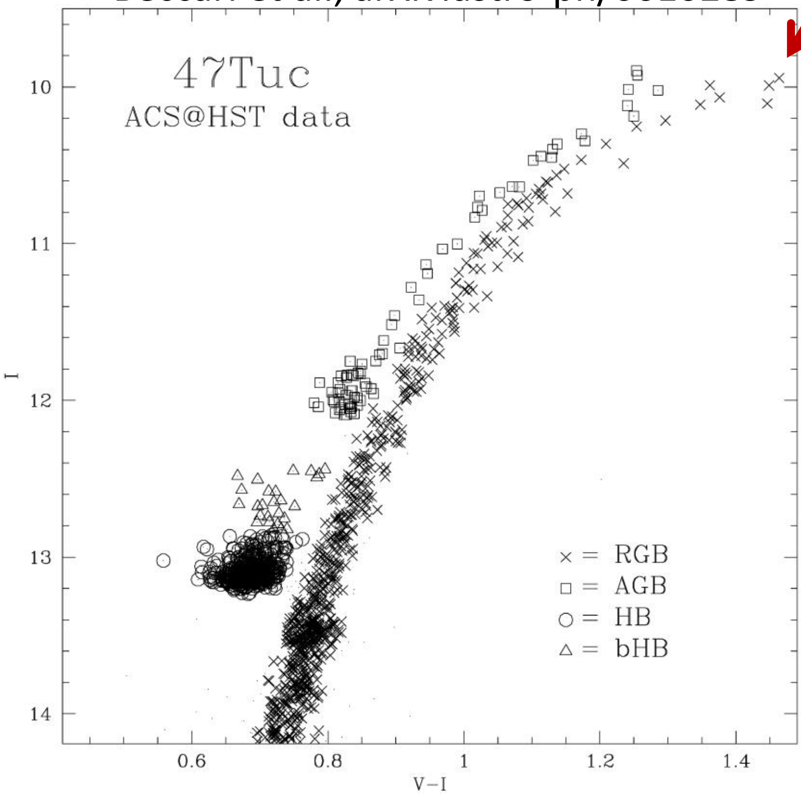

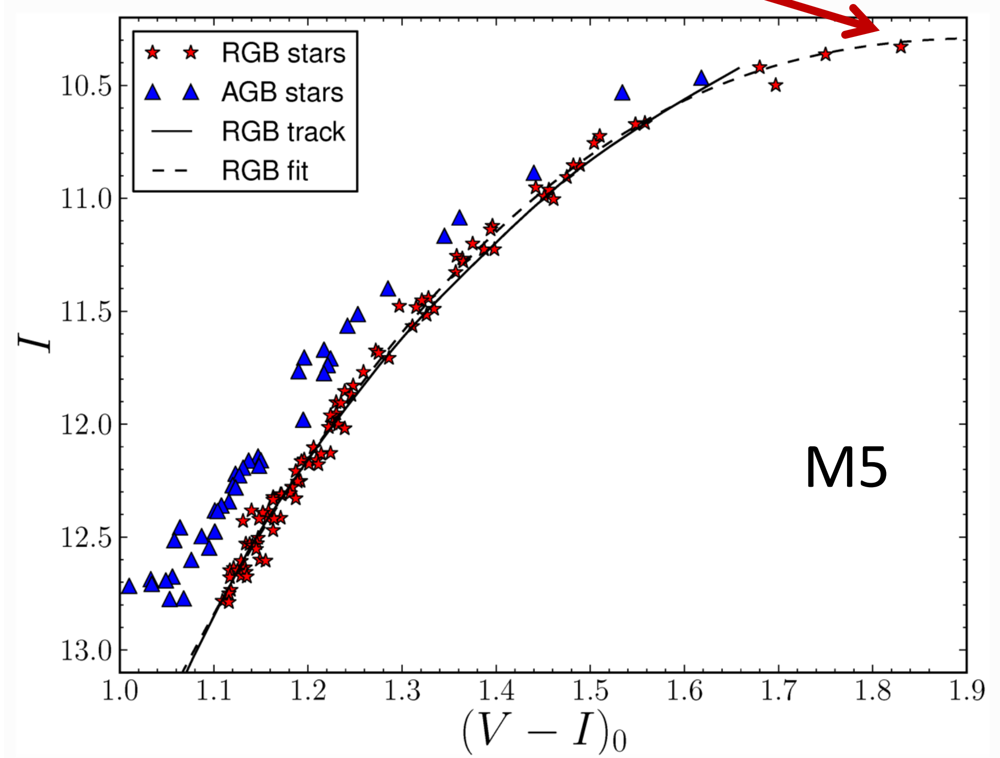

Straniero et al., arXiv:2010.03833

Viaux et al., arXiv:1308.4627

Limits on Axion-Electron Coupling from GC M5

I-band brightness
of tip of red-giant branch
[magnitudes]

- Uncertainty dominated by distance
- Can be improved in future (GAIA mission)

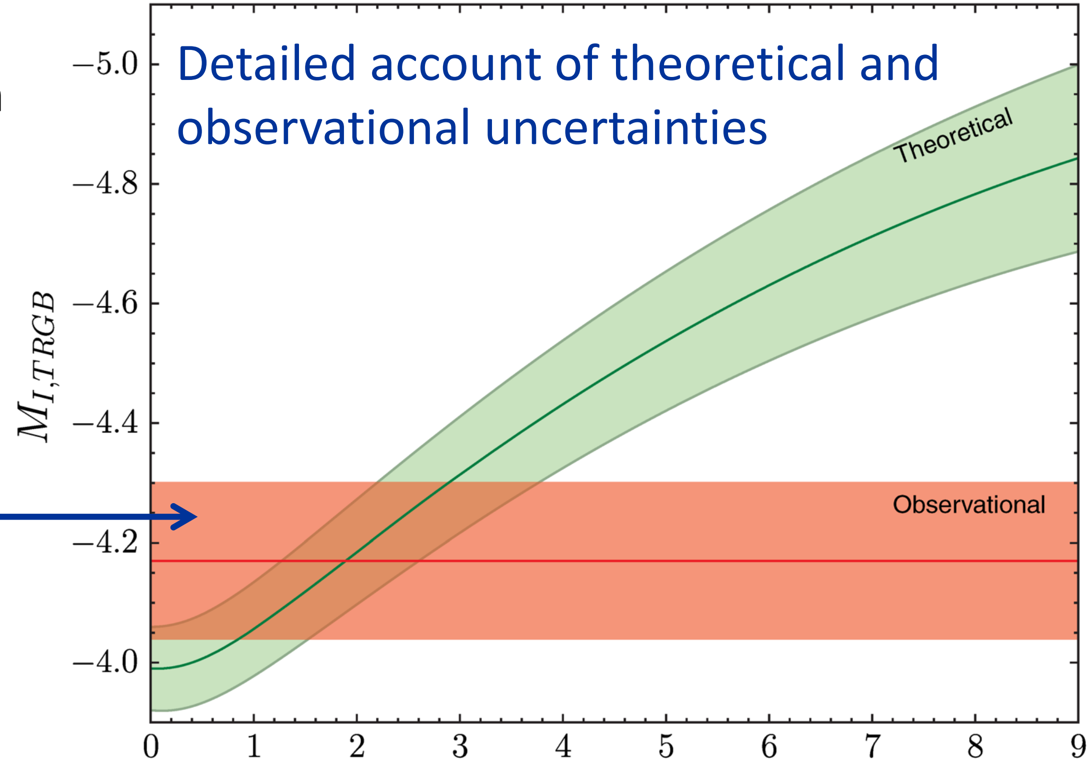

Axion-electron Yukawa $g_{ae} \times 10^{13}$

Limit on axion-electron Yukawa

$$g_{ae} < \begin{cases} 2.6 \times 10^{-13} & (68\%\ \mathrm{CL}) \\ 4.3 \times 10^{-13} & (95\%\ \mathrm{CL}) \end{cases}$$

Mass limit in DFSZ model

$$m_a \cos^2\beta < \begin{cases} 9.3\ \mathrm{meV} & (68\%\ \mathrm{CL}) \\ 15.4\ \mathrm{meV} & (95\%\ \mathrm{CL}) \end{cases}$$

Viaux, Catelan, Stetson, Raffelt, Redondo, Valcarce & Weiss, arXiv:1311.1669

New TRGB Calibration from 22 Globular Clusters

Straniero et al., arXiv:2010.03833 (8 Oct. 2020)

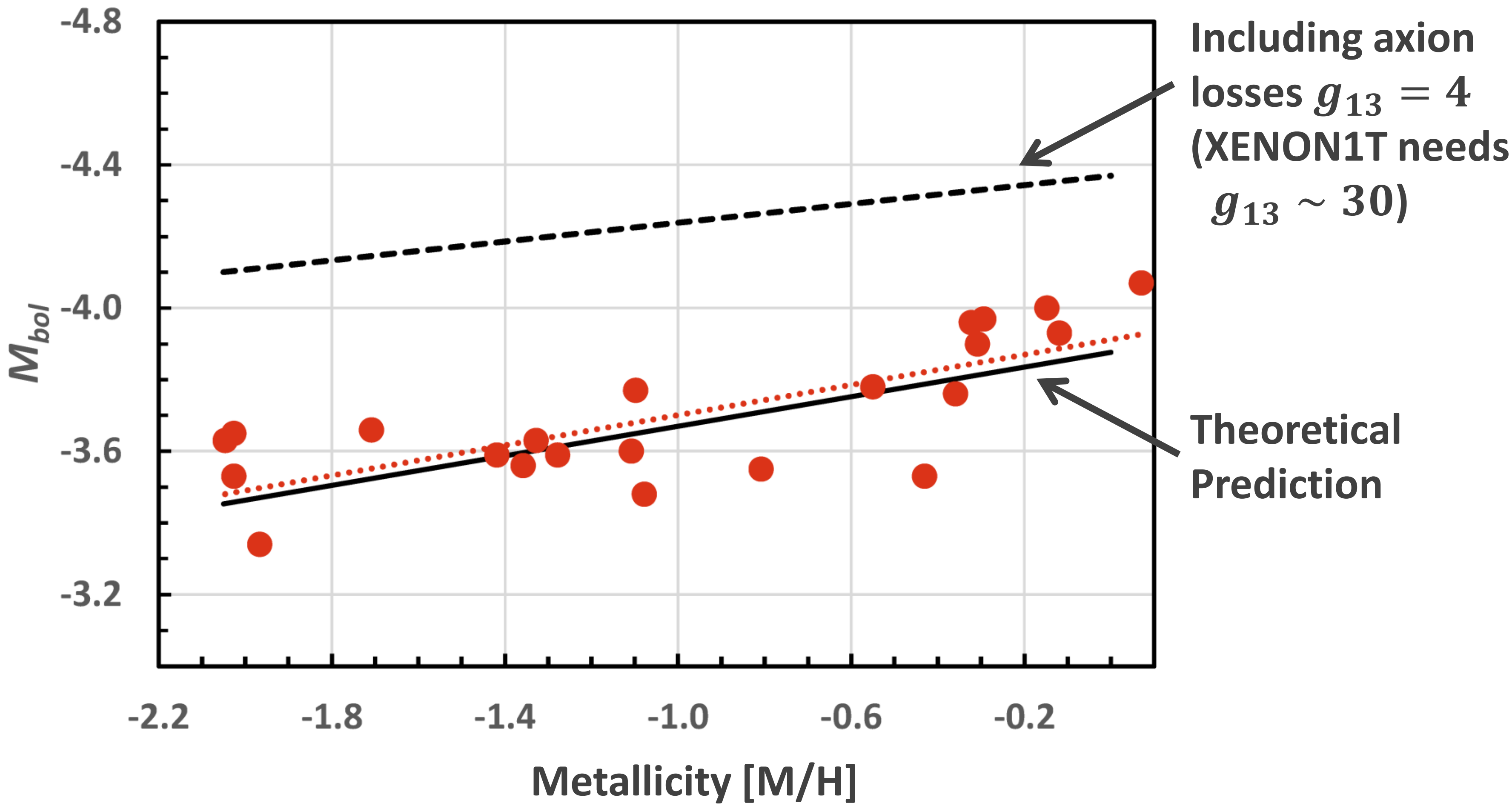

Their final axion limit: $g_{ae} < 1.2 \times 10^{-13}$ (95% CL)

Tip of the Red-Giant Branch in the Galaxy NGC 4258

The Astrophysical Journal, 835:28 (17pp), 2017 January 20 Jang & Lee

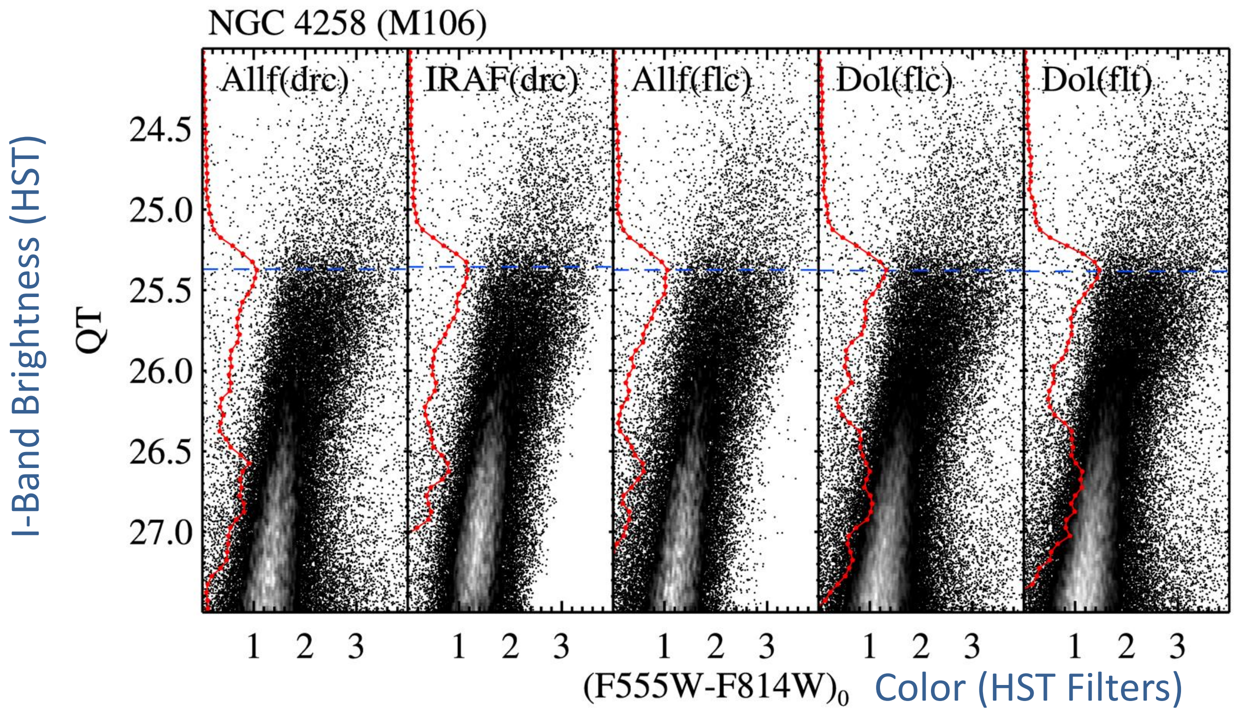

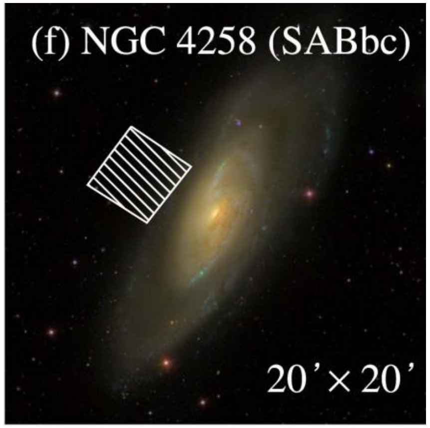

Figure 7. *QT* − (F555W − F814W)$_0$ CMDs of NGC 4258 from five different reduction methods : ALLFRAME on drc, IRAF/DAOPHOT on drc, ALLFRAME on flc, DOLPHOT on flc, and DOLPHOT on flt (from left to right). Edge detection responses are shown by the solid lines. Note that the estimated TRGB magnitudes (dashed lines) agree very well.

NGC 4258 hosts a water megamaser
→ Quasi-geometric distance determination
→ Among the best absolute TRGB calibrations

TRGB in Different Filters

Freedman et al., ApJ 891 (2020) 57

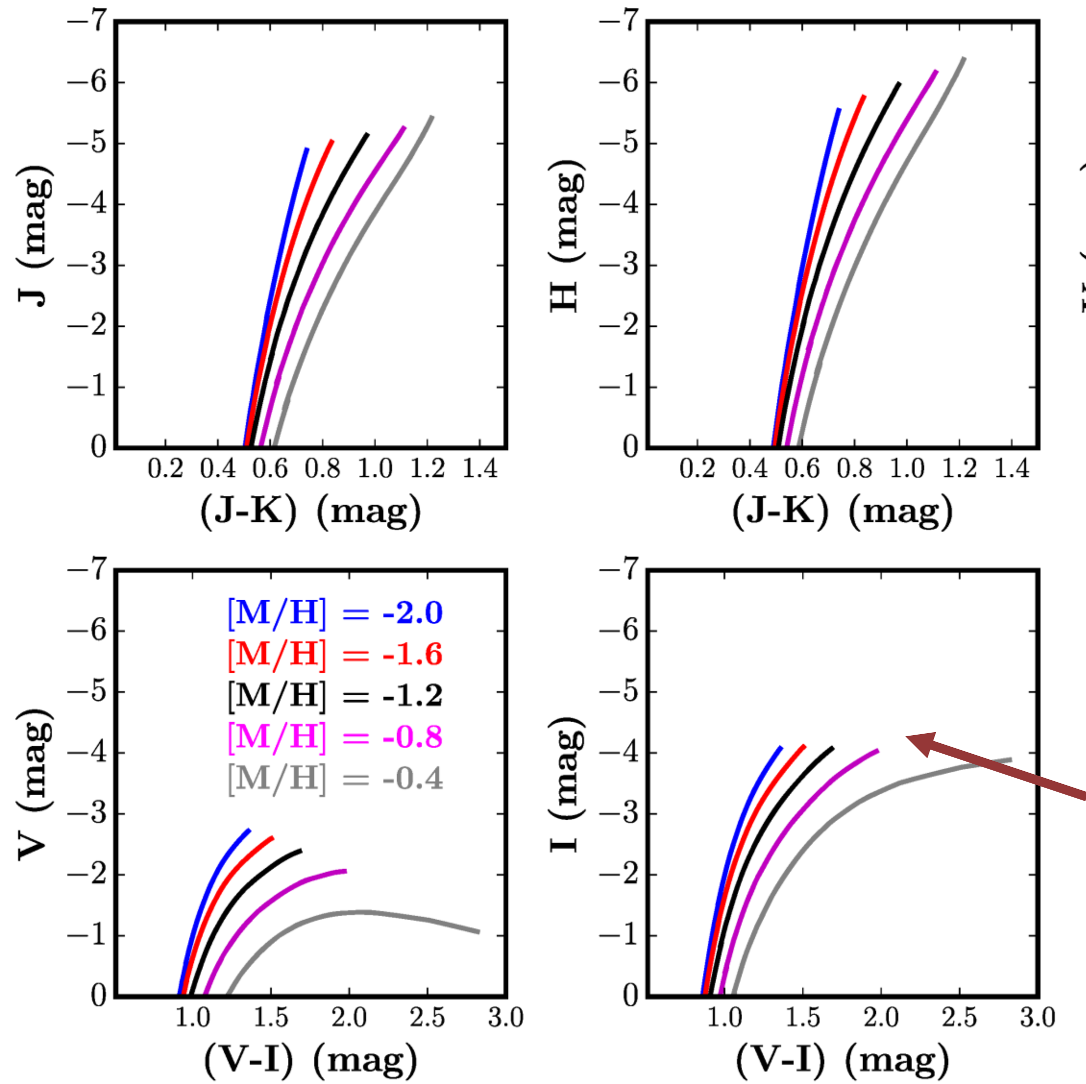

- Upper RGB for different metallicities in different color filters
- The TRGB is practically horizontal in the (I,V–I) color-magnitude diagram (CMD)

Determinations of the Hubble Constant

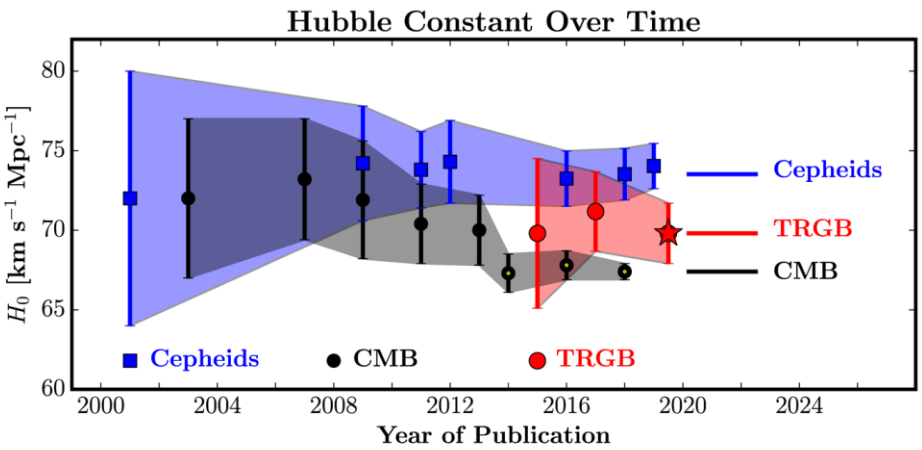

Freedman et al. 2019, ApJ 882:34

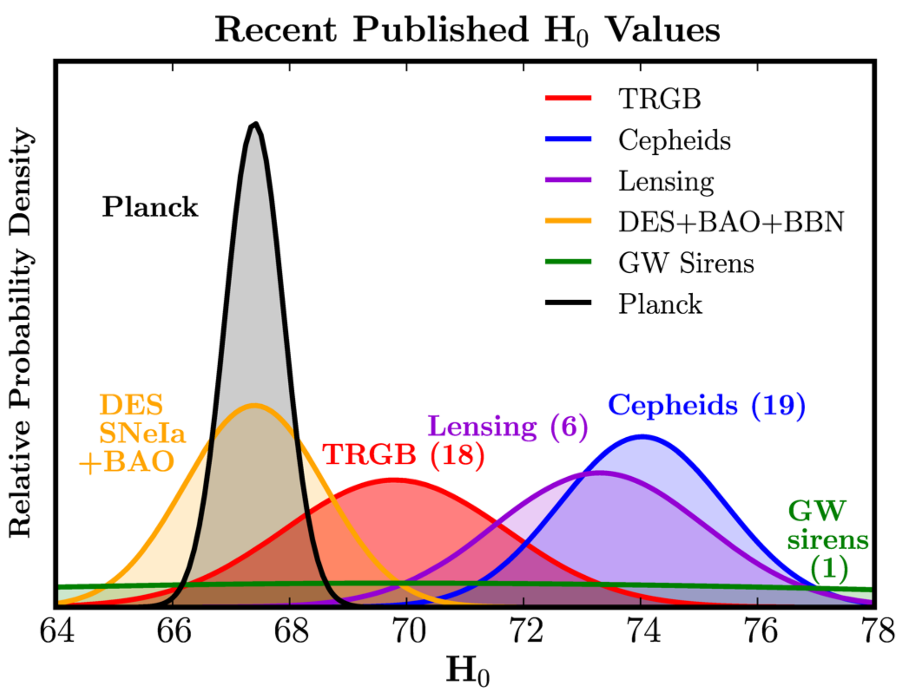

Freedman et al. 2020 ApJ 891:57

Axion Bounds from TRGB Calibrations

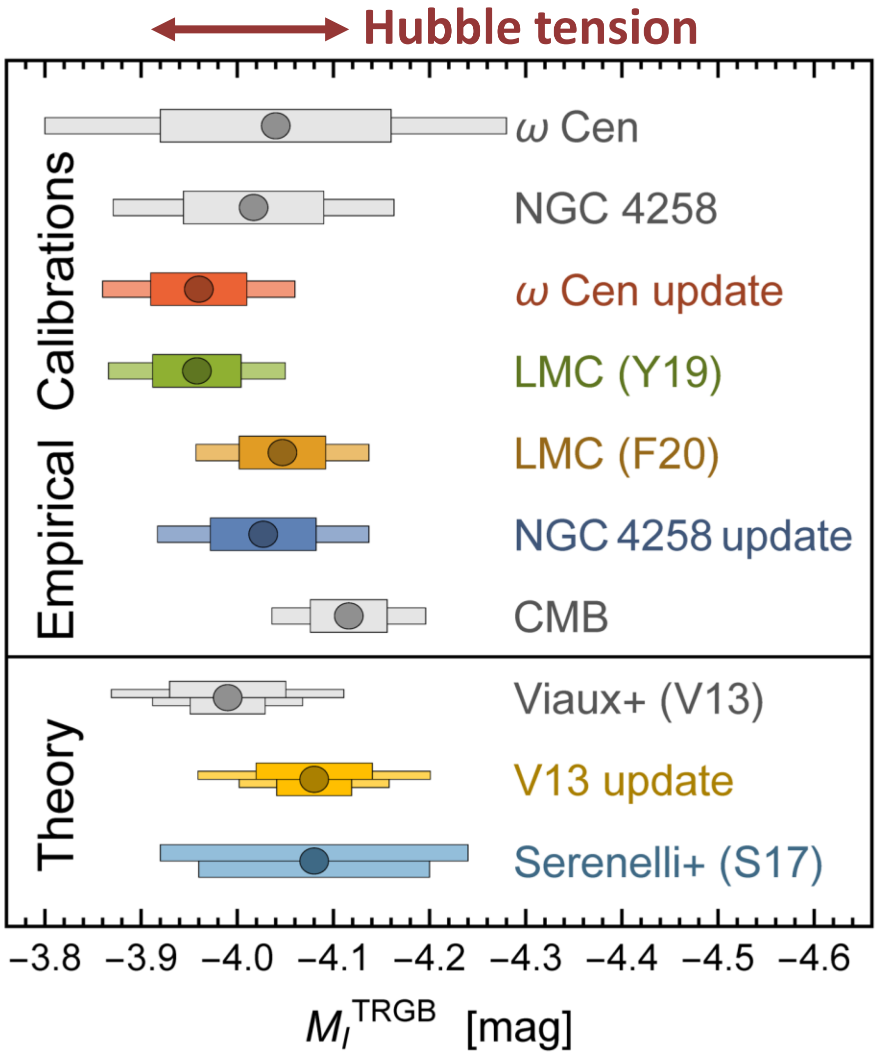

Updated TRGB Calibrations
Capozzi & Raffelt, arXiv:2007.03694

Bounds from "water megamaser" galaxy NGC 4258, compared with stellar evolution theory (95% CL)

$$g_{ae} < 1.6 \times 10^{-13}$$

$$\mu_\nu < 1.5 \times 10^{-12} \mu_{\rm B}$$

XENON1T interpretation:

$$g_{ae} \sim 30 \times 10^{-13}$$

$$\mu_\nu \sim 20 \times 10^{-12} \mu_{\rm B}$$

Color-Magnitude Diagram for Globular Clusters

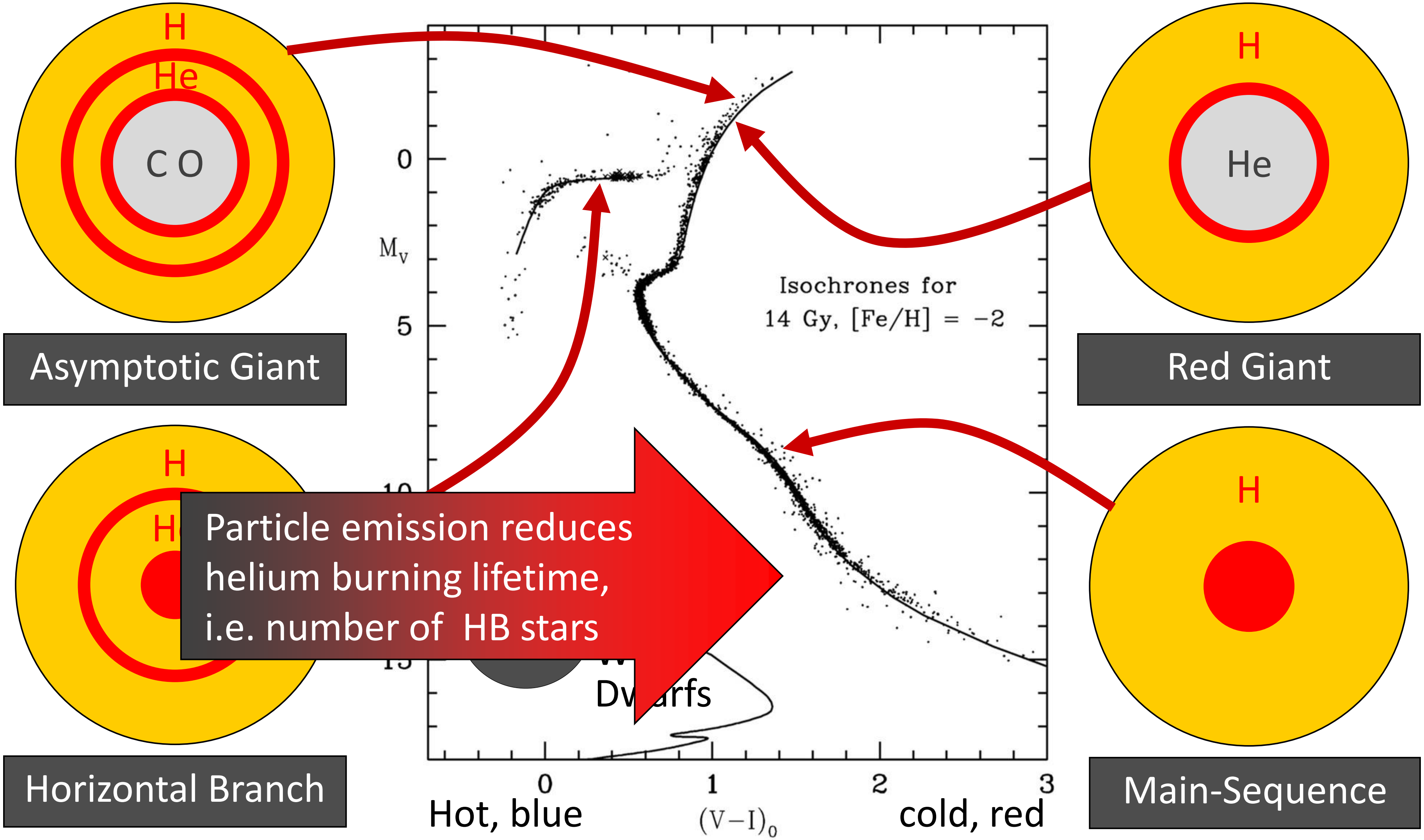

Color-magnitude diagram synthesized from several low-metallicity globular clusters and compared with theoretical isochrones (W.Harris, 2000)

ALP Limits from Globular Clusters

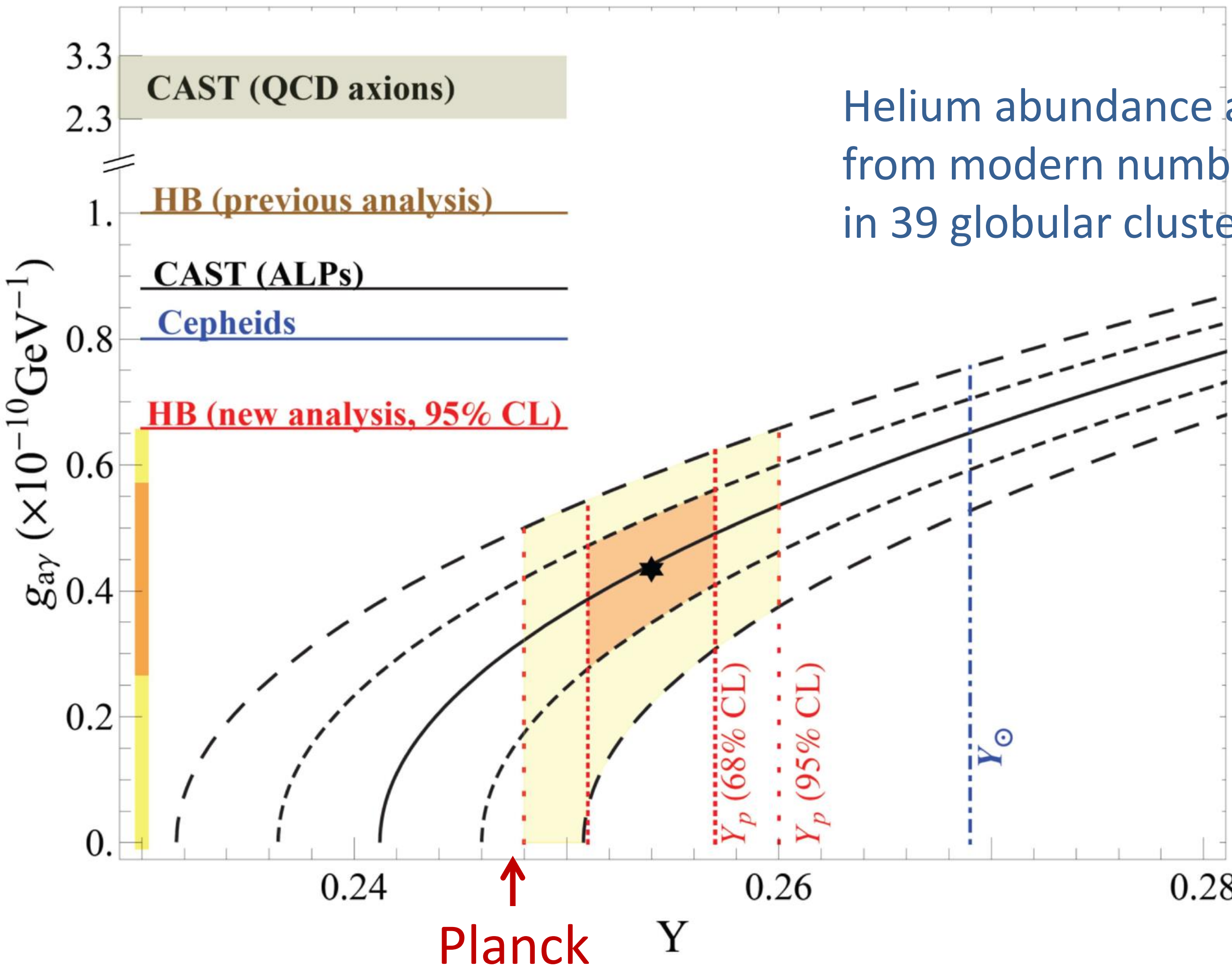

Helium abundance and energy loss rate from modern number counts HB/RGB in 39 globular clusters

Ayala, Dominguez, Giannotti, Mirizzi & Straniero, arXiv:1406.6053

White Dwarf Luminosity Function

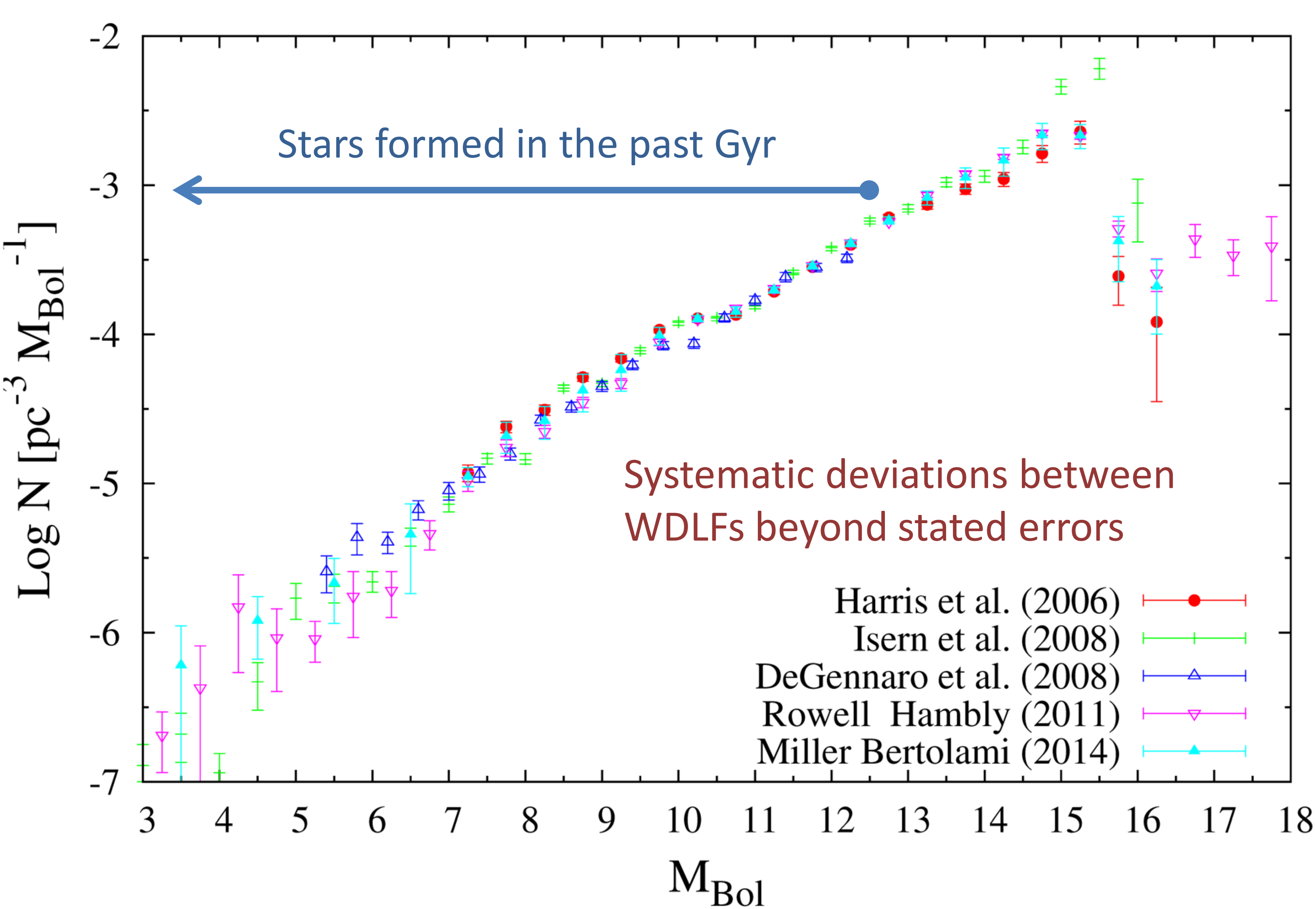

Miller Bertolami, Melendez, Althaus & Isern, arXiv:1406.7712

Axion Bounds from WD Luminosity Function

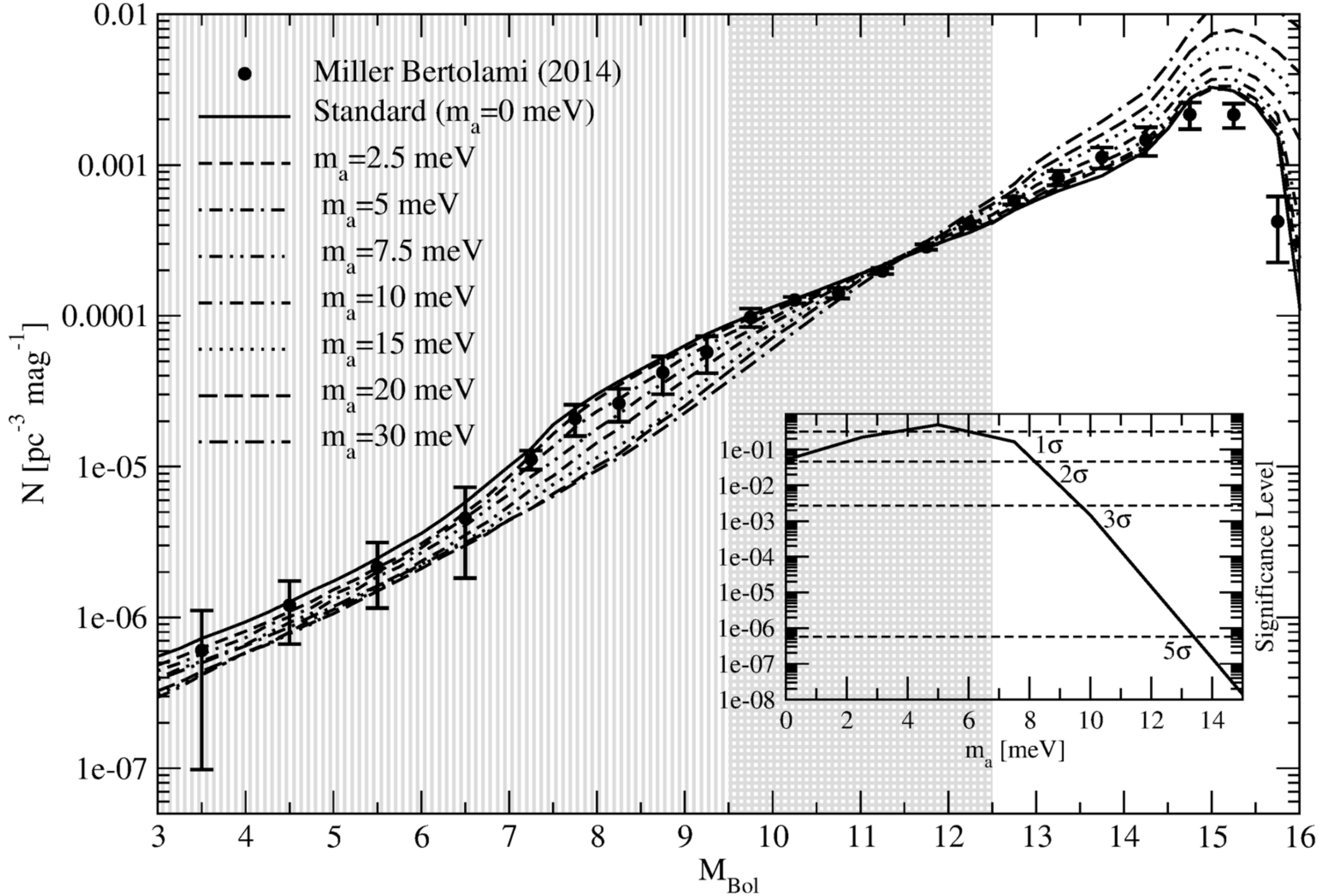

Limits on axion-electron coupling and mass limit in DFSZ model:

$g_{ae} \lesssim 3 \times 10^{-13}$ $\quad$ $m_a \cos^2\beta \lesssim 10\ \mathrm{meV}$

Miller Bertolami, Melendez, Althaus & Isern, arXiv:1406.7712, 1410.1677

For extensions and review see: Isern, arXiv:2002.08069

Period Change of Variable White Dwarfs

Period change $\dot{\Pi}$ of pulsating white darfs depends on cooling speed

White dwarf G117−B15A

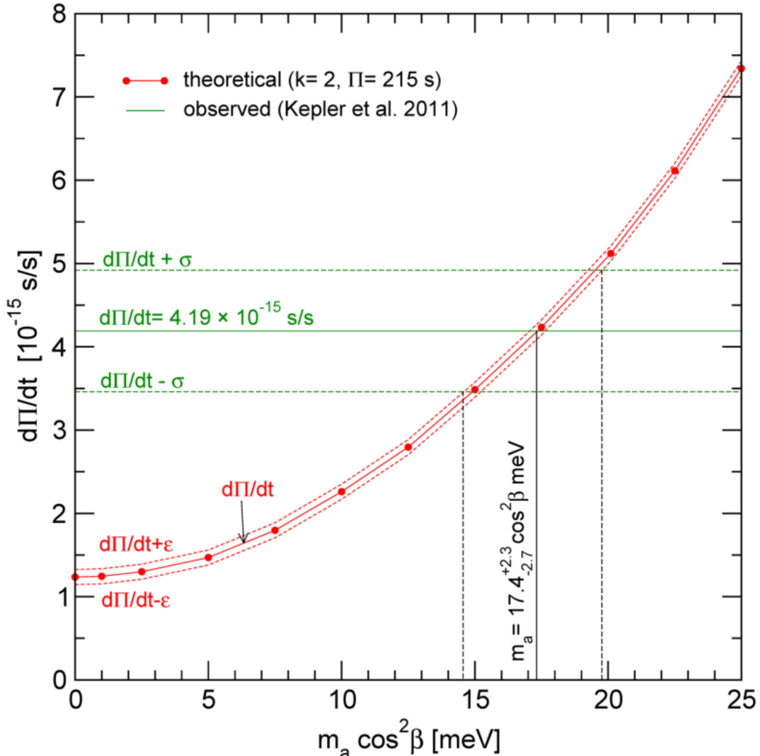

Favored by $\dot{\Pi}$

Córsico et al., arXiv:1205.6180

White dwarf PG 1351+489

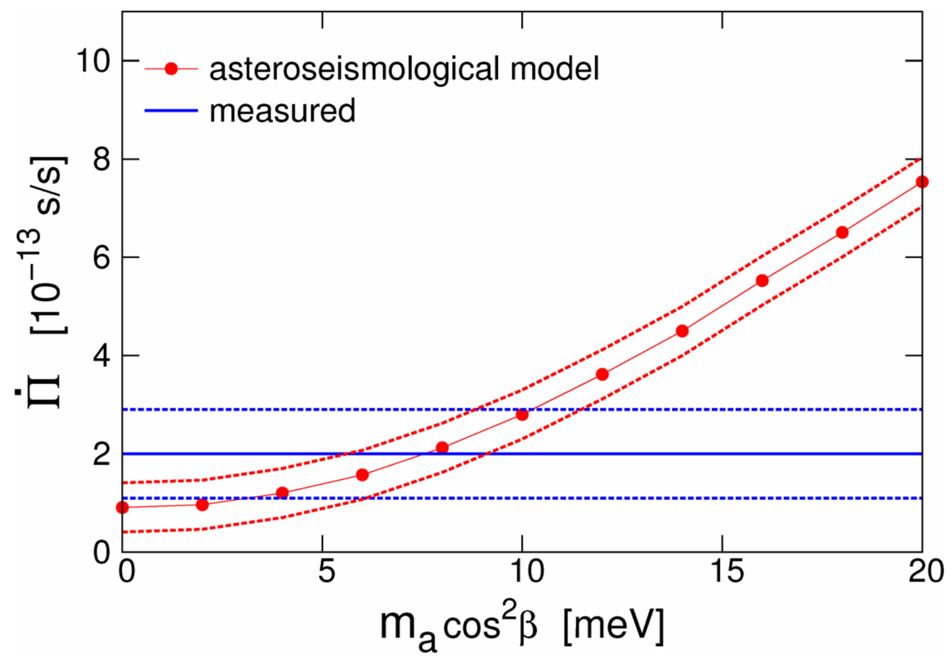

Limited by $\dot{\Pi}$

Battich et al., arXiv:1605.07668

Córsico, Althaus, Miller Bertolami & Kepler: Pulsating white dwarfs: new insights, Astron. Astrophys. Rev. 27 (2019) 7 [1907.00115]

White Dwarf Bounds or Cooling Hint?

Isern: White dwarfs as advanced physics laboratories. The Axion case [2002.08069]

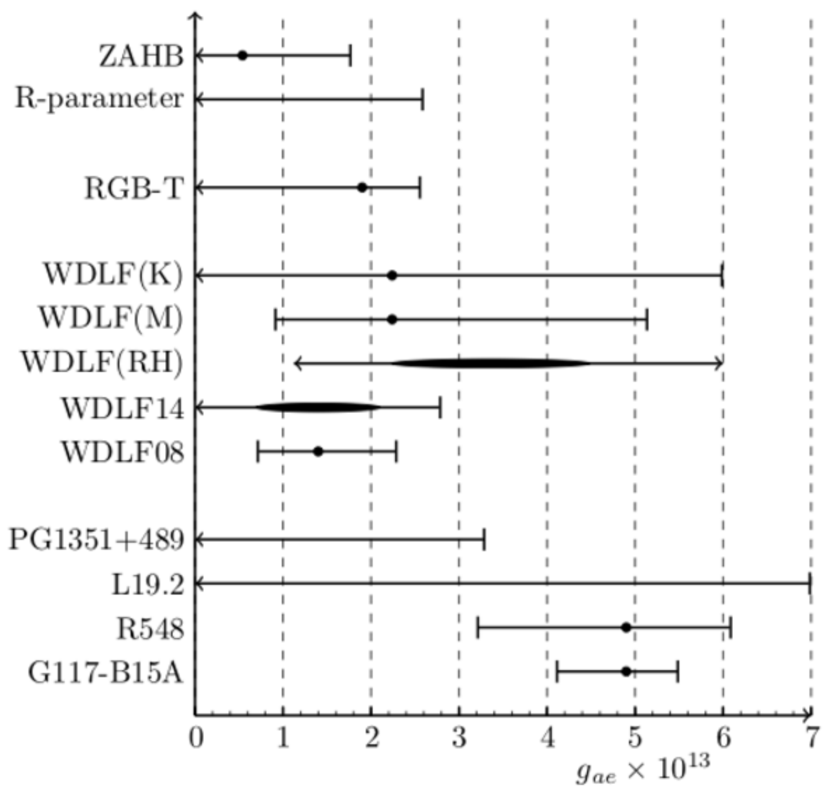

Physics potential of the International Axion Observatory (IAXO) [1904.09155]

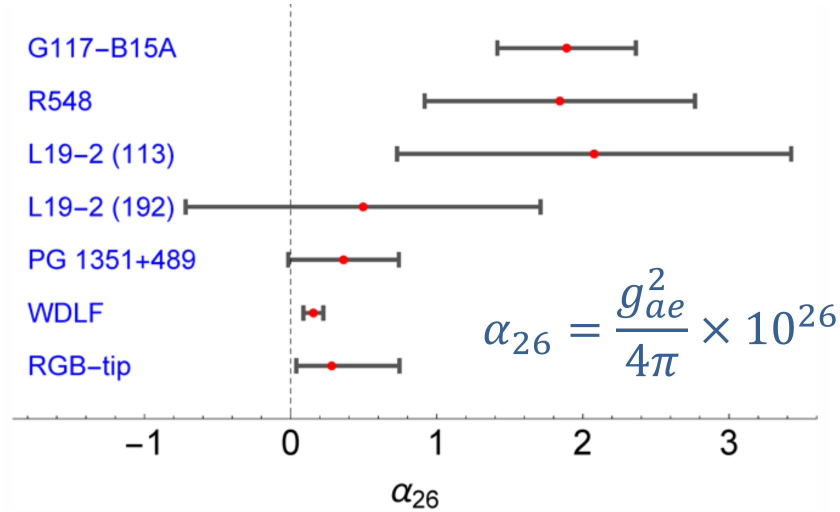

$$\alpha_{26} = \frac{g_{ae}^2}{4\pi} \times 10^{26}$$

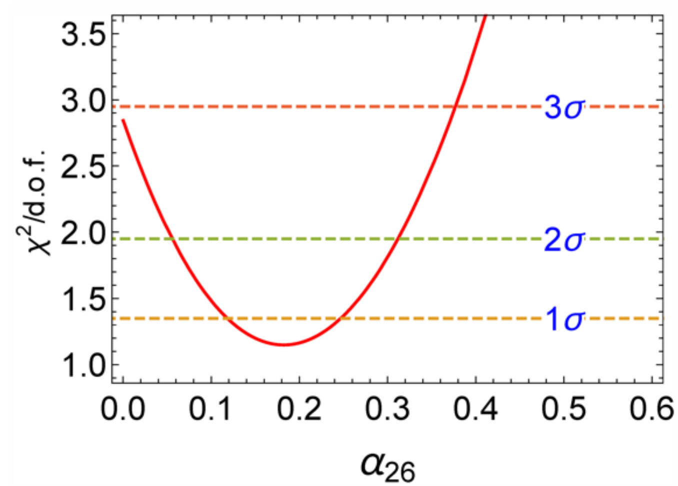

All results improve with a bit of extra cooling …

Photon Dispersion Relation in Stars

Non-relativistic plasma of electrons and nuclei

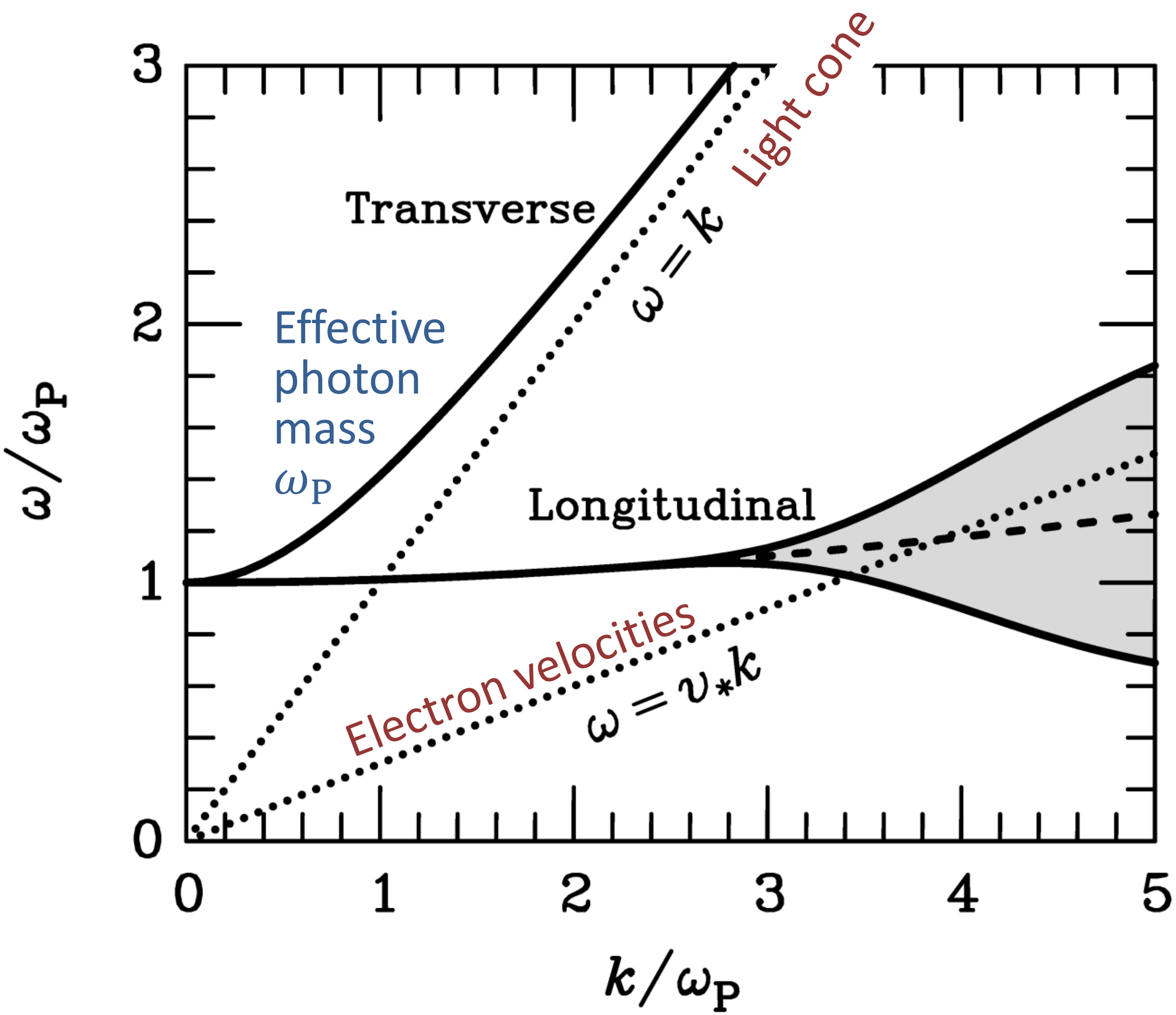

Plasma frequency

$$\omega_P^2 = \frac{4\pi\alpha\, n_e}{m_e}$$

Landau damping
(Cherenkov absorption
on electrons)

Resonant Production of Hidden Photons & Friends

Non-relativistic plasma of electrons and nuclei

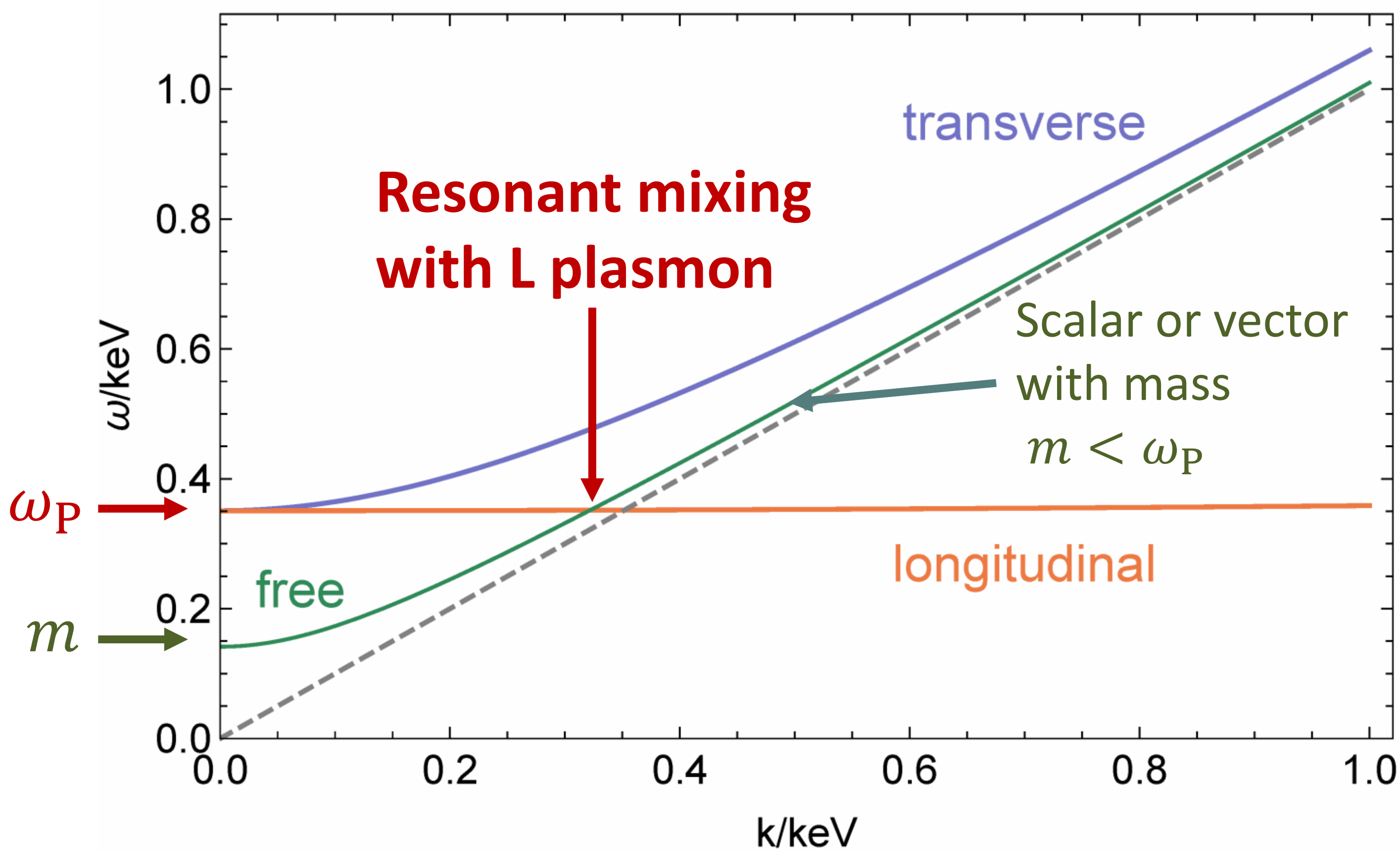

Hardy & Lasenby, arXiv:1611.05852

Hidden Photon Bounds

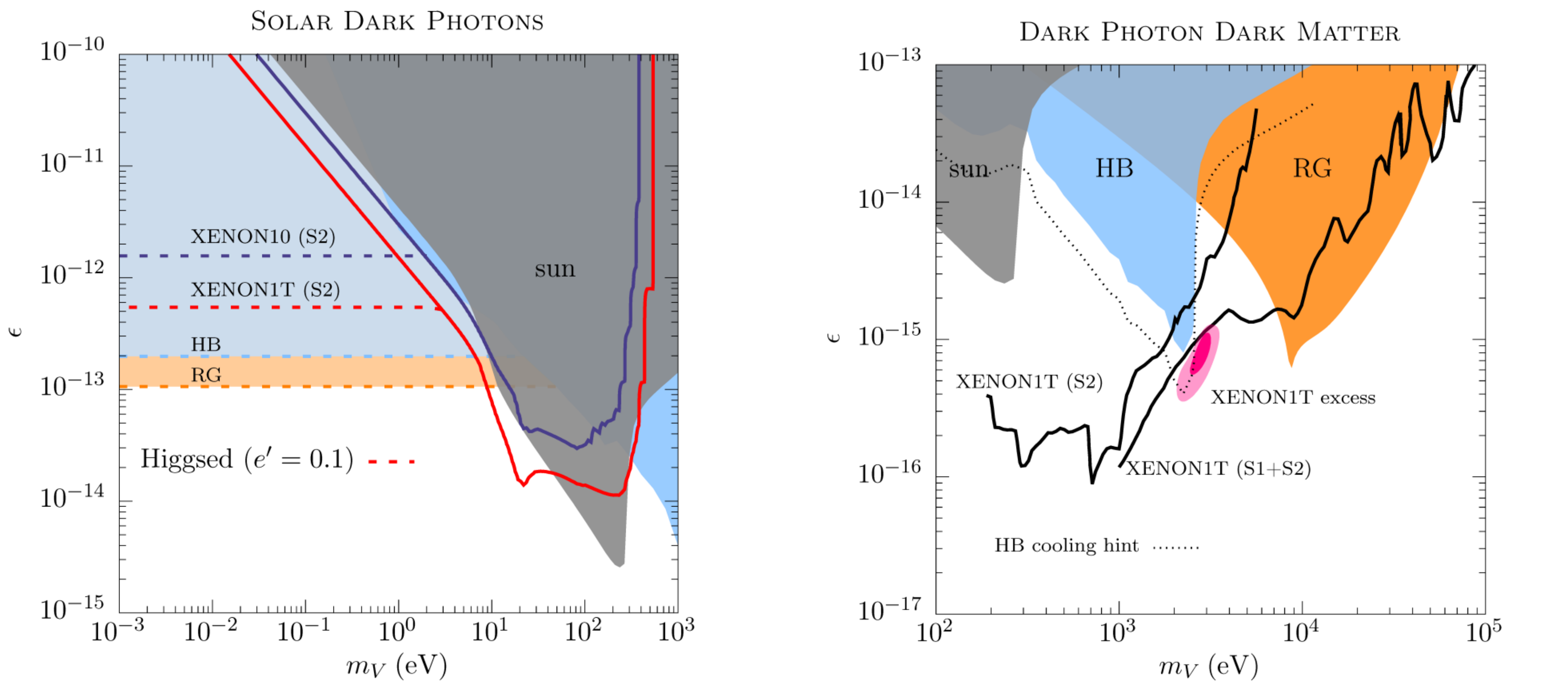

FIG. 1. *Left panel:* Direct detection constraints at 90% C.L. on solar-generated dark photon fluxes in the parameter space of vector mass $m_{A'}$ versus kinetic mixing parameter ϵ. The red (blue) line is derived from the S2-only reported data by XENON1T [8] (XENON10 [26]). Solid lines apply to a "hard" Stückelberg mass and dashed lines show how the constraint continues for a "soft" Higgsed dark photon mass with $e' = 0.1$ and following [22]. Cooling constraints from the sun, and for HB and RG stars as labeled are derived following [6, 24]. *Right panel:* Dark photon dark matter parameter space showing the favored region from a fit to XENON1T data [9] (1σ and 2σ ellipses). Official limits by the XENON1T collaboration using S2 [8] and S1+S2 [9] data are shown by the solid black lines as labeled. The HB constraint (and cooling hint, dotted line) are taken from [31] and the solar and RG constraints are derived following [6, 24]; see the main text for a discussion of the latter bounds.

An, Pospelov, Pradler & Ritz, arXiv:2006.13929 (24 June 2020)

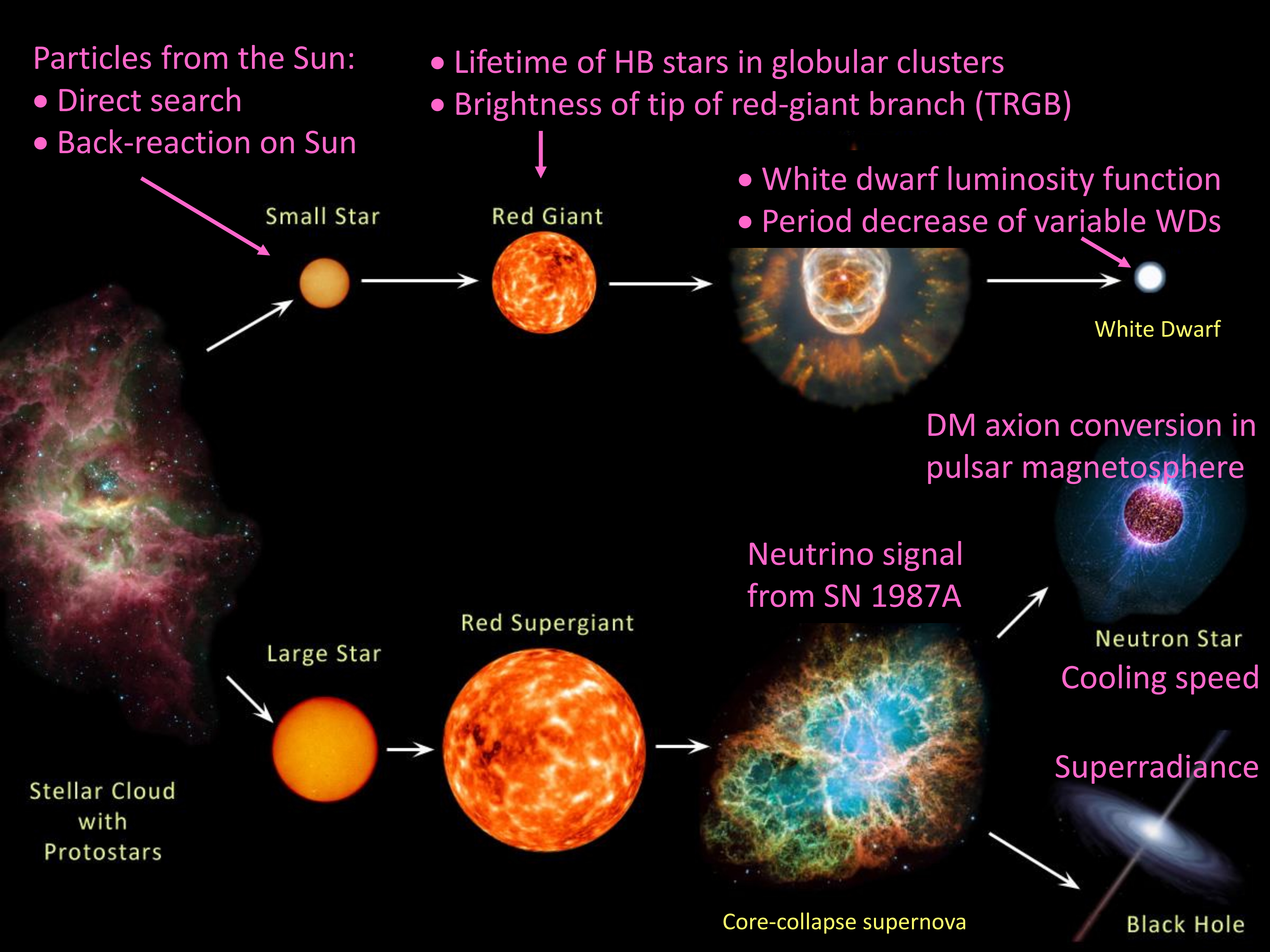
Particles from the Sun:
• Direct search
• Back-reaction on Sun
• Lifetime of HB stars in globular clusters
• Brightness of tip of red-giant branch (TRGB)
Small Star
Red Giant
• White dwarf luminosity function
• Period decrease of variable WDs
White Dwarf
DM axion conversion in pulsar magnetosphere
Neutrino signal from SN 1987A
Neutron Star
Cooling speed
Large Star
Red Supergiant
Superradiance
Stellar Cloud with Protostars
Core-collapse supernova
Black Hole

Crab Nebula – Remnant of SN 1054

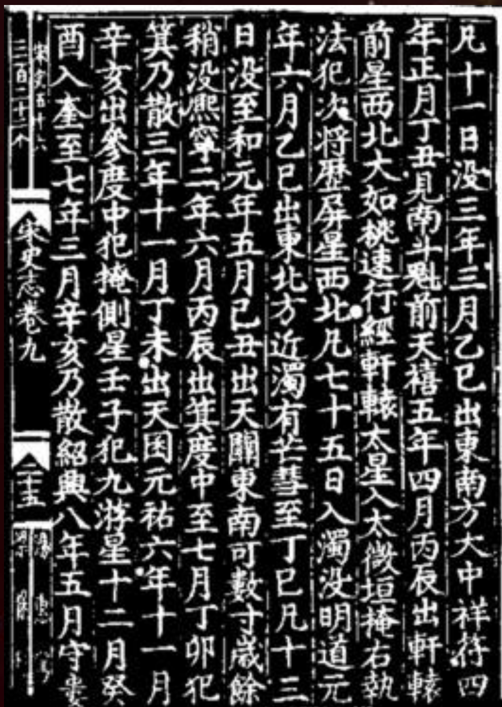

凡十一日沒三年三月乙巳出東南方大中祥符四
年正月丁丑見南斗魁前天禧五年四月丙辰出軒轅
前星西北大如桃速行經軒轅太星入太微垣掩右執
法犯次將歷屏星西北凡七十五日入濁沒明道元
年六月乙巳出東北方近濁有芒彗至丁巳凡十三
日沒至和元年五月己丑出天關東南可數寸歲餘
稍沒熙寧二年六月丙辰出箕度中至七月丁卯犯
箕乃散三年十一月丁未出天囷元祐六年十一月
辛亥出參度中犯掩側星壬子犯九斿星十二月癸
酉入奎至七年三月辛亥乃散紹興八年五月守婁

宋史志卷九

Crab Pulsar

Chandra x-ray images

Supernova Remnant in Cas A (SN 1680?)

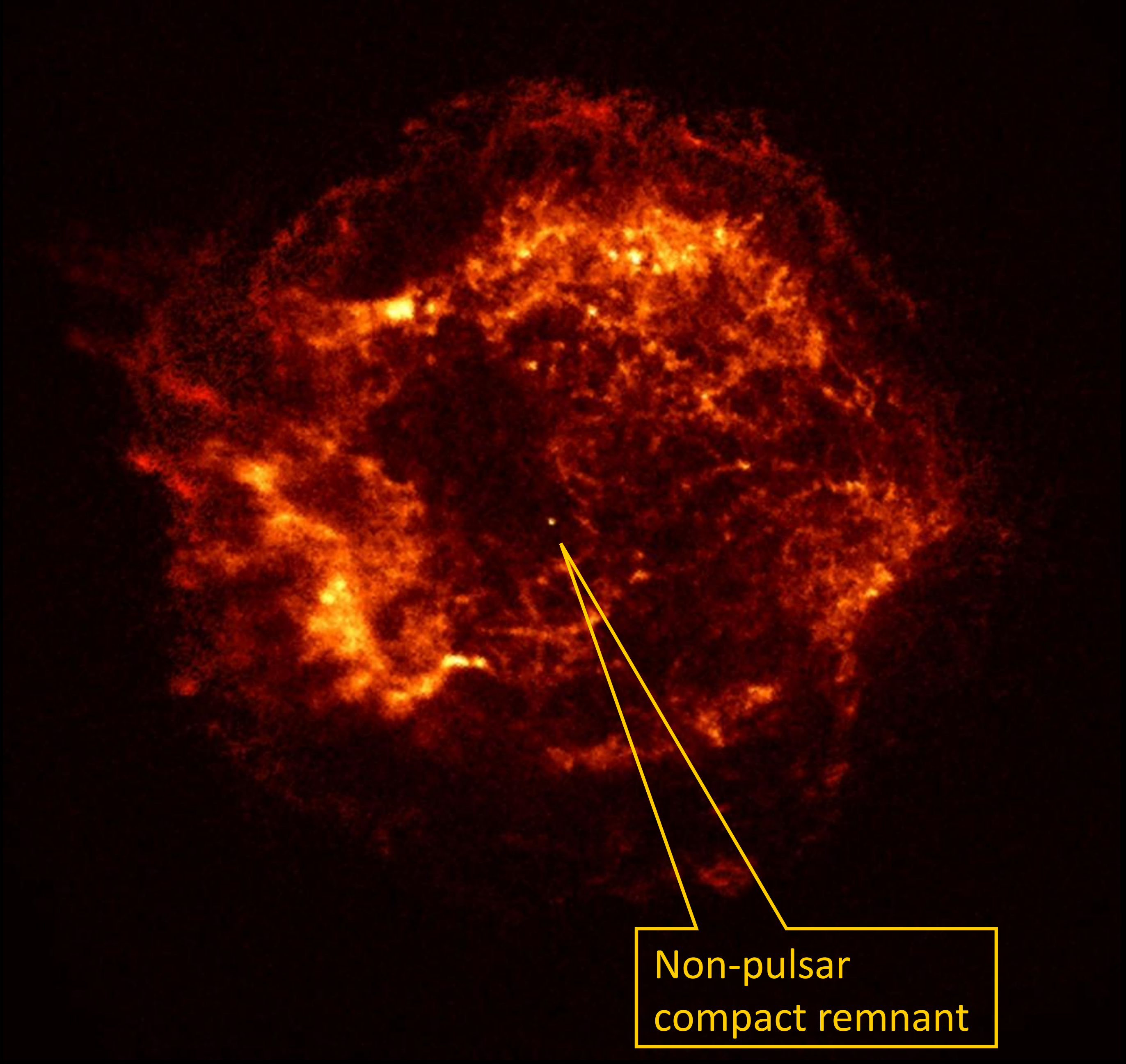

Chandra
x-ray image

Stellar Collapse and Supernova Explosion

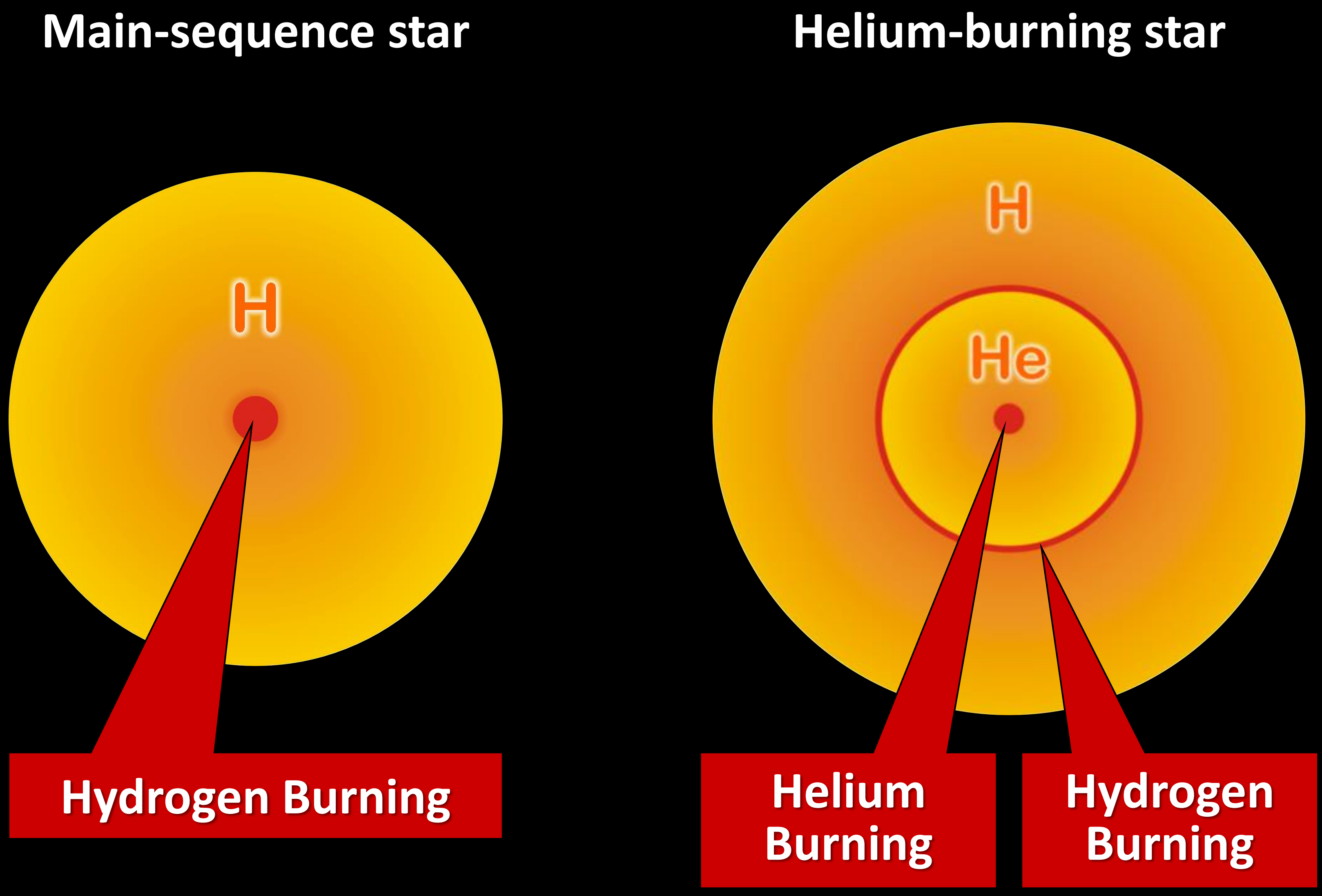

Stellar Collapse and Supernova Explosion

Onion structure

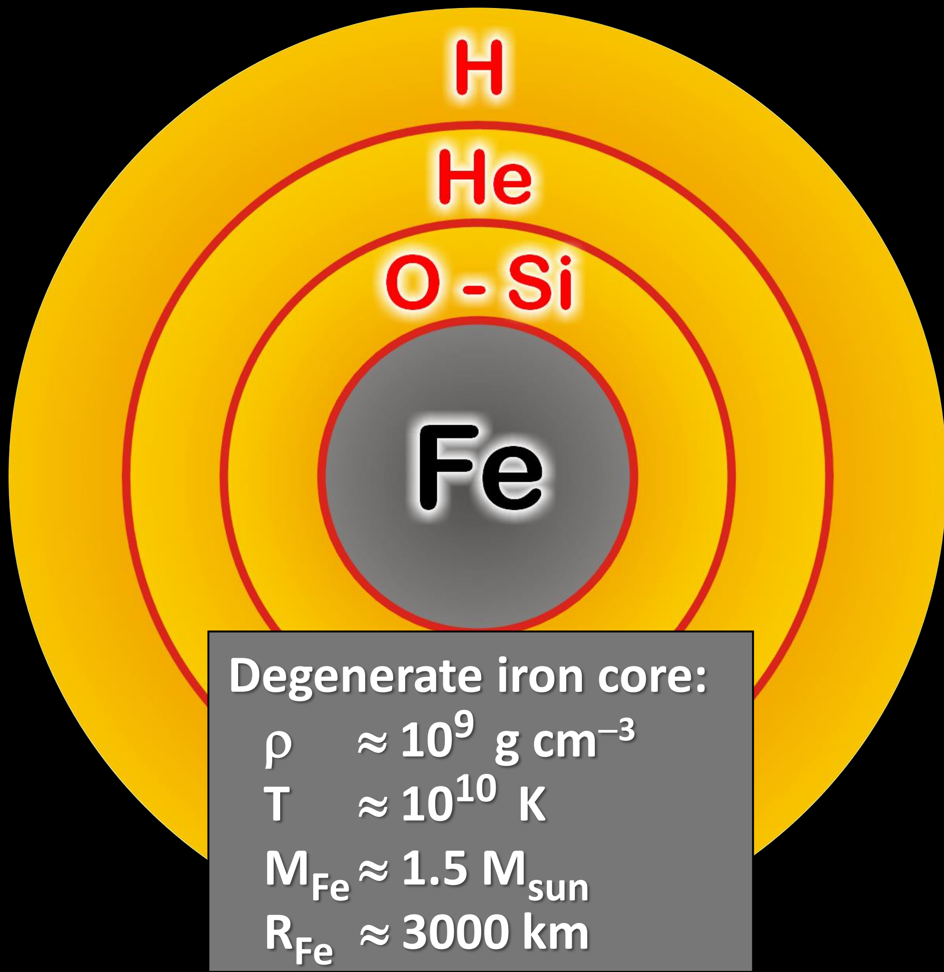

Helium-burning star

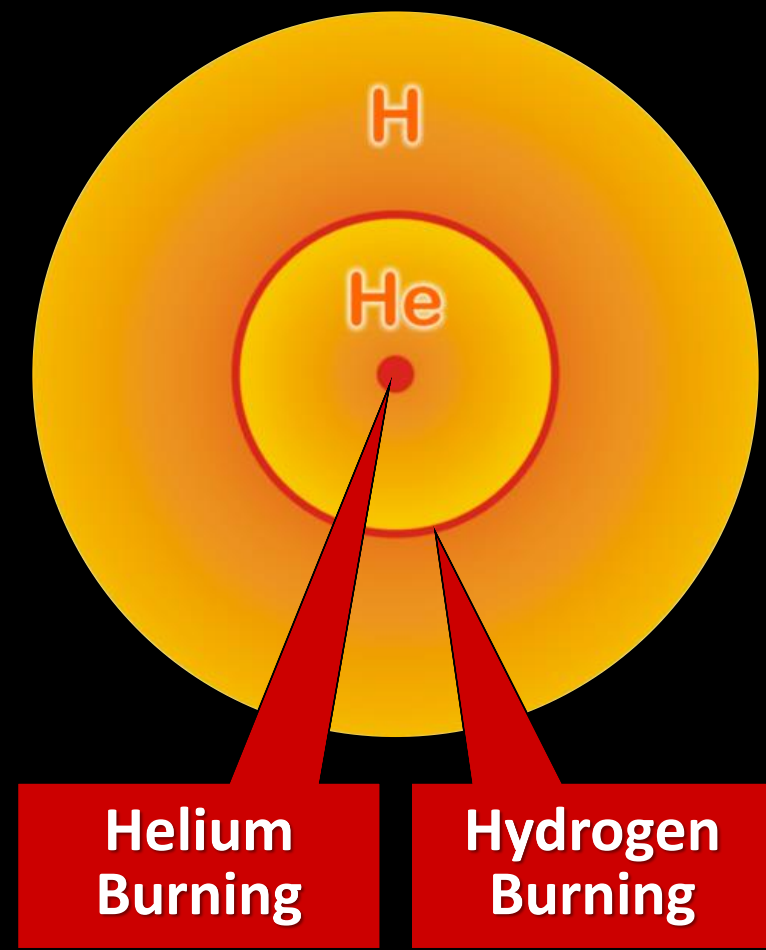

Stellar Collapse and Supernova Explosion

Onion structure | **Collapse (implosion)**

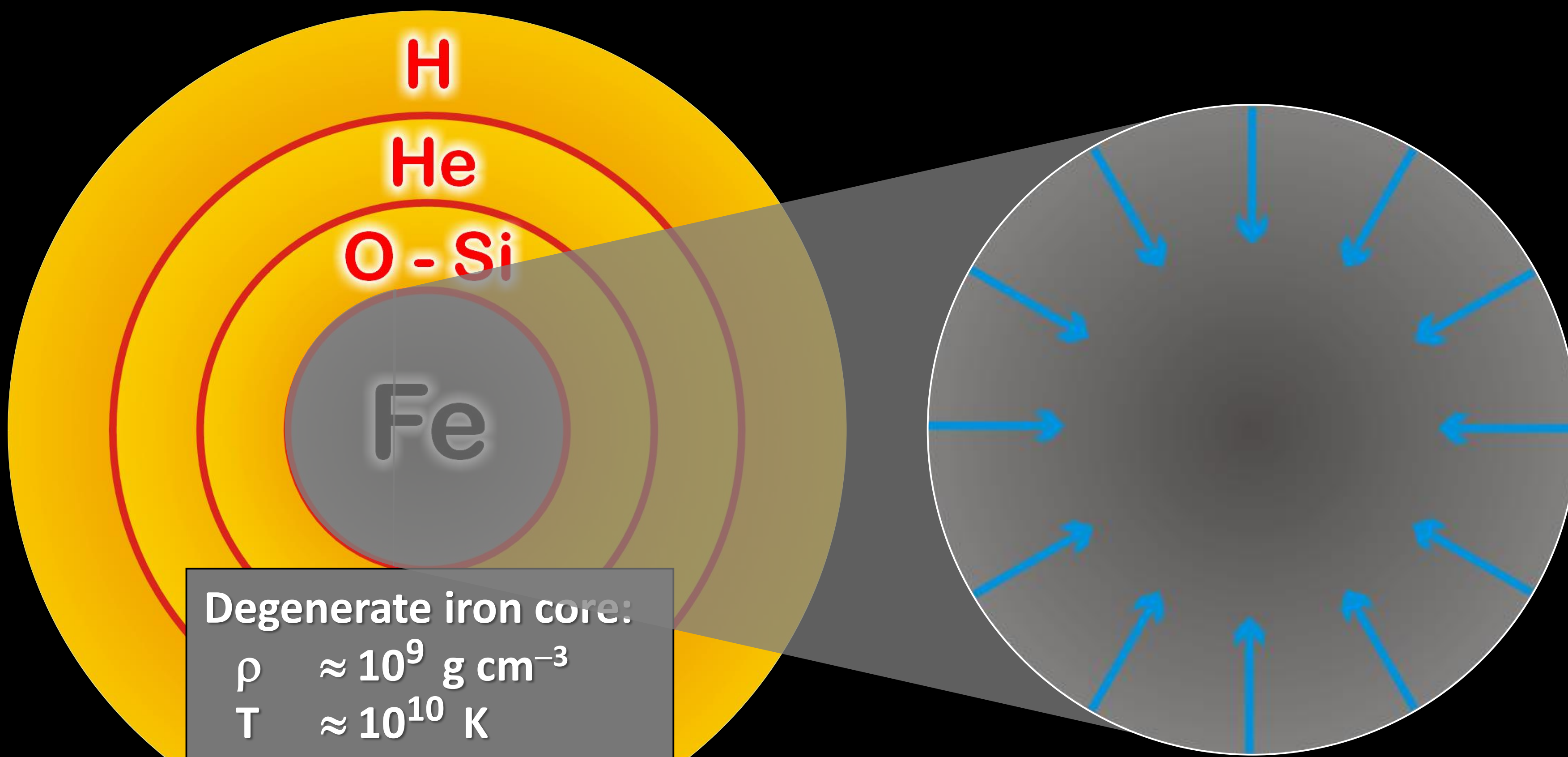

Degenerate iron core:

- $\rho \approx 10^{9}$ g cm^{-3}
- $T \approx 10^{10}$ K
- $M_{Fe} \approx 1.5\ M_{sun}$
- $R_{Fe} \approx 3000$ km

Stellar Collapse and Supernova Explosion

Newborn Neutron Star | **Explosion**

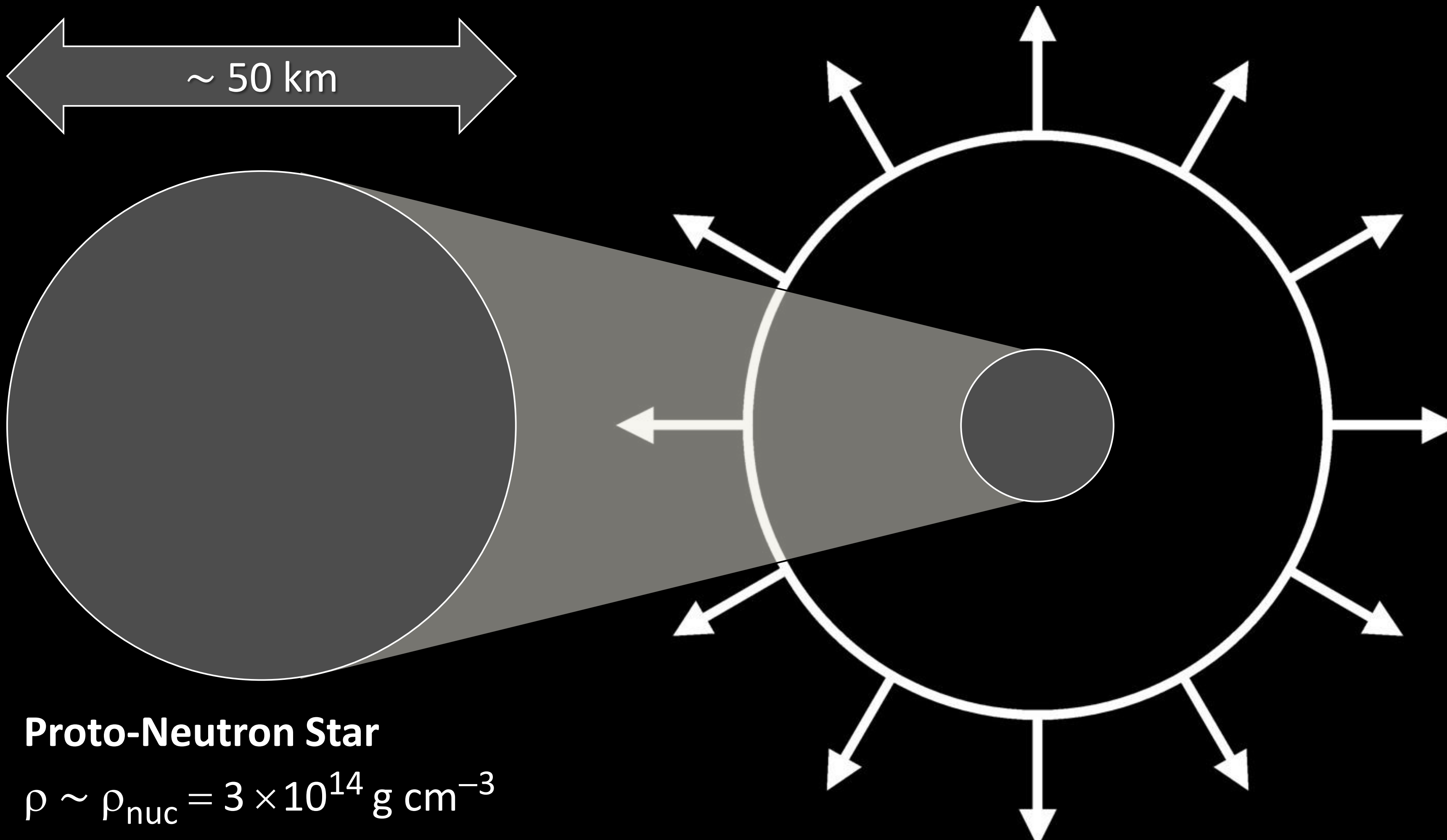

Proto-Neutron Star

$\rho \sim \rho_{nuc} = 3 \times 10^{14}\ \mathrm{g\ cm^{-3}}$

$T \sim 10\ \mathrm{MeV}$

Stellar Collapse and Supernova Explosion

Newborn Neutron Star

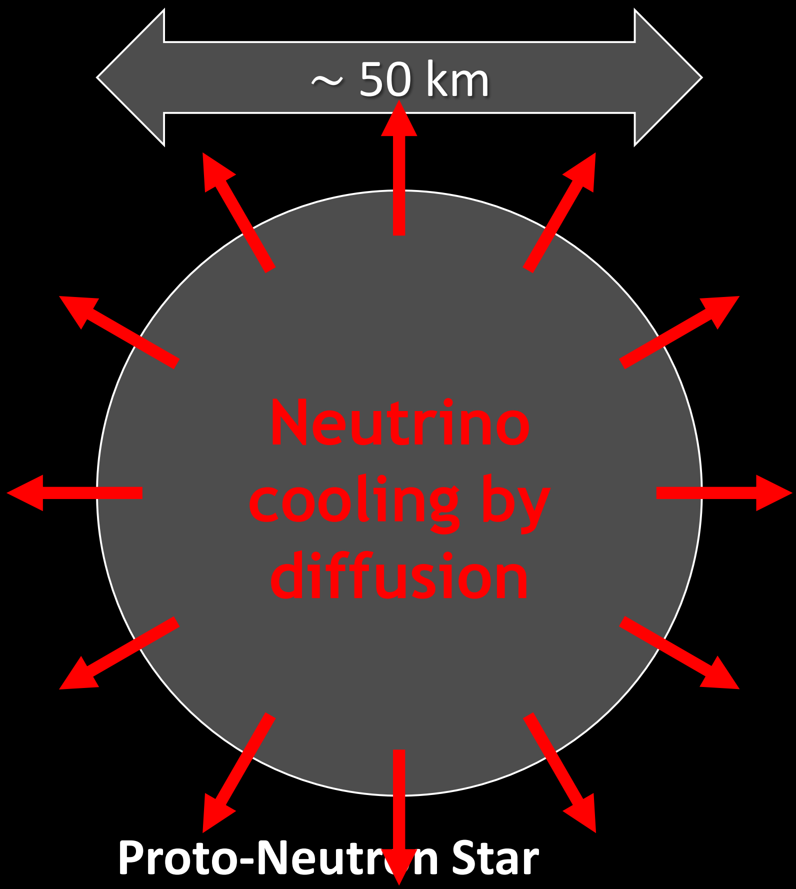

Proto-Neutron Star

$\rho \sim \rho_{nuc} = 3 \times 10^{14}\ \mathrm{g\ cm^{-3}}$

$T \sim 10$ MeV

Gravitational binding energy

$$E_b \approx 3 \times 10^{53}\ \mathrm{erg} \approx 17\%\ M_{SUN}\, c^2$$

This shows up as

99% Neutrinos

1% Kinetic energy of explosion

0.01% Photons, outshine host galaxy

Neutrino luminosity

$$L_\nu \sim 3 \times 10^{53}\ \mathrm{erg} / 3\ \mathrm{sec}$$
$$\sim 3 \times 10^{19}\ L_{SUN}$$

While it lasts, outshines the entire visible universe

Why No Prompt Explosion?

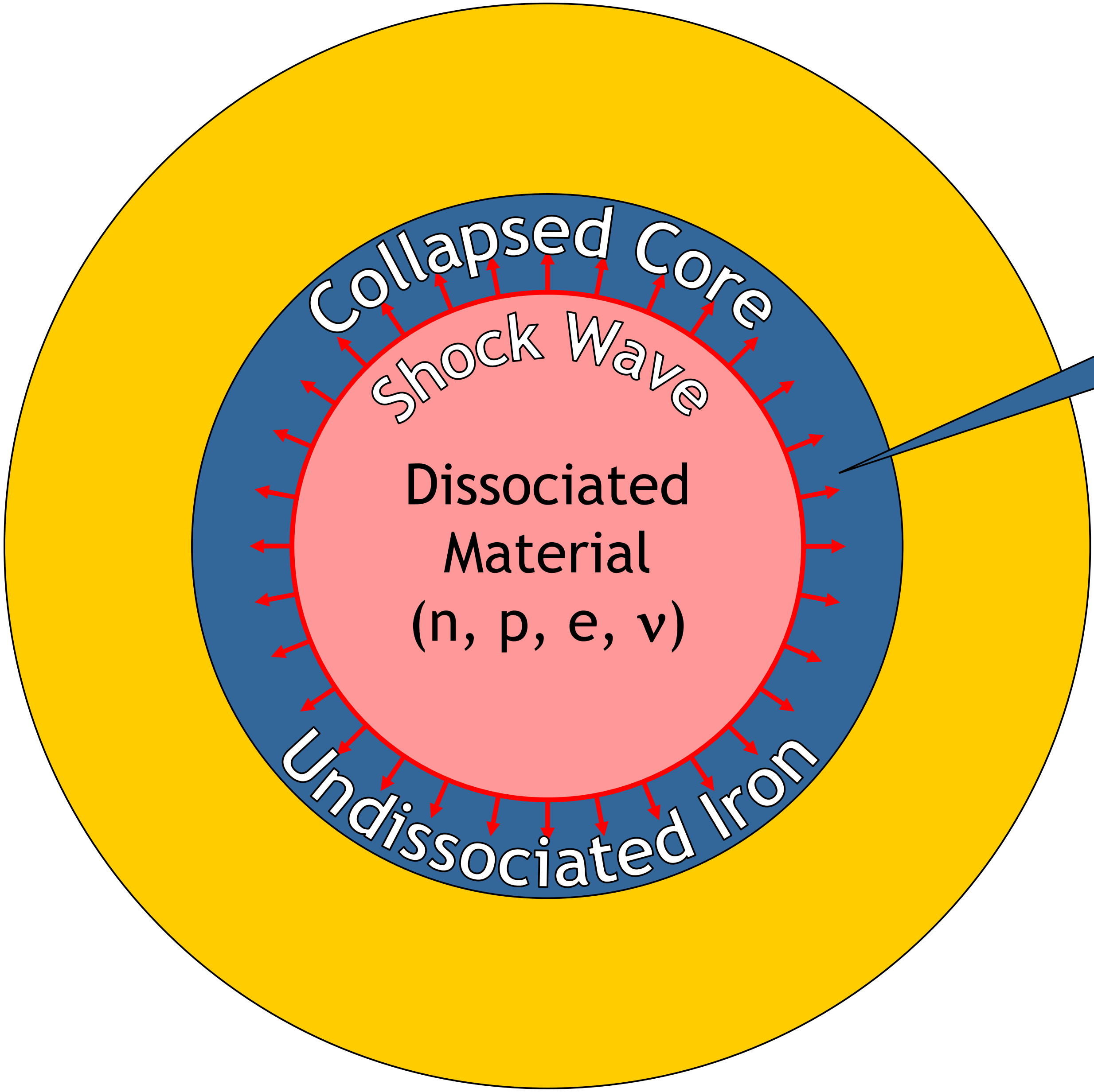

- $0.1\ M_{sun}$ of iron has a nuclear binding energy $\approx 1.7 \times 10^{51}$ erg
- Comparable to explosion energy

- **Shock wave forms within the iron core**
- **Dissipates its energy by dissociating the remaining layer of iron**

Supernova Delayed Explosion Scenario

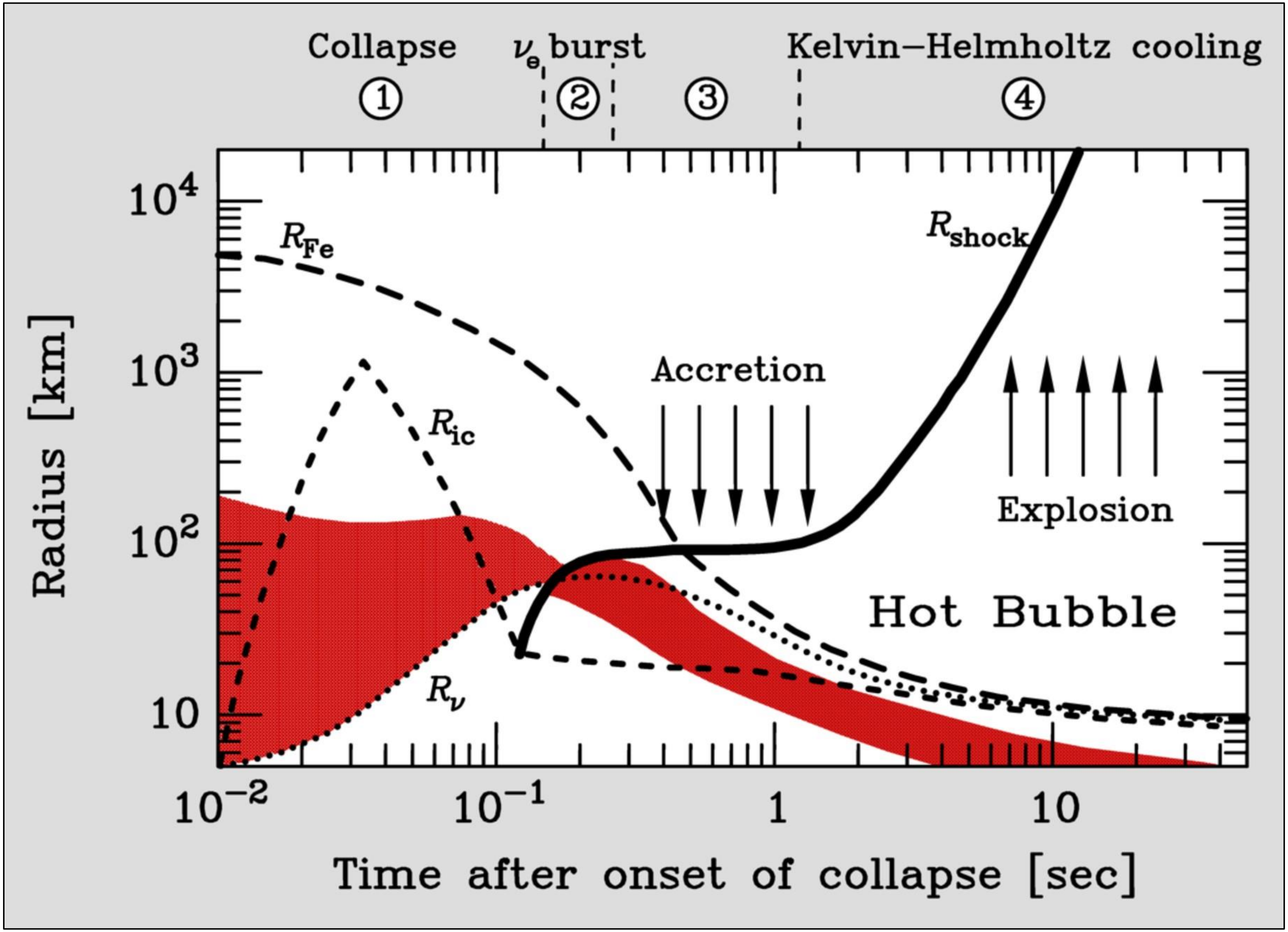

Three Phases of Neutrino Emission

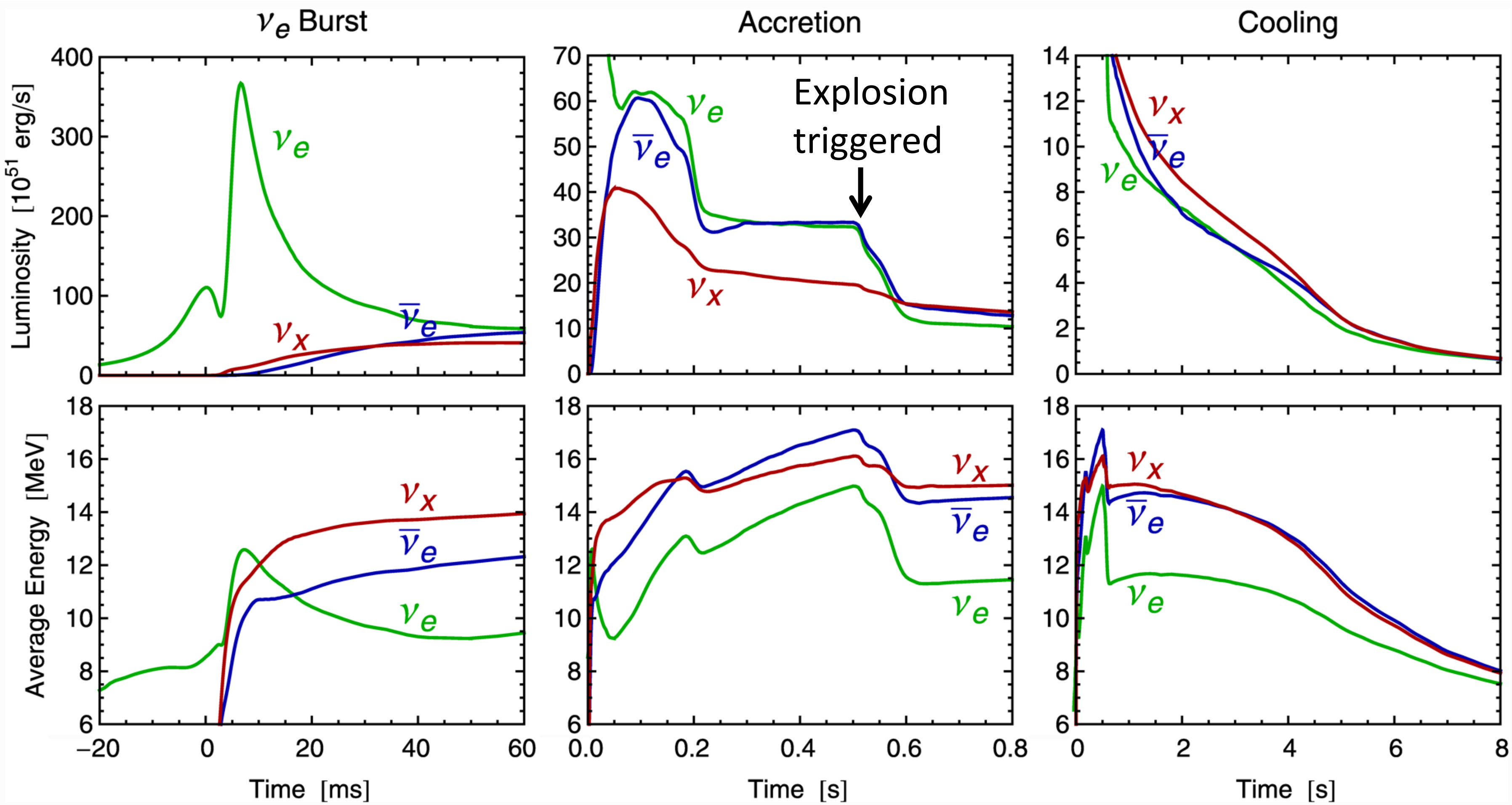

- Shock breakout
- De-leptonization of outer core layers

- Shock stalls ~ 150 km
- Neutrinos powered by infalling matter

Cooling on neutrino diffusion time scale

Spherically symmetric Garching model (25 $M_\odot$) with Boltzmann neutrino transport

Death Watch of a Million Supergiants

- Monitoring 27 galaxies within 10 Mpc for many years
- Visit typically twice per year
- 10^6 supergiants (lifetime 10^6 years)
- Combined SN rate: about 1 per year

First 7 years of survey:

- 6 successful core-collapse SNe
- 1 candidate failed SN

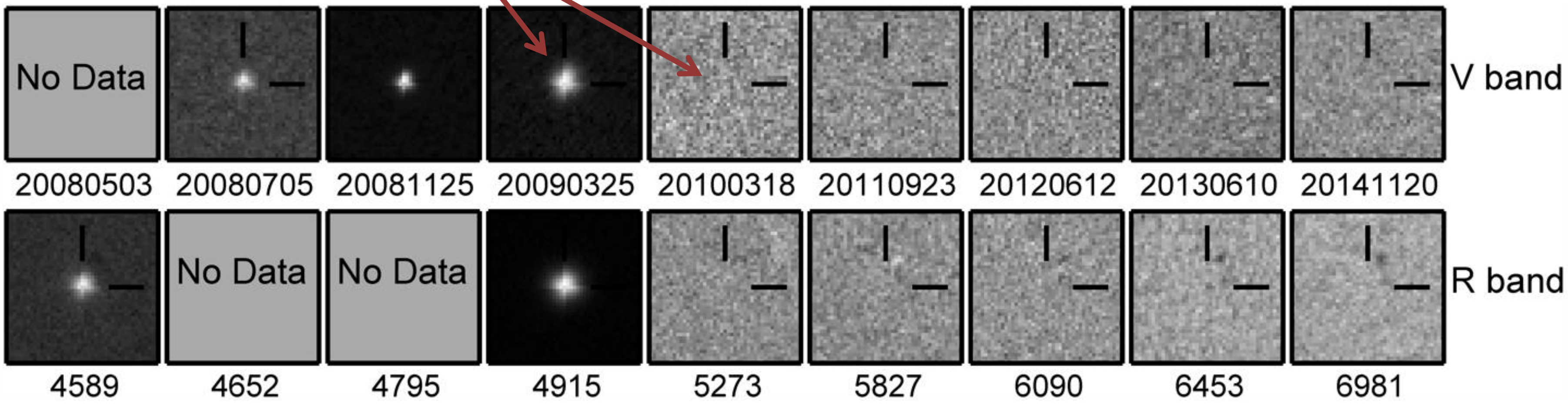

Gerke, Kochanek & Stanek, arXiv:1411.1761

Adams, Kochanek, Gerke, Stanek (& Dai), arXiv:1610.02402 (1609.01283)

Neutrino-Driven Mechanism – Modern Version

- Stalled accretion shock pushed out to ~150 km as matter piles up on the PNS
- Heating (gain) region develops within some tens of ms after bounce
- Convective overturn & shock oscillations (SASI) enhance efficiency of ν-heating, finally revives shock
- Successful explosions in 1D and 2D for different progenitor masses (e.g. Garching group)
- Details important (treatment of GR, ν interaction rates, etc.)
- First self-consistent 3D studies being performed, sometimes successful explosions

→ 3D Model of Princeton Group

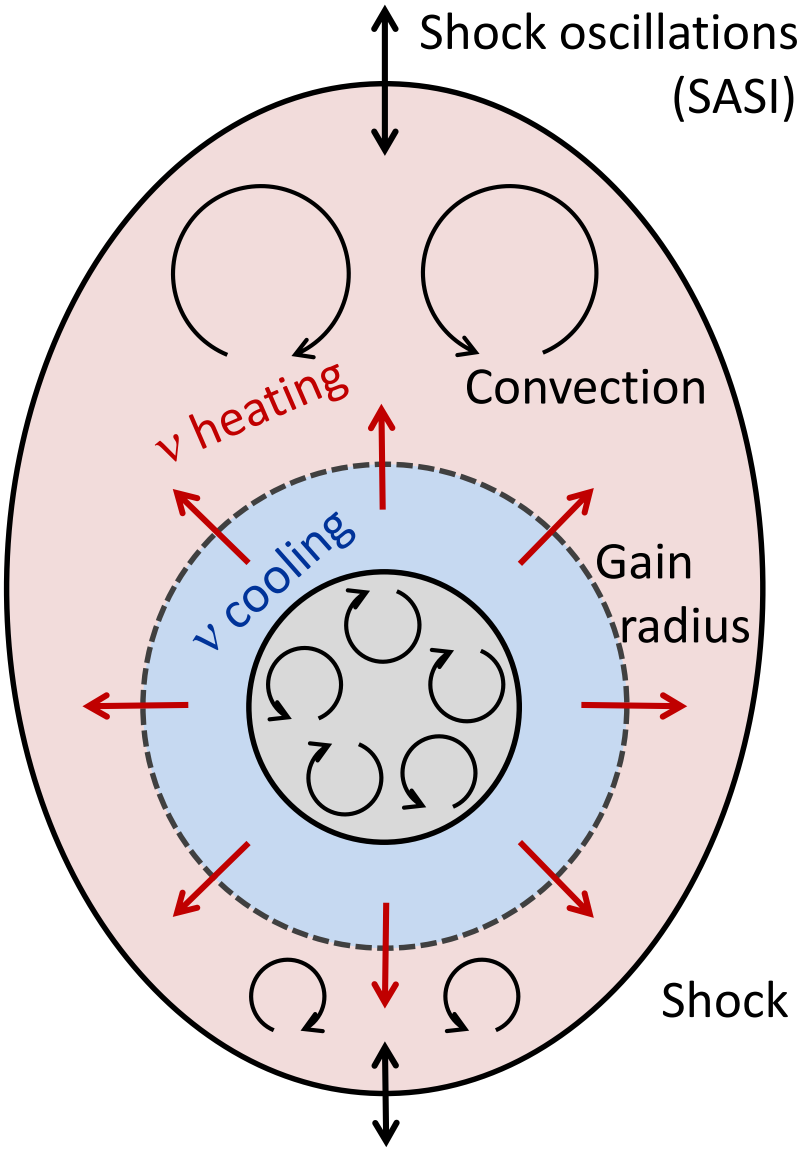

Adapted from B. Müller

Exploding 3D Garching Model (20 M_{SUN})

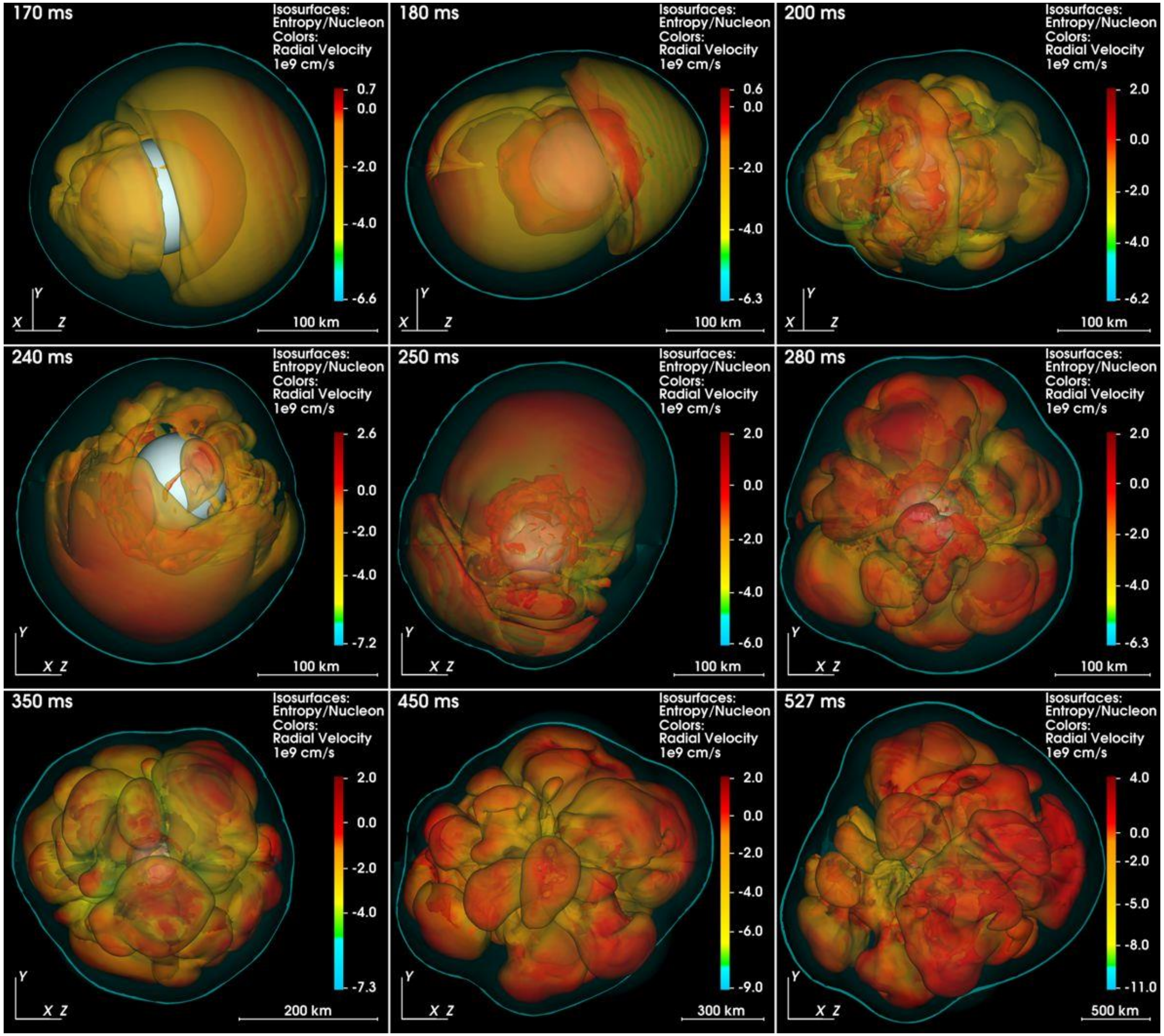

Melson, Janka, Bollig, Hanke, Marek & Müller, arXiv:1504.07631


Sanduleak –69 202


Tarantula Nebula


Large Magellanic Cloud
Distance 50 kpc
(160.000 light years)

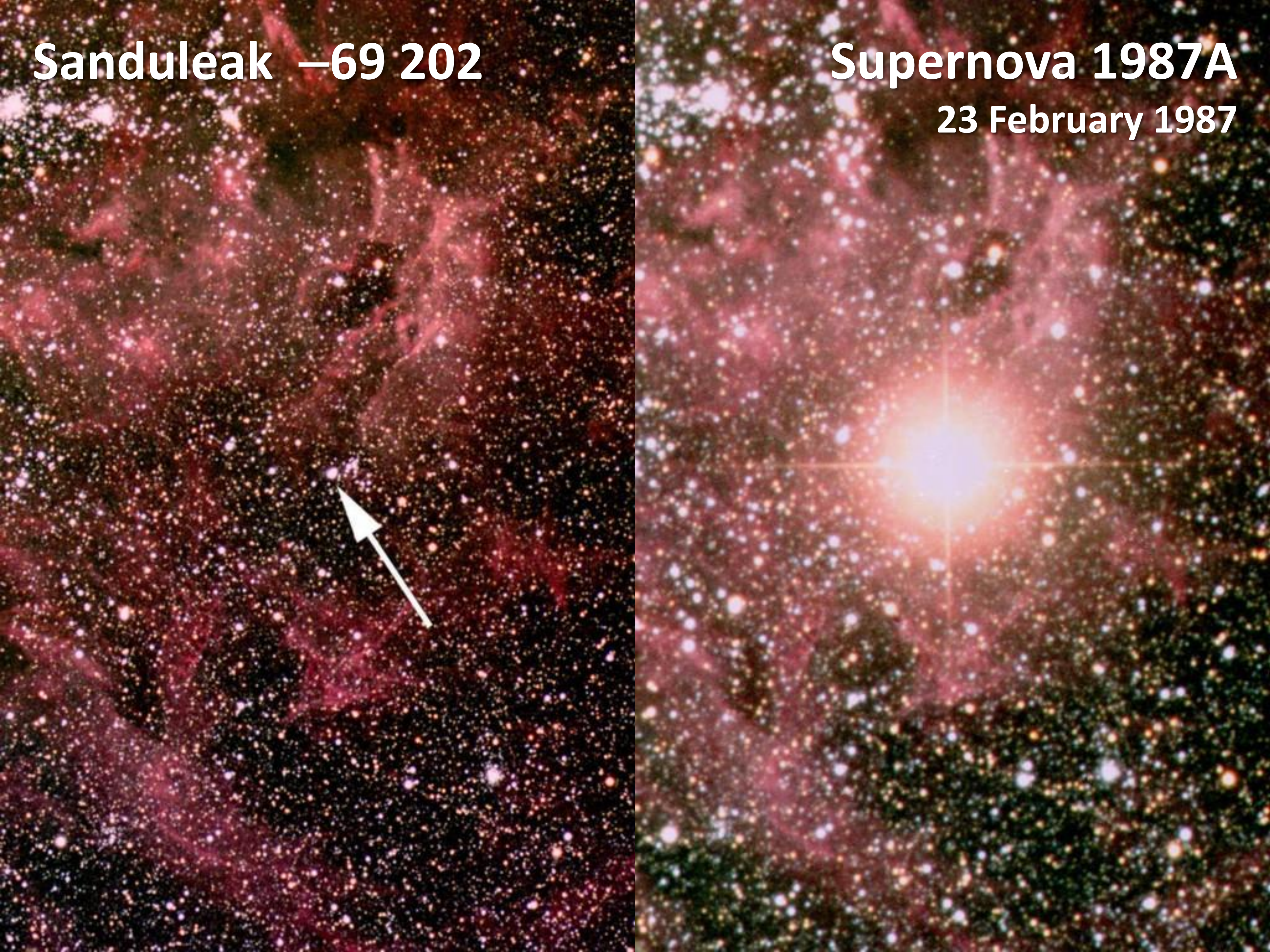
Sanduleak –69 202
Supernova 1987A
23 February 1987

SN 1987A Rings (Hubble Space Telescope 4/1994)

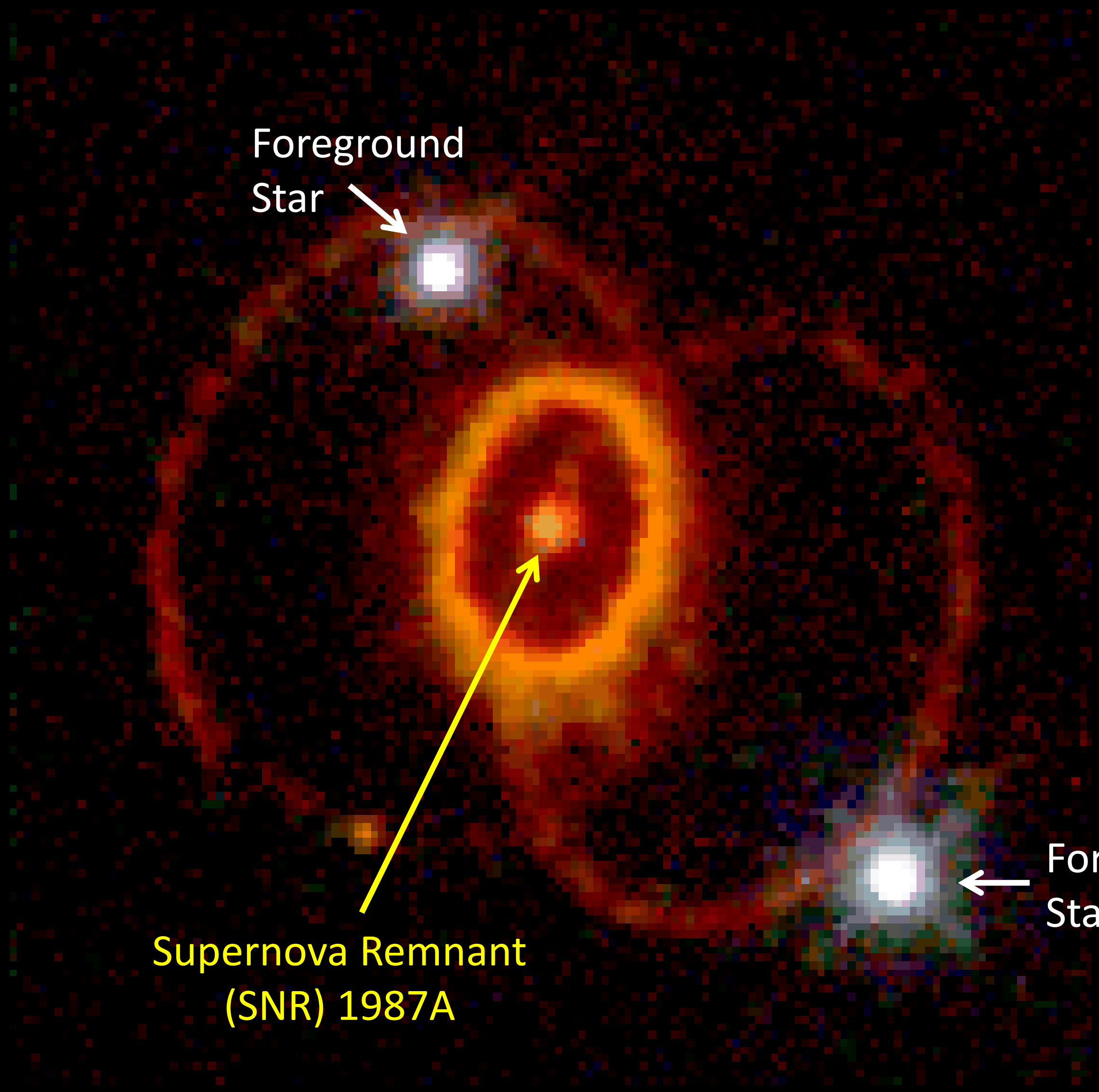

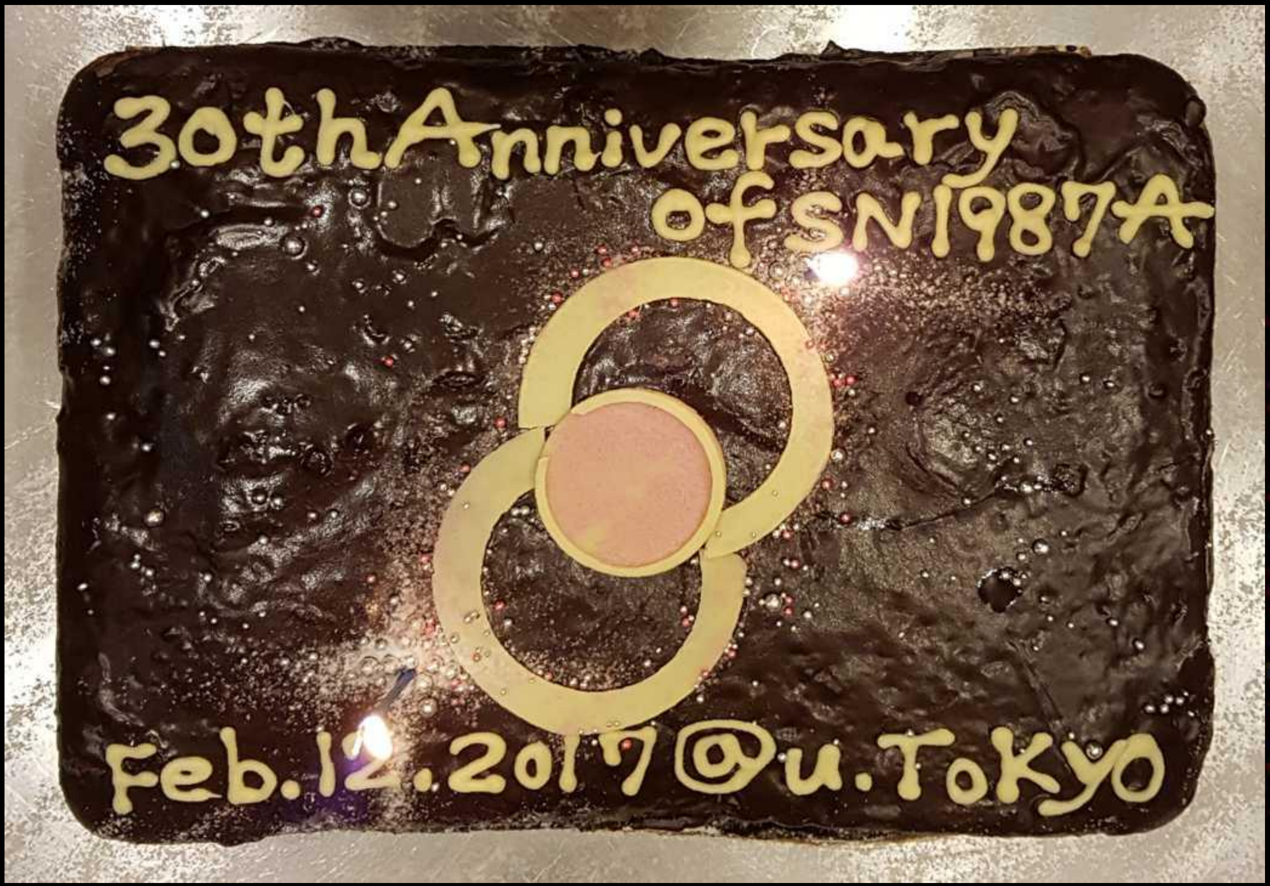
30th Anniversary
of SN1987A
Feb.12.2017@u.Tokyo

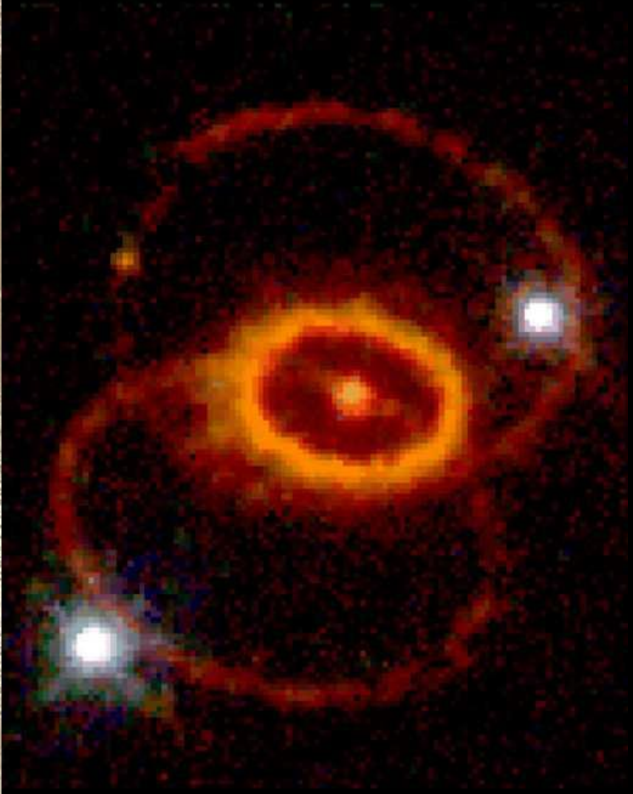

Neutrino Signal of Supernova 1987A

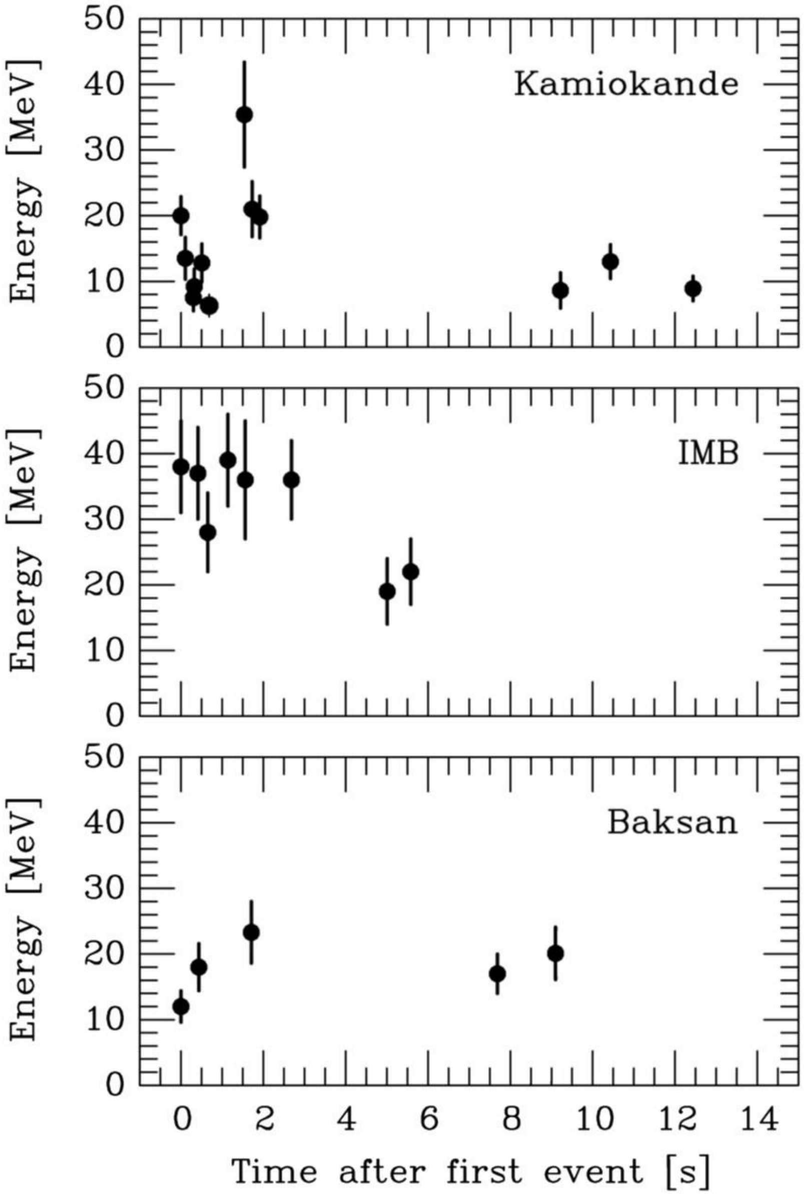

Kamiokande-II (Japan)
Water Cherenkov detector
2140 tons
Clock uncertainty ±1 min

Irvine-Michigan-Brookhaven (US)
Water Cherenkov detector
6800 tons
Clock uncertainty ±50 ms

Baksan Scintillator Telescope
(Soviet Union), 200 tons
Random event cluster ~ 0.7/day
Clock uncertainty +2/–54 s

Within clock uncertainties, all signals are contemporaneous

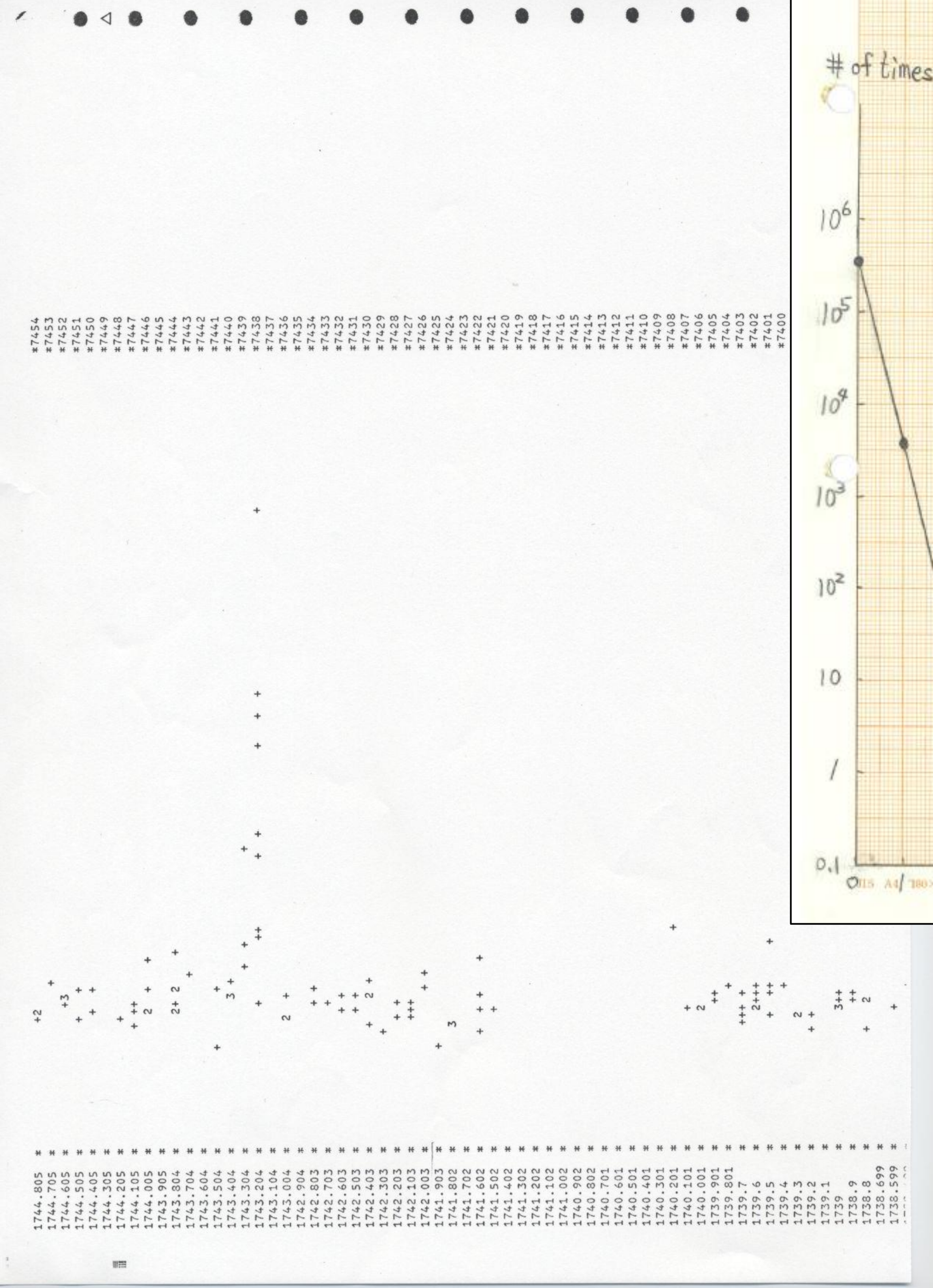

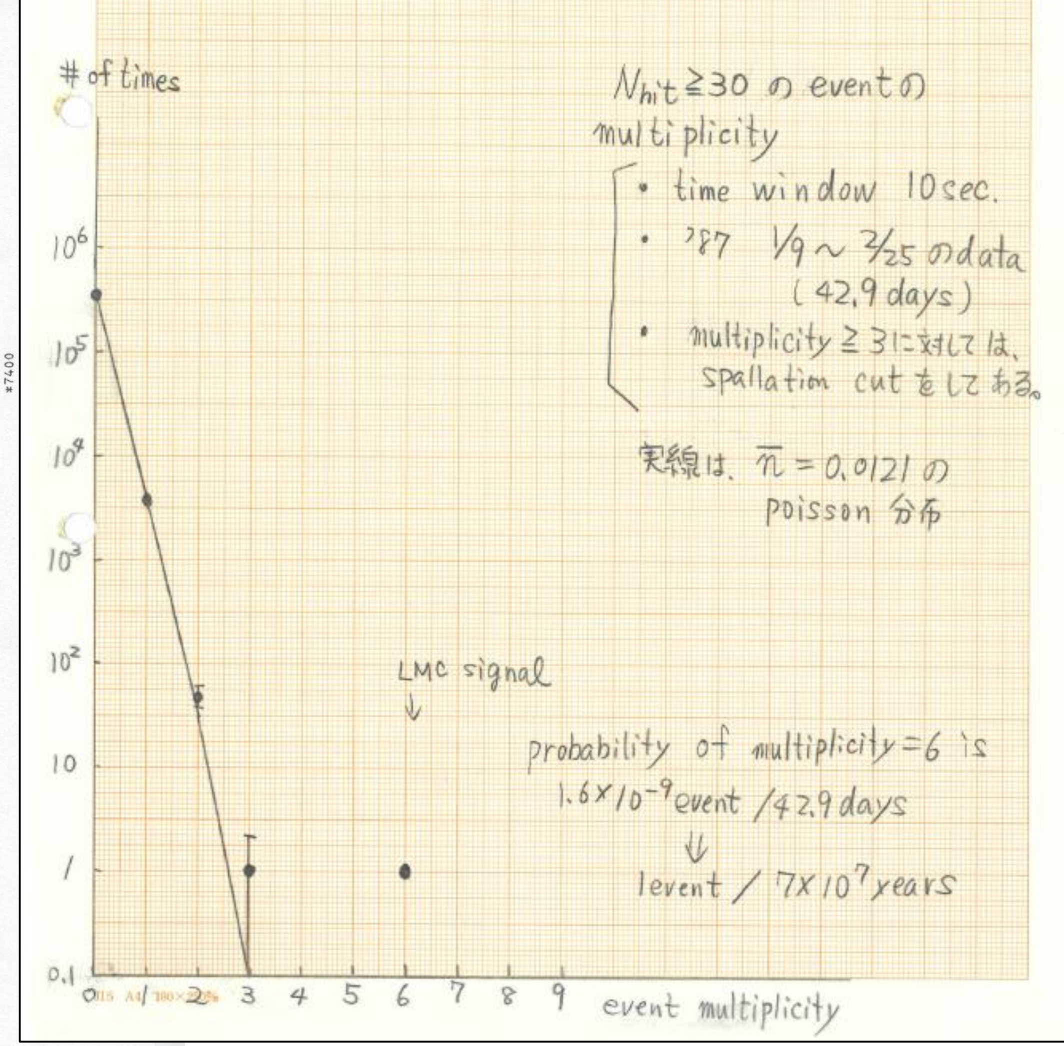

M.Nakahata's notes after the analysis (now director of Kamioka Observatory)

SN 1987A Event No.9 in Kamiokande

Kamiokande-II Detector
(2140 tons of water)

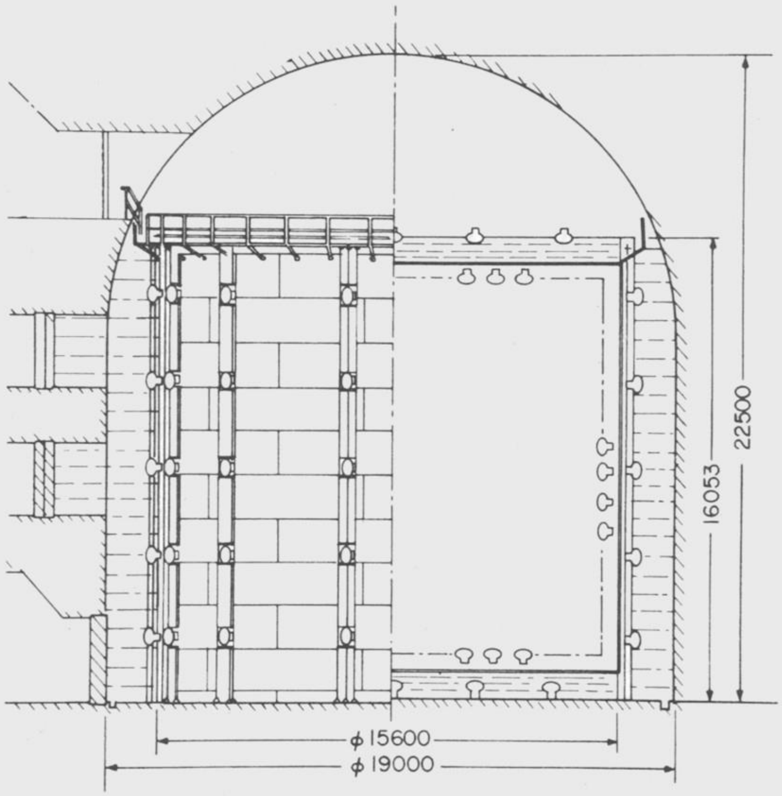

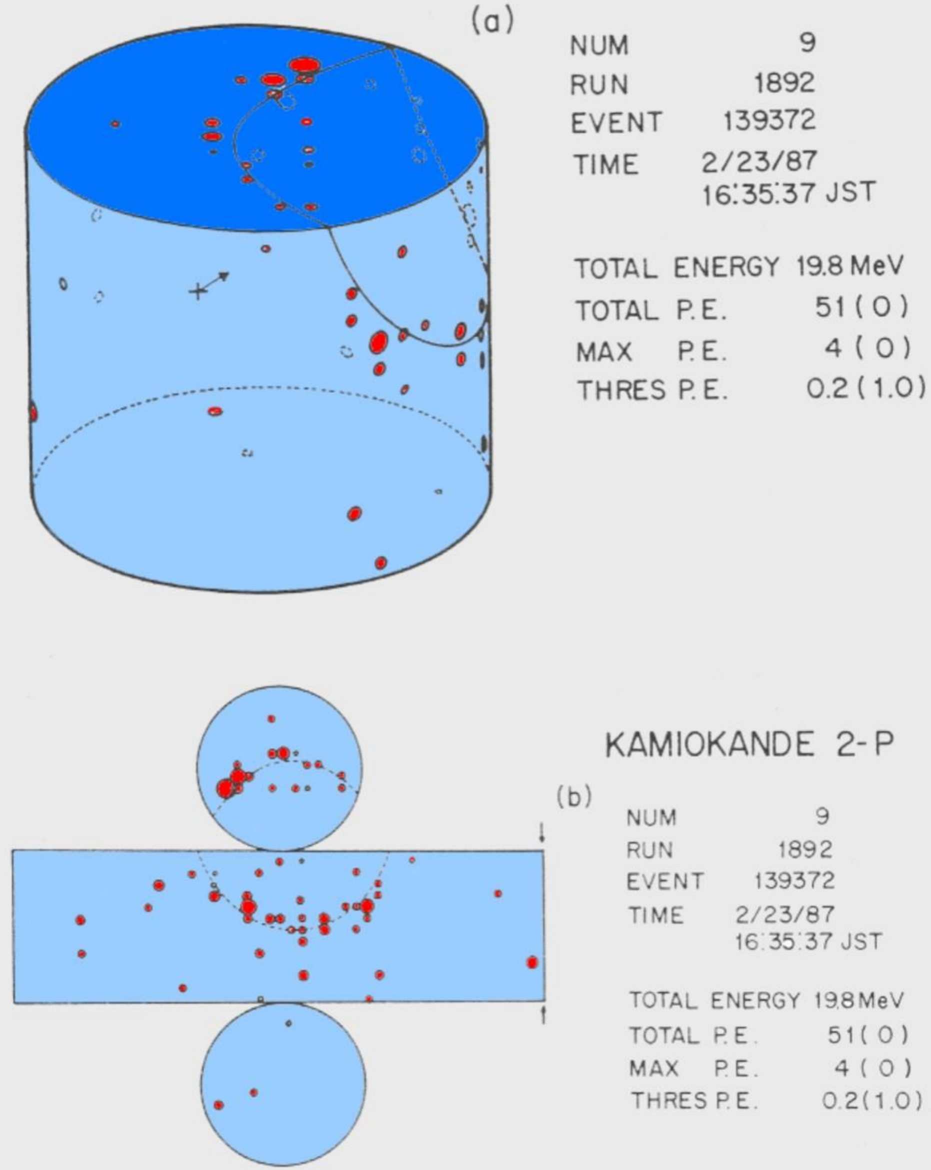

Hirata et al., PRD 38 (1988) 448

Irvine-Michigan-Brookhaven (IMB) Detector

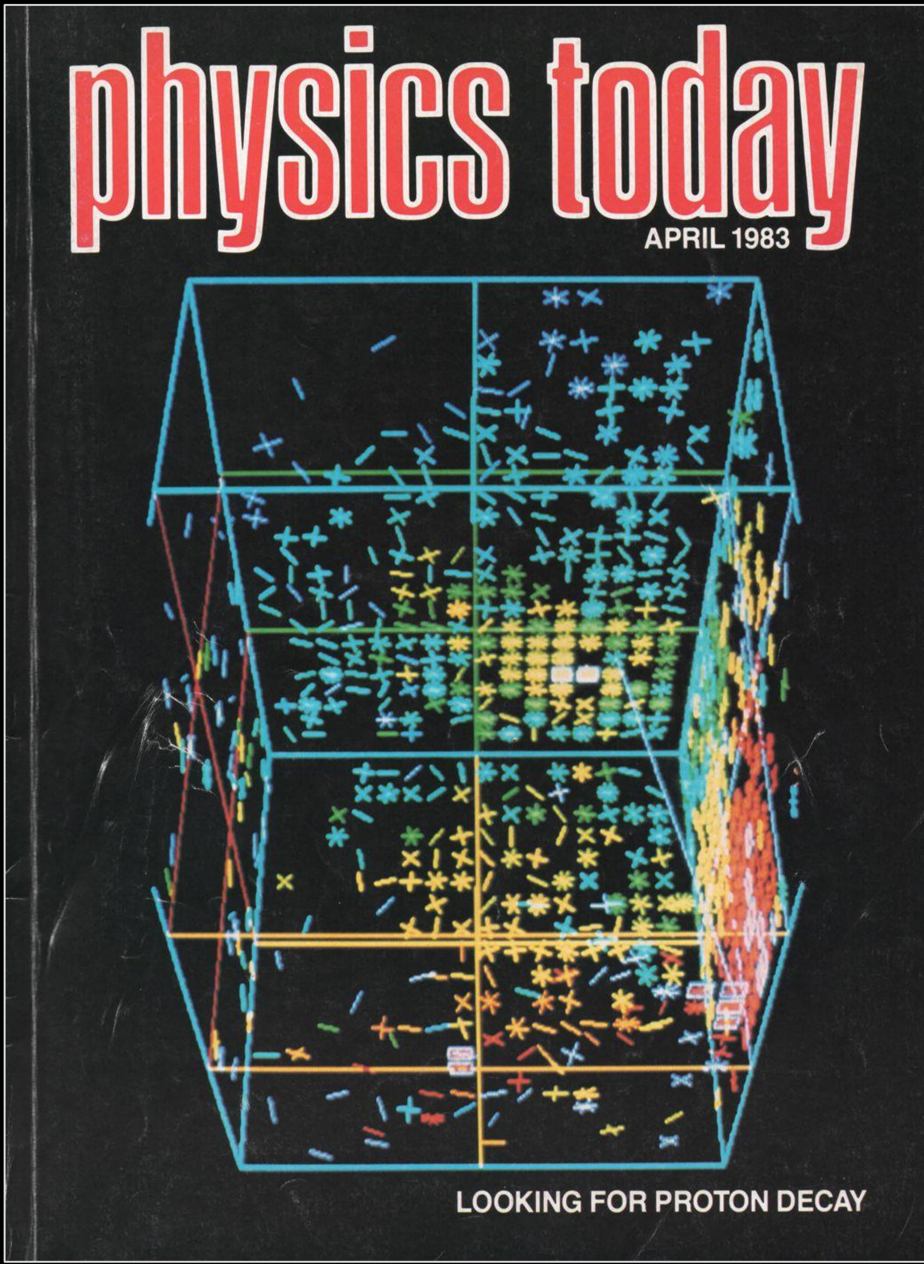

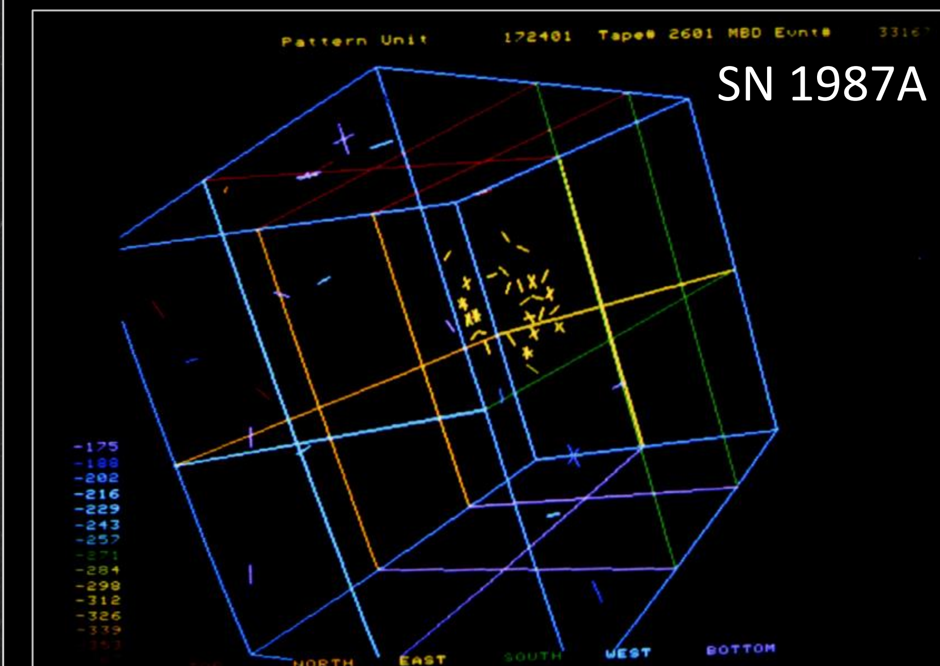

2002 Physics Nobel Prize for Neutrino Astronomy

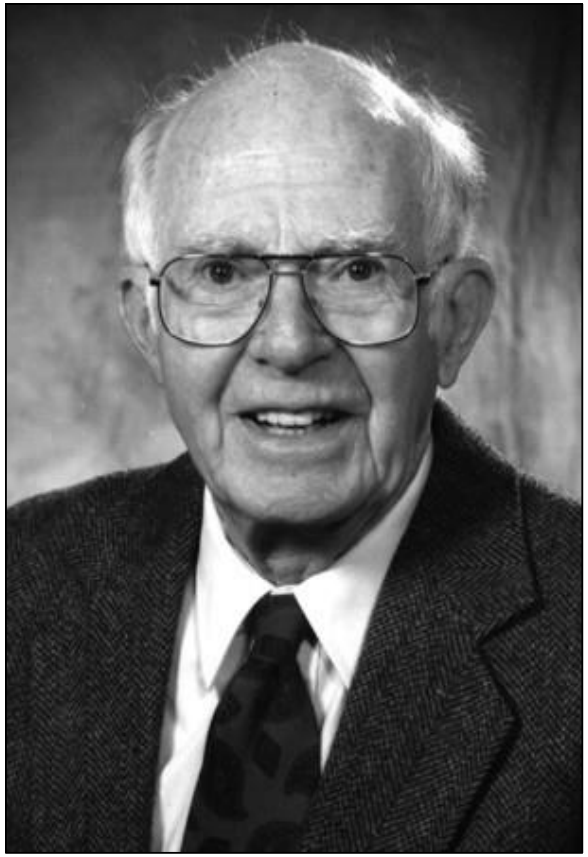

Ray Davis Jr.
(1914–2006)

Masatoshi Koshiba
(*1926)

"for pioneering contributions to astrophysics, in particular for the detection of cosmic neutrinos"

Early Lightcurve of SN 1987A

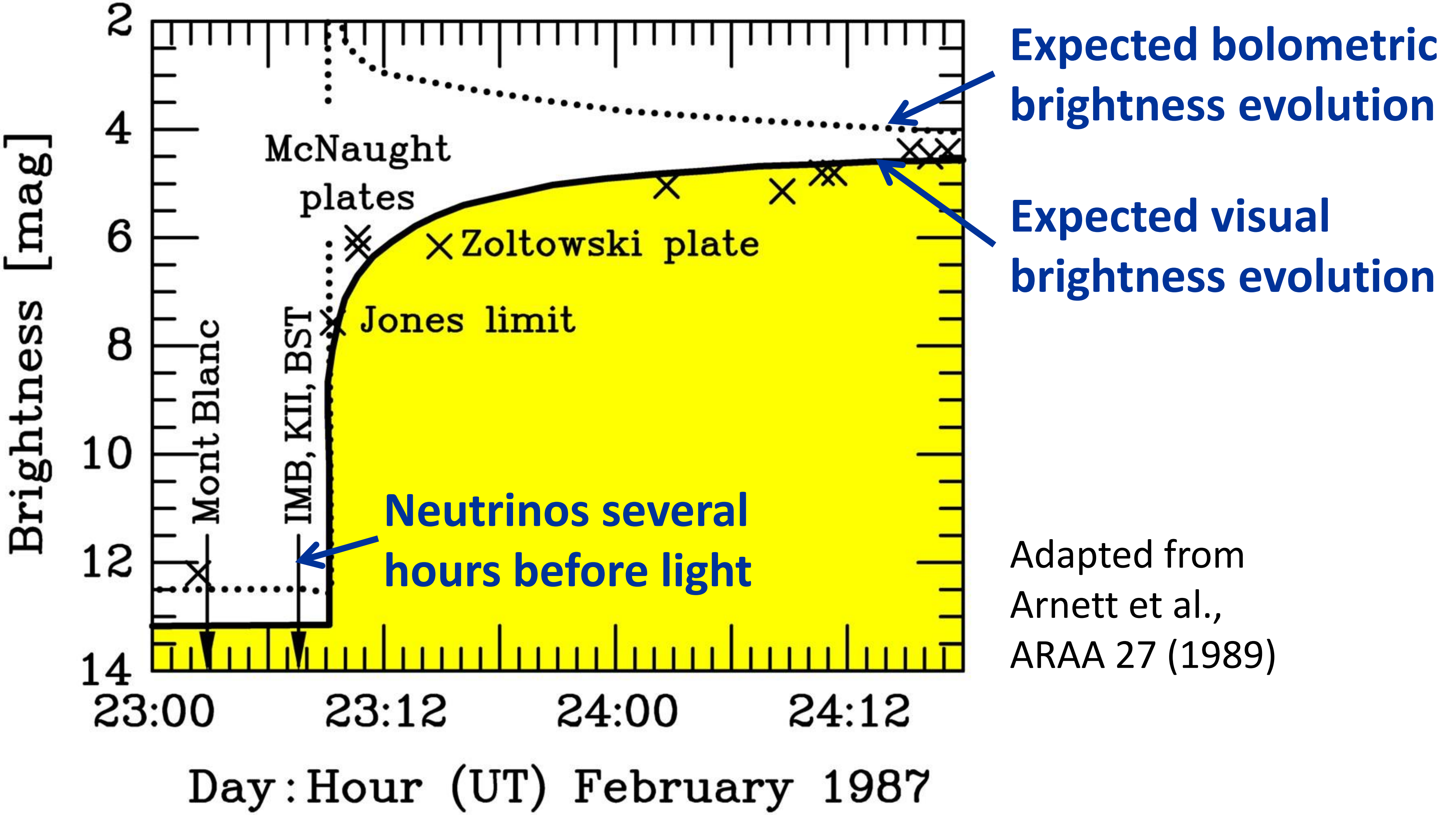

Adapted from Arnett et al., ARAA 27 (1989)

Do Neutrinos Gravitate?

Early light curve of SN 1987A

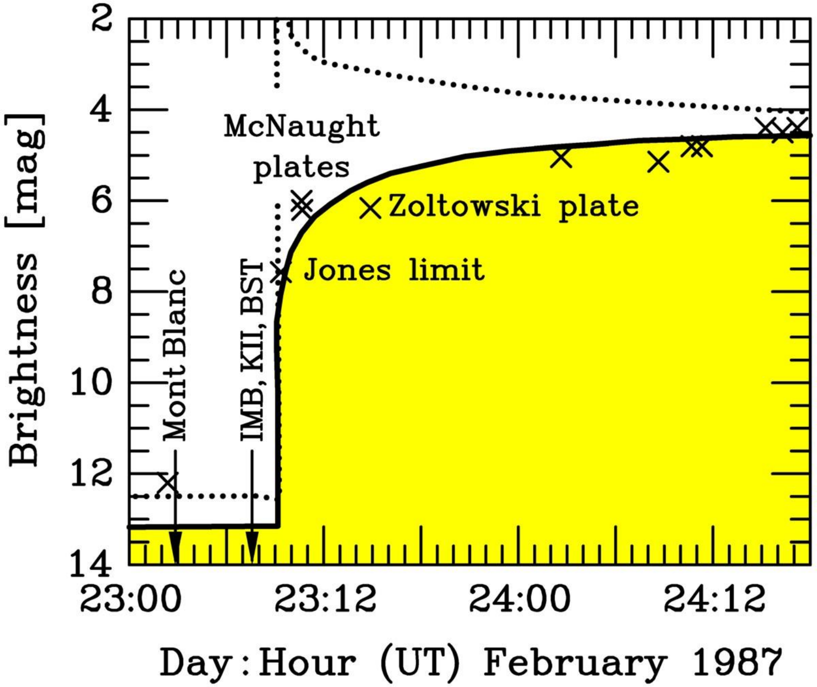

- Neutrinos arrived several hours before photons as expected
- Transit time for ν and γ same (160.000 yr) within a few hours

Shapiro time delay for particles moving in a gravitational potential

$$\Delta t = -2 \int_A^B dt\, \Phi[r(t)]$$

For trip from LMC to us, depending on galactic model,

$$\Delta t \approx 1\text{–}5 \text{ months}$$

Neutrinos and photons respond to gravity the same to within

$$1\text{–}4 \times 10^{-3}$$

Longo, PRL 60:173, 1988
Krauss & Tremaine, PRL 60:176, 1988

Interpreting SN 1987A Neutrinos

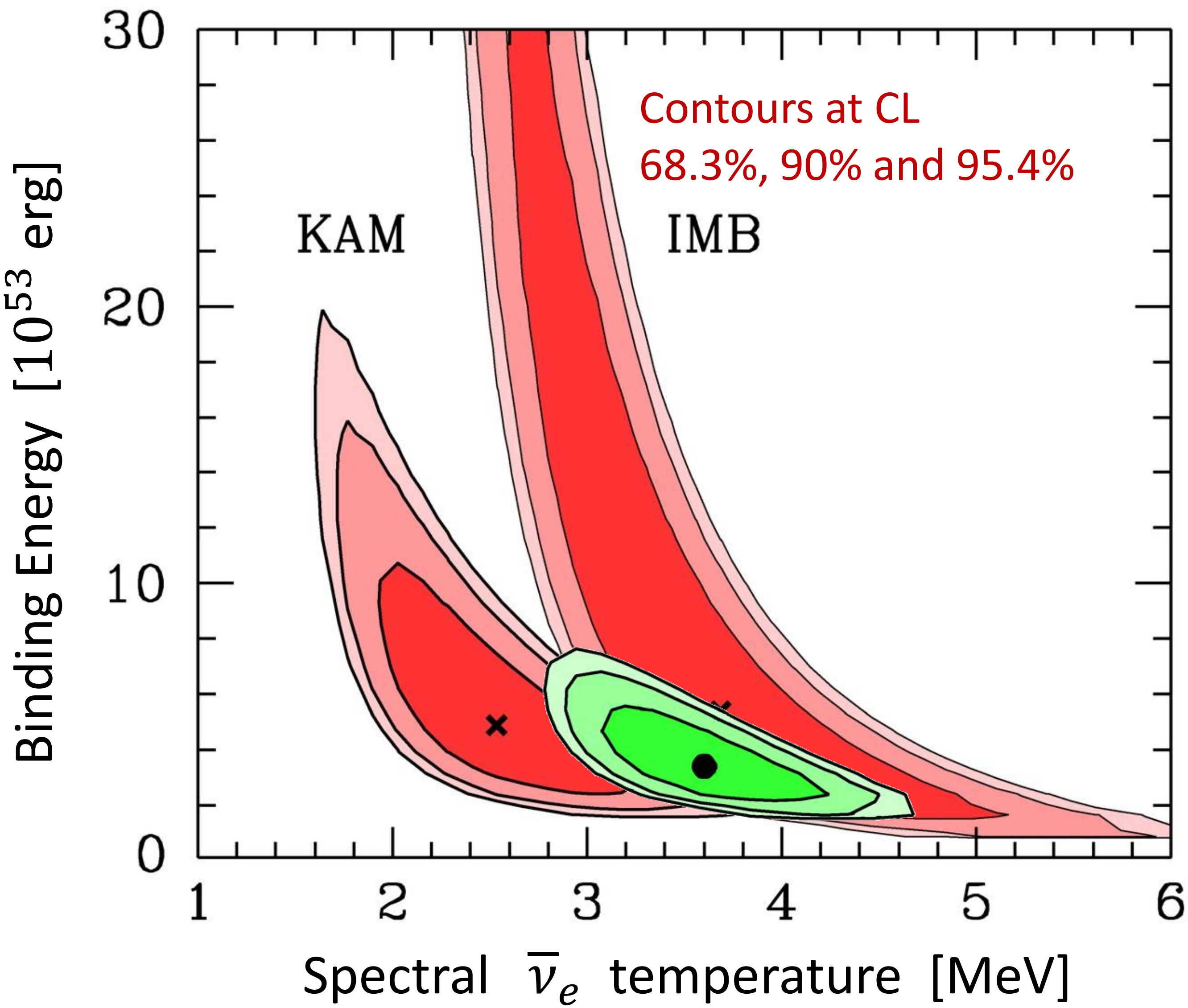

Assume
- Thermal spectra
- Equipartition of energy between $\nu_e, \overline{\nu}_e, \nu_\mu, \overline{\nu}_\mu, \nu_\tau$ and $\overline{\nu}_\tau$

Jegerlehner, Neubig & Raffelt, PRD 54 (1996) 1194

Interpreting SN 1987A Neutrinos

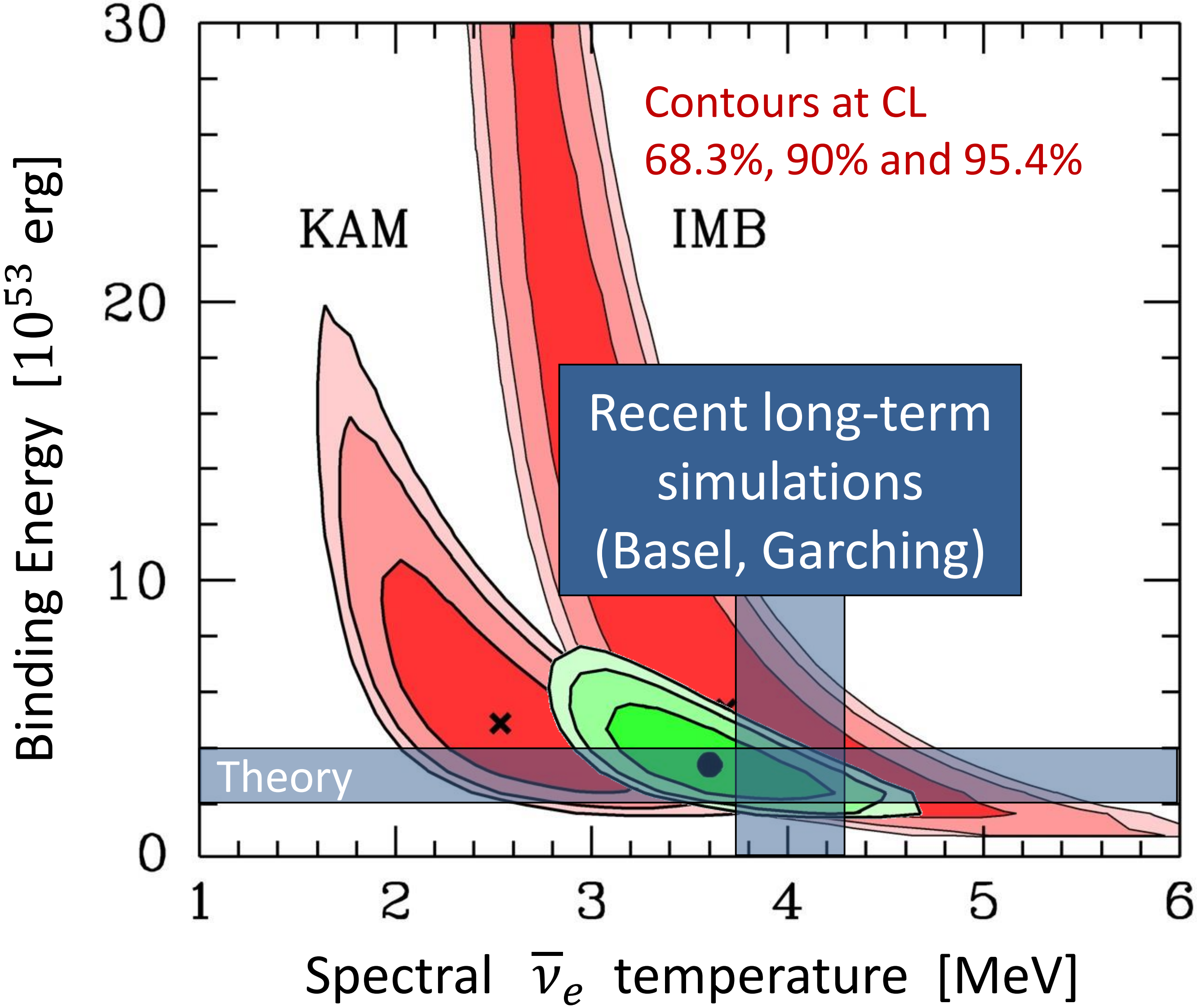

Assume
- Thermal spectra
- Equipartition of energy between $\nu_e, \overline{\nu}_e, \nu_\mu, \overline{\nu}_\mu, \nu_\tau$ and $\overline{\nu}_\tau$

Jegerlehner, Neubig & Raffelt, PRD 54 (1996) 1194

SN 1987A Burst of Neutrino Papers

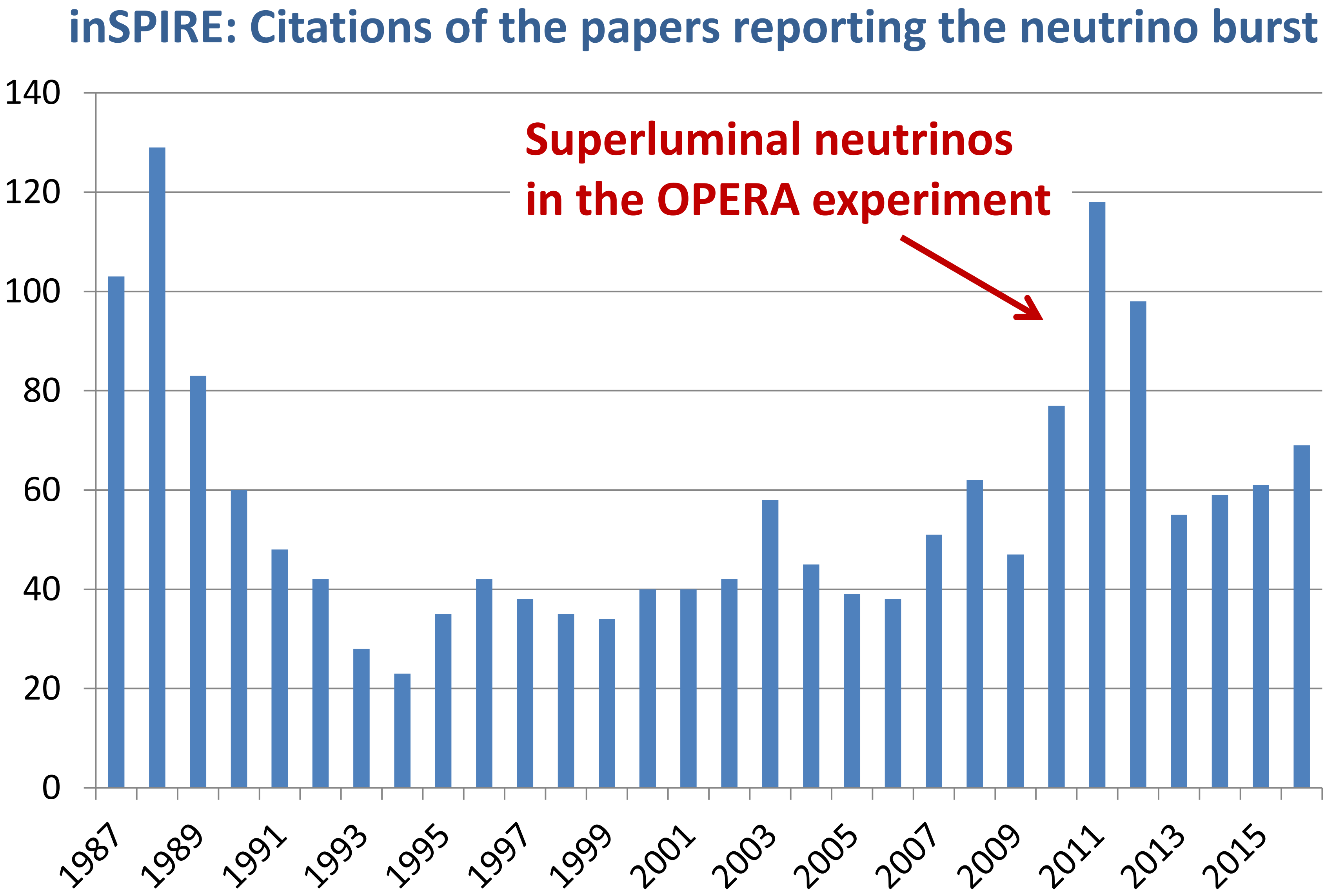

Supernova 1987A Energy-Loss Argument

SN 1987A neutrino signal

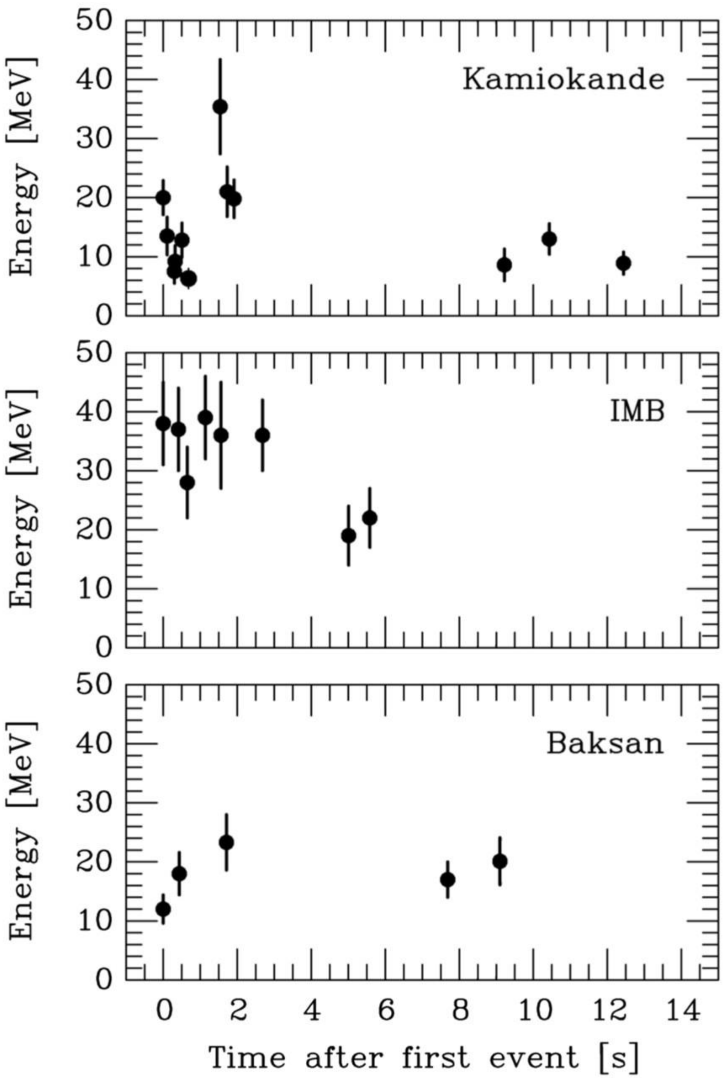

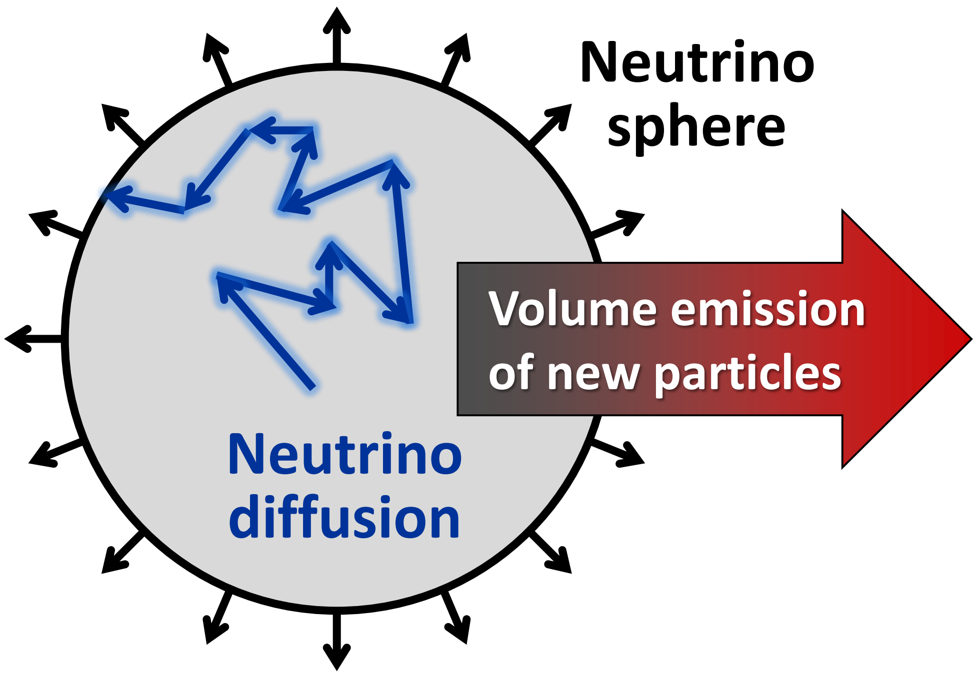

Emission of very weakly interacting particles would "steal" energy from the neutrino burst and shorten it.
(Early neutrino burst powered by accretion, not sensitive to volume energy loss.)

Late-time signal most sensitive observable

Cooling Time Scale

Exponential cooling model: $T = T_0\, e^{-t/4\tau}$, constant radius, $L = L_0\, e^{-t/\tau}$

Fit parameters are T_0, τ, radius, 3 offset times for KII, IMB & BST detectors

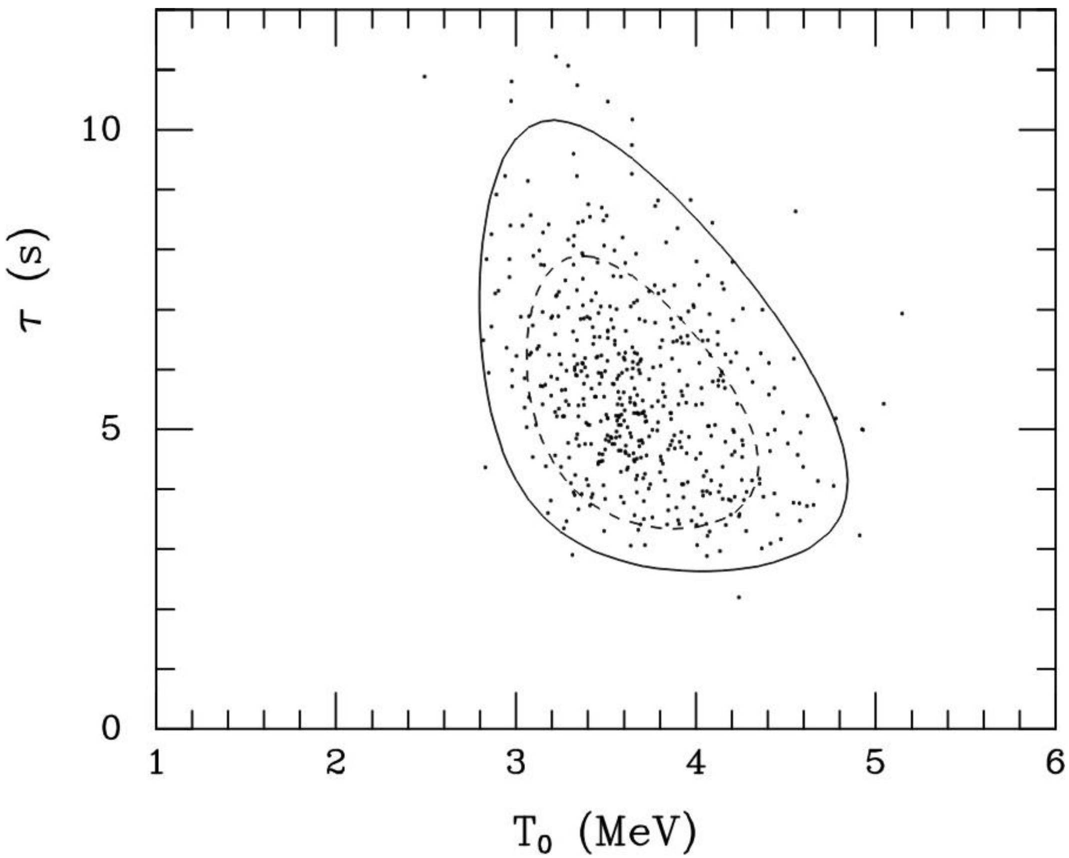

Loredo and Lamb, Bayesian analysis
astro-ph/0107260

Axion Emission from a Nuclear Medium

Axion-nucleon interaction: $\mathcal{L}_{\rm int} = \frac{C_N}{2f_a}\,\overline{\Psi}_N\gamma_\mu\gamma_5\Psi_N\partial^\mu a = \frac{C_N}{2f_a}J_\mu^A\partial_a^\mu$

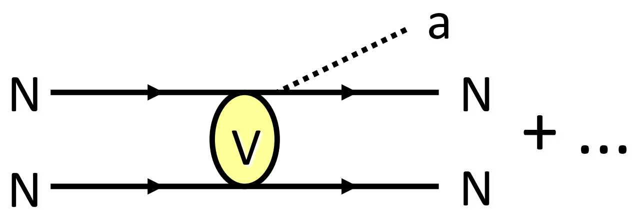

Nucleon-Nucleon Bremsstrahlung

Axial-vector interaction implies dominance of spin-dependent process

- Interaction potential (one-pion exchange OPE often used, but too simplistic)
- In-medium coupling constants
- In-medium effective nucleon properties
- Correlation effects (static and dynamical spin-spin correlations)

→ For latest discussion see Carenza et al. arXiv:1906.11844v3 (28 May 2020)

Thermal π^- contribute significantly (dominantly?)

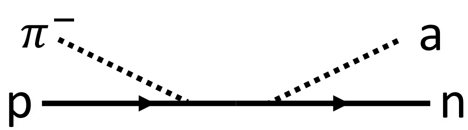

→ For latest discussion see Carenza et al. arXiv:2010.02943 (06 Oct 2020)

SN 1987A Axion Limits from Burst Duration

- Raffelt, Lect. Notes Phys. 741 (2008) 51 [hep-ph/0611350]
  Burst duration calibrated by early numerical studies
  "Generic" emission rates inspired by OPE rates
  $f_a \gtrsim 4 \times 10^8$ GeV and $m_a \lesssim 16$ meV (KSVZ, based on proton coupling)
- Chang, Essig & McDermott, JHEP 1809 (2018) 051 [1803.00993]
  Various correction factors to emission rates, specific SN core models
  $f_a \gtrsim 1 \times 10^8$ GeV and $m_a \lesssim 60$ meV (KSVZ, based on proton coupling)
- Carenza, Fischer, Giannotti, Guo, Martínez-Pinedo & Mirizzi,
  JCAP 10 (2019) 016 & Erratum [1906.11844v3]
  Beyond OPE emission rates, specific SN core models: similar to Chang et al.
  $f_a \gtrsim 4 \times 10^8$ GeV and $m_a \lesssim 15$ meV (KSVZ, based on proton coupling)
- Carenza, Fore, Giannotti, Mirizzi & Reddy [arXiv:2010.02943]
  Including thermal pions $\pi^- + p \to n + a$ (factor 3 larger emission)
  $f_a \gtrsim 5 \times 10^8$ GeV and $m_a \lesssim 11$ meV (KSVZ, based on proton coupling)
- Bar, Blum & D'Amico, Is there a supernova bound on axions? [1907.05020]
  Alternative picture of SN explosion (thermonuclear event)
  Observed signal not PNS cooling. SN1987A neutron star (or pulsar) not yet found.
  (but see "NS 1987A in SN 1987A", Page et al. arXiv:2004.06078)

Operational Detectors for Supernova Neutrinos

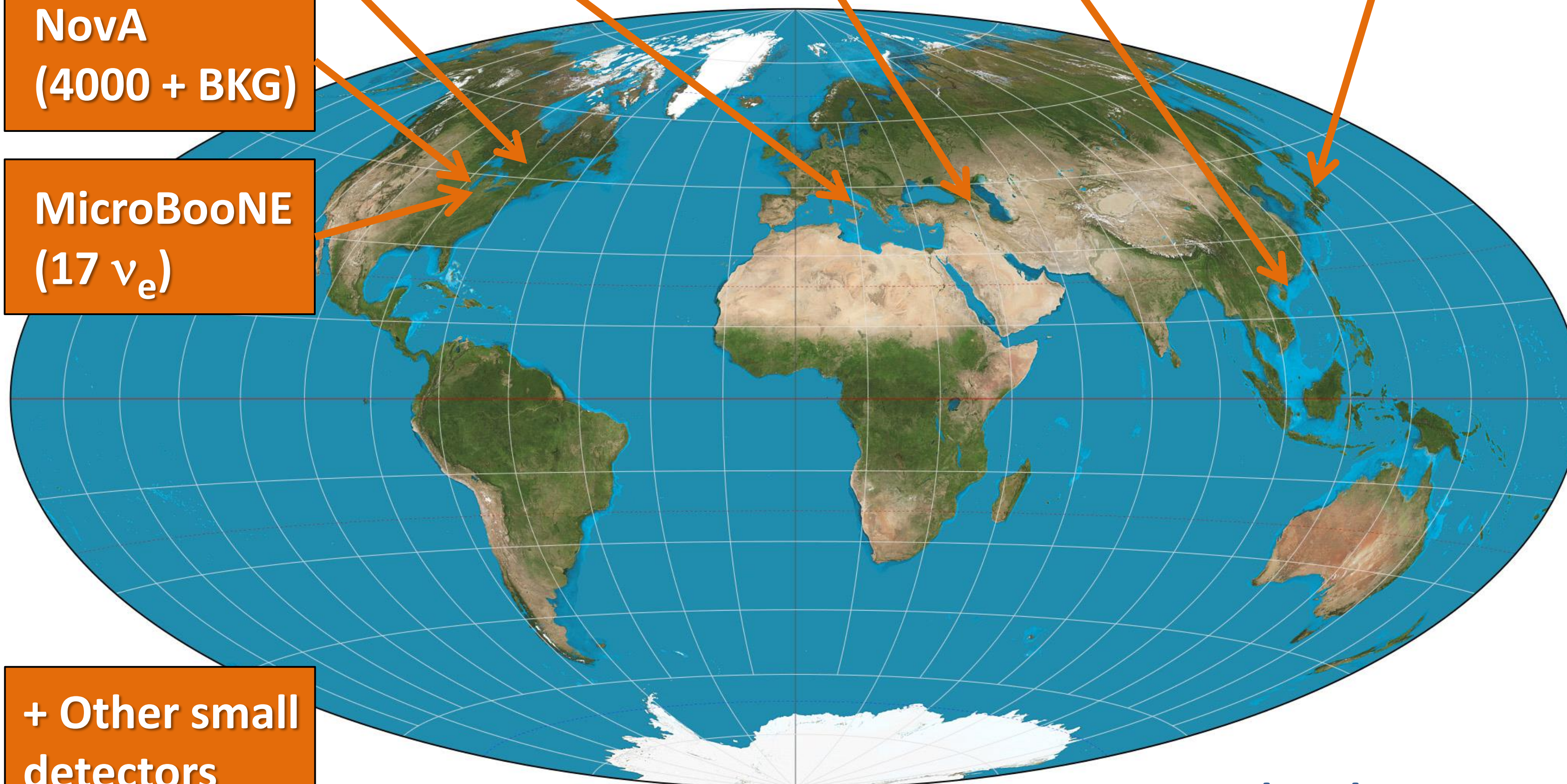

+ Other small detectors with some SN sensitivity

In brackets events for a "fiducial SN" at distance 10 kpc

Local Group of Galaxies

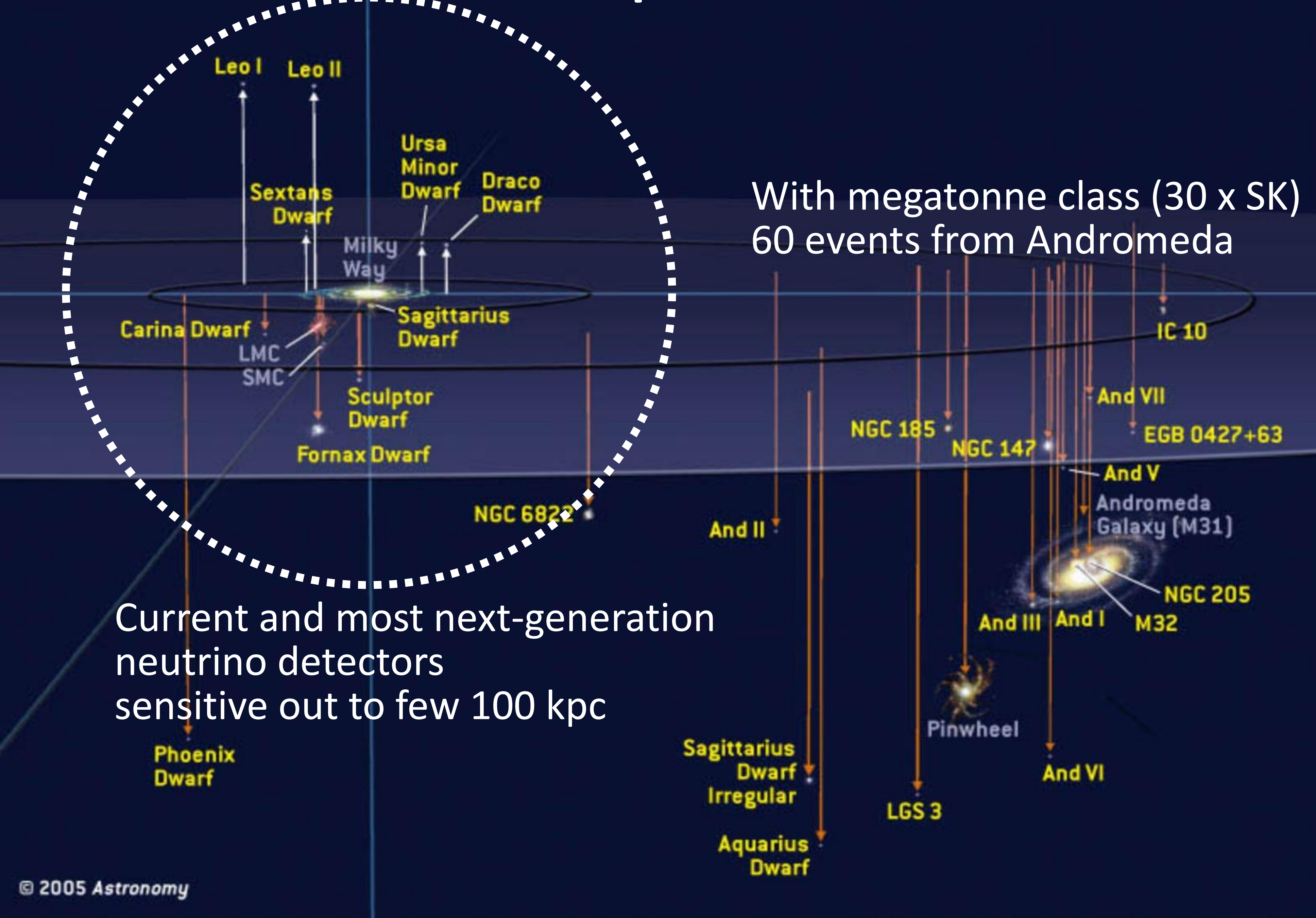

With megatonne class (30 x SK)
60 events from Andromeda

Current and most next-generation neutrino detectors
sensitive out to few 100 kpc

Many large detectors online for next decades

Every year a 3% chance

I am optimistic to see more SN neutrinos!

Neutron Star Cooling

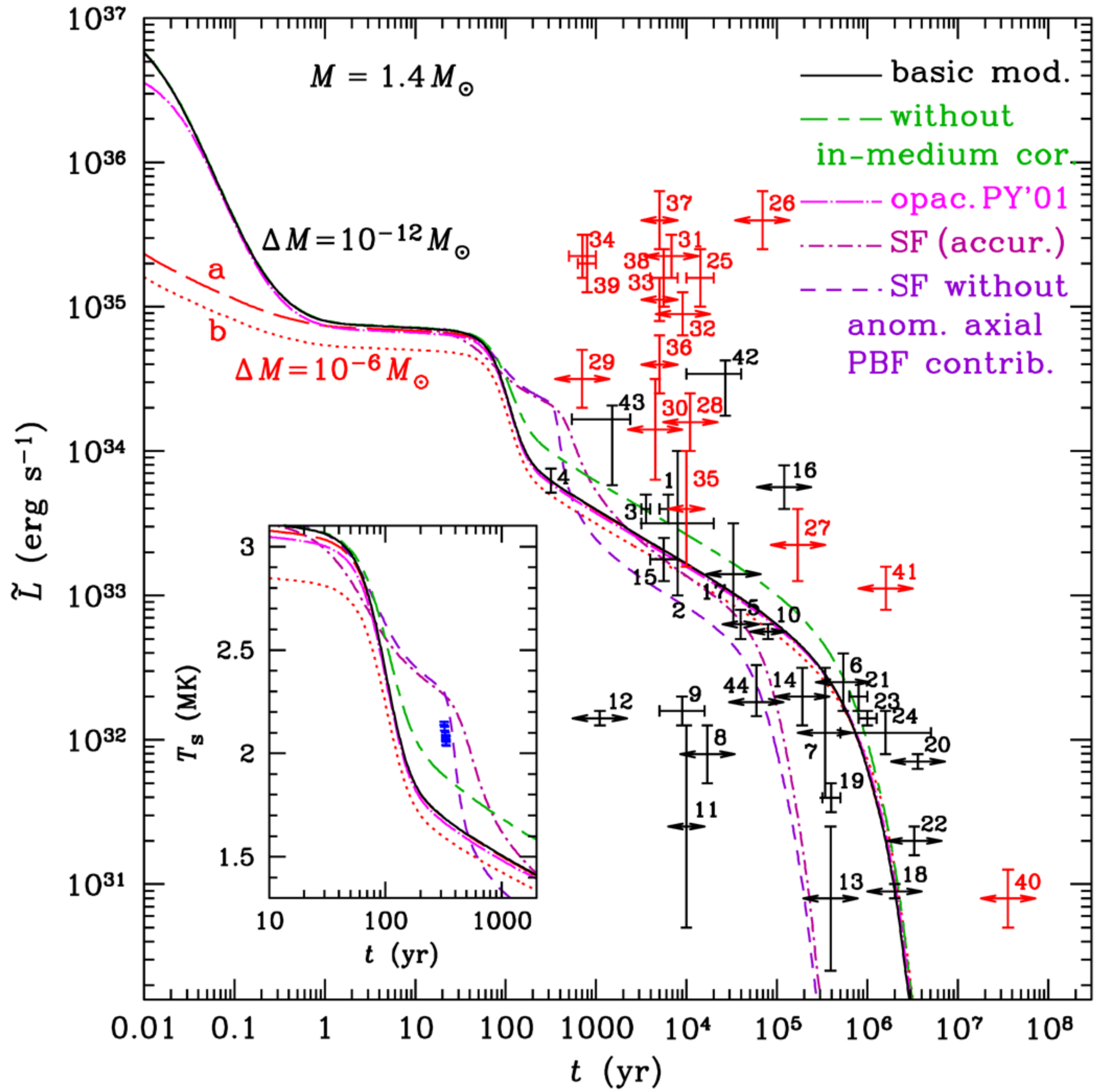

Potekhin & Chabrier: Magnetic neutron star cooling and microphysics [1711.07662]

Axion Limits from Neutron Star Cooling

Selection of pulsars at different age:

- Umeda, Iwamoto, Tsuruta, Qin & Nomoto, astro-ph/9806337
- A. Sedrakian, arXiv:1512.07828 (hadronic axions)
- A. Sedrakian, arXiv:1810.00190 (non-hadronic axions)

Supernova Remnant Cas A (320 years)

- Leinson, arXiv:1405.6873
- Hamaguchi, Nagata, Yanagi & Zheng, arXiv:1806.07151

Supernova Remnant HESS J1731-347 (27 kyears)

- Beznogov, Rrapaj, Page & Reddy, arXiv:1806.07991
  $g_{an}^2 < 0.77 \times 10^{-19}$
- Leinson, arXiv:1909.03941
  $g_{an}^2 < 1.1 \times 10^{-19}$

$$C_n m_a \lesssim 2\ \mathrm{meV}$$

Limits broadly comparable to SN 1987A bounds (m_a tens of meV range)

- Protons superconducting – bremsstrahlung from neutrons
- Neutron-axion coupling can be very small or vanish

Cooling of Neutron Star in Cas A

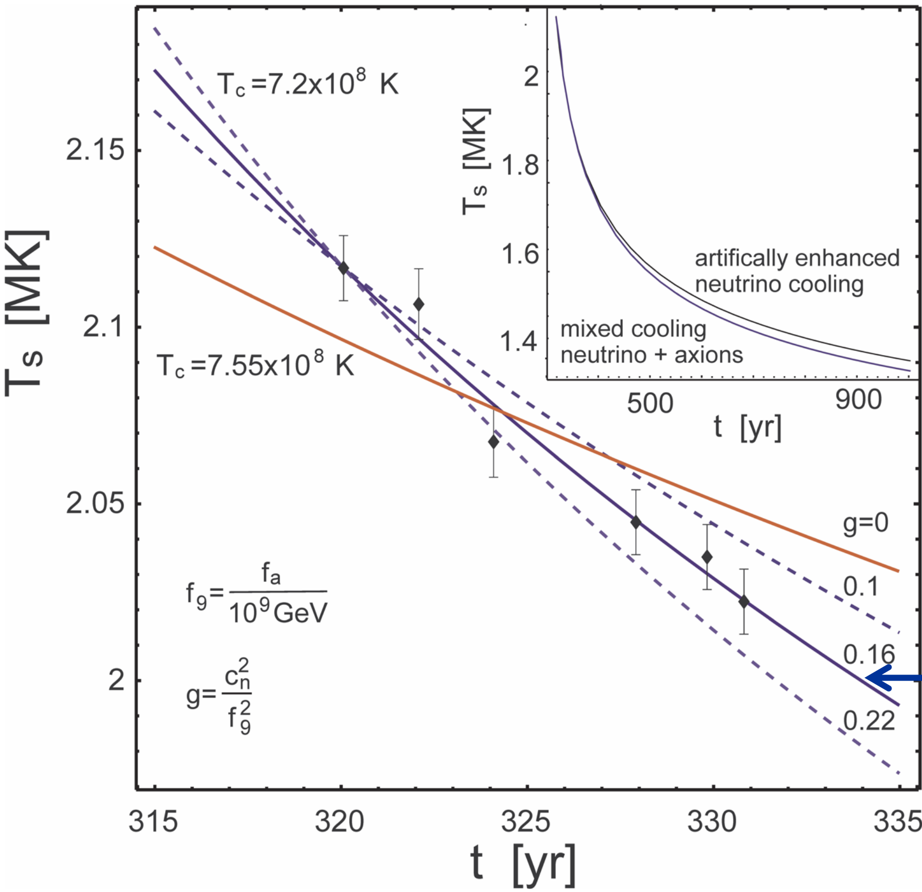

$C_n m_a \sim 2.4$ meV

Chandra x-ray image of non-pulsar compact remnant

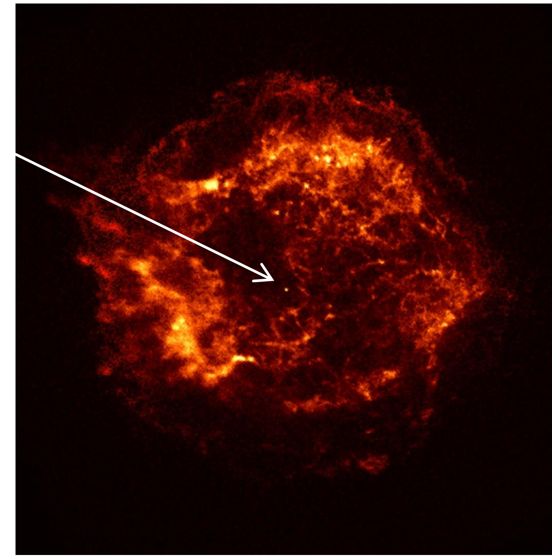

Measured surface temperature over 10 years reveals unusually fast cooling rate

- Neutron Cooper pair breaking and formation (PBF) as neutrino emission process?
- Evidence for extra cooling (by axions)?

Leinson, arXiv:1405.6873

Axion Bounds from Magnetic WDs and NSs

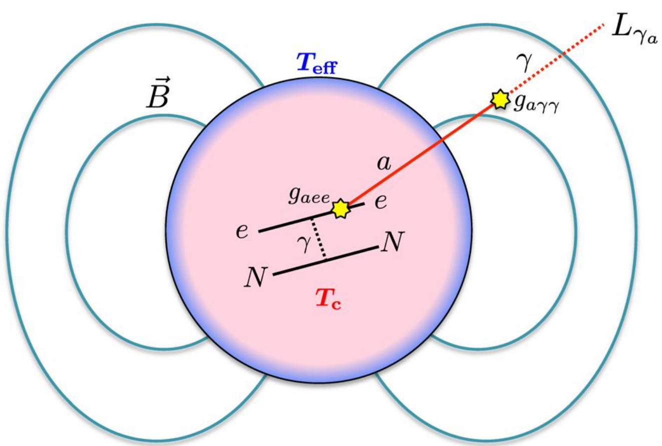

Magnetic White Dwarf

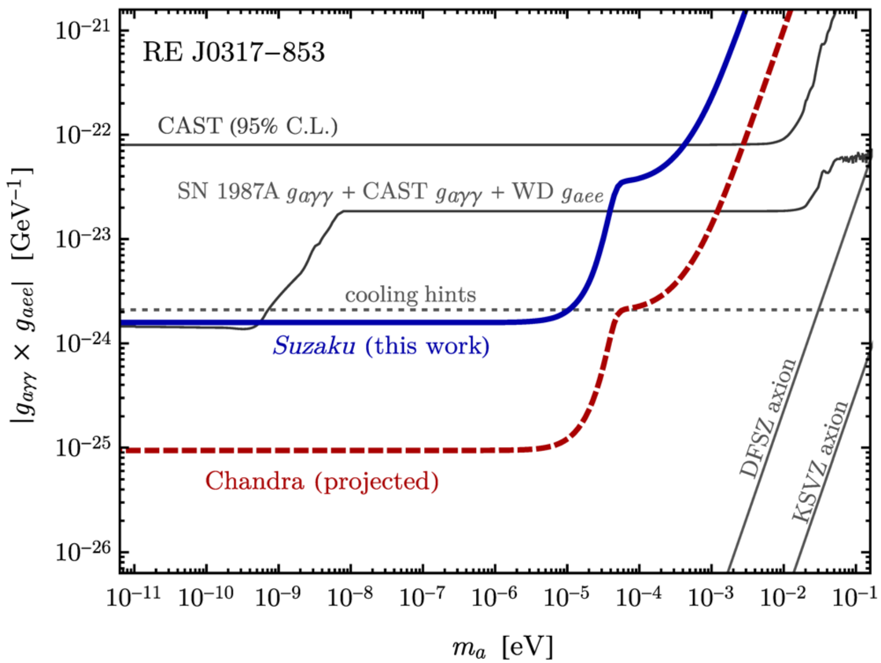

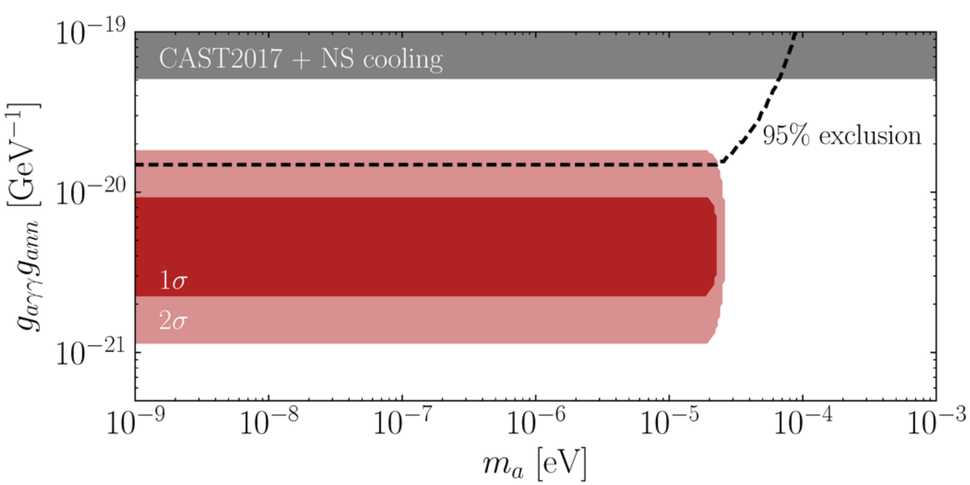

Magnificent Seven Neutron Stars
X-Ray limits and excess

- Buschmann, Co, Dessert & Safdi:
  X-Ray Search for Axions from Nearby Isolated Neutron Stars, arXiv:1910.04164
- Dessert, Long & Safdi: *X-Ray Signatures of Axion Conversion in Magnetic White Dwarf Stars*, PRL 123 (2019) 061104, arXiv:1903.05088

Radio Search for Axion Dark Matter in Pulsars

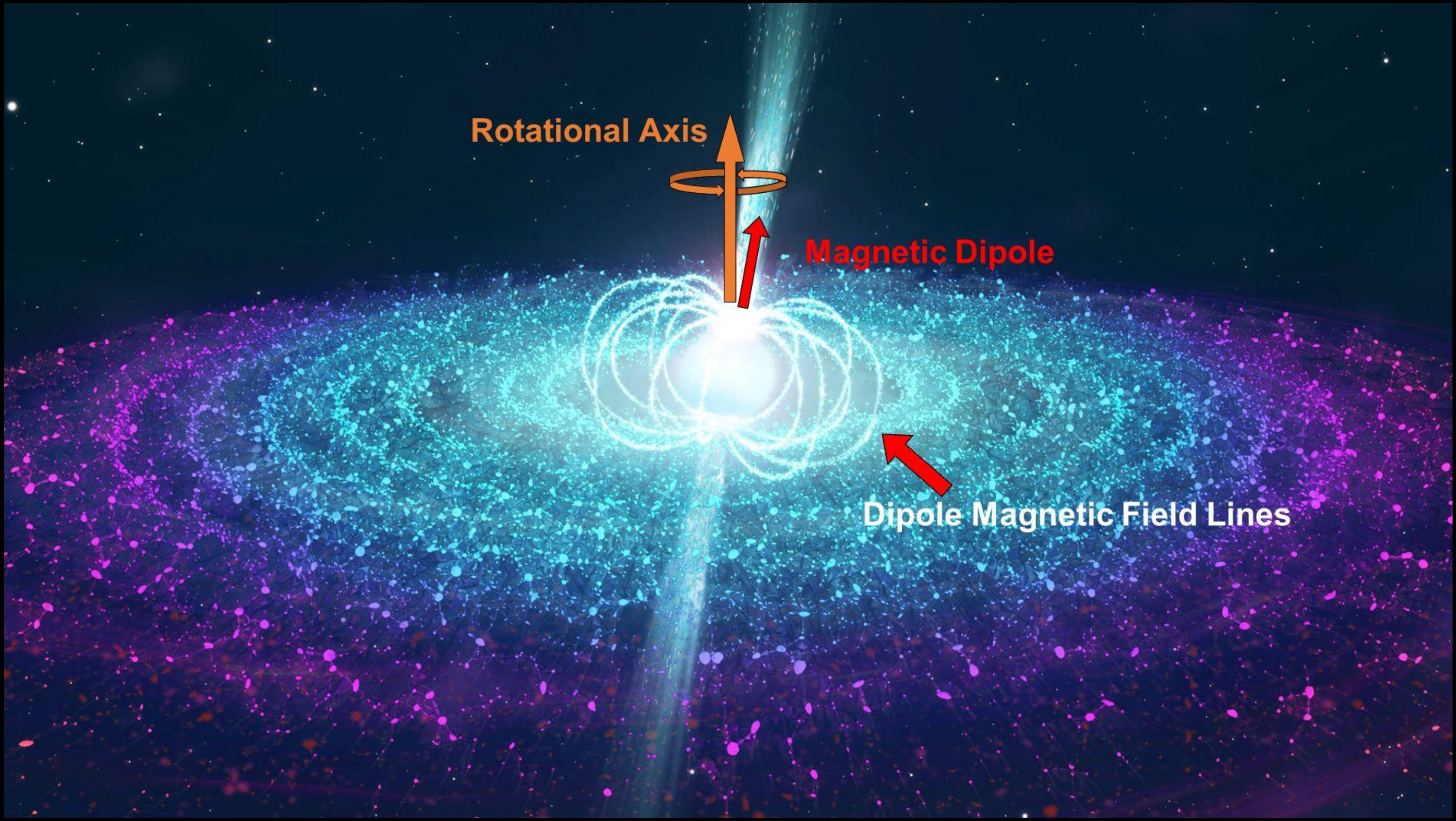

See Josh Foster, 9 Oct 2020, https://indico.cern.ch/event/950670/

Radio Search for Axion Dark Matter in Pulsars

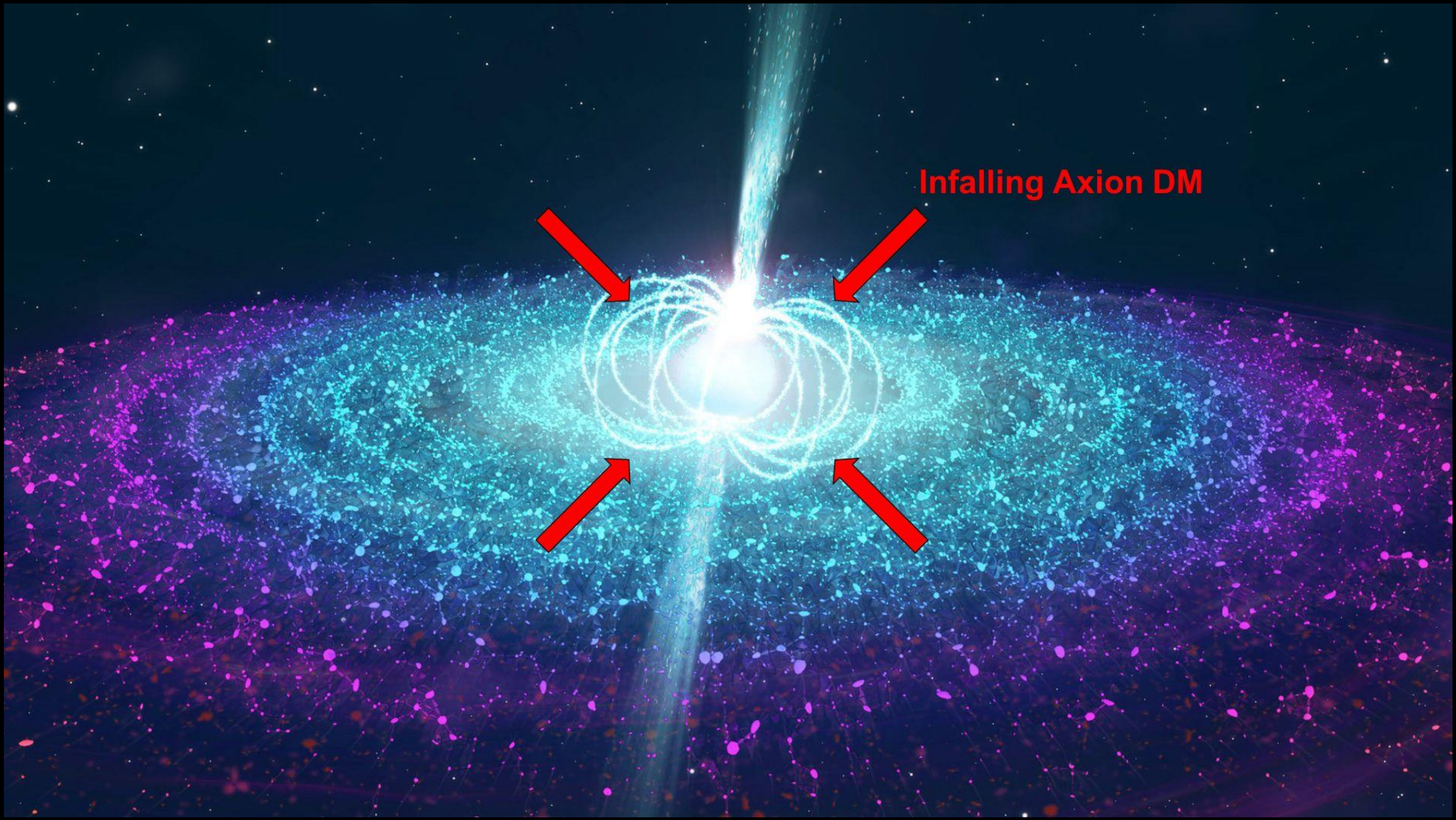

See Josh Foster, 9 Oct 2020, https://indico.cern.ch/event/950670/

Radio Search for Axion Dark Matter in Pulsars

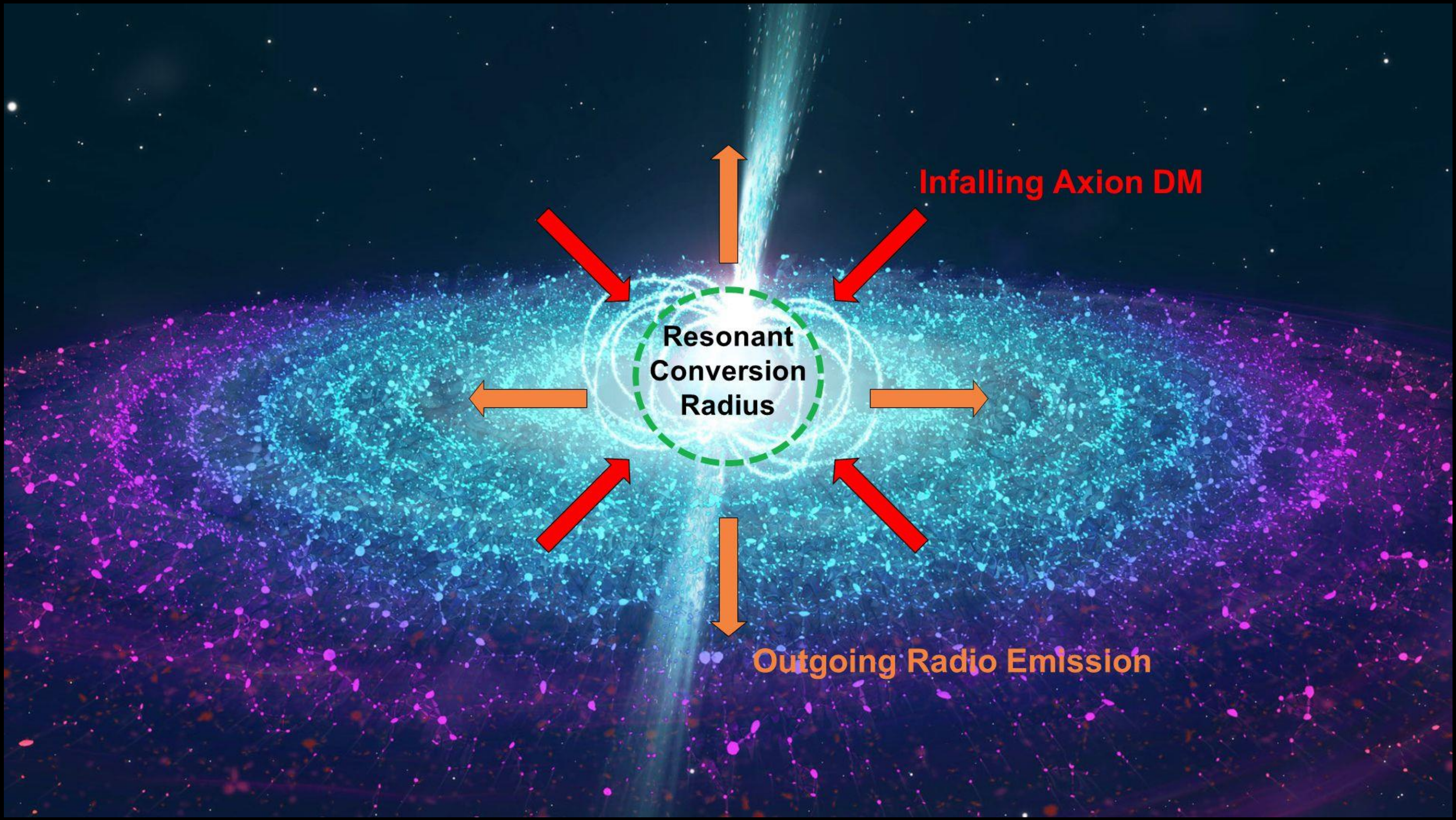

See Josh Foster, 9 Oct 2020, https://indico.cern.ch/event/950670/

Radio Search for Axion Dark Matter in Pulsars

Two viable strategies

1. Observe isolated neutron stars in clean environments
2. Observe high density targets in messy environments

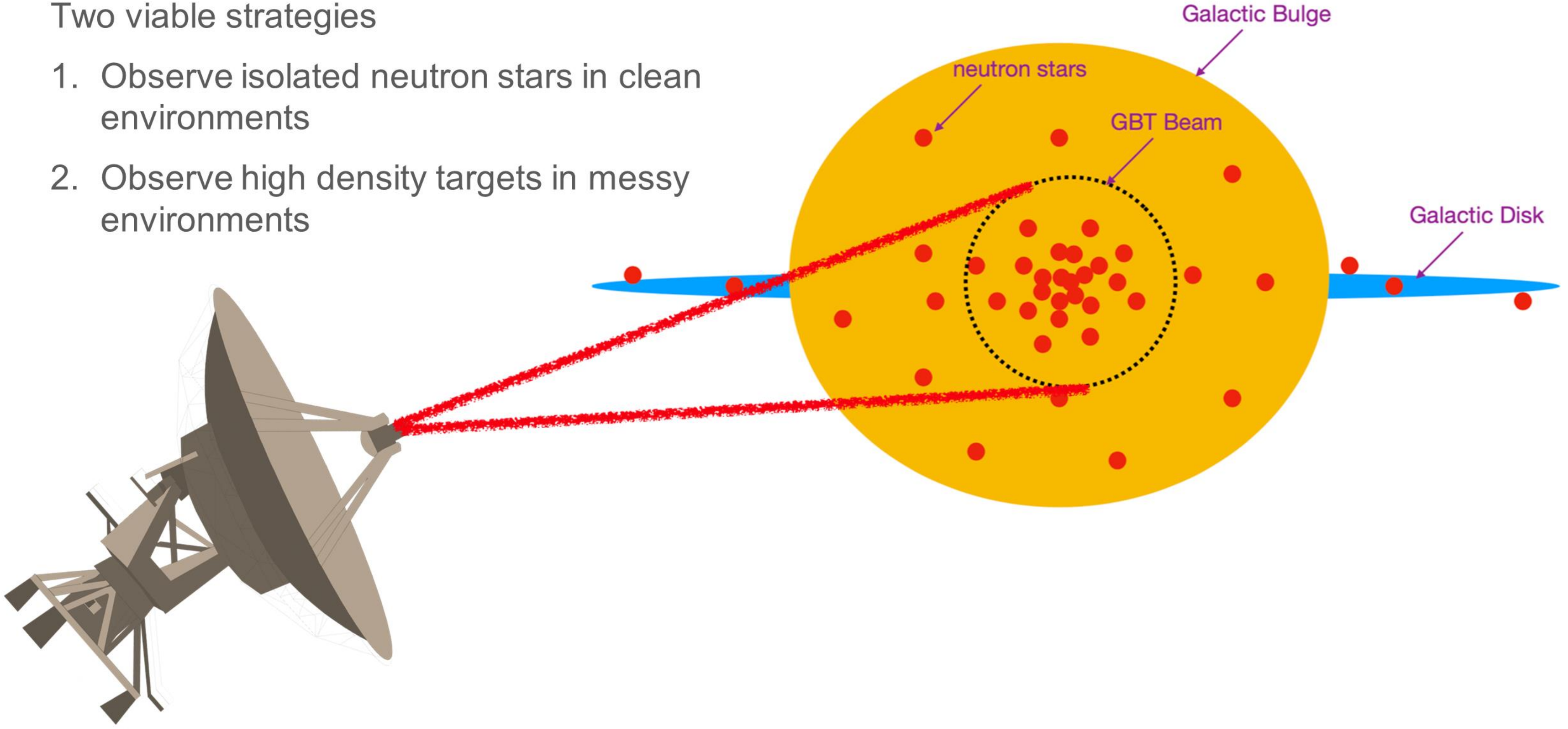

See Josh Foster, 9 Oct 2020, https://indico.cern.ch/event/950670/

Superradiance

Initially slow particle scattering in the ergoregion speeds up by extracting angular momentum and energy from the BH;

Waves similarly increase in amplitude

Particles/waves trapped in orbit around the BH repeat this process continuously

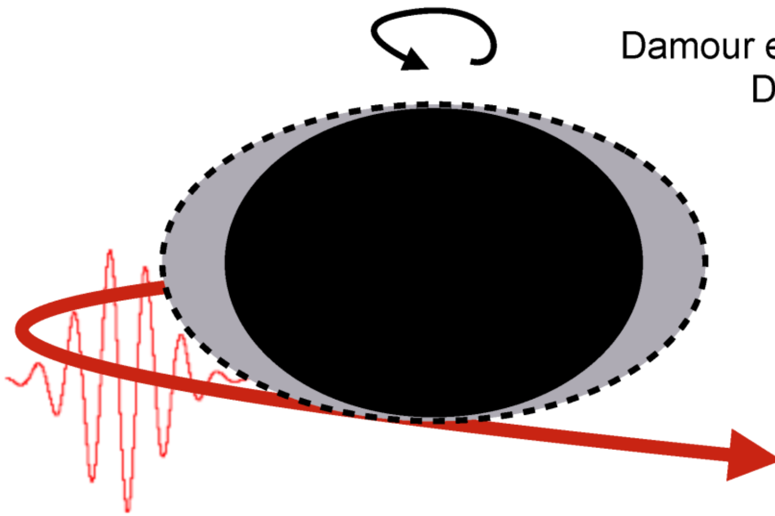

Damour et al; Zouros & Eardley; Detweiler; Gaina

Superradiance condition:

Angular velocity of particle slower than angular velocity of BH horizon

$$\frac{\omega_a}{m} < \Omega_{BH}$$

(m = magnetic quantum number)

Particles in orbits that satisfy the SR condition are amplified:
"Black hole bomb"

Kinematic, not resonant condition

Black Hole Spins

Five currently measured black holes combine to set limit:

$$2 \times 10^{-11} > \mu_a > 6 \times 10^{-13} \text{ eV}$$
$$3 \times 10^{17} < f_a < 1 \times 10^{19} \text{ GeV}$$

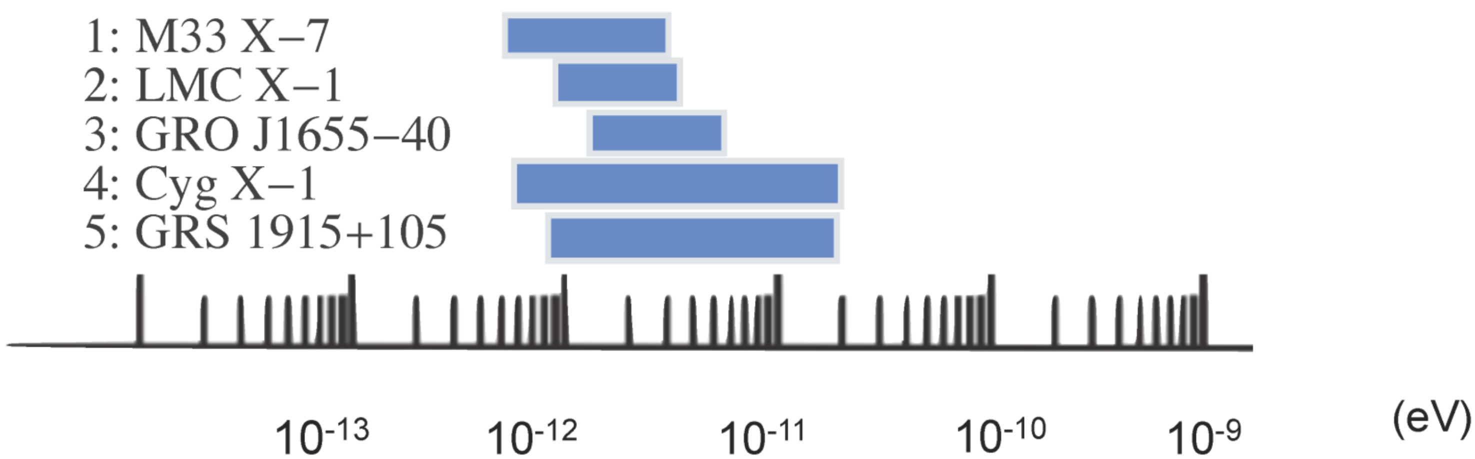

Arvanitaki , Baryakhtar & Huang, arXiv:1411.2263, PRD 91 (2015) 084011

But see Fernandez, Ghalsasi & Profumo, arXiv:1911.07862

Masha Baryakhtar, Talk at Invisibles 2016, https://indico.cern.ch/event/464402/

Gravitational Wave Signals

- Transitions between levels

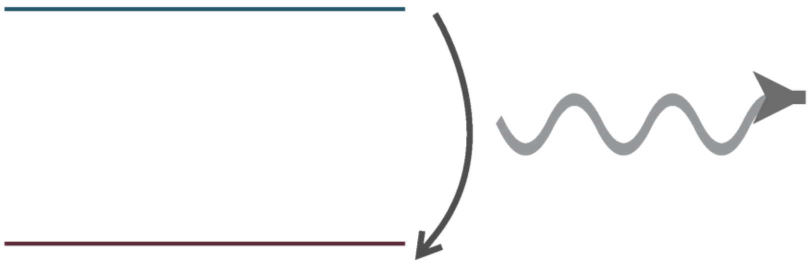

- Annihilations to gravitons

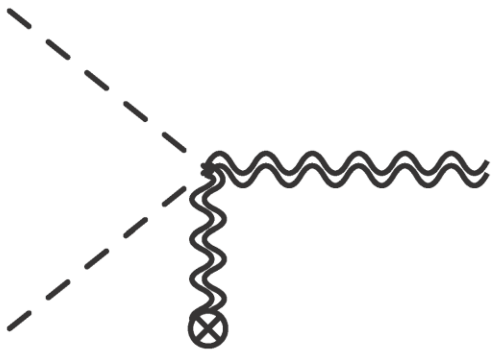

Arvanitaki, Baryakhtar, Dimopoulos, Dubovsky & Lasenby, arXiv:1604.03958

Direct Constraints on the Ultralight Boson Mass from Searches of Continuous Gravitational Waves

C. Palomba,[1] S. D'Antonio,[2] P. Astone,[1] S. Frasca,[3,1] G. Intini,[3,1] I. La Rosa,[4] P. Leaci,[3,1] S. Mastrogiovanni,[5] A. L. Miller,[3,1,6] F. Muciaccia,[3] O. J. Piccinni,[3,1] L. Rei,[7] and F. Simula[1]

Superradiance limits from LIGO O2 all-sky search for periodic GWs

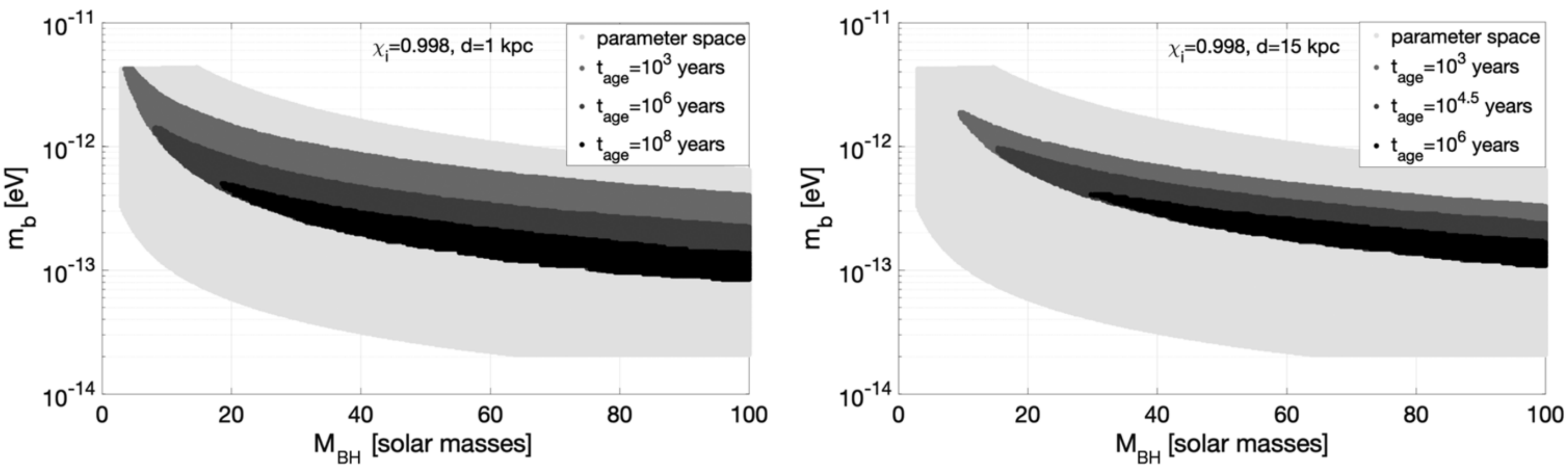

FIG. 2. 95% C.L. exclusion regions in the plane $m_b - M_{\rm BH}$ assuming a maximum distance $d = 1$ kpc (left plot) and $d = 15$ kpc (right plot), a black hole initial adimensional spin $\chi_i = 0.998$, and three possible values for $t_{\rm age}$: 10^3, 10^6, 10^8 yr (left plot) and 10^3, $10^{4.5}$, 10^6 yr (right plot). The larger light gray area is the accessible parameter space. As expected, the extension of the excluded region decreases for increasing $t_{\rm age}$ (corresponding to darker color).

See also:
Search for ultralight bosons in Cygnus X-1 with Advanced LIGO, arXiv:1909.11267

Axions and Stars

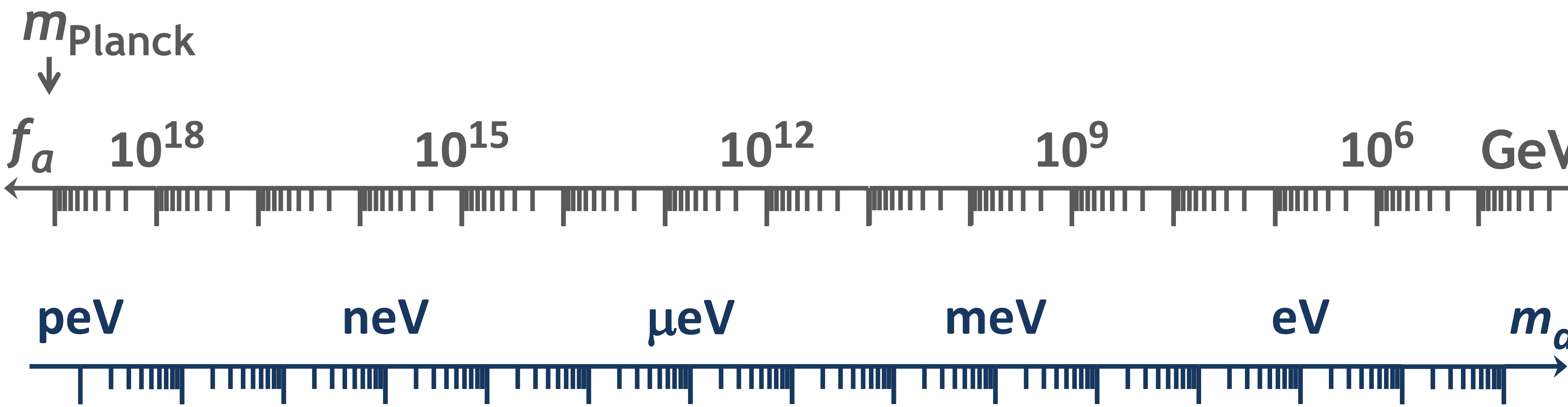

Opportunities for detection

Astrophysical Bounds (Energy loss of stars)

Super Radiance

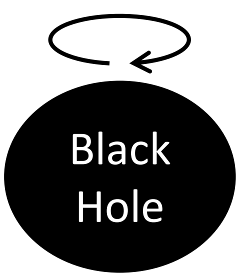

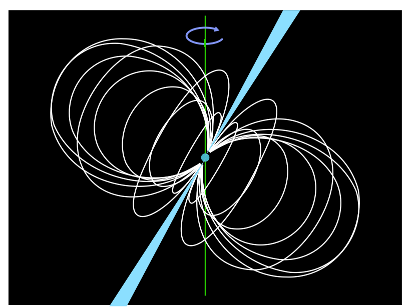

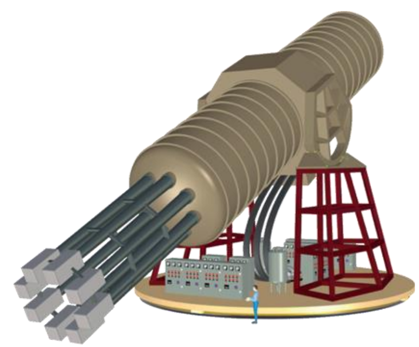

IAXO Solar Axion Telescope

Axion conversion in neutron star magnetospheres